EPFL

Advanced Control Systems

Prof. Alireza Karimi

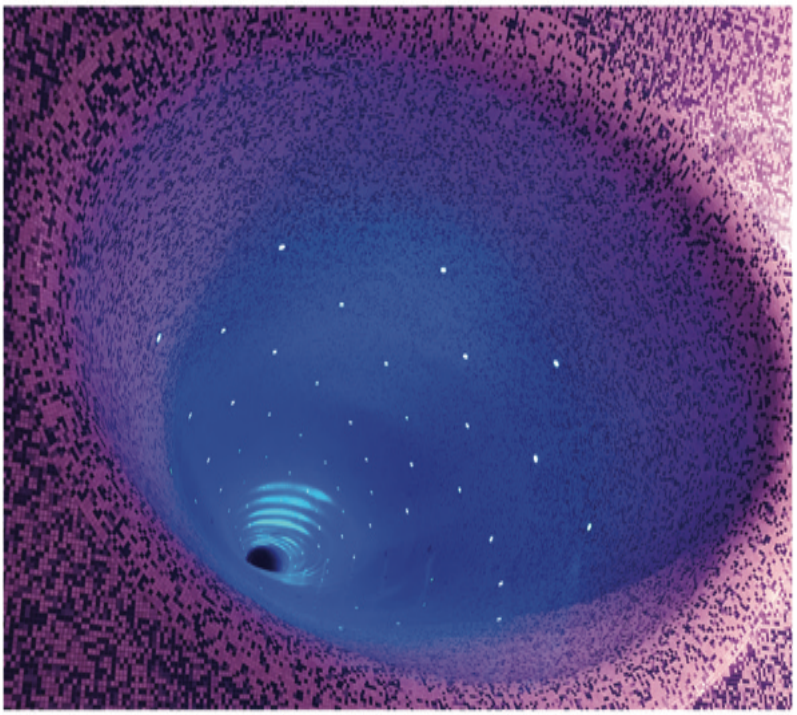

Lausanne
Spring 2025

PREFACE

These course notes have been prepared for a graduate course on Advanced Control Systems for students of Ecole Polytechnique Fédérale de Lausanne (EPFL). The course covers theoretical and practical aspects of robust and adaptive control for students involved in control system design.

The first chapter provides a summary of the first six chapters of Feedback Control Theory by Doyle, Francis, and Tannenbaum published in 1992 by Maxwell Macmillan (available online), with the addition of a section on stochastic uncertainty modeling. The chapter covers stability and performance of control systems, the concept of model uncertainty, robust stability, and robust performance in the $\mathcal{H}_2/\mathcal{H}_\infty$ framework.

The second chapter presents the essentials of controller design in the $\mathcal{H}_2$ and $\mathcal{H}_\infty$ framework using convex optimization algorithms and linear matrix inequalities. After a brief introduction to convex optimization, the chapter covers $\mathcal{H}_2$ and $\mathcal{H}_\infty$ state feedback controller design using Linear Matrix Inequalities (LMIs), introduces the concept of an augmented plant using linear fractional transformation, and discusses $\mathcal{H}_2/\mathcal{H}_\infty$ output feedback controller design. The chapter concludes with a new method for robust controller design developed in the Automatic Control Laboratory of EPFL (thanks to Christoph Kammer, Philippe Schuchert and Vaibhav Gupta), which uses frequency-domain data and convex optimization algorithms to design fixed structure controllers for uncertain systems.

The third chapter introduces the concept of robust adaptive control and reviews digital controller design methods using two-degree of freedom polynomial controllers. It then covers the robust pole placement technique using Q-parameterization and provides a detailed overview of parameter adaptation algorithms. The chapter concludes by discussing direct, indirect, and switching adaptive control. This chapter is a concise version of Chapters 1-3, 7-8, 10-13 of Adaptive Control, Algorithms, Analysis and Applications by Landau, Lozano, M'Saad and Karimi published in 2011 by Springer.

Lausanne, Spring 2025

Contents

Chapter 1

STABILITY, PERFORMANCE AND ROBUSTNESS

1.1 Introduction

The process of designing a control system generally involves many steps. A typical scenario is as follows [2]:

1. Study the system to be controlled and decide what types of sensors and actuators will be used and where they will be placed.
2. Model the resulting system to be controlled.
3. Simplify the model if necessary so that it is tractable.
4. Analyze the resulting model; determine its properties.
5. Decide on performance specifications.
6. Decide on the type of controller to be used.
7. Design a controller to meet the specs, if possible; if not, modify the specs or generalize the type of controller sought.
8. Simulate the resulting controlled system, either on a computer or in a pilot plant.
9. Repeat from step 1 if necessary.
10. Choose hardware and software and implement the controller.
11. Tune the controller on-line if necessary.

It must be kept in mind that a control engineer's role is not merely one of designing control systems for fixed plants, of simply "wrapping a little feedback" around an already fixed physical system. It also involves assisting in the choice and configuration of hardware by taking a system-wide view of performance. For this reason it is important that a theory of feedback not only lead to good designs when these are possible, but also indicate directly and unambiguously when the performance objectives cannot be met.

It is also important to realize at the outset that practical problems have uncertain, non-minimum-phase plants (non-minimum-phase means the existence of right half-plane zeros, so the inverse is unstable); that there are inevitably unmodeled dynamics that produce substantial uncertainty, usually at high frequency; and that sensor noise and input signal level constraints limit the achievable benefits of feedback. A theory that excludes some of these practical issues can still be useful in limited application domains. For example, many process control problems are so dominated by plant uncertainty and right half-plane zeros that sensor noise and input signal level constraints can be neglected. Some spacecraft problems, on the other hand, are so dominated by tradeoffs between sensor noise, disturbance rejection, and input signal level (e.g., fuel consumption) that plant uncertainty and non-minimum-phase effects are negligible. Nevertheless, any general theory should be able to treat all these issues explicitly and give quantitative and qualitative results about their impact on system performance.

Now we continue with a discussion of the issues in general.

Control objectives: Generally speaking, the objective in a control system is to make some output, say y, behave in a desired way by manipulating some input, say u. The simplest objective might be to keep y small (or close to some equilibrium point), *a regulator problem*, or to keep $y - r$ small for r, a reference or command signal, in some set, *a servomechanism or servo problem*. Examples:

- On a commercial airplane, the vertical acceleration should be less than a certain value for passenger comfort.
- In an audio amplifier, the power of noise signals at the output must be sufficiently small for high fidelity.
- In paper making, the moisture content must be kept between prescribed values.

There might be the side constraint of keeping u itself small as well, because it might be constrained (e.g., the flow rate from a valve has a maximum value, determined when the valve is fully open) or it might be too expensive to use a large input. But what is small for a signal? It is natural to introduce norms for signals; then "y small" means "$\|y\|$ small". Which norm is appropriate depends on the particular application.

In summary, performance objectives of a control system naturally lead to the introduction of norms; then the specs are given as norm bounds on certain key signals of interest.

Models: Before discussing the issue of modeling a physical system it is important to distinguish among four different objects:

1. Real physical system: the one "out there".
2. Ideal physical model: obtained by schematically decomposing the real physical system into ideal building blocks; composed of resistors, masses, beams, kilns, isotropic media, Newtonian fluids, electrons, and so on.

3. Ideal mathematical model: obtained by applying natural laws to the ideal physical model; composed of nonlinear partial differential equations, and so on.
4. Reduced mathematical model: obtained from the ideal mathematical model by linearization, lumping, and so on; usually a rational transfer function.

Sometimes language makes a fuzzy distinction between the real physical system and the ideal physical model. For example, the word *resistor* applies to both the actual piece of ceramic and metal and the ideal object satisfying Ohm's law. Of course, the adjectives *real* and *ideal* could be used to disambiguate.

No mathematical system can precisely model a real physical system; there is always uncertainty. Uncertainty means that we cannot predict exactly what the output of a real physical system will be even if we know the input, so we are uncertain about the system. Uncertainty arises from two sources: unknown or unpredictable inputs (disturbance, noise, etc.) and unpredictable dynamics.

What should a model provide? It should predict the input-output response in such a way that we can use it to design a control system, and then be confident that the resulting design will work on the real physical system. Of course, this is not possible. A "leap of faith" will always be required on the part of the engineer. This cannot be eliminated, but it can be made more manageable with the use of effective modeling, analysis, and design techniques.

Mathematical models: The models in this chapter are finite-dimensional, linear, and time-invariant. The main reason for this is that they are the simplest models for treating the fundamental issues in control system design. The resulting design techniques work remarkably well for a large class of engineering problems, partly because most systems are built to be as close to linear time-invariant as possible so that they are more easily controlled. Also, a good controller will keep the system in its linear regime. The uncertainty description is as simple as possible as well.

The basic form of the plant model is

$$y = (G + \Delta)u + n.$$

Here y is the output, u the input, and G the nominal plant transfer function. The model uncertainty comes in two forms:

n: unknown noise or disturbance;

Δ: unknown plant perturbation.

Both n and Δ will be assumed to belong to sets, that is, some *a priori* information is assumed about n and Δ. Then every input u is capable of producing a set of outputs, namely, the set of all outputs $(G + \Delta)u + n$ as n and Δ range over their sets. Models capable of producing sets of outputs for a single input are said to be nondeterministic. There are two main ways of obtaining models, as described next.

Models from science: The usual way of getting a model is by applying the laws of physics, chemistry, and so on. Consider an electromechanical system. One can write down differential equations based on physical principles (e.g., Newton's or Kirchhoff's laws) and making idealizing assumptions (e.g., the mechanical parts are rigid or the resistors have no capacitive or inductive effect). The coefficients in the differential equations will depend on physical constants, such as masses and physical dimensions. These can be measured. This method of applying physical laws and taking measurements is most successful in electromechanical systems, such as aerospace vehicles and robots. Some systems are difficult to model in this way, either because they are too complex or because their governing laws are unknown.

Models from experimental data: The second way of getting a model is by doing experiments on the physical system. Let's start with a simple thought experiment, one that captures many essential aspects of the relationships between physical systems and their models and the issues in obtaining models from experimental data. Consider a real physical system, *the plant to be controlled*, with one input, u, and one output, y. To design a control system for this plant, we must understand how u affects y.

The experiment runs like this. Suppose that the real physical system is in a rest state before an input u is applied (i.e., $u = y = 0$). Now apply some input signal u, resulting in some output signal y. Observe the pair (u, y). Repeat this experiment several times. Pretend that these data pairs are all we know about the real physical system. (This is the black box scenario. Usually, we know something about the internal workings of the system.)

After doing this experiment we will notice several things. First, the same input signal at different times produces different output signals. Second, if we hold $u = 0$, y will fluctuate in an unpredictable manner. Thus the real physical system produces just one output for any given input, so it itself is deterministic. However, we observers are uncertain because we cannot predict what that output will be.

Ideally, the model should cover the data in the sense that it should be capable of producing every experimentally observed input-output pair. (Of course, it would be better to cover not just the data observed in a finite number of experiments, but anything that can be produced by the real physical system. Obviously, this is impossible.) If nondeterminism that reasonably covers the range of expected data is not built into the model, we will not trust that designs based on such models will work on the real system.

In summary, for a useful theory of control design, plant models must be nondeterministic, having uncertainty built in explicitly.

Synthesis problem: A synthesis problem is a theoretical problem, precise and unambiguous. Its purpose is primarily pedagogical: It gives us something clear to focus on for the purpose of study. The hope is that the principles learned from studying a formal synthesis problem will be useful when it comes to designing a real control system.The most general

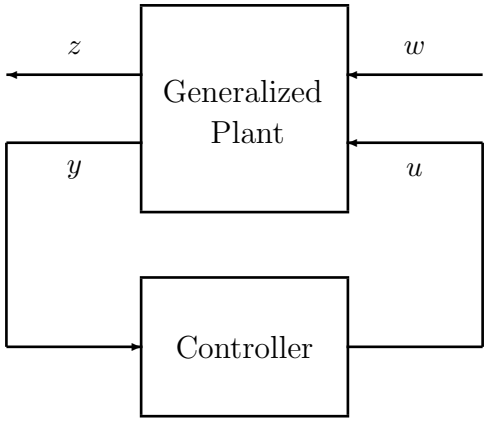

Figure 1.1: Most general control system.

block diagram of a control system is shown in Figure 1.1. The generalized plant consists of everything that is fixed at the start of the control design exercise: the plant, actuators that generate inputs to the plant, sensors measuring certain signals, analog-to-digital and digital-to-analog converters, and so on. The controller consists of the designable part: it may be an electric circuit, a programmable logic controller, a general-purpose computer, or some other such device.

The signals w, z, y, and u are, in general, vector-valued functions of time. The components of w are all the exogenous inputs: references, disturbances, sensor noises, and so on. The components of z are all the signals we wish to control: tracking errors between reference signals and plant outputs, actuator signals whose values must be kept between certain limits, and so on. The vector y contains the outputs of all sensors. Finally, u contains all controlled inputs to the generalized plant. (Even open-loop control fits in; the generalized plant would be so defined that y is always constant.)

Very rarely is the exogenous input w a fixed, known signal. One of these rare instances is where a robot manipulator is required to trace out a definite path, as in welding. Usually, w is not fixed but belongs to a set that can be characterized to some degree. Some examples:

- In a thermostat-controlled temperature regulator for a house, the reference signal is always piecewise constant: at certain times during the day the thermostat is set to a new value. The temperature of the outside air is not piecewise constant but varies slowly within bounds.
- In a vehicle such as an airplane or ship the pilot's commands on the steering wheel, throttle,pedals, and so on come from a predictable set, and the gusts and wave motions have amplitudes and frequencies that can be bounded with some degree of confidence.

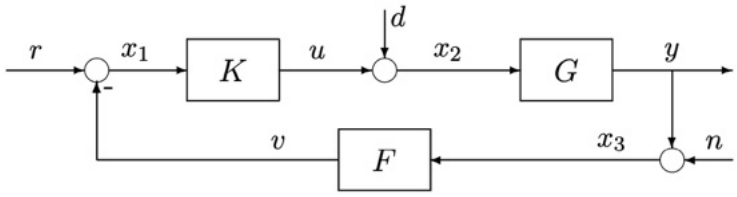

Figure 1.2: Basic feedback loop

- The load power drawn on an electric power system has predictable characteristics.

Sometimes the designer does not attempt to model the exogenous inputs. Instead, she or he designs for a suitable response to a test input, such as a step, a sinusoid, or white noise. The designer may know from past experience how this correlates with actual performance in the field. Desired properties of z generally relate to how large it is according to various measures, as discussed above.

1.2 Stability

1.2.1 Basic Feedback Loop

The most elementary feedback control system has three components: a plant (the object to be controlled, no matter what it is, is always called the plant), a sensor to measure the output of the plant, and a controller to generate the plant's input. Usually, actuators are lumped in with the plant. We begin with the block diagram in Figure 1.2. The signals in this figure have the following interpretations:

r: reference or command input
v: sensor output
u: actuating signal, plant input
d: external disturbance
y: plant output and measured signal
n: sensor noise

The three signals coming from outside, r, d and n, are called exogenous inputs.

In what follows we shall consider a variety of performance objectives, but they can be summarized by saying that y should approximate some prespecified function of r, and it should do so in the presence of the disturbance d, sensor noise n, with uncertainty in the plant. We may also want to limit the size of u. Frequently, it makes more sense to describe the performance objective in terms of the measurement v rather than y, since often the only knowledge of y is obtained from v.

This section ends with the notion of *properness* and *well-posedness*.

Definition 1.1. (Properness) *A transfer function $G(s)$ said to be proper if $G(j\infty)$ is finite (degree of denominator $\geq$ degree of numerator), strictly proper if $G(j\infty) = 0$ (degree of denominator $>$ degree of numerator), and biproper if $G(s)$ and $G^{-1}(s)$ are both proper (degree of denominator = degree of numerator).*

Definition 1.2. (Well-posedness) *It means that in Figure 1.2 all closed-loop transfer functions exist, that is, all transfer functions from the three exogenous inputs to all internal signals, namely, u, y, v, and the outputs of the summing junctions.*

The analysis to follow is done in the frequency domain. For well-posedness it suffices to look at the nine transfer functions from r, d, n to x_1, x_2, x_3. (The other transfer functions are obtainable from these.) Write the equations at the summing junctions:

$$\begin{aligned} x_1(s) &= r(s) - F(s)x_3(s) \\ x_2(s) &= d(s) + K(s)x_1(s) \\ x_3(s) &= n(s) + G(s)x_2(s) \end{aligned}$$

In matrix form these are

$$\begin{bmatrix} 1 & 0 & F \\ -K & 1 & 0 \\ 0 & -G & 1 \end{bmatrix} \begin{bmatrix} x_1 \\ x_2 \\ x_3 \end{bmatrix} = \begin{bmatrix} r \\ d \\ n \end{bmatrix}$$

Thus, the system is well-posed if and only if the above 3×3 matrix is nonsingular, that is, the determinant $1 + GKF$ is not identically equal to zero. [For instance, the system with $G(s) = 1, K(s) = 1, F(s) = -1$ is not well-posed.] Then the nine transfer functions are obtained from the equation

$$\begin{bmatrix} x_1 \\ x_2 \\ x_3 \end{bmatrix} = \begin{bmatrix} 1 & 0 & F \\ -K & 1 & 0 \\ 0 & -G & 1 \end{bmatrix}^{-1} \begin{bmatrix} r \\ d \\ n \end{bmatrix}$$

that is

$$\begin{bmatrix} x_1 \\ x_2 \\ x_3 \end{bmatrix} = \frac{1}{1+GKF} \begin{bmatrix} 1 & -GF & -F \\ K & 1 & -KF \\ GK & G & 1 \end{bmatrix} \begin{bmatrix} r \\ d \\ n \end{bmatrix} \tag{1.1}$$

A stronger notion of well-posedness that makes sense when G, K, and F are proper is that the nine transfer functions above are proper. A necessary and sufficient condition for this is that $1 + GKF$ not be strictly proper [i.e., $GKF(\infty) \neq -1$].

One might argue that the transfer functions of all physical systems are strictly proper: If a sinusoid of ever-increasing frequency is applied to a (linear, time-invariant) system, the amplitude of the output will go to zero. This is somewhat misleading because a real system will cease to behave linearly as the frequency of the input increases. Furthermore, our transfer functions will be used to parametrize an uncertainty set, and as we shall see, it may be convenient to allow some of them to be only proper.

Notice that the feedback system is automatically well-posed, in the stronger sense, if G, K, and F are proper and one is strictly proper. In the sequel, we shall make the following *standing assumption*, under which all closed-loop transfer functions are proper: G is strictly proper, K and F are proper.

1.2.2 Internal Stability

Consider a system with input u, output y, and transfer function G, assumed stable and proper. We can write $G = G_0 + G_1$ where G_0 is constant and G_1 is strictly proper.

$$\text{Example: } G(s) = \frac{s}{s+1} = 1 - \frac{1}{s+1}$$

In the time domain the output equation is:

$$y(t) = G_0 u(t) + \int_{-\infty}^{\infty} g_1(t-\tau)u(\tau)d\tau$$

if $|u(t)| \leq c$ for all t, then

$$|y(t)| \leq |G_0|c + \int_{-\infty}^{\infty} c|g_1(\tau)|d\tau$$

The right-hand side is finite. Thus the output is bounded whenever the input is bounded.

If the nine transfer functions in (1.1) are stable, then the feedback system is said to be internally stable. As a consequence, if the exogenous inputs are bounded in magnitude, so too are all output signals. So internal stability guarantees bounded internal signals for all bounded exogenous signals.The idea behind this definition of internal stability is that it is not enough to look only at input-output transfer functions, such as from r to y, for example. This transfer function could be stable, so that y is bounded when r is, and yet an internal signal could be unbounded, probably causing internal damage to the physical system.

Example 1.1. Take

$$K(s) = \frac{s-1}{s+1}, \qquad G(s) = \frac{1}{s^2-1}, \qquad F(s) = 1.$$

Check that the transfer function from r to y is stable, but that from d to y is not. The feedback system is therefore not internally stable. As we will see later, this offense is caused by the cancellation of the controller zero and the plant pole at the point $s = 1$.

We shall develop a test for internal stability which is easier than examining nine transfer functions. For the remainder of this chapter, for simplicity we specialize to the

unity-feedback case, $F = 1$. Write G and K as ratios of coprime polynomials (i.e., polynomials with no common factors):

$$G = \frac{N_G}{M_G}, \qquad K = \frac{N_K}{M_K}$$

The *characteristic polynomial* of the feedback system is the one formed by taking the product of the two numerators plus the product of the two denominators:

$$N_G N_K + M_G M_K$$

The closed-loop poles are the zeros of the characteristic polynomial.

Theorem 1.1. *The feedback system is internally stable if and only if there are no closed-loop poles in Re $s \geq 0$.*

Proof. From (1.1) we have

$$\begin{bmatrix} x_1 \\ x_2 \\ x_3 \end{bmatrix} = \frac{1}{1+GK} \begin{bmatrix} 1 & -G & -1 \\ K & 1 & -K \\ GK & G & 1 \end{bmatrix} \begin{bmatrix} r \\ d \\ n \end{bmatrix}$$

Substitute in the ratios and clear fractions to get

$$\begin{bmatrix} x_1 \\ x_2 \\ x_3 \end{bmatrix} = \frac{1}{N_G N_K + M_G M_K} \begin{bmatrix} M_G M_K & -N_G M_K & -M_G M_K \\ M_G N_K & M_G M_K & -M_G N_K \\ N_G N_K & N_G M_K & M_G M_K \end{bmatrix} \begin{bmatrix} r \\ d \\ n \end{bmatrix} \tag{1.2}$$

Note that the characteristic polynomial equals $N_G N_K + M_G M_K$. Sufficiency is now evident; the feedback system is internally stable if the characteristic polynomial has no zeros in Re $s \geq 0$.

Necessity involves a subtle point. Suppose that the feedback system is internally stable. Then all nine transfer functions in (1.2) are stable, that is, they have no poles in Re $s \geq 0$. But we cannot immediately conclude that the polynomial $N_G N_K + M_G M_K$ has no zeros in Re $s \geq 0$ because this polynomial may conceivably have a right half-plane zero which is also a zero of all nine numerators in (1.2), and hence is canceled to form nine stable transfer functions. However, the characteristic polynomial has no zero which is also a zero of all nine numerators, $N_G N_K, M_G M_K$, and so on. Proof of this statement is left as an exercise. (It follows from the fact that we took coprime factors to start with, that is, N_G and M_G are coprime, as are the other numerator-denominator pairs.) □

By Theorem 1.1 internal stability can be determined simply by checking the zeros of a polynomial.There is another test that provides additional insight.

Theorem 1.2. *The feedback system is internally stable if and only if the following two conditions hold:*

(a) *The transfer function* $1 + GK$ *has no zeros in Re* $s \geq 0$.

(b) *There is no pole-zero cancellation in Re* $s \geq 0$ *when the product* GK *is formed.*

Proof. Recall that the feedback system is internally stable if and only if all nine transfer functions

$$\frac{1}{1+GK}\begin{bmatrix} 1 & -G & -1 \\ K & 1 & -K \\ GK & G & 1 \end{bmatrix}$$

are stable.

($\Rightarrow$) Assume that the feedback system is internally stable. Then in particular $(1 + GK)^{-1}$ is stable (i.e., it has no poles in Re $s \geq 0$). Hence $(1 + GK)$ has no zeros there. This proves (a).

To prove (b), write G and K as ratios of coprime polynomials:

$$G = \frac{N_G}{M_G}, \qquad K = \frac{N_K}{M_K}$$

By Theorem 1.1 the characteristic polynomial $N_G N_K + M_G M_K$ has no zeros in Re $s \geq 0$. Thus the pair (N_G, M_K) have no common zero in Re $s \geq 0$, and similarly for the other numerator-denominator pairs.

($\Leftarrow$) Assume (a) and (b). Factor G, K as above, and let s_0 be a zero of the characteristic polynomial, that is,

$$N_G N_K + M_G M_K = 0.$$

We must show that Re $s_0 < 0$; this will prove internal stability by Theorem 1.1. Suppose to the contrary that Re $s_0 \geq 0$. If $(M_G M_K)(s_0) = 0$, then $(N_G N_K)(s_0) = 0$. But this violates (b). Thus $(M_G M_K)(s_0) \neq 0$, so we can divide by it above to get

$$1 + \frac{N_G N_K}{M_G M_K}(s_0) = 0,$$

that is, $1 + (GK)(s_0) = 0$, which violates (a). □

Finally, let us recall for later use the Nyquist stability criterion. It can be derived from Theorem 1.2 and the principle of the argument. Begin with the curve $\mathcal{D}$ in the complex plane: It starts at the origin, goes up the imaginary axis, turns into the right half-plane following a semicircle of infinite radius, and comes up the negative imaginary axis to the origin again.

As a point s makes one circuit around this curve, the point $G(s)K(s)$ traces out a curve called the Nyquist plot of GK. If GK has a pole on the imaginary axis, then $\mathcal{D}$ must have a small indentation to avoid it.

Nyquist criterion: Construct the Nyquist plot of GK, indenting to the left around poles on the imaginary axis. Let n denote the total number of poles of G and K in Re $s \geq 0$. Then the feedback system is internally stable if and only if the Nyquist plot does not pass through the point -1 and encircles it exactly n times counterclockwise.

1.3 Performance

One way to describe the performance of a control system is in terms of the size of certain signals of interest. For example, the performance of a tracking system could be measured by the size of the error signal. This section looks at several ways of defining a signal's size (i.e., at several norms for signals). Which norm is appropriate depends on the situation at hand. Also introduced are norms for a system's transfer function. Then two very useful tables are developed summarizing input-output norm relationships. The asymptotic tracking is recalled and the nominal closed-loop performance is defined in terms of a norm of the weighted sensitivity function.

1.3.1 Norms for Signals

We consider signals mapping $(-\infty, \infty)$ to $\mathbb{R}$. They are assumed to be piecewise continuous. Of course, a signal may be zero for $t < 0$ (i.e., it may start at time $t = 0$).

We are going to introduce several different norms for such signals. First, recall that a norm must have the following four properties:

1. $\|u\| \geq 0$ (positivity)
2. $\|au\| = |a| \, \|u\|, \forall a \in \mathbb{R}$ (homogeneity)
3. $\|u\| = 0 \Longleftrightarrow u(t) = 0 \quad \forall t$
4. $\|u + v\| \leq \|u\| + \|v\|$ (triangle inequality)

1-Norm: The 1-norm of a signal $u(t)$ is the integral of its absolute value:

$$\|u\|_1 = \int_{-\infty}^{\infty} |u(t)| dt$$

2-Norm: The 2-norm of $u(t)$ is

$$\|u\|_2 = \left(\int_{-\infty}^{\infty} u^2(t) dt \right)^{1/2}$$

For example, suppose that u is the current through a 1 Ω resistor. Then the instantaneous power equals $u^2(t)$ and the total energy equals the integral of this, namely, $\|u\|_2^2$. We shall generalize this interpretation: The *instantaneous power* of a signal $u(t)$ is defined to be $u^2(t)$ and its energy is defined to be the square of its 2-norm.

∞-Norm: The ∞-norm of a signal is the least upper bound of its absolute value:

$$\|u\|_\infty = \sup_t |u(t)|$$

For example, the ∞-norm of $(1 - e^{-t})1(t)$ equals 1. Here, $1(t)$ denotes the unit step function.

1.3.2 Norms for Systems

We consider systems that are linear, time-invariant, causal, and (usually) finite-dimensional. In the time domain an input-output model for such a system has the form of a convolution equation,

$$y = g * u, \qquad \text{that is} \qquad y(t) = \int_{-\infty}^{\infty} g(t-\tau)u(\tau)d\tau.$$

Causality means that $g(t) = 0$ for $t < 0$. Let $G(s)$ denote the transfer function, the Laplace transform of $g(t)$. Then $G(s)$ is rational (by finite-dimensionality) with real coefficients. We say that $G(s)$ is stable if it is analytic in the closed right half-plane (Re $s \geq 0$). We introduce two norms for the transfer function G.

2-Norm: $$\|G\|_2 = \left(\frac{1}{2\pi}\int_{-\infty}^{\infty} |G(j\omega)|^2 d\omega\right)^{1/2}.$$

∞-Norm: $$\|G\|_\infty = \sup_\omega |G(j\omega)|.$$

Note that if $G(s)$ is stable, then by Parseval's theorem

$$\|G\|_2 = \left(\frac{1}{2\pi}\int_{-\infty}^{\infty} |G(j\omega)|^2 d\omega\right)^{1/2} = \left(\int_{-\infty}^{\infty} g^2(t)dt\right)^{1/2}$$

The ∞-norm of G equals the distance in the complex plane from the origin to the farthest point on the Nyquist plot of G. It also appears as the peak value on the Bode magnitude plot of G. An important property of the ∞-norm is that it is submultiplicative:

$$\|GH\|_\infty \leq \|G\|_\infty \|H\|_\infty$$

It is easy to tell when these two norms are finite.

Lemma 1.1. *The 2-norm of G is finite if and only if G is strictly proper and has no poles on the imaginary axis; the ∞-norm is finite if and only if is proper and has no poles on the imaginary axis.*

Proof. Assume that G is strictly proper, with no poles on the imaginary axis. Then the Bode magnitude plot rolls off at high frequency. It is not hard to see that the plot of $c/(\tau s+1)$ dominates that of G for sufficiently large positive c and sufficiently small positive τ, that is,

$$\left|\frac{c}{\tau j\omega+1}\right| \geq |G(j\omega)|, \qquad \forall \omega.$$

But $c/(\tau s+1)$ has finite 2-norm; its 2-norm equals $c/\sqrt{2\tau}$ (how to do this computation is shown below). Hence G has finite 2-norm. The rest of the proof follows similar lines. □

How to compute the 2-Norm: Suppose that G is strictly proper and has no poles on the imaginary axis (so its 2-norm is finite). We have

$$\|G\|_2^2 = \frac{1}{2\pi}\int_{-\infty}^{\infty} |G(j\omega)|^2 d\omega = \frac{1}{2\pi j}\int_{-j\infty}^{j\infty} G(-s)G(s)ds = \frac{1}{2\pi j}\oint G(-s)G(s)ds$$

The last integral is a contour integral up the imaginary axis, then around an infinite semicircle in the left half-plane; the contribution to the integral from this semicircle equals zero because G is strictly proper. By the residue theorem, $\|G\|_2^2$ equals the sum of the residues of $G(-s)G(s)$ at its poles in the left half-plane.

Example 1.2. Take $G(s) = 1/(\tau s+1), \tau > 0$. The left half-plane pole of $G(-s)G(s)$ is at $s = -1/\tau$. The residue at this pole equals

$$\lim_{s\to -1/\tau}\left(s+\frac{1}{\tau}\right)\frac{1}{-\tau s+1}\frac{1}{\tau s+1} = \frac{1}{2\tau}.$$

Hence $\|G\|_2 = 1/\sqrt{2\tau}$.

How to compute the ∞-Norm: This requires a search. Set up a fine grid of frequency points $\{\omega_1, \ldots, \omega_N\}$, then an estimate for $\|G\|_\infty$ is: $\max_{1\leq k\leq N} |G(j\omega_k)|$. Alternatively, one could find where $|G(j\omega)|$ is maximum by solving the equation

$$\frac{d|G(j\omega)|^2}{d\omega} = 0$$

This derivative can be computed in closed form because G is rational. It then remains to compute the roots of a polynomial.

Example 1.3. Consider

$$G(s) = \frac{as+1}{bs+1}$$

with $a, b > 0$. Look at the Bode magnitude plot: For $a \geq b$ it is increasing (high-pass); else, it is decreasing (low-pass). Thus

$$\|G\|_\infty = \begin{cases} a/b, & a \geq b \\ 1, & a < b. \end{cases}$$

Norm of multivariable systems:

Given $G(s)$ a multi-input multi-output system, we can define:

2-Norm:

$$\|G\|_2 = \left(\frac{1}{2\pi}\int_{-\infty}^{\infty} \text{trace}[G^*(j\omega)G(j\omega)]d\omega\right)^{1/2}$$

where $G^*(j\omega)$ is the complex conjugate transpose of $G(j\omega)$.

∞-Norm:

$$\|G\|_\infty = \sup_\omega \|G(j\omega)\| = \sup_\omega \bar{\sigma}[G(j\omega)]$$

where $\bar{\sigma}[G(j\omega)]$ is the maximum singular value of $G(j\omega)$ defined as:

$$\bar{\sigma}[G(j\omega)] = \sqrt{\lambda_{\max}[G^*(j\omega)G(j\omega)]}$$

where $\lambda_{\max}$ is the maximum eigenvalue. The two and infinity norm of strictly proper stable systems are called respectively $\mathcal{H}_2$ and $\mathcal{H}_\infty$ norm.

Computing the norms by state-space methods: Consider a state-space model for a stable strictly proper system of the form:

$$\begin{aligned}\dot{x}(t) &= Ax(t) + Bu(t)\\ y(t) &= Cx(t)\end{aligned}$$

2-Norm: The $\mathcal{H}_2$ norm can be computed using the following lemma.

Lemma 1.2. *The $\mathcal{H}_2$ norm of G is given by: $\|G\|_2 = \sqrt{trace[CLC^T]}$, where $L = L^T \succ 0$[1] is a symmetric positive definite solution to the following equation:*

$$AL + LA^T + BB^T = 0$$

Proof. The impulse response of the system is given by:

$$g(t) = Ce^{tA}B, \qquad t > 0$$

Calling on Parseval we get:

$$\begin{aligned}\|G\|_2^2 = \|g\|_2^2 &= \text{trace}\int_0^\infty g(t)g^T(t)dt\\ &= \text{trace}\int_0^\infty Ce^{tA}BB^Te^{tA^T}C^Tdt = \text{trace}[CLC^T]\end{aligned}$$

[1] We use $\succ$ instead of $>$ to emphasize the positive definiteness of a matrix.

where

$$L = \int_0^\infty e^{tA} B B^T e^{tA^T} dt$$

Now, integrate both sides of the equation:

$$\frac{d}{dt} e^{tA} B B^T e^{tA^T} = A e^{tA} B B^T e^{tA^T} + e^{tA} B B^T e^{tA^T} A^T$$

from 0 to ∞, noting that e^{tA} converges to zero because the real part of eigenvalues of A are negative (the system supposed to be stable), to get $-BB^T = AL + LA^T$. □

∞-Norm: The $\mathcal{H}_\infty$ norm of G can be computed using the bounded real lemma.

Lemma 1.3. *Consider a strictly proper stable LTI system. Then $\|G\|_\infty < \gamma$ (with $\gamma > 0$), if and only if the Hamiltonian matrix H has no eigenvalue on the imaginary axis.*

$$H = \begin{bmatrix} A & \gamma^{-2} B B^T \\ -C^T C & -A^T \end{bmatrix}$$

Proof. The proof of this theorem is a bit involved, so only sufficiency is considered. The full proof for proper systems ($D \neq 0$) can be found in [9].

We start with showing that

$$I + \begin{bmatrix} 0 & \gamma^{-1} B^T \end{bmatrix} (sI - H)^{-1} \begin{bmatrix} \gamma^{-1} B \\ 0 \end{bmatrix} = \Phi^{-1}(s) \tag{1.3}$$

where $\Phi(s) = [I - \gamma^{-2} G^T(-s) G(s)]$. Using the matrix inversion lemma (see Lemma 3.1) the inverse of the term in the left hand side is:

$$\begin{aligned}
&= I - \begin{bmatrix} 0 & \gamma^{-1} B^T \end{bmatrix} \left\{ (sI - H) + \begin{bmatrix} \gamma^{-1} B \\ 0 \end{bmatrix} \begin{bmatrix} 0 & \gamma^{-1} B^T \end{bmatrix} \right\}^{-1} \begin{bmatrix} \gamma^{-1} B \\ 0 \end{bmatrix} \\
&= I - \begin{bmatrix} 0 & \gamma^{-1} B^T \end{bmatrix} \begin{bmatrix} sI - A & 0 \\ C^T C & sI + A^T \end{bmatrix}^{-1} \begin{bmatrix} \gamma^{-1} B \\ 0 \end{bmatrix} \\
&= I - \begin{bmatrix} 0 & \gamma^{-1} B^T \end{bmatrix} \begin{bmatrix} (sI - A)^{-1} & 0 \\ -(sI + A^T)^{-1} C^T C (sI - A)^{-1} & (sI + A^T)^{-1} \end{bmatrix} \begin{bmatrix} \gamma^{-1} B \\ 0 \end{bmatrix} \\
&= I + \gamma^{-1} B^T (sI + A^T)^{-1} C^T C (sI - A)^{-1} B \gamma^{-1} \\
&= I - \gamma^{-2} G^T(-s) G(s)
\end{aligned}$$

It is clear that $\|G\|_\infty < \gamma$ if and only if $\Phi(j\omega) \succ 0$ for all $\omega \in \mathbb{R}$. Since $G(s)$ is strictly proper $\Phi(j\infty) = I \succ 0$ and since $\Phi(j\omega)$ is a continuous function of ω, $\Phi(j\omega) \succ 0$ for all $\omega \in \mathbb{R}$ if and only if $\Phi(j\omega)$ is nonsingular. That is $\Phi(s)$ has no imaginary axis zero or $\Phi^{-1}(s)$ has no imaginary axis pole. However, Equation (1.3) shows that the poles of $\Phi^{-1}(s)$ are contained in the eigenvalues of H. Therefore, if H has no eigenvalues on the imaginary axis, then $\|G\|_\infty < \gamma$. □

The lemma suggests an iterative way to compute the infinity norm: Select a positive number γ; test if $\|G\|_\infty < \gamma$ by calculating the eigenvalues of H or the existence of a positive solution to the matrix inequality; increase or decrease γ accordingly; repeat. A quiet efficient search method is the bisection algorithm.

Bisection algorithm:

1. Select an upper bound γ_u and a lower bound γ_l such that $\gamma_l \leq \|G\|_\infty \leq \gamma_u$.
2. If $(\gamma_u - \gamma_l)/\gamma_l <$ specified level, stop; $\|G\|_\infty \approx (\gamma_u + \gamma_l)/2$. Otherwise go to the next step.
3. Set $\gamma = (\gamma_u + \gamma_l)/2$;
4. Test if $\|G\|_\infty < \gamma$ by calculating the eigenvalues of H for the given γ.
5. If H has an eigenvalue on the imaginary axis, set $\gamma_l = \gamma$, otherwise set $\gamma_u = \gamma$ and go back to step 2.

Input-Output Relationships

The question of interest in this section is: If we know how big the input is, how big is the output going to be? Consider a linear system with input $u(t)$, output $y(t)$, and transfer function $G(s)$, assumed stable and strictly proper. The results are summarized in two tables below. Suppose that $u(t)$ is the unit impulse, $\delta(t)$. Then the 2-norm of y equals the 2-norm of g, which by Parseval's theorem equals the 2-norm of G; this gives entry (1,1) in Table 1.1. The second row is for the ∞-norm, and the second column is for a sinusoidal input. The ∞ in the (1,2) entry is true as long as $G(j\omega) \neq 0$.

Table 1.1: Output Norms for Two Inputs

	$u(t) = \delta(t)$	$u(t) = \sin(\omega t)$
$\|y\|_2$	$\|G\|_2$	∞
$\|y\|_\infty$	$\|g\|_\infty$	$\|G(j\omega)\|$

Proofs for Table 1.1:

Entry (1,1): If $u(t) = \delta(t)$ then $y(t) = g(t)$, so $\|y\|_2 = \|g\|_2$. But by Parseval's theorem, $\|g\|_2 = \|G\|_2$.

Entry (2,1): Again, since $y(t) = g(t)$.

Entry (1,2): With the input $u(t) = \sin(\omega t)$, the output is

$$y(t) = |G(j\omega)| \sin[\omega t + \arg G(j\omega)]. \tag{1.4}$$

The 2-norm of this signal is infinite as long as $G(j\omega) \neq 0$, that is, the system's transfer function does not have a zero at the frequency of excitation.

Entry (2,2): The amplitude of the sinusoid (1.4) equals $|G(j\omega)|$.

Now suppose that $u(t)$ is not a fixed signal but that it can be any signal of 2-norm ≤ 1. It turns out that the least upper bound on the 2-norm of the output, that is, $\sup\{\|y\|_2 : \|u\|_2 \leq 1\}$, which we can call the 2-norm/2-norm system gain, equals the ∞-norm of G; this provides entry (1,1) in Table 1.2. The other entries are the other system gains. The ∞ in the (1,2) is true as long as $G \equiv 0$, that is, as long as there is some ω for which $G(j\omega) = 0$.

Table 1.2: System Gains

	$\|u\|_2$	$\|u\|_\infty$
$\|y\|_2$	$\|G\|_\infty$	∞
$\|y\|_\infty$	$\|G\|_2$	$\|g\|_1$

Proofs for Table 1.2: In this paragraph we denote $Y(s) = \mathcal{L}[y(t)]$ and $U(s) = \mathcal{L}[u(t)]$.

Entry (1,1): First we see that $\|G\|_\infty$ is an upper bound on the 2-norm/2-norm system gain:

$$\begin{aligned} \|y\|_2^2 = \|Y\|_2^2 = \frac{1}{2\pi}\int_{-\infty}^{\infty} |G(j\omega)|^2 |U(j\omega)|^2 d\omega &\leq \|G\|_\infty^2 \frac{1}{2\pi}\int_{-\infty}^{\infty} |U(j\omega)|^2 d\omega \\ &= \|G\|_\infty^2 \|u\|_2^2 \end{aligned}$$

To show that $\|G\|_\infty$ is the least upper bound, first choose a frequency ω_0 where $|G(j\omega)|$ is maximum, that is,

$$|G(j\omega_0)| = \|G\|_\infty.$$

Now choose the input u so that

$$|U(j\omega)| = \begin{cases} c, & \text{if} \quad |\omega - \omega_0| < \epsilon \text{ or } |\omega + \omega_0| < \epsilon \\ 0, & \text{otherwise,} \end{cases}$$

where ϵ is a small positive number and c is chosen so that u has unit 2-norm (i.e., $c = \sqrt{\pi/2\epsilon}$). Then

$$\|Y\|_2^2 \approx \frac{1}{2\pi}\left[|G(-j\omega_0)|^2\pi + |G(j\omega_0)|^2\pi\right] = |G(j\omega_0)|^2 = \|G\|_\infty^2.$$

Entry (2,1): According to the Cauchy-Schwartz inequality

$$\begin{aligned} |y(t)| = \left| \int_{-\infty}^{\infty} g(t-\tau)u(\tau)d\tau \right| &\leq \left(\int_{-\infty}^{\infty} g^2(t-\tau)d\tau \right)^{1/2} \left(\int_{-\infty}^{\infty} u^2(\tau)d\tau \right)^{1/2} \\ &= \|g\|_2\|u\|_2 = \|G\|_2\|u\|_2 \end{aligned}$$

Hence

$$\|y\|_\infty \leq \|G\|_2\|u\|_2$$

To show that $\|G\|_2$ is the least upper bound, apply the input

$$u(t) = g(-t)/\|G\|_2.$$

Then $\|u\|_2 = 1$ and $|y(0)| = \|g\|_2$, so $\|y\|_\infty \geq \|g\|_2$.

Entry (1,2): Apply a sinusoidal input of unit amplitude and frequency ω such that $j\omega$ is not a zero of G. Then $\|u\|_\infty$=1, but $\|y\|_2 = \infty$.

Entry (2,2): First, $\|g\|_1$ is an upper bound on the ∞-norm/∞-norm system gain:

$$\begin{aligned} |y(t)| &= \left| \int_{-\infty}^{\infty} g(\tau)u(t-\tau)d\tau \right| \leq \int_{-\infty}^{\infty} |g(\tau)u(t-\tau)|d\tau \\ &\leq \|u\|_\infty \int_{-\infty}^{\infty} |g(\tau)|d\tau = \|g\|_1\|u\|_\infty. \end{aligned}$$

That $\|g\|_1$ is the least upper bound can be seen as follows. Fix t and set

$$u(t-\tau) := \operatorname{sgn}(g(\tau)), \qquad \forall\tau.$$

Then $\|u\|_\infty = 1$ and

$$y(t) = \int_{-\infty}^{\infty} g(\tau)u(t-\tau)d\tau = \int_{-\infty}^{\infty} |g(\tau)|d\tau = \|g\|_1.$$

So $\|y\|_\infty \geq \|g\|_1$.

A typical application of these tables is as follows. Suppose that our control analysis or design problem involves, among other things, a requirement of disturbance attenuation: The controlled system has a disturbance input, say u, whose effect on the plant output, say y, should be small. Let $g(t)$ denote the impulse response from u to y. The controlled system will be required to be stable, so the transfer function $G(s)$ will be stable. Typically, it will be strictly proper, too (or at least proper). The tables tell us how much u affects y according to various measures. For example, if u is known to be a sinusoid of fixed frequency (maybe u comes from a power source at 60 Hz), then the second column of Table 1.1 gives the relative size of y according to the two measures. More commonly, the disturbance signal will not be known *a priori*, so Table 1.2 will be more relevant.

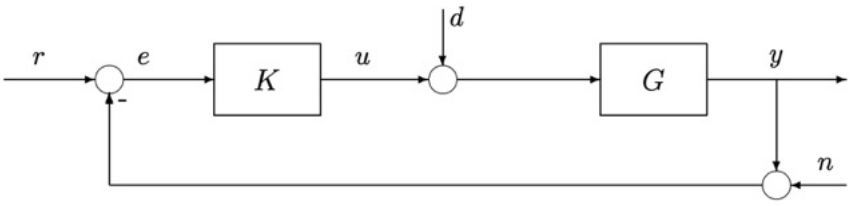

Figure 1.3: Unity-feedback loop

Example 1.4. A system with transfer function $1/(10s+1)$ has a disturbance input $d(t)$ known to have the energy bound $\|d\|_2 \leq 0.4$. Suppose that we want to find the best estimate of the ∞-norm of the output $y(t)$. Table 1.2 says that the 2-norm/∞-norm gain equals the 2-norm of the transfer function, which equals $1/\sqrt{20}$. Thus

$$\|y\|_\infty \leq \frac{0.4}{\sqrt{20}}$$

1.3.3 Asymptotic Tracking

In this section we look at a typical performance specification, perfect asymptotic tracking of a reference signal. Consider the block diagram as in Figure 1.3. Here e is the tracking error; with $n = d = 0$, e equals the reference input (ideal response), r, minus the plant output (actual response), y.

We wish to study this system's capability of tracking certain test inputs asymptotically as time tends to infinity. The two test inputs are the step

$$r(t) = \begin{cases} c, & \text{if } t \geq 0 \\ 0, & \text{if } t < 0 \end{cases}$$

and the ramp

$$r(t) = \begin{cases} \text{ct}, & \text{if } t \geq 0 \\ 0, & \text{if } t < 0 \end{cases}$$

(c is a nonzero real number). As an application of the former think of the temperature-control thermostat in a room; when you change the setting on the thermostat (step input), you would like the room temperature eventually to change to the new setting (of course, you would like the change to occur within a reasonable time). A situation with a ramp input is a radar dish designed to track orbiting satellites. A satellite moving in a circular orbit at constant angular velocity sweeps out an angle that is approximately a linear function of time (i.e., a ramp). Define the loop transfer function $L(s) := G(s)K(s)$. The transfer function from reference input r to tracking error e is

$$\mathcal{S}(s) := \frac{1}{1 + L(s)}$$

called the *sensitivity function*. The ability of the system to track steps and ramps asymptotically depends on the number of zeros of $\mathcal{S}(s)$ at $s = 0$.

Theorem 1.3. *Assume that the feedback system is internally stable and $n = d = 0$.*

(a) *if $r(t)$ is a step, then $e(t) \to 0$ as $t \to \infty$ if and only if $\mathcal{S}$ has at least one zero at the origin.*

(b) *if $r(t)$ is a ramp, then $e(t) \to 0$ as $t \to \infty$ if and only if $\mathcal{S}$ has at least two zeros at the origin.*

Proof. The proof is an application of the final-value theorem: If $Y(s) = \mathcal{L}[y(t)]$ is a rational Laplace transform that has no poles in Re $s \geq 0$ except possibly a simple pole at $s = 0$, then $\lim_{t\to\infty} y(t)$ exists and it equals $\lim_{s\to 0} sY(s)$.

(a) The Laplace transform of the foregoing step is $\mathcal{L}[r(t)] = c/s$. The transfer function from r to e equals $\mathcal{S}$, so

$$\mathcal{L}[e(t)] = \mathcal{S}(s)\frac{c}{s}.$$

Since the feedback system is internally stable, $\mathcal{S}(s)$ is a stable transfer function. It follows from the final-value theorem that $e(t)$ does indeed converge as $t \to \infty$, and its limit is the residue of the function $\mathcal{L}[e(t)]$ at the pole $s = 0$:

$$e(\infty) = \mathcal{S}(0)c.$$

The right-hand side equals zero if and only if $\mathcal{S}(0) = 0$.

(b) Similarly with $\mathcal{L}[r(t)] = c/s^2$.

□

Note that $\mathcal{S}(s)$ has a zero at $s = 0$ if and only if $L(s)$ has a pole there. Thus, from the theorem we see that if the feedback system is internally stable and either $G(s)$ or $K(s)$ has a pole at the origin (i.e., an inherent integrator), then the output $y(t)$ will asymptotically track any step input $r(t)$.

Example 1.5. To see how this works, take the simplest possible example,

$$G(s) = \frac{1}{s}, \qquad K(s) = 1.$$

Then the transfer function from r to e equals

$$\mathcal{S}(s) = \frac{1}{1 + s^{-1}} = \frac{s}{s + 1}$$

So the open-loop pole at $s = 0$ becomes a closed-loop zero of the error transfer function; then this zero cancels the pole of $\mathcal{L}[r(t)]$, resulting in no unstable poles in $\mathcal{L}[e(t)]$. Similar remarks apply for a ramp input.

Theorem 1.3 is a special case of an elementary principle: For perfect asymptotic tracking, the loop transfer function $L(s)$ must contain an internal model of the unstable poles of $\mathcal{L}[r(t)]$.

A similar analysis can be done for the situation where $r = n = 0$ and d is a sinusoid, say $d(t) = \sin(\omega t)1(t)$ (1 is the unit step). You can show this: If the feedback system is internally stable, then $y(t) \to 0$ as $t \to \infty$ if and only if either $G(s)$ has a zero at $s = j\omega$ or $K(s)$ has a pole at $s = j\omega$.

1.3.4 Nominal Performance

In this section we again look at tracking a reference signal, but whereas in the preceding section we considered perfect asymptotic tracking of a *single* signal, we will now consider a *set* of reference signals and a bound on the steady-state error. This performance objective will be quantified in terms of a weighted norm bound.

In the analysis to follow, it will always be assumed that the feedback system is internally stable, so $\mathcal{S}(s)$ is a stable, proper transfer function. Observe that since $L(s)$ is strictly proper (since $G(s)$ is), $\mathcal{S}(j\infty) = 1$.

The name *sensitivity function* comes from the following idea. Let $\mathcal{T}(s)$ denote the transfer function from r to y:

$$\mathcal{T}(s) = \frac{G(s)K(s)}{1 + G(s)K(s)}$$

One way to quantify how sensitive $\mathcal{T}$ is to variations in G is to take the limiting ratio of a relative perturbation in $\mathcal{T}$ (i.e., $\Delta\mathcal{T}/\mathcal{T}$) to a relative perturbation in G (i.e., $\Delta G/G$). Thinking of G as a variable and $\mathcal{T}$ as a function of it, we get

$$\lim_{\Delta G \to 0} \frac{\Delta\mathcal{T}/\mathcal{T}}{\Delta G/G} = \frac{d\mathcal{T}}{dG}\frac{G}{\mathcal{T}}$$

The right-hand side is easily evaluated to be $\mathcal{S}$. In this way, $\mathcal{S}$ is the sensitivity of the closed-loop transfer function $\mathcal{T}$ to an infinitesimal perturbation in G.

Now we have to decide on a performance specification, a measure of goodness of tracking. This decision depends on two things: what we know about $r(t)$ and what measure we choose to assign to the tracking error. Usually, $r(t)$ is not known in advance, few control systems are designed for one and only one input. Rather, a set of possible $r(t)$s will be known or at least postulated for the purpose of design.

Let us first consider sinusoidal inputs. Suppose that $r(t)$ can be any sinusoid of amplitude ≤ 1 and we want $e(t)$ to have amplitude $< \epsilon$. Then the performance specification can be expressed succinctly as

$$\|\mathcal{S}\|_\infty < \epsilon.$$

Here we used Table 1.1: the maximum amplitude of $e(t)$ equals the ∞-norm of the transfer function. Or if we define the (trivial, in this case) weighting function $W_1(s) = 1/\epsilon$, then the performance specification is $\|W_1\mathcal{S}\|_\infty < 1$.

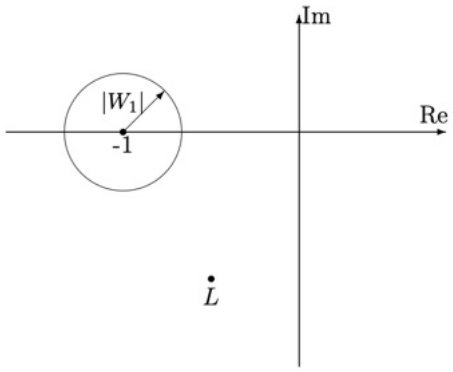

Figure 1.4: Performance specification graphically

The situation becomes more realistic and more interesting with a frequency-dependent weighting function. Assume that $W_1(s)$ is real-rational; you will see below that only the magnitude of $W_1(j\omega)$ is relevant, so any poles or zeros in Re $s > 0$ can be reflected into the left half-plane without changing the magnitude. Let us consider two scenarios giving rise to an ∞-norm bound on $W_1\mathcal{S}$. The first one requires $W_1(s)$ to be stable.

1. Suppose that the family of reference inputs is all signals of the form $W_1(s)R_{pf}(s)$, where $R_{pf}(s)$ is the Laplace transform of a pre-filtered sinusoid input of amplitude ≤ 1. Thus the set of $r(t)$s consists of sinusoids with frequency-dependent amplitudes. Then the maximum amplitude of $e(t)$ equals $\|W_1\mathcal{S}\|_\infty$.
2. In several applications, for example aircraft flight-control design, designers have acquired through experience desired shapes for the Bode magnitude plot of $\mathcal{S}$. In particular, suppose that good performance is known to be achieved if the plot of $|\mathcal{S}(j\omega)|$ lies under some curve. We could rewrite this as

$$|\mathcal{S}(j\omega)| < |W_1(j\omega)|^{-1}, \qquad \forall\omega,$$

   or in another words, $\|W_1\mathcal{S}\|_\infty < 1$.

There is a nice graphical interpretation of the norm bound $\|W_1\mathcal{S}\|_\infty < 1$. Note that

$$\|W_1\mathcal{S}\|_\infty < 1 \Leftrightarrow \left|\frac{W_1(j\omega)}{1+L(j\omega)}\right| < 1 \qquad \forall\omega, \quad \Leftrightarrow \quad |W_1(j\omega)| < |1+L(j\omega)|, \qquad \forall\omega$$

The last inequality says that at every frequency, the point $L(j\omega)$ on the Nyquist plot lies outside the disk of center -1, radius $|W_1(j\omega)|$(Figure 1.4).

Other performance problems could be posed by focusing on the response to the other two exogenous inputs, d and n. Note that the transfer functions from d, n to e are given by $-G(s)\mathcal{S}(s)$ and $-\mathcal{S}(s)$, respectively. In the same way, the transfer functions from d, n to u are $-\mathcal{T}(s)$ and $-K(s)\mathcal{S}(s)$, where

$$\mathcal{T}(s) := 1 - \mathcal{S}(s) = \frac{G(s)K(s)}{1+G(s)K(s)},$$

called the *complementary sensitivity function.*

Various performance specifications could be made using weighted versions of the transfer functions above. Note that a performance spec with weight W on $G\mathcal{S}$ is equivalent to the weight WG on $\mathcal{S}$. Similarly, a weight W on $K\mathcal{S} = \mathcal{T}/G$ is equivalent to the weight W/G on $\mathcal{T}$. Thus performance specs that involve e result in weights on $\mathcal{S}$ and performance specs on u result in weights on $\mathcal{T}$. Essentially all problems in this book boil down to weighting $\mathcal{S}$ or $\mathcal{T}$ or some combination, and the tradeoff between making $\mathcal{S}$ small and making $\mathcal{T}$ small is the main issue in design.

1.4 Robustness

No mathematical system can exactly model a physical system. For this reason, we must be aware of how modeling errors might adversely affect the performance of a control system. This section begins with a treatment of various models of plant uncertainty. Then robust stability, stability in the face of plant uncertainty, is studied using the small-gain theorem. The final topic is robust performance, guaranteed tracking in the presence of plant uncertainty.

1.4.1 Model Uncertainty

The basic technique is to model the plant as belonging to a set $\mathbb{G}$. Such a set can be either structured or unstructured. For an example of a structured set consider the plant model

$$G(s) = \frac{1}{s^2 + as + 1}$$

This is a standard second-order transfer function with natural frequency 1 rad/s and damping ratio $a/2$. It could represent, for example, a mass-spring-damper setup or an R-L-C circuit. Suppose that the constant a is known only to the extent that it lies in some interval $[a_{\min}, a_{\max}]$. Then the plant belongs to the structured set

$$\mathbb{G} = \left\{ \frac{1}{s^2 + as + 1} : a_{\min} \le a \le a_{\max} \right\}$$

Thus one type of structured set is parametrized by a finite number of scalar parameters (one parameter, a, in this example). Another type of structured uncertainty is a discrete set of plants, not necessarily parametrized explicitly.

$$\mathbb{G} = \{G_1(s), G_2(s), \ldots, G_n(s)\}$$

Unstructured sets are also important, for two reasons. First, we believe that all models used in feedback design should include some unstructured uncertainty to cover unmodeled dynamics, particularly at high frequency. Other types of uncertainty, though important,

may or may not arise naturally in a given problem. Second, for a specific type of unstructured uncertainty, disk uncertainty, we can develop simple, general analysis methods. Thus the basic starting point for an unstructured set is that of disk-like uncertainty. In what follows, multiplicative disk uncertainty is chosen for detailed study. This is only one type of unstructured perturbation. The important point is that we use disk uncertainty instead of a more complicated description. We do this because it greatly simplifies our analysis and lets us say some fairly precise things. The price we pay is conservativeness.

Multiplicative Uncertainty

Suppose that the nominal plant transfer function is $G(s)$ and consider perturbed plant transfer functions of the form

$$\tilde{G}(s) = [1 + \Delta(s)W_2(s)]G(s).$$

Here $W_2(s)$, the weight, is a fixed stable transfer function and $\Delta(s)$ is a variable stable transfer function satisfying $\|\Delta\|_\infty < 1$. Furthermore, it is assumed that no unstable poles of $G(s)$ are canceled in forming $\tilde{G}(s)$. Thus, $G(s)$ and $\tilde{G}(s)$ have the same unstable poles. Such a perturbation $\Delta(s)$ is said to be *allowable*.

The idea behind this uncertainty model is that $\Delta(s)W_2(s)$ is the normalized plant perturbation away from 1:

$$\frac{\tilde{G}(s)}{G(s)} - 1 = \Delta(s)W_2(s).$$

Hence if $\|\Delta\|_\infty \leq 1$, then

$$\left|\frac{\tilde{G}(j\omega)}{G(j\omega)} - 1\right| \leq |W_2(j\omega)|, \qquad \forall\omega,$$

so $|W_2(j\omega)|$ provides the uncertainty profile. This inequality describes a disk in the complex plane: At each frequency the point $\tilde{G}(j\omega)/G(j\omega)$ lies in the disk with center 1, radius $|W_2(j\omega)|$. Typically, $|W_2(j\omega)|$ is a (roughly) increasing function of ω: Uncertainty increases with increasing frequency. The main purpose of Δ is to account for phase uncertainty and to act as a scaling factor on the magnitude of the perturbation (i.e., $|\Delta|$ varies between 0 and 1). Thus, this uncertainty model is characterized by a nominal plant $G(s)$ together with a weighting function $W_2(s)$. How does one get the weighting function $W_2(s)$ in practice? This is illustrated by a few examples.

Example 1.6. Suppose that the plant is stable and its transfer function is arrived at by means of frequency-response experiments: Magnitude and phase are measured at a number of frequencies, $\omega_i, i = 1, ..., m$, and this experiment is repeated several, say n, times. Let the magnitude-phase measurement for frequency ω_i and experiment k be denoted (M_{ik}, ϕ_{ik}). Based on these data select nominal magnitude-phase pairs (M_i, ϕ_i)

for each frequency ω_i, and fit a nominal transfer function $G(s)$ to these data. Then fit a weighting function $W_2(s)$ so that

$$\left|\frac{M_{ik}e^{j\phi_{ik}}}{M_i e^{j\phi_i}} - 1\right| \le |W_2(j\omega_i)|, \qquad i = 1, \ldots, m; \quad k = 1, \ldots, n.$$

Example 1.7. Assume that the nominal plant transfer function is a double integrator:

$$G(s) = \frac{1}{s^2}.$$

For example, a dc motor with negligible viscous damping could have such a transfer function. You can think of other physical systems with only inertia, no damping. Suppose that a more detailed model has a time delay, yielding the transfer function

$$\tilde{G}(s) = e^{-\tau s}\frac{1}{s^2},$$

and suppose that the time delay is known only to the extent that it lies in the interval $0 \le \tau \le 0.1$. This time-delay factor $\exp(-\tau s)$ can be treated as a multiplicative perturbation of the nominal plant by embedding $\tilde{G}$ in the family

$$\{(1 + \Delta W_2)G : \|\Delta\|_\infty \le 1\}.$$

To do this, the weight W_2 should be chosen so that the normalized perturbation satisfies

$$\left|\frac{\tilde{G}(j\omega)}{G(j\omega)} - 1\right| \le |W_2(j\omega)|, \qquad \forall \omega, \tau,$$

that is,

$$|e^{-\tau j\omega} - 1| \le |W_2(j\omega)|, \qquad \forall \omega, \tau.$$

A little time with Bode magnitude plots shows that a suitable first-order weight is

$$W_2(s) = \frac{0.21s}{0.1s + 1}.$$

Figure 1.5 is the Bode magnitude plot of this W_2 and $\exp(-\tau s) - 1$ for $\tau = 0.1$, the worst value.

To get a feeling for how conservative this is, compare at a few frequencies ω the actual uncertainty set

$$\left\{\frac{\tilde{G}(j\omega)}{G(j\omega)} - 1 : 0 \le \tau \le 0.1\right\} = \{e^{-\tau j\omega} - 1 : 0 \le \tau \le 0.1\}$$

with the covering disk

$$\{s : |s - 1| \le |W_2(j\omega)|\}.$$

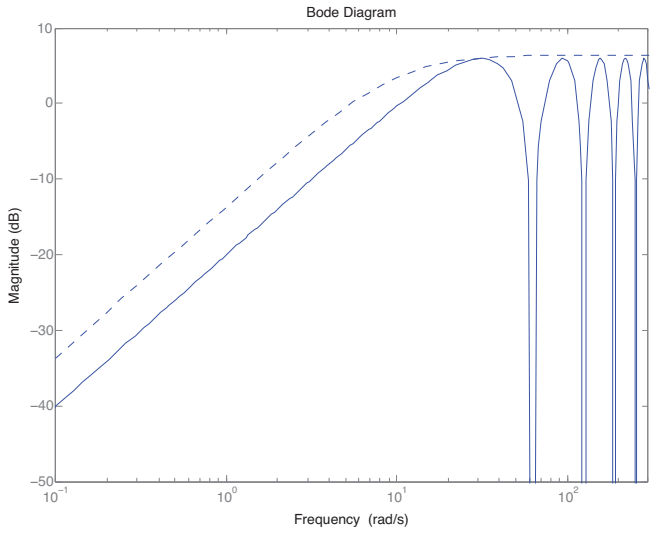

Figure 1.5: Bode plots of W_2 (dash) and $\exp(-0.1\tau s) - 1$ (solid)

Example 1.8. Suppose that the plant transfer function is

$$\tilde{G}(s) = \frac{k}{s-2},$$

where the gain k is uncertain but is known to lie in the interval $[0.1, 10]$. This plant too can be embedded in a family consisting of multiplicative perturbations of a nominal plant

$$G(s) = \frac{k_0}{s-2}.$$

The weight W_2 must satisfy

$$\left| \frac{\tilde{G}(j\omega)}{G(j\omega)} - 1 \right| \leq |W_2(j\omega)|, \qquad \forall \omega, k,$$

that is,

$$\max_{0.1 \leq k \leq 10} \left| \frac{k}{k_0} - 1 \right| \leq |W_2(j\omega)|, \qquad \forall \omega.$$

The left-hand side is minimized by $k_0 = 5.05$, for which the left-hand side equals $4.95/5.05$. In this way we get the nominal plant

$$G(s) = \frac{5.05}{s-2}$$

and constant weight $W_2(s) = 4.95/5.05$.

The multiplicative perturbation model is not suitable for every application because the disk covering the uncertainty set is sometimes too coarse an approximation. In this case a controller designed for the multiplicative uncertainty model would probably be too conservative for the original uncertainty model.

The discussion above illustrates an important point. In modeling a plant we may arrive at a certain plant set. This set may be too awkward to cope with mathematically, so we may embed it in a larger set that is easier to handle. Conceivably, the achievable performance for the larger set may not be as good as the achievable performance for the smaller; that is, there may exist, even though we cannot find it, a controller that is better for the smaller set than the controller we design for the larger set. In this sense the latter controller is conservative for the smaller set.

In this book we stick with plant uncertainty that is disk-like. It will be conservative for some problems, but the payoff is that we obtain some very nice theoretical results. The resulting theory is remarkably practical as well.

Other Perturbations

Other uncertainty models are possible besides multiplicative perturbations, as illustrated by the following example.

Example 1.9. As at the start of this section, consider the family of plant transfer functions

$$\tilde{G}(s) = \frac{1}{s^2 + as + 1} : 0.4 \le a \le 0.8.$$

Thus $a = 0.6 + 0.2\Delta, \quad -1 \le \Delta \le 1$, so the family can be expressed as

$$\frac{G(s)}{1 + \Delta W_2(s) G(s)}, \quad -1 \le \Delta \le 1,$$

where

$$G(s) := \frac{1}{s^2 + 0.6s + 1}, \qquad W_2(s) := 0.2s$$

Note that G is the nominal plant transfer function for the value $a = 0.6$, the midpoint of the interval. The block diagram corresponding to this representation of the plant is shown in Figure 1.6. Thus the original plant has been represented as a feedback uncertainty around a nominal plant.

The following list summarizes the common uncertainty models:

$$(1 + \Delta W_2)G, \quad G + \Delta W_2, \quad G/(1 + \Delta W_2 G), \quad G/(1 + \Delta W_2)$$

Appropriate assumptions would be made on Δ and W_2 in each case. Typically, we can relax the assumption that Δ be stable; but then the theorems to follow would be harder to prove.

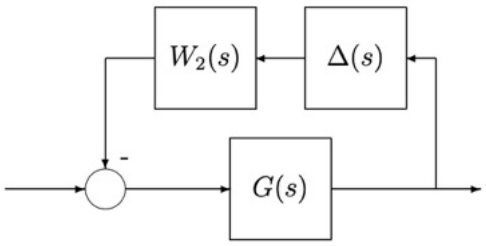

Figure 1.6: Feedback uncertainty

1.4.2 Stochastic Uncertainty

When the model of the system is identified using some noisy data, the identified model will have some stochastic uncertainty. Since these models are usually in discrete-time, in this part of the course-notes, we use $G(q^{-1})$ and $G(e^{-j\omega})$, respectively for time- and frequency-domain models. The stochastic uncertainty can be computed for nonparametric as well as parametric models. Then, they can be transformed to unstructured multiplicative or additive uncertainty. The stochastic uncertainty sets are usually smaller than deterministic ones and so have less conservatism and leads to higher performance controllers. However, the robust stability conditions presented in 1.4.3 do not guarantee the closed-loop stability in a deterministic sense.

Nonparametric Uncertainty

Consider the input signal $u(t)$ and the output signal $y(t)$ of a discrete-time system $G(q^{-1})$ are available for a finite number of $t = 1, \ldots, N$, where q^{-1} is backward shift operator. Assume that the data are noise-free and the initial and final conditions for u and y are zero, i.e $u(t) = y(t) = 0$ for $t \leq 0$ and $t > N$. Then

$$\hat{G}(e^{-j\omega}) = \frac{Y(\omega)}{U(\omega)} \tag{1.5}$$

where $U(\omega)$ and $Y(\omega)$ are defined by :

$$U(\omega) = \frac{1}{\sqrt{N}} \sum_{t=1}^{N} u(t) e^{-j\omega t} \qquad ; \qquad Y(\omega) = \frac{1}{\sqrt{N}} \sum_{t=1}^{N} y(t) e^{-j\omega t}$$

The model in (1.5) has no uncertainty (i.e., $W_2(j\omega) \equiv 0$). For noisy data (1.5) gives a spectral model which is asymptotically unbiased. The estimates $\mathrm{Re}\{\hat{G}(e^{j\omega})\}$ and $\mathrm{Im}\{\hat{G}(e^{j\omega})\}$ are asymptotically uncorrelated and normally distributed with a variance of $\Phi_v(\omega)/2|U(\omega)|^2$, where $\Phi_v(\omega)$ is the spectrum of the disturbance $v(t)$ at the output of the plant. Since $v(t)$ is not measurable, it can be estimated using the unbiased estimate

of the plant model, i.e., $\hat{v}(t) = y(t) - \hat{G}(q^{-1})u(t)$. So its spectrum is given by:

$$\Phi_{\hat{v}}(\omega) = \Phi_y(\omega) - \frac{|\Phi_{yu}(\omega)|^2}{\Phi_u(\omega)} \tag{1.6}$$

where, $\Phi_y(\omega)$ and $\Phi_u(\omega)$ are the output and input spectra respectively. The cross spectral density between y and u is denoted by $\Phi_{yu}(\omega)$. In order to see the shape of this uncertainty in the complex plan, we can define a multivariate random variable vector $\hat{G}_{vec}(\omega)$ as

$$\hat{G}_{vec}(\omega) = [\mathrm{Re}\{\hat{G}(e^{-j\omega})\}\ \mathrm{Im}\{\hat{G}(e^{-j\omega})\}]^T \tag{1.7}$$

As a result, the additive uncertainty $\Delta_{add}(\omega) = \hat{G}_{vec}(\omega) - G_{vec}(\omega)$ is a zero-mean random variable and has a joint normal distribution with a diagonal covariance matrix (because of the uncorrelation of real and imaginary parts of the estimates):

$$C_G(\omega) = \mathrm{cov}\left(\hat{G}_{vec}(\omega)\right) = \mathbb{E}\{\Delta_{add}(\omega)\Delta_{add}^T(\omega)\} = \frac{\Phi_{\hat{v}}(\omega)}{2|U(\omega)|^2}\begin{bmatrix} 1 & 0 \\ 0 & 1 \end{bmatrix} \tag{1.8}$$

It represents a disk in the complex plane. The radius of the additive uncertainty disk depends on the distribution of the radius (as a random variable), its standard deviation σ and the probability level for which the true plant model belongs to the disk. For example, if the distribution of the radius was Gaussian, the uncertainty disk would have a radius of 2σ for a probability level of 0.95. Now, we should find the distribution of the magnitude of the additive uncertainty $\Delta_{add}(\omega)$. We know from the probability theory, that $|\Delta_{add}(\omega)|$ has a Rayleigh distribution[2] with the standard deviation

$$\sigma(\omega) = \sqrt{\frac{\Phi_{\hat{v}}(\omega)}{2|U(\omega)|^2}} \tag{1.9}$$

Therefore, the true plant model $G(e^{-j\omega})$ belongs with 0.95 probability to a disk centered at $\hat{G}(e^{-j\omega})$ with a radius of $|W_3(j\omega)| = 2.45\sigma(\omega)$.

Example 1.10. The input/output data of an electromechanical laboratory setup are given in Fig. 1.7. The input signal is a Pseudo Random Binary Sequence (PRBS) and the sampling period is $T_s = 40$ ms. A spectral model and its covariance matrix can be computed using the spectral analysis method of Identification Toolbox of Matlab. For $\omega_0 = 4$ rad/s we obtain:

$$\hat{G}(e^{-j\omega_0}) = 0.9527 - j0.4884 \qquad ; \qquad C_G(\omega_0) = \begin{bmatrix} 0.0277 & 0 \\ 0 & 0.0277 \end{bmatrix}$$

[2] $R \sim \mathrm{Rayleigh}(\sigma)$ is Rayleigh distributed if $R = \sqrt{X^2 + Y^2}$, where $X \sim N(0, \sigma^2)$ and $Y \sim N(0, \sigma^2)$ are independent normal random variables. The distribution of R^2 is chi-squared $\mathcal{X}_2^2$ with two degree of freedom. For Rayleigh(σ) distribution, a realization is less than 2.45σ, 2.65σ and 3.05σ with a probability of 0.95, 0.97 and 0.99, respectively.

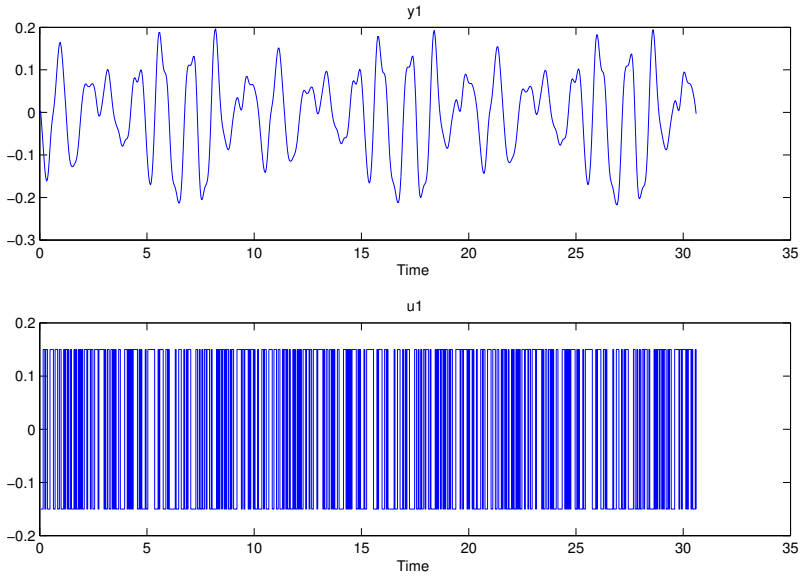

Figure 1.7: Input/output data of an electromechanical system

The covariance matrix shows that the estimates of the real and imaginary part are uncorrelated and have the same variance ($\sigma^2 = 0.0277$). In the Nyquist diagram, this uncertainty can be presented with a disk of radius $W_3(j\omega_0) = 2.45\sqrt{0.0277} = 0.4077$ centered at $0.9527 - j0.4884$ for a probability level of 0.95 . Figure 1.8 shows the Nyquist diagram of the identified nonparametric model together with the uncertainty disks at some frequencies (use `nyquist(G,'sd',2.45)`).

Parametric Uncertainty

In many practical applications a model of the system is available, but its parameters are not exactly known. In most cases, the parameters can be considered as random variables with known mean, variance and distribution. This is the case for parametric models obtained by system identification from a set of noisy data. In physical modelling of the systems, the parameters are measured by an instrument that has some accuracy. Therefore, the measured value can be considered as a random variable whose mean and variance can be estimated by repeating measurements. Even in the deterministic case when each parameter belongs to an interval, a stochastic approach can be used to represent the uncertainty.

Example 1.11. Suppose that $\theta \in [\theta_{\min}, \theta_{\max}]$. Then, assuming that θ is a uniformly distributed random variable, compute its mean and variance.

Solution: The probability density function $p(\theta)$ of the uniform distribution $\mathcal{U}(\theta_{\min}, \theta_{\max})$ has a pulse shape with amplitude $(\theta_{\max} - \theta_{\min})^{-1}$ (to have the integral equal

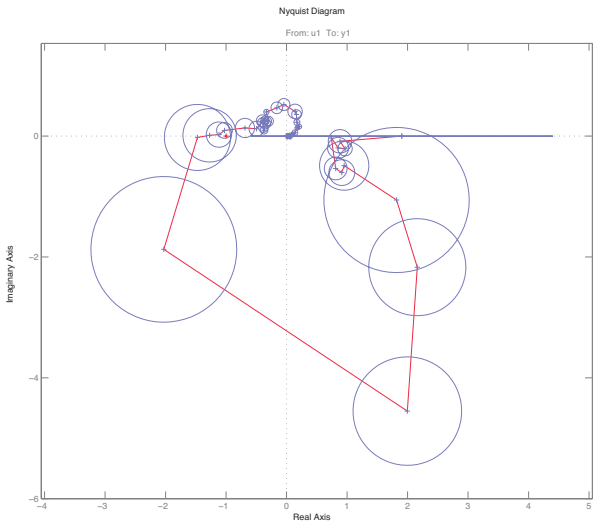

Figure 1.8: The Nyquist diagram of the spectral model together with the uncertainty disks

to one!) and is drawn in Fig. 1.9.

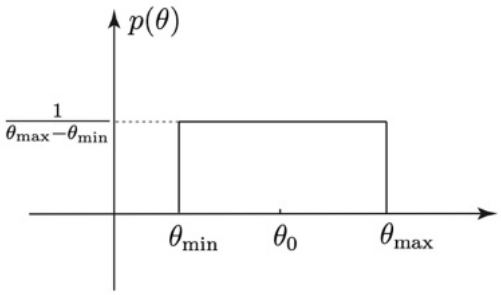

Figure 1.9: The probability density function of the uniform distribution $\mathcal{U}(\theta_{\min}, \theta_{\max})$

The mean value is given by:

$$\theta_0 = \mathbb{E}\{\theta\} = \int_{-\infty}^{\infty} \theta p(\theta) d\theta = \int_{\theta_{\min}}^{\theta_{\max}} \frac{\theta}{\theta_{\max} - \theta_{\min}} d\theta = \frac{\theta_{\min} + \theta_{\max}}{2}$$

and the variance by:

$$\begin{aligned} \mathrm{var}(\theta) = \mathbb{E}\{(\theta - \theta_0)^2\} &= \int_{-\infty}^{\infty} (\theta - \theta_0)^2 p(\theta) d\theta = \int_{\theta_{\min}}^{\theta_{\max}} \frac{(\theta - \theta_0)^2}{\theta_{\max} - \theta_{min}} d\theta \\ &= \frac{(\theta - \theta_0)^3}{3(\theta_{\max} - \theta_{\min})}\Bigg|_{\theta_{\min}}^{\theta_{\max}} = \frac{(\theta_{\max} - \theta_{\min})^2}{12} \end{aligned}$$

Example 1.12. In the previous example, the parametric interval uncertainty can also be approximated with a normally distributed random variable such that it belongs to the interval with a probability of 0.95. Compute the mean and variance of the parameter.

Solution: In this case the mean value is again θ_0. For a probability of 0.95 with a Gaussian distribution, we have $\theta_{\max} - \theta_0 = 2\sigma$ or $\theta_{\max} - \theta_{\min} = 4\sigma$, therefore:

$$\text{var}(\theta) = \sigma^2 = \frac{(\theta_{\max} - \theta_{\min})^2}{16}$$

In order to convert stochastic parametric uncertainty to additive or multiplicative uncertainty in frequency domain, we recall first the principle of the transformation of the estimators.

Principle of the transformation of the estimators: Assume that $\hat{\theta}$ is an efficient estimator of the system parameters obtained for example from a parametric identification method. Consider a nonlinear function of the parameters $f(\theta)$. This function maybe the frequency response of the system, the poles, the step response or any other nonlinear function of the parameters. The principle of the transformation of the parameters in estimation theory says that an efficient estimator of $f(\theta)$ is $f(\hat{\theta})$.

If $\hat{\theta}$ is a scalar unbiased estimator of θ with variance σ^2 and $f(\theta) = a\theta + b$ is an affine function of θ, then $f(\hat{\theta}) = a\hat{\theta} + b$. Therefore, it is clear that $f(\hat{\theta})$ is an unbiased estimator of $f(\theta)$ with

$$\text{var}\left(f(\hat{\theta})\right) = \left(\frac{\partial f}{\partial \hat{\theta}}\right)^2 \sigma^2 = a^2\sigma^2$$

In general, when θ is an n-dimensional vector and $f(\theta)$ is an affine m-dimensional vector, $f(\hat{\theta})$ is unbiased with the following covariance matrix:

$$\text{cov}\left(f(\hat{\theta})\right) = \left(\frac{\partial f}{\partial \hat{\theta}}\right)^T \text{cov}(\hat{\theta}) \left(\frac{\partial f}{\partial \hat{\theta}}\right) \tag{1.10}$$

where $\partial f/\partial\hat{\theta}$ is an $n \times m$ matrix. If $f(\hat{\theta})$ is a nonlinear function, the above relation is true only approximately because $f(\hat{\theta})$ can always be linearized around its mean value. The approximation is better when the covariance of $\hat{\theta}$ is smaller. In parametric system identification, the covariance of the estimates is proportional to $1/N$ when N is the number of data. Therefore, (1.10) is asymptotically correct (when $N \to \infty$).

Shape of uncertainty: The additive uncertainty in the frequency domain can be obtained by estimating the covariance of $\hat{G}_{vec}(\omega)$ in (1.7) from the covariance of its parameters using a linear approximation. In this case, we compute the covariance matrix of real and imaginary part of $\hat{G}$ using the principle of the transformation of the estimators:

$$C_G(\omega) = \left(\frac{\partial \hat{G}_{vec}(\omega)}{\partial \hat{\theta}}\right)^T \text{cov}(\hat{\theta}) \left(\frac{\partial \hat{G}_{vec}(\omega)}{\partial \hat{\theta}}\right) \tag{1.11}$$

where

$$\left(\frac{\partial \hat{G}_{vec}(\omega)}{\partial \hat{\theta}}\right)_{n\times 2} = \left[\frac{\partial \mathrm{Re}\{\hat{G}\}}{\partial \hat{\theta}} \qquad \frac{\partial \mathrm{Im}\{\hat{G}\}}{\partial \hat{\theta}}\right]$$

This covariance is computed in the identification Toolbox of Matlab and can be used to compute an uncertainty model set for robust controller design. Note that the covariance matrix in this case is not diagonal, contrarily to that of (1.8), because $\mathrm{cov}(\hat{\theta})$ is not in general diagonal. In the Nyquist diagram, this uncertainty is represented by an ellipse instead of a disk in the case of nonparametric uncertainty (use `nyquist(G,'sd',2.45)` to plot the Nyquist diagram with 2.45σ bounds). The distribution of the magnitude of the additive uncertainty, however, is no longer a Rayleigh distribution because of the correlation between the real and imaginary part[3]. If the correlation is small, we can approximately consider a Rayleigh distribution for computing the confidence region for a given probability (e.g. 2.45σ for 0.95 probability).

Example 1.13. If we identify a parametric model for the electromechanical system in Example 1.11, the covariance of the model parameters are also computed. Then using (1.11), the covariance of $[\mathrm{Re}\{\hat{G}(e^{-j\omega})\}\ \mathrm{Im}\{\hat{G}(e^{-j\omega})\}]^T$ can be computed at each desired frequency. For example, for $\omega_0 = 4$ rad/s we have

$$\hat{G}(e^{-j\omega_0}) = 1.6405 - j0.6662 \qquad C_G(\omega_0) = \begin{bmatrix} 0.0067 & -0.0012 \\ -0.0012 & 0.0065 \end{bmatrix}$$

Figure 1.10 shows the Nyquist diagram of the identified 4-th order parametric model of the plant together with uncertainty ellipses in some frequencies (computed for a probability of 0.95 based on Rayleigh distribution, i.e. 2.45σ). In this case, the spectral model cannot be represented directly by a disk multiplicative or additive uncertainty model. A conservative solution is to consider the smallest disk that covers an ellipse. The magnitude of the uncertainty filter W_3 will be equal to the semi-major axis of the ellipse.

A less conservative alternative is to represent the stochastic parametric uncertainty with multimodel uncertainty. This approach is useful for the methods that can solve efficiently robust control problems for systems with multimodel uncertainty. Let's consider an n_q-side polygon of minimum area that circumscribes each ellipse. Therefore, the uncertainty set, e.g. for a probability of 0.95 based on Rayleigh distribution, can be approximated by the convex combination of the vertices (that represent a multimodel uncertainty) of the polygon.

$$G(\lambda) = \sum_{k=1}^{n_q} \lambda_i \tilde{G}_k(e^{-j\omega}) : \tag{1.12}$$

where

$$\tilde{G}_k(e^{-j\omega}) = \hat{G}(e^{-j\omega}) + [1 \ \ j]2.45\sqrt{C_G(\omega)} \begin{bmatrix} \frac{\cos(2\pi k/n_q)}{\cos(\pi/n_q)} \\ \frac{\sin(2\pi k/n_q)}{\cos(\pi/n_q)} \end{bmatrix} \tag{1.13}$$

[3]In case of correlation between two Gaussian variables X and Y, $\sqrt{X^2+Y^2}$ has a Hoyt distribution.

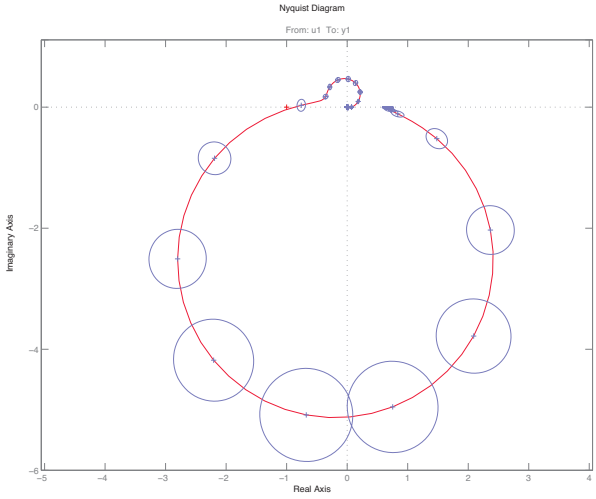

Figure 1.10: The Nyquist diagram of the parametric model together with the uncertainty ellipses

The last vector in (1.13) gives the coordinates of a vertex of a polygon circumscribing the unit circle and $2.45\sqrt{C_G}$ is a 2×2 matrix that defines the size and direction of the uncertainty (for 0.95 probability). In fact $2.45\sqrt{C_G}$ projects the unit circle to an ellipse with the size of uncertainty and consequently it projects the polygon circumscribed the unit circle to a polygon circumscribed about the ellipse. For the preceding example, we can compute four models ($n_q = 4$) that circumscribe the uncertainty ellipse at $\omega_0 = 4$ rad/s. These models are given by:

$$\begin{aligned}
\tilde{G}_1(e^{-j\omega_0}) &= 1.6405 - j0.6662 - 0.0264 + j0.2770 = 1.6141 - j0.3891 \\
\tilde{G}_2(e^{-j\omega_0}) &= 1.6405 - j0.6662 - 0.2815 + j0.0264 = 1.3590 - j0.6397 \\
\tilde{G}_3(e^{-j\omega_0}) &= 1.6405 - j0.6662 + 0.0264 - j0.2770 = 1.6670 - j0.9432 \\
\tilde{G}_4(e^{-j\omega_0}) &= 1.6405 - j0.6662 + 0.2815 - j0.0264 = 1.9220 - j0.6926
\end{aligned}$$

and are plotted in Fig. 1.11 together with the uncertainty ellipse. The quality of this approximation can be improved by increasing n_q to 8, which is shown in the same figure.

1.4.3 Robust Stability

The notion of robustness can be described as follows. Suppose that the plant transfer function G belongs to a set $\mathbb{G}$, as in the preceding section. Consider some characteristic of the feedback system, for example, that it is internally stable. A controller K is robust with respect to this characteristic if this characteristic holds for every plant in $\mathbb{G}$. The notion of robustness therefore requires a controller, a set of plants, and some characteristic of the system. For us, the two most important variations of this notion are robust stability, treated in this section, and robust performance, treated in the next.

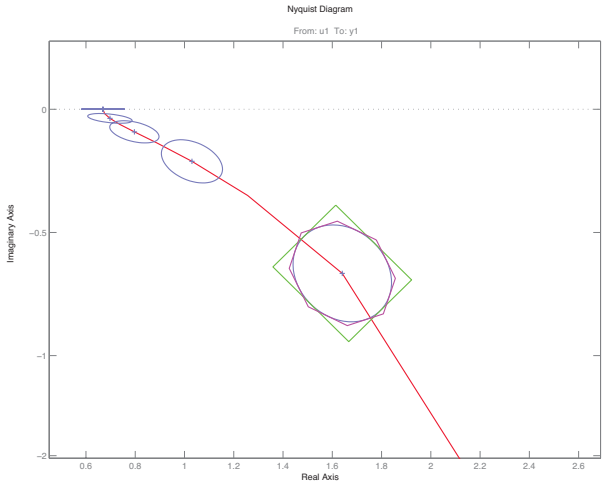

Figure 1.11: Approximation of the uncertainty ellipses with n_q-side polygons

A controller K provides *robust stability* if it provides internal stability for every plant in $\mathbb{G}$. We might like to have a test for robust stability, a test involving K and $\mathbb{G}$. Or if $\mathbb{G}$ has an associated size, the maximum size such that K stabilizes all of $\mathbb{G}$ might be a useful notion of stability margin.

The Nyquist plot gives information about stability margin (see Figure 1.12). Note that the distance from the critical point -1 to the nearest point on the Nyquist plot of L, called *modulus margin*, equals $1/\|\mathcal{S}\|_\infty$:

$$\begin{aligned} \text{modulus margin } M_m &= \inf_\omega |-1-L(j\omega)| = \inf_\omega |1+L(j\omega)| \\ &= \left[\sup_\omega \frac{1}{1+L(j\omega)}\right]^{-1} = \|\mathcal{S}\|_\infty^{-1} \end{aligned}$$

Thus if $\|\mathcal{S}\|_\infty \gg 1$, the Nyquist plot comes close to the critical point, and the feedback system is nearly unstable. However, as a measure of stability margin this distance is not entirely adequate because it contains no frequency information. More precisely, if the nominal plant G is perturbed to $\tilde{G}$, having the same number of unstable poles as has G and satisfying the inequality

$$|\tilde{G}(j\omega)K(j\omega) - G(j\omega)K(j\omega)| < \|\mathcal{S}\|_\infty^{-1}, \qquad \forall\omega,$$

then internal stability is preserved (the number of encirclements of the critical point by the Nyquist plot does not change). But this is usually very conservative; for instance, larger perturbations could be allowed at frequencies where $G(j\omega)K(j\omega)$ is far from the critical point. Better stability margins are obtained by taking explicit frequency-dependent perturbation models: for example, the multiplicative perturbation model, $\tilde{G} = (1+\Delta W_2)G$. Fix a positive number β and consider the family of plants

$$\{\tilde{G} : \Delta \text{ is stable and } \|\Delta\|_\infty \le \beta\}.$$

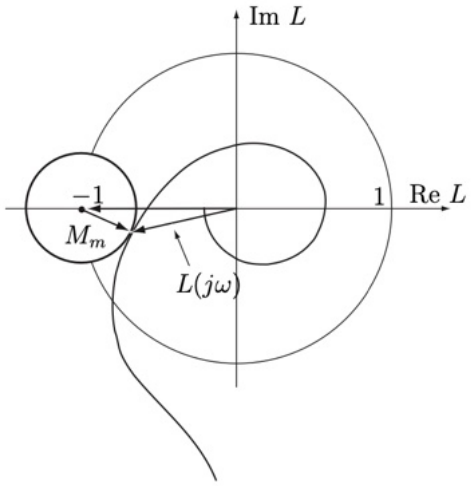

Figure 1.12: Modulus margin M_m

Now a controller K that achieves internal stability for the nominal plant G will stabilize this entire family if β is small enough. Denote by β_{sup} the least upper bound on β such that K achieves internal stability for the entire family. Then β_{sup} is a stability margin (with respect to this uncertainty model). Analogous stability margins could be defined for the other uncertainty models.

We turn now to two classical measures of stability margin, gain and phase margin. Assume that the feedback system is internally stable with plant G and controller K. Now perturb the plant to kG, with k a positive real number. The upper gain margin, denoted $k_{\max}$, is the first value of k greater than 1 when the feedback system is not internally stable; that is, $k_{\max}$ is the maximum number such that internal stability holds for $1 \leq k < k_{\max}$. If there is no such number, then set $k_{\max} := \infty$. Similarly, the lower gain margin, $k_{\min}$, is the least nonnegative number such that internal stability holds for $k_{\min} < k \leq 1$. These two numbers can be read off the Nyquist plot of L; for example, $-1/k_{\max}$ is the point where the Nyquist plot intersects the segment (-1, 0) of the real axis, the closest point to -1 if there are several points of intersection.

Now perturb the plant to $e^{-j\phi}G$, with ϕ a positive real number. The phase margin, $\phi_{\max}$, is the maximum number (usually expressed in degrees) such that internal stability holds for $0 \leq \phi < \phi_{\max}$. You can see that $\phi_{\max}$ is the angle through which the Nyquist plot must be rotated until it passes through the critical point, -1; or, in radians, $\phi_{\max}$ equals the arc length along the unit circle from the Nyquist plot to the critical point.

Thus gain and phase margins measure the distance from the critical point to the Nyquist plot in certain specific directions. Gain and phase margins have traditionally been important measures of stability robustness: if either is small, the system is close to instability. Notice, however, that the gain and phase margins can be relatively large and yet the Nyquist plot of L can pass close to the critical point; that is, simultaneous small

changes in gain and phase could cause internal instability. We return to these margins in Chapters 2 and 3.

Now we look at a typical robust stability test, one for the multiplicative perturbation model. Assume that the nominal feedback system (i.e., with $\Delta = 0$) is internally stable for controller K. Bring in again the complementary sensitivity function

$$\mathcal{T} = 1 - \mathcal{S} = \frac{L}{1+L} = \frac{GK}{1+GK}.$$

Theorem 1.4. *For multiplicative uncertainty model, K provides robust stability if and only if $\|W_2\mathcal{T}\|_\infty < 1$.*

Proof. ($\Leftarrow$) Assume that $\|W_2\mathcal{T}\|_\infty < 1$. Construct the Nyquist plot of L, indenting $\mathcal{D}$, the Nyquist contour, to the left around poles on the imaginary axis. Since the nominal feedback system is internally stable, we know this from the Nyquist criterion: The Nyquist plot of L does not pass through -1 and its number of counterclockwise encirclements equals the number of poles of G in Re $s \geq 0$ plus the number of poles of K in Re $s \geq 0$.

Fix an allowable Δ. Construct the Nyquist plot of $\tilde{G}K = (1 + \Delta W_2)L$. No additional indentations are required since ΔW_2 introduces no additional imaginary axis poles. We have to show that the Nyquist plot of $(1+\Delta W_2)L$ does not pass through -1 and its number of counterclockwise encirclements equals the number of poles of $(1 + \Delta W_2)G$ in Re $s \geq 0$ plus the number of poles of K in Re $s \geq 0$; equivalently, the Nyquist plot of $(1 + \Delta W_2)L$ does not pass through -1 and encircles it exactly as many times as does the Nyquist plot of L. We must show, in other words, that the perturbation does not change the number of encirclements. The key equation is

$$1 + (1 + \Delta W_2)L = (1 + L)(1 + \Delta W_2\mathcal{T}). \tag{1.14}$$

Since

$$\|\Delta W_2\mathcal{T}\|_\infty \leq \|W_2\mathcal{T}\|_\infty < 1,$$

the point $1 + \Delta W_2\mathcal{T}$ always lies in some closed disk with center 1, radius < 1, for all points s on $\mathcal{D}$. Thus from (1.14), as s goes once around $\mathcal{D}$, the net change in the angle of $1 + (1 + \Delta W_2)L$ equals the net change in the angle of $1 + L$. This gives the desired result.

($\Rightarrow$) Suppose that $\|W_2\mathcal{T}\|_\infty \geq 1$. We will construct an allowable Δ that destabilizes the feedback system. Since $\mathcal{T}$ is strictly proper, at some frequency ω,

$$|W_2(j\omega)\mathcal{T}(j\omega)| = 1. \tag{1.15}$$

Suppose that $\omega = 0$. Then $W_2(0)\mathcal{T}(0)$ is a real number, either +1 or -1. If $\Delta = W_2(0)\mathcal{T}(0)$, then Δ is allowable and $1+\Delta W_2(0)\mathcal{T}(0) = 0$. From (1.14) the Nyquist plot of $(1+\Delta W_2)L$ passes through the critical point, so the perturbed feedback system is not internally stable.

If $\omega > 0$, constructing an admissible Δ takes a little more work; the details are omitted. □

The theorem can be used effectively to find the stability margin $\beta_{\sup}$ defined previously. The simple scaling technique

$$\begin{aligned}\{\tilde{G} = (1 + \Delta W_2)G : \|\Delta\|_\infty \leq \beta\} &= \{\tilde{G} = (1 + \beta^{-1}\Delta\beta W_2)G : \|\beta^{-1}\Delta\|_\infty \leq 1\} \\ &= \{\tilde{G} = (1 + \Delta_1\beta W_2)G : \|\Delta_1\|_\infty \leq 1\}\end{aligned}$$

together with the theorem shows that

$$\beta_{\sup} = \sup\{\beta : \|\beta W_2\mathcal{T}\|_\infty < 1\} = 1/\|W_2\mathcal{T}\|_\infty.$$

The condition $\|W_2\mathcal{T}\|_\infty < 1$ also has a nice graphical interpretation. Note that

$$\begin{aligned}\|W_2\mathcal{T}\|_\infty < 1 &\Leftrightarrow \left|\frac{W_2(j\omega)L(j\omega)}{1 + L(j\omega)}\right| < 1, \qquad \forall\omega \\ &\Leftrightarrow |W_2(j\omega)L(j\omega)| < |1 + L(j\omega)|, \qquad \forall\omega.\end{aligned}$$

The last inequality says that at every frequency, the critical point, -1, lies outside the disk of center $L(j\omega)$, radius $|W_2(j\omega)L(j\omega)|$ (Figure 1.13).

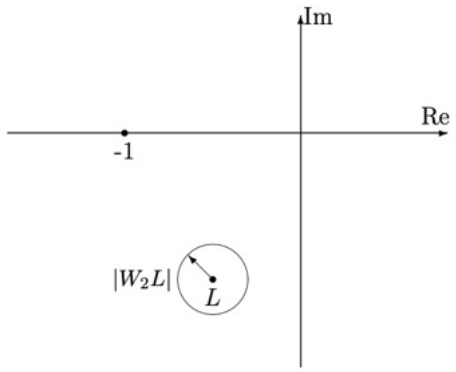

Figure 1.13: Robust stability graphically

There is a simple way to see the relevance of the condition $\|W_2\mathcal{T}\|_\infty < 1$. First, draw the block diagram of the perturbed feedback system, but ignoring inputs (Figure 1.14). The transfer function from the output of Δ around to the input of Δ equals $-W_2\mathcal{T}$, so the block diagram collapses to the configuration shown in Figure 1.15. The maximum loop gain in Figure 1.15 equals $\| - \Delta W_2\mathcal{T}\|_\infty$, which is < 1 for all allowable Δs if and only if the small-gain condition $\|W_2\mathcal{T}\|_\infty < 1$ holds.

The foregoing discussion is related to the *small-gain theorem*, a special case of which is this: If L is stable and $\|L\|_\infty < 1$, then $(1 + L)^{-1}$ is stable too. An easy proof uses the Nyquist criterion.

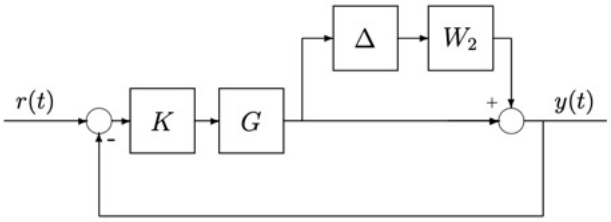

Figure 1.14: Perturbed feedback system

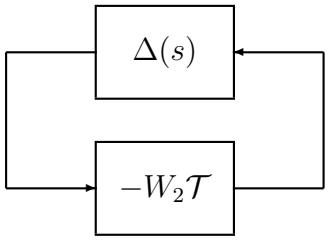

Figure 1.15: Collapsed block diagram

Summary of robust stability tests: Table 1.3 summarizes the robust stability tests for the other uncertainty models.

Note that we get the same four transfer functions, $\mathcal{T}, K\mathcal{S}, G\mathcal{S}, \mathcal{S}$, as we did in Section 1.3.4. This should not be too surprising since (up to sign) these are the only closed-loop transfer functions for a unity feedback SISO system.

1.4.4 Robust Performance

Now we look into performance of the perturbed plant. Suppose that the plant transfer function belongs to a set $\mathbb{G}$. The general notion of robust performance is that internal stability and performance, of a specified type, should hold for all plants in $\mathbb{G}$. Again we focus on multiplicative perturbations.

Recall that when the nominal feedback system is internally stable, the nominal performance condition is $\|W_1\mathcal{S}\|_\infty < 1$ and the robust stability condition is $\|W_2\mathcal{T}\|_\infty < 1$. If $\mathbb{G}$ is perturbed to $(1 + \Delta W_2)G$, $\mathcal{S}$ is perturbed to

$$\frac{1}{1 + (1 + \Delta W_2)L} = \frac{\mathcal{S}}{1 + \Delta W_2\mathcal{T}}$$

Clearly, the *robust performance* condition should therefore be

$$\|W_2\mathcal{T}\|_\infty < 1 \quad \text{and} \quad \left\| \frac{W_1\mathcal{S}}{1 + \Delta W_2\mathcal{T}} \right\|_\infty < 1, \qquad \forall \Delta.$$

Table 1.3: Robust stability conditions for different model perturbations

Perturbation	Condition
$(1+\Delta W_2)G$	$\|W_2\mathcal{T}\|_\infty < 1$
$G+\Delta W_2$	$\|W_2K\mathcal{S}\|_\infty < 1$
$G/(1+\Delta W_2G)$	$\|W_2G\mathcal{S}\|_\infty < 1$
$G/(1+\Delta W_2)$	$\|W_2\mathcal{S}\|_\infty < 1$

Here Δ must be allowable. The next theorem gives a test for robust performance in terms of the function

$$s \mapsto |W_1(s)\mathcal{S}(s)| + |W_2(s)\mathcal{T}(s)|$$

which is denoted $|W_1\mathcal{S}| + |W_2\mathcal{T}|$.

Theorem 1.5. *A necessary and sufficient condition for robust performance is*

$$\||W_1\mathcal{S}| + |W_2\mathcal{T}|\|_\infty < 1. \tag{1.16}$$

Proof. ($\Leftarrow$) Assume (1.16), or equivalently,

$$\|W_2\mathcal{T}\|_\infty < 1 \quad \text{and} \quad \left\| \frac{W_1\mathcal{S}}{1-|W_2\mathcal{T}|} \right\|_\infty < 1 \tag{1.17}$$

Fix Δ. In what follows, functions are evaluated at an arbitrary point $j\omega$, but this is suppressed to simplify notation. We have

$$1 = |1 + \Delta W_2\mathcal{T} - \Delta W_2\mathcal{T}| \le |1 + \Delta W_2\mathcal{T}| + |W_2\mathcal{T}|$$

and therefore

$$1 - |W_2\mathcal{T}| \le |1 + \Delta W_2\mathcal{T}|.$$

This implies that

$$\left\| \frac{W_1\mathcal{S}}{1-|W_2\mathcal{T}|} \right\|_\infty \ge \left\| \frac{W_1\mathcal{S}}{1+\Delta W_2\mathcal{T}} \right\|_\infty$$

This and (1.17) yield

$$\left\| \frac{W_1\mathcal{S}}{1+\Delta W_2\mathcal{T}} \right\|_\infty < 1.$$

($\Rightarrow$) Assume that

$$\|W_2\mathcal{T}\|_\infty < 1 \quad \text{and} \quad \left\| \frac{W_1\mathcal{S}}{1+\Delta W_2\mathcal{T}} \right\|_\infty < 1, \qquad \forall\Delta. \tag{1.18}$$

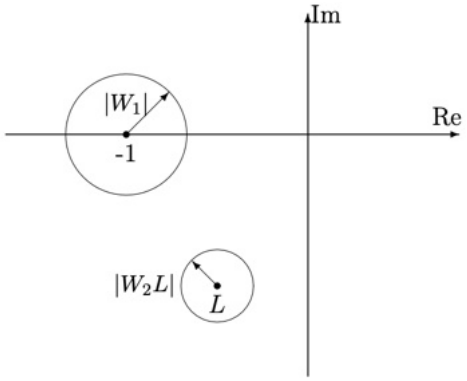

Figure 1.16: Robust performance graphically

Pick a frequency ω where

$$\frac{|W_1\mathcal{S}|}{1-|W_2\mathcal{T}|}$$

is maximum. Now pick Δ so that

$$1-|W_2\mathcal{T}| = |1+\Delta W_2\mathcal{T}|$$

The idea here is that $\Delta(j\omega)$ should rotate $W_2(j\omega)\mathcal{T}(j\omega)$ so that $\Delta(j\omega)W_2(j\omega)\mathcal{T}(j\omega)$ is negative real. The details of how to construct such an allowable Δ are omitted. Now we have

$$\begin{aligned}\left\|\frac{W_1\mathcal{S}}{1-|W_2\mathcal{T}|}\right\|_\infty &= \frac{|W_1\mathcal{S}|}{1-|W_2\mathcal{T}|} = \frac{|W_1\mathcal{S}|}{1+\Delta W_2\mathcal{T}} \\ &\leq \left\|\frac{W_1\mathcal{S}}{1+\Delta W_2\mathcal{T}}\right\|_\infty\end{aligned}$$

So from this and (1.18) there follows (1.17). □

Test (1.16) also has a nice graphical interpretation. For each frequency ω, construct two closed disks: one with center -1, radius $|W_1(j\omega)|$; the other with center $L(j\omega)$, radius $|W_2(j\omega)L(j\omega)|$. Then (1.16) holds if and only if for each ω these two disks are disjoint (Figure 1.16).

1.5 Limit of Performance

Before we see how to design control systems for the robust performance specification, it is useful to determine the basic limitations on achievable performance. In this chapter we study design constraints arising from two sources: from algebraic relationships that must hold among various transfer functions; from the fact that closed-loop transfer functions must be stable (i.e., analytic in the right half-plane). It is assumed throughout this section that the feedback system is internally stable.

1.5.1 Algebraic Constraints

There are three items in this section.

1. The identity $\mathcal{S} + \mathcal{T} = 1$ always holds. This is an immediate consequence of the definitions of $\mathcal{S}$ and $\mathcal{T}$. So in particular, $|\mathcal{S}(j\omega)|$ and $|\mathcal{T}(j\omega)|$ cannot both be less than $1/2$ at the same frequency ω.
2. A necessary condition for robust performance is that the weighting functions satisfy

$$\min\{|W_1(j\omega)|, |W_2(j\omega)|\} < 1, \forall\omega.$$

Proof. Fix ω and assume that $|W_1| \leq |W_2|$ (the argument $j\omega$ is suppressed). Then

$$\begin{aligned} |W_1| &= |W_1(\mathcal{S} + \mathcal{T})| \\ &\leq |W_1\mathcal{S}| + |W_1\mathcal{T}| \\ &\leq |W_1\mathcal{S}| + |W_2\mathcal{T}|. \end{aligned}$$

So robust performance (see Theorem 1.5), that is, $\||W_1\mathcal{S}| + |W_2\mathcal{T}|\|_\infty < 1$, implies that $|W_1| < 1$, and hence $\min\{|W_1|, |W_2|\} < 1$. The same conclusion can be drawn when $|W_2| \leq |W_1|$. □

So at every frequency either $|W_1|$ or $|W_2|$ must be less than 1. Typically, $|W_1(j\omega)|$ is monotonically decreasing, for good tracking of low-frequency signals, and $|W_2(j\omega)|$ is monotonically increasing (uncertainty increases with increasing frequency).

3. If p is a pole of L in Re $s \geq 0$ and z is a zero of L in the same half-plane, then

$$\mathcal{S}(p) = 0, \quad \mathcal{S}(z) = 1, \tag{1.19}$$
$$\mathcal{T}(p) = 1, \quad \mathcal{T}(z) = 0. \tag{1.20}$$

These interpolation constraints are immediate from the definitions of $\mathcal{S}$ and $\mathcal{T}$. For example,

$$\mathcal{S}(p) = \frac{1}{1 + L(p)} = \frac{1}{\infty} = 0.$$

1.5.2 Analytic Constraints

In this section we derive some constraints concerning achievable performance obtained from analytic function theory. The first subsection presents some mathematical preliminaries.

Preliminaries

Introduce the symbol $\mathcal{M}$ for the family of all stable, proper, real-rational functions. Notice that $\mathcal{M}$ is closed under addition and multiplication: If $F, G \in \mathcal{M}$, then $F+G$, $FG \in \mathcal{M}$. Also, $1 \in \mathcal{M}$. (Thus $\mathcal{M}$ is a commutative ring with identity.)

Theorem 1.6. ***(Maximum Modulus Theorem)*** *Suppose that Ω is a region (nonempty, open, connected set) in the complex plane and F is a function that is analytic in Ω. Suppose that F is not equal to a constant. Then $|F|$ does not attain its maximum value at an interior point of Ω.*

A simple application of this theorem, with Ω equal to the open right half-plane, shows that for F in $\mathcal{M}$

$$\|F\|_\infty = \sup_{\text{Re } s>0} |F(s)|$$

Theorem 1.7. ***(Cauchy's Theorem)*** *Suppose that Ω is a bounded open set with connected complement and $\mathcal{D}$ is a non-self-intersecting closed contour in Ω. If F is analytic in Ω, then*

$$\oint_{\mathcal{D}} F(s)ds = 0$$

Cauchy's integral formula: Suppose that F is analytic on a non-self-intersecting closed contour $\mathcal{D}$ and in its interior Ω. Let s_0 be a point in Ω. Then

$$F(s_0) = \frac{1}{2\pi j} \oint_{\mathcal{D}} \frac{F(s)}{s - s_0} ds.$$

We shall also need the Poisson integral formula, which says that the value of a bounded analytic function at a point in the right half-plane is completely determined by the coordinates of the point together with the values of the function on the imaginary axis.

Lemma 1.4. *Let F be analytic and of bounded magnitude in Re $s \geq 0$ and let $s_0 = \sigma_0 + j\omega_0$ be a point in the complex plane with $\sigma_0 > 0$. Then*

$$F(s_0) = \frac{1}{\pi} \int_{-\infty}^{\infty} F(j\omega) \frac{\sigma_0}{\sigma_0^2 + (\omega - \omega_0)^2} d\omega.$$

Proof. Construct the Nyquist contour $\mathcal{D}$ in the complex plane taking the radius, r, large enough so that the point s_0 is encircled by $\mathcal{D}$. Cauchy's integral formula gives

$$F(s_0) = \frac{1}{2\pi j} \oint_{\mathcal{D}} \frac{F(s)}{s - s_0} ds.$$

Also, since $-\bar{s}_0$ is not encircled by $\mathcal{D}$, Cauchy's theorem gives

$$0 = \frac{1}{2\pi j} \oint_{\mathcal{D}} \frac{F(s)}{s + \bar{s}_0} ds.$$

Subtract these two equations to get

$$F(s_0) = \frac{1}{2\pi j} \oint_{\mathcal{D}} F(s) \frac{\bar{s}_0 + s_0}{(s - s_0)(s + \bar{s}_0)} ds.$$

Thus $F(s_0) = I_1 + I_2$, where

$$\begin{aligned} I_1 &:= \frac{1}{\pi} \int_{-r}^{r} F(j\omega) \frac{\sigma_0}{(s_0 - j\omega)(\bar{s}_0 + j\omega)} d\omega = \frac{1}{\pi} \int_{-r}^{r} F(j\omega) \frac{\sigma_0}{\sigma_0^2 + (\omega - \omega_0)^2} d\omega \\ I_2 &:= \frac{1}{\pi j} \int_{-\pi/2}^{\pi/2} F(re^{j\theta}) \frac{\sigma_0}{(re^{j\theta} - s_0)(re^{j\theta} + \bar{s}_0)} rje^{j\theta} d\theta \end{aligned}$$

As $r \to \infty$

$$I_1 \to \frac{1}{\pi} \int_{-\infty}^{\infty} F(j\omega) \frac{\sigma_0}{\sigma_0^2 + (\omega - \omega_0)^2} d\omega$$

So it remains to show that $I_2 \to 0$ as $r \to \infty$. We have

$$I_2 \leq \frac{\sigma_0}{\pi} \|F\|_\infty \frac{1}{r} \int_{-\pi/2}^{\pi/2} \frac{1}{|e^{j\theta} - s_0 r^{-1}||e^{j\theta} + \bar{s}_0 r^{-1}|} d\theta.$$

The integral

$$\int_{-\pi/2}^{\pi/2} \frac{1}{|e^{j\theta} - s_0 r^{-1}||e^{j\theta} + \bar{s}_0 r^{-1}|} d\theta$$

converges as $r \to \infty$. Thus $I_2 \leq \text{constant}/r$, which gives the desired result. □

All-pass transfer functions: A function in $\mathcal{M}$ is *all-pass* if its magnitude equals 1 at all points on the imaginary axis. The terminology comes from the fact that a filter with an all-pass transfer function passes without attenuation input sinusoids of all frequencies. It is not difficult to show that such a function has pole-zero symmetry about the imaginary axis in the sense that a point s_0 is a zero if and only if its reflection, $-\bar{s}_0$, is a pole. Consequently, the function being stable, all its zeros lie in the right half-plane. Thus an all-pass function is, up to sign, the product of factors of the form

$$\frac{s - s_0}{s + \bar{s}_0}, \quad \text{Re } s > 0.$$

Examples of all-pass functions are

$$1, \quad \frac{s - 1}{s + 1}, \quad \frac{s^2 - s + 2}{s^2 + s + 2}$$

Minimum-phase transfer functions: A function in $\mathcal{M}$ is *minimum-phase* if it has no zeros in Re $s > 0$. This terminology can be explained as follows. Let G be a minimum-phase transfer function. There are many other transfer functions having the same magnitude as G, for example FG where F is all-pass. But all these other transfer functions have greater phase. Thus, of all the transfer functions having Gs magnitude, the one with the minimum phase is G. Examples of minimum-phase functions are

$$1, \quad \frac{1}{s+1}, \quad \frac{s}{s+1}, \quad \frac{s+2}{s^2+s+1}$$

It is a useful fact that every function in $\mathcal{M}$ can be written as the product of two such factors: for example

$$\frac{4(s-2)}{s^2+s+1} = \left(\frac{s-2}{s+2}\right)\left(\frac{4(s+2)}{s^2+s+1}\right).$$

Lemma 1.5. *For each function G in $\mathcal{M}$ there exist an all-pass function G_{ap} and a minimum-phase function G_{mp} such that $G = G_{ap}G_{mp}$. The factors are unique up to sign.*

Proof. Let G_{ap} be the product of all factors of the form

$$\frac{s-s_0}{s+\bar{s}_0}$$

where s_0 ranges over all zeros of G in Re $s > 0$, counting multiplicities, and then define $G_{mp} = G/G_{ap}$. The proof of uniqueness is left as an exercise. □

To proceed, it is useful to include the following lemma which will be used subsequently.

Lemma 1.6. *For every point $s_0 = \sigma_0 + j\omega_0$ with $\sigma_0 > 0$,*

$$\log|\mathcal{S}_{mp}(s_0)| = \frac{1}{\pi}\int_{-\infty}^{\infty} \log|\mathcal{S}(j\omega)| \frac{\sigma_0}{\sigma_0^2+(\omega-\omega_0)^2} d\omega.$$

Proof. Set $F(s) := \ln \mathcal{S}_{mp}(s)$. Then F is analytic and of bounded magnitude in Re $s \geq 0$. (This follows from the properties $\mathcal{S}_{mp}, \mathcal{S}_{mp}^{-1} \in \mathcal{M}$; the idea is that since $\mathcal{S}_{mp}$ has no poles or zeros in the right half-plane, $\ln \mathcal{S}_{mp}$ is well-behaved there.) Apply Lemma 1.4 to get

$$F(s_0) = \frac{1}{\pi}\int_{-\infty}^{\infty} F(j\omega) \frac{\sigma_0}{\sigma_0^2+(\omega-\omega_0)^2} d\omega.$$

Now take real parts of both sides:

$$\text{Re } F(s_0) = \frac{1}{\pi}\int_{-\infty}^{\infty} \text{Re } F(j\omega) \frac{\sigma_0}{\sigma_0^2+(\omega-\omega_0)^2} d\omega. \tag{1.21}$$

But $\mathcal{S}_{mp} = e^F = e^{\text{Re } F} e^{j\text{Im } F}$, so $|\mathcal{S}_{mp}| = e^{\text{Re } F}$, that is, $\ln |\mathcal{S}_{mp}| = \text{Re } F$. Thus from (1.21)

$$\ln |\mathcal{S}_{mp}(s_0)| = \frac{1}{\pi} \int_{-\infty}^{\infty} \ln |\mathcal{S}_{mp}(j\omega)| \frac{\sigma_0}{\sigma_0^2 + (\omega - \omega_0)^2} d\omega,$$

or since $|\mathcal{S}| = |\mathcal{S}_{mp}|$ on the imaginary axis,

$$\ln |\mathcal{S}_{mp}(s_0)| = \frac{1}{\pi} \int_{-\infty}^{\infty} \ln |\mathcal{S}(j\omega)| \frac{\sigma_0}{\sigma_0^2 + (\omega - \omega_0)^2} d\omega.$$

Finally, since $\log x = \log e \ln x$, the result follows upon multiplying the last equation by $\log e$. □

Bounds on W_1 and W_2

Suppose that the loop transfer function L has a zero z in Re $s \geq 0$. Then

$$\|W_1 \mathcal{S}\|_\infty \geq |W_1(z)| \tag{1.22}$$

This is a direct consequence of the maximum modulus theorem and (1.19):

$$|W_1(z)| = |W_1(z)\mathcal{S}(z)| \leq \sup_{\text{Re } s \geq 0} |W_1(s)\mathcal{S}(s)| = \|W_1 \mathcal{S}\|_\infty.$$

So a necessary condition that the performance criterion $\|W_1\mathcal{S}\|_\infty < 1$ be achievable is that the weight satisfy $|W_1(z)| < 1$. In words, the magnitude of the weight at a right half-plane zero of G or K must be less than 1. Similarly, suppose that L has a pole p in Re $s \geq 0$. Then

$$\|W_2 \mathcal{T}\|_\infty \geq |W_2(p)| \tag{1.23}$$

so a necessary condition for the robust stability criterion $\|W_2\mathcal{T}\|_\infty < 1$ is that the weight W_2 satisfy $|W_2(p)| < 1$.

For technical reasons we assume for the remainder of this section that L has no poles on the imaginary axis. Factor the sensitivity function as $\mathcal{S} = \mathcal{S}_{ap}\mathcal{S}_{mp}$. Then S_{mp} has no zeros on the imaginary axis (such zeros would be poles of L) and $\mathcal{S}_{mp}$ is not strictly proper (since $\mathcal{S}$ is not). Thus $\mathcal{S}_{mp}^{-1} \in \mathcal{M}$. As a simple example of the use of all-pass functions, suppose that G has a zero at z with $z > 0$, a pole at p with $p > 0$; also, suppose that K has neither poles nor zeros in the closed right half-plane. Then

$$\mathcal{S}_{ap} = \frac{s - p}{s + p}, \quad \mathcal{T}_{ap}(s) = \frac{s - z}{s + z}.$$

It follows from the preceding section that $\mathcal{S}(z) = 1$, and hence

$$\mathcal{S}_{mp}(z) = \mathcal{S}_{ap}^{-1}(z) = \frac{z + p}{z - p}.$$

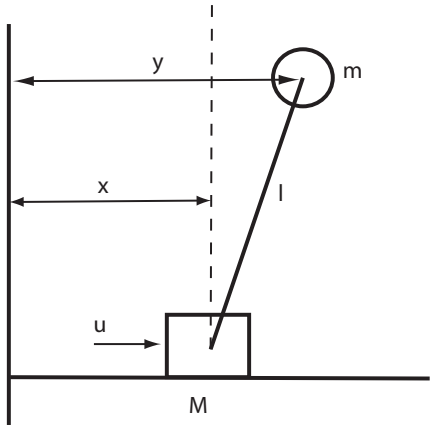

Figure 1.17: Cart-pendulum example

Similarly,

$$\mathcal{T}_{mp}(p) = \mathcal{T}_{ap}^{-1}(p) = \frac{p+z}{p-z}.$$

Then

$$\|W_1\mathcal{S}\|_\infty = \|W_1\mathcal{S}_{mp}\|_\infty \geq |W_1(z)\mathcal{S}_{mp}(z)| = \left|W_1(z)\frac{z+p}{z-p}\right|$$

and

$$\|W_2\mathcal{T}\|_\infty \geq \left|W_2(p)\frac{p+z}{p-z}\right| \tag{1.24}$$

Thus, if there are a pole and zero close to each other in the right half-plane, they can greatly amplify the effect that either would have alone.

Example 1.14. An interesting stabilization problem is afforded by the cart-pendulum example, a common toy control system. The setup is shown in Figure 1.17. The system consists of a cart of mass M that slides in one dimension x on a horizontal surface, with a ball of mass m at the end of a rigid massless pendulum of length l. The cart and ball are treated as point masses, with the pivot at the center of the cart. There is assumed to be no friction and no air resistance. Let $G_x(s)$ be the linearized transfer function u-to-x for the up position of the pendulum, that is,

$$G_x(s) = \frac{ls^2 - g}{s^2[Mls^2 - (M+m)g]}.$$

Define the ratio $r := m/M$ of pendulum mass to cart mass. The zero and pole of G_x in $\operatorname{Re} s > 0$ are

$$z = \sqrt{\frac{g}{l}}, \quad p = z\sqrt{1+r}.$$

Note that for r fixed, a larger value of l means a smaller value of p, and this in turn means that the system is easier to stabilize (the time constant is slower). The foregoing two inequalities on $\|W_1\mathcal{S}\|_\infty$ and $\|W_2\mathcal{T}\|_\infty$ apply. Since the cart-pendulum is a stabilization task, let us focus on (1.24). The robust stabilization problem becomes harder the larger the value of the right-hand side of (1.24). The scaling factor in this inequality is

$$\frac{p+z}{p-z} = \frac{\sqrt{r+1}+1}{\sqrt{1+r}-1} \tag{1.25}$$

This quantity is always greater than 1, and it approaches 1 only when r approaches ∞, that is, only when the pendulum mass is much larger than the cart mass. There is a tradeoff, however, in that a large value of r means a large value of p, the unstable pole; for a typical W_2 (high-pass) this in turn means a relatively large value of $|W_2(p)|$ in (1.24). So at least for small uncertainty, the worst-case scenario is a short pendulum with a small mass m relative to the cart mass M.

In contrast, the u-to-y linearized transfer function

$$G_y(s) = \frac{-g}{s^2[Mls^2 - (M+m)g]}$$

has no zeros, so the constraint there is simply $\|W_2\mathcal{T}\|_\infty \geq |W_2(p)|$. If robust stabilization were the only objective, we could achieve equality by careful selection of the controller. Note that for this case there is no apparent tradeoff in making m/M large. The difference between the two cases, measuring x and measuring y, again highlights the important fact that sensor location can have a significant effect on the difficulty of controlling a system or on the ultimate achievable performance.

Some simple experiments can be done to illustrate the points made in this example. Obtain several sticks of various lengths and try to balance them in the palm of your hand. You will notice that it is easier to balance longer sticks, because the dynamics are slower and p above is smaller. It is also easier to balance the sticks if you look at the top of the stick (measuring y) rather than at the bottom (measuring x). In fact, even for a stick that is easily balanced when looking at the top, it will be impossible to balance it while looking only at the bottom. There is also feedback from the forces that your hand feels, but this is similar to measuring x.

The Waterbed Effect

Consider a tracking problem where the reference signals have their energy spectra concentrated in a known frequency range, say $[\omega_1, \omega_2]$. This is the idealized situation where W_1 is a bandpass filter. Let M_1 denote the maximum magnitude of $\mathcal{S}$ on this frequency band,

$$M_1 := \max_{\omega_1 \leq \omega \leq \omega_2} |\mathcal{S}(j\omega)|,$$

and let M_2 denote the maximum magnitude over all frequencies, that is, $\|\mathcal{S}\|_\infty$. Then good tracking capability is characterized by the inequality $M_1 << 1$. On the other hand, we cannot permit M_2 to be too large: Remember that $1/M_2$ equals the distance from the critical point to the Nyquist plot of L, so large M_2 means small stability margin (a typical upper bound for M_2 is 2). Notice that M_2 must be at least 1 because this is the value of $\mathcal{S}$ at infinite frequency. So the question arises: Can we have M_1 very small and M_2 not too large? Or does it happen that very small M_1 necessarily means very large M_2? The latter situation might be compared to a waterbed: As $|\mathcal{S}|$ is pushed down on one frequency range, it pops up somewhere else. It turns out that non-minimum-phase plants exhibit the waterbed effect.

Theorem 1.8. *Suppose that G has a zero at z with Re $z > 0$. Then there exist positive constants c_1 and c_2, depending only on ω_1, ω_2, and z, such that*

$$c_1 \log M_1 + c_2 \log M_2 \geq \log |\mathcal{S}_{ap}^{-1}(z)| \geq 0.$$

Proof. Since z is a zero of G, it follows that $\mathcal{S}(z) = 1$, and hence $\mathcal{S}_{mp}(z) = \mathcal{S}_{ap}^{-1}(z)$. Apply Lemma 1.6 with $s_0 = z = \sigma_0 + j\omega_0$ to get

$$\log |\mathcal{S}_{ap}^{-1}(z)| = \frac{1}{\pi} \int_{-\infty}^{\infty} \log |\mathcal{S}(j\omega)| \frac{\sigma_0}{\sigma_0^2 + (\omega - \omega_0)^2} d\omega.$$

Thus $\log |\mathcal{S}_{ap}^{-1}(z)| \leq c_1 \log M_1 + c_2 \log M_2$, where c_1 is defined to be the integral of

$$\frac{1}{\pi} \frac{\sigma_0}{\sigma_0^2 + (\omega - \omega_0)^2}$$

over the set $[-\omega_2, -\omega_1] \bigcup [\omega_1, \omega_2]$ and c_2 equals the same integral but over the complementary set. It remains to observe that $|\mathcal{S}_{ap}(z)| \leq 1$ by the maximum modulus theorem, so $\log |\mathcal{S}_{ap}^{-1}(z)| \geq 0$. □

Example 1.15. As an illustration of the theorem consider the plant transfer function

$$G(s) = \frac{s - 1}{(s + 1)(s - p)},$$

where $p > 0, p \neq 1$. It has been shown that $\mathcal{S}$ must interpolate zero at the unstable poles of $G(s)$ to have internal stability, so $\mathcal{S}(p) = 0$. Thus the all-pass factor of $\mathcal{S}$ must contain the factor $(s - p)/(s + p)$, that is.

$$\mathcal{S}_{ap}(s) = \frac{s - p}{s + p} P(s)$$

for some all-pass function P. Since $|P(1)| \leq 1$ (maximum modulus theorem), there follows

$$|\mathcal{S}_{ap}(1)| \leq \left| \frac{1 - p}{1 + p} \right|.$$

So the theorem gives

$$c_1 \log M_1 + c_2 \log M_2 \geq \log \left| \frac{1-p}{1+p} \right|.$$

Note that the right-hand side is very large if p is close to 1. This example illustrates again a general fact: The waterbed effect is amplified if the plant has a pole and a zero close together in the right half-plane. We would expect such a plant to be very difficult to control. It is emphasized that the waterbed effect applies to non-minimum-phase plants only. In fact, the following can be proved: If G has no zeros in Re $s > 0$ nor on the imaginary axis in the frequency range $[\omega_1, \omega_2]$, then for every $\epsilon > 0$ and $\delta > 1$ there exists a controller K so that the feedback system is internally stable, $M_1 < \epsilon$, and $M_2 < \delta$. As a very easy example, take

$$G(s) = \frac{1}{s+1}$$

The controller $K(s) = k$ is internally stabilizing for all $k > 0$, and then

$$\mathcal{S}(s) = \frac{s+1}{s+1+k}.$$

So $\|\mathcal{S}\|_\infty = 1$ and for every $\epsilon > 0$ and ω_2. if k is large enough, then $|\mathcal{S}(j\omega)| < \epsilon, \quad \forall \omega \leq \omega_2$.

The Area Formula

Herein is derived a formula for the area bounded by the graph of $|\mathcal{S}(j\omega)|$ (log scale) plotted as a function of ω (linear scale). The formula is valid when the relative degree of L is large enough. Relative degree equals degree of denominator minus degree of numerator. Let $\{p_i\}$ denote the set of poles of L in Re $s > 0$.

Theorem 1.9. *Assume that the relative degree of L is at least 2. Then*

$$\int_0^\infty \log |\mathcal{S}(j\omega)| d\omega = \pi (\log e)(Re \sum_i p_i).$$

Proof. In Lemma 1.6 take $\omega_0 = 0$ to get

$$\log |\mathcal{S}_{mp}(s_0)| = \frac{1}{\pi} \int_{-\infty}^\infty \log |\mathcal{S}(j\omega)| \frac{\sigma_0}{\sigma_0^2 + \omega^2} d\omega,$$

or equivalently,

$$\int_0^\infty \log |\mathcal{S}(j\omega)| \frac{\sigma_0}{\sigma_0^2 + \omega^2} d\omega = \frac{\pi}{2} \log |\mathcal{S}_{mp}(\sigma_0)|.$$

Multiply by σ_0:

$$\int_0^\infty \log |\mathcal{S}(j\omega)| \frac{\sigma_0^2}{\sigma_0^2 + \omega^2} d\omega = \frac{\pi}{2} \sigma_0 \log |\mathcal{S}_{mp}(\sigma_0)|.$$

It can be shown that the left-hand side converges to

$$\int_0^\infty \log|\mathcal{S}(j\omega)|d\omega$$

as $\sigma_0 \to \infty$. [The idea is that for very large σ_0 the function $\sigma_0^2/(\sigma_0^2+\omega^2)$ equals nearly 1 up to large values of ω. On the other hand, $\log|\mathcal{S}(j\omega)|$ tends to zero as ω tends to ∞.] So it remains to show that

$$\lim_{\sigma\to\infty} \frac{\sigma}{2}\log|\mathcal{S}(\sigma)| = (\log e)(\text{Re } \sum_i p_i). \tag{1.26}$$

We can write $\mathcal{S} = \mathcal{S}_{ap}\mathcal{S}_{mp}$, where

$$\mathcal{S}_{ap}(s) = \prod_i \frac{s-p_i}{s+\bar{p}_i}.$$

It is claimed that $\lim_{\sigma\to\infty} \ln \mathcal{S}(\sigma) = 0$. To see this, note that since L has relative degree at least 2 we can write $L(\sigma) \approx c/\sigma^k$ as $\sigma \to \infty$ for some $k \geq 2$. Thus as $\sigma \to \infty$

$$\sigma \ln \mathcal{S}(\sigma) = -\sigma \ln[1+L(\sigma)] \approx -\sigma \ln\left(1+\frac{c}{\sigma^k}\right).$$

Now use the Maclaurin's series $\ln(1+x) = x - x^2/2 + \cdots$ to get

$$\sigma \ln \mathcal{S}(\sigma) \approx -\sigma\left(\frac{c}{\sigma^2} - \cdots\right).$$

The right-hand side converges to zero as σ tends to ∞. This proves the claim. In view of the claim, to prove (1.26) it remains to show that

$$\lim_{\sigma\to\infty} \frac{\sigma}{2}\ln|\mathcal{S}_{ap}^{-1}(\sigma)| = \text{Re } \sum_i p_i \tag{1.27}$$

Now

$$\ln(\mathcal{S}_{ap}^{-1}(\sigma)) = \ln\prod_i \frac{\sigma+\bar{p}_i}{\sigma-p_i} = \sum_i \ln\frac{\sigma+\bar{p}_i}{\sigma-p_i},$$

so to prove (1.27) it suffices to prove

$$\lim_{\sigma\to\infty} \frac{\sigma}{2}\ln\left|\frac{\sigma+\bar{p}_i}{\sigma-p_i}\right| = \text{Re } p_i. \tag{1.28}$$

Let $p_i = x + jy$ and use the Maclaurin's series again as follows:

$$\begin{aligned}
\frac{\sigma}{2}\ln\left|\frac{\sigma+\bar{p}_i}{\sigma-p_i}\right| &= \frac{\sigma}{2}\ln\left|\frac{1+\sigma^{-1}\bar{p}_i}{1-\sigma^{-1}p_i}\right| = \frac{\sigma}{4}\ln\frac{(1+x\sigma^{-1})^2+(y\sigma^{-1})^2}{(1-x\sigma^{-1})^2+(y\sigma^{-1})^2} \\
&= \frac{\sigma}{4}\left\{\ln[(1+x\sigma^{-1})^2+(y\sigma^{-1})^2] - \ln[(1-x\sigma^{-1})^2+(y\sigma^{-1})^2]\right\} \\
&= \frac{\sigma}{4}\left\{2\frac{x}{\sigma}+2\frac{x}{\sigma}+\cdots\right\} = x+\cdots = \text{Re } p_i + \cdots
\end{aligned}$$

Letting $\sigma \to \infty$ gives (1.28). □

Example 1.16. Take the plant and controller

$$G(s) = \frac{1}{(s-1)(s+2)}, \quad K(s) = 10.$$

The feedback system is internally stable and L has relative degree 2. Consider the plot of $|\mathcal{S}(j\omega)|$, log scale, versus ω, linear scale. The area below the line $|\mathcal{S}| = 1$ is negative, the area above, positive. The theorem says that the net area is positive, equaling $\pi(\log e)(\text{Re } \sum_i p_i)$. So the negative area, required for good tracking over some frequency range, must unavoidably be accompanied by some positive area.

The waterbed effect applies to non-minimum-phase systems, whereas the area formula applies in general (except for the relative degree assumption). In particular, the area formula does not itself imply a peaking phenomenon, only an area conservation. However, one can infer a type of peaking phenomenon from the area formula when another constraint is imposed, namely, controller bandwidth, or more precisely, the bandwidth of the loop transfer function GK. For example, suppose that the constraint is

$$|GK| < \frac{1}{\omega^2}, \quad \forall \omega \geq \omega_1,$$

where $\omega_1 > 1$. This is one way of saying that the loop bandwidth is constrained to be $\leq \omega_1$. Then for $\omega \geq \omega_1$

$$|\mathcal{S}| \leq \frac{1}{1-|GK|} < \frac{1}{1-\omega^{-2}} = \frac{\omega^2}{\omega^2-1}.$$

Hence

$$\int_{\omega_1}^{\infty} \log |\mathcal{S}(j\omega)| d\omega \leq \int_{\omega_1}^{\infty} \log \frac{\omega^2}{\omega^2-1} d\omega.$$

The latter integral, denote it by I, is finite. This is proved by the following computation:

$$\begin{aligned} I &= \frac{1}{\ln 10} \int_{\omega_1}^{\infty} \ln \frac{1}{1-\omega^{-2}} d\omega = -\frac{1}{\ln 10} \int_{\omega_1}^{\infty} \ln(1-\omega^{-2}) d\omega \\ &= \frac{1}{\ln 10} \int_{\omega_1}^{\infty} \left(\omega^{-2} + \frac{\omega^{-4}}{2} + \frac{\omega^{-6}}{3} + \cdots \right) d\omega \\ &= \frac{1}{\ln 10} \left(\omega_1^{-1} + \frac{\omega_1^{-3}}{2} + \frac{\omega_1^{-5}}{3} + \cdots \right) < \infty \end{aligned}$$

Hence the possible positive area over the interval $[\omega_1, \infty)$ is limited. Thus if $|\mathcal{S}|$ is made smaller and smaller over some subinterval of $[0, \omega_1]$, incurring a larger and larger debt of negative area, then $|\mathcal{S}|$ must necessarily become larger and larger somewhere else in $[0, \omega_1]$. Roughly speaking, with a loop bandwidth constraint the waterbed effect applies even to minimum-phase plants.

Chapter 2

ROBUST CONTROLLER DESIGN

2.1 Introduction

In the previous chapter, we showed that the nominal performance, robust stability and robust performance can be represented by some constraints on the 2- or infinity-norm of weighted closed-loop sensitivity functions. We also showed how the weighting filters can be computed to obtain desired performance or to convert real uncertainties to unstructured frequency-domain additive or multiplicative uncertainty. It turned out that a robust control design problem can be converted to an optimization problem under constraints. This optimization problem is, in general, nonlinear with respect to the controller parameters.

Although there are some numerical solutions to nonlinear optimization problems, their complexity usually increase polynomially or even exponentially with the number of optimization variables. Moreover, the convergence of the algorithms to a global optimal solution of the problem cannot be guaranteed. The global optimization techniques can be used with the cost of increasing the computation time, if the number of optimization variables is small. However, a control design problem is by nature an iterative procedure in which the desired performance and the practical constraints are revealed gradually in an iterative procedure by designing and implementing of the controllers. Therefore, it is reasonable that the controller design step be carried out with a convex optimization approach that can produce an optimal and efficient solution.

Depending on the controller structure (state-feedback, output feedback, fixed structure), the desired performance (loop shaping, two-norm or infinity-norm optimization) and the model representation (continuous-time, discrete-time, frequency-domain models) different sorts of control problems can be defined. In this chapter, we try to solve some of the standard problems using convex optimization techniques.

This chapter will start with a brief introduction to convex optimization problems. Then, $\mathcal{H}_2$ and $\mathcal{H}_\infty$ control problems are defined in a model-based design framework. An overview of state feedback and output feedback optimal controller design will be given. It

will be shown that how these methods can be implemented in Matlab using a simulation example. Finally, a new data-driven method for controller design is introduced. This method needs only the frequency response of the system and can be used for fixed structure controller design with loop shaping, $\mathcal{H}_2$ and $\mathcal{H}_\infty$ performance. The development of the method together with stability conditions are detailed. The effectiveness of the method is illustrated by application to two experimental setups.

2.2 Introduction to Convex Optimization

The robust control design methods presented in this course-notes are based on convex optimization methods using linear matrix inequalities (LMIs) taken mostly from [8]. The objective of this section is to provide a brief introduction to convex sets and convex optimization problems with applications to control theory.

2.2.1 Convex Sets and Convex Functions

Convex sets: A set $\mathbb{S}$ in a vector space is convex if

$$x_1, x_2 \in \mathbb{S} \Rightarrow \lambda x_1 + (1-\lambda)x_2 \in \mathbb{S} \qquad \forall \lambda \in [0\,,\,1]$$

In geometric terms, it means that the line segment between any two points of a convex set lies inside the set (see Fig. 2.1). In general, the empty set is considered to be convex.

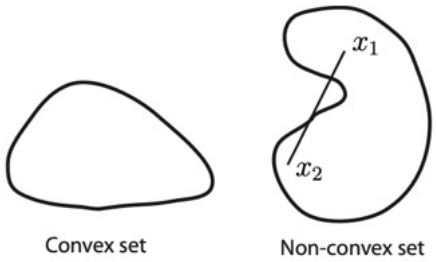

Figure 2.1: Convex and non-convex sets

The point $\lambda x_1 + (1-\lambda)x_2$ for a given $\lambda \in [0\,,\,1]$ is called a convex combination of the two points x_1 and x_2. More generally, convex combinations are defined as follows.

Convex combinations: Let $\mathbb{S}$ be a subset of a vector space and let $x_1, \ldots, x_n \in \mathbb{S}$. Then

$$x = \sum_{i=1}^{n} \lambda_i x_i \qquad \text{with} \quad \lambda_i \geq 0 \quad \text{and} \quad \sum_{i=1}^{n} \lambda_i = 1$$

is called a convex combination of $x_1, \ldots, x_n$.

Convex hull: For any set $\mathbb{S}$ in a vector space, the convex hull consists of *all* convex combinations of the elements of $\mathbb{S}$ and is a convex set.

Properties of convex sets: Let $\mathbb{S}_1$ and $\mathbb{S}_2$ be two convex sets. Then

- The set $\alpha\mathbb{S}_1 = \{x | x = \alpha c_1, c_1 \in \mathbb{S}_1\}$ is convex for any scalar α.
- The set $\mathbb{S}_1 + \mathbb{S}_2 = \{x | x = c_1 + c_2,\ c_1 \in \mathbb{S}_1,\ c_2 \in \mathbb{S}_2\}$ is convex.
- The intersection $\mathbb{S}_1 \cap \mathbb{S}_2 = \{x | x \in \mathbb{S}_1 \text{ and } x \in \mathbb{S}_2\}$ is convex.

Convex functions: A function $f : \mathbb{S} \to \mathbb{R}$ is convex if

1. $\mathbb{S}$ is a convex set and
2. for all $x_1, x_2 \in \mathbb{S}$ and $\lambda \in [0\,,\ 1]$ there holds that

$$f(\lambda x_1 + (1-\lambda)x_2) \leq \lambda f(x_1) + (1-\lambda) f(x_2)$$

Note that the domain of a convex function is by definition a convex set. In geometric terms, the function $f(x)$ is always below the segment of a line that connects any two points on the curve of $f(x)$ (see Fig. 2.2). $f(x)$ is called strictly convex if the above inequality is strict for $x_1 \neq x_2$.

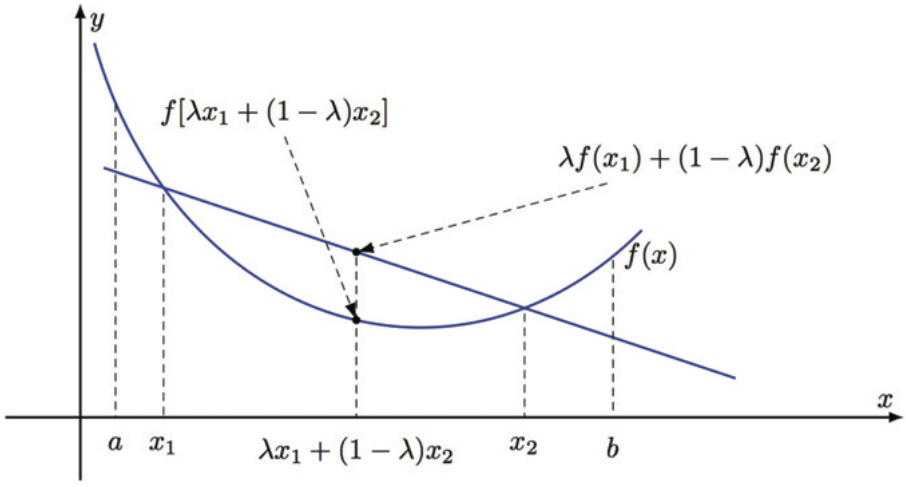

Figure 2.2: A convex function

Example 2.1. Show that $f(x) = x^2$ on $\mathbb{R}$ is a convex function.
Solution: Let's take $x_1, x_2 \in \mathbb{R}$, then we should show that

$$\lambda^2 x_1^2 + (1-\lambda)^2 x_2^2 + 2\lambda(1-\lambda)x_1 x_2 \leq \lambda x_1^2 + (1-\lambda)x_2^2$$

If we bring everything to the left side, we have:

$$\lambda^2 x_1^2 + x_2^2 + \lambda^2 x_2^2 - 2\lambda x_2^2 + 2\lambda x_1 x_2 - 2\lambda^2 x_1 x_2 - \lambda x_1^2 - x_2^2 + \lambda x_2^2 \leq 0$$

$$(\lambda^2 - \lambda) x_1^2 - 2(\lambda^2 - \lambda) x_1 x_2 + (\lambda^2 - \lambda) x_2^2 \leq 0$$

$$(\lambda^2 - \lambda)(x_1 - x_2)^2 \leq 0$$

which is always true because $(\lambda^2 - \lambda) \leq 0$ for all $\lambda \in [0\,,\,1]$.

In fact any twice differentiable function is convex if its domain is convex and its second derivative is non-negative. Using this rule for the above example, we have $f''(x) = 2 > 0$ that results in the convexity of $f(x)$. In the same way $f(x) = -x^2$ is not a convex function.

Example 2.2. Let x belong to a vector space, then show any norm of x is a convex function.

Solution: We should show that $f(x) = \|x\|$ is a convex function, i.e.

$$\|\lambda x_1 + (1-\lambda) x_2\| \leq \lambda \|x_1\| + (1-\lambda)\|x_2\| \tag{2.1}$$

Every norm function by definition follows the triangle inequality:

$$\|\lambda x_1 + (1-\lambda) x_2\| \leq \|\lambda x_1\| + \|(1-\lambda) x_2\|$$

On the other hand, because of the homogeneity property of norms and the non-negativity of λ and $1-\lambda$ the inequality in (2.1) results.

Properties of convex functions:

1. Linear and affine functions are convex because their second derivative is zero (non-negative).
2. If $f(y)$ is convex and $y = g(x)$ is linear, then $f \circ g = f(g(x))$ is convex.
3. If $f_1, \ldots, f_n$ are convex functions, then their convex combination

$$g = \sum_{i=1}^{n} \lambda_i f_i \qquad \lambda_i \in [0 \quad 1] \quad \text{and} \quad \sum_{i=1}^{n} \lambda_i = 1$$

   is also convex.
4. If $f(x)$ is a convex function, then $\mathbb{D} = \{x \mid f(x) \leq 0\}$ is a convex set.
5. If $f(x)$ is a linear function on $\mathbb{R}$ then $f(x) \leq 0$, $f(x) \geq 0$ and $f(x) = 0$ define the convex sets.
6. Let $f_1, \ldots, f_n$ be convex functions then $\mathbb{D} = \{x \mid f_i(x) \leq 0 \quad \text{for } i = 1, \ldots, n\}$ is the intersection of convex sets and defines a convex set.
7. If $f(x)$ is a nonlinear convex function, neither $f(x) \geq 0$ nor $-f(x) \leq 0$ defines a convex set.

2.2.2 Linear Matrix Inequalities

A linear matrix inequality is an expression of the form:

$$F(x) = F_0 + \sum_{i=1}^{m} x_i F_i \succ 0$$

where $x = [x_1, \ldots, x_m]$ is a vector of m decision variables and $F_i = F_i^T \in \mathbb{R}^{n \times n}$, for $i = 0, \ldots, m$. The special inequality $\succ 0$, means positive definite i.e. $F \succ 0$ if and only if $u^T F u > 0$ for all $u \in \mathbb{R}^n$ and $u \neq 0$.

The matrix $F = F^T$ is positive definite if and only if all eigenvalues of F are positive. This is equivalent to requiring that all its leading principal minors (i.e., the determinants of its leading principal submatrices) are positive. In this course, we consider the positive definiteness of symmetric matrices unless stated otherwise.

Properties of positive matrices: If $F \succ 0$ then

1. All diagonals of F are positive.
2. The determinant of F is positive.
3. Eigenvalues and singular values of F are equal.
4. F is invertible and the inverse is also positive definite $F^{-1} \succ 0$.
5. If $\lambda > 0$ is a real number, then $\lambda F \succ 0$.
6. If $G \succ 0$ then $F + G \succ 0$ and $GFG \succ 0$ and $FGF \succ 0$ and $\mathrm{tr}(FG) > 0$. The product FG is also positive definite if $FG = GF$.
7. Let M be a nonsingular full rank matrix, then $F \succ 0$ if and only if $M^T F M \succ 0$. In the same way, $F \prec 0$ if and only if $M^T F M \prec 0$.
8. There is $\delta > 0$ such that $F \succeq \delta I$ (it means that $F - \delta I \succeq 0$).

Geometry of LMIs:

The LMIs $F(x) \succ 0$ and $F(x) \prec 0$ define convex sets on x i.e.:

$$F(\lambda x_1 + (1-\lambda)x_2) = \lambda F(x_1) + (1-\lambda)F(x_2) \succ 0$$

This can be shown easily using the properties 5 and 6. For example take $x = [x_1\ x_2]$, then $F(x) = x_2 - x_1 > 0$ is an LMI (of dimension 1 !) with $F_0 = 0$, $F_1 = -1$ and $F_2 = 1$. If we plot the set corresponding to $x_2 - x_1 > 0$ in the space of x_1 and x_2 a half plane is obtained that is a convex set (see Fig. 2.3 a) [1].

The following two dimensional LMI [1]:

$$F(x) = \begin{bmatrix} 1 & x_1 \\ x_1 & x_2 \end{bmatrix} \succ 0$$

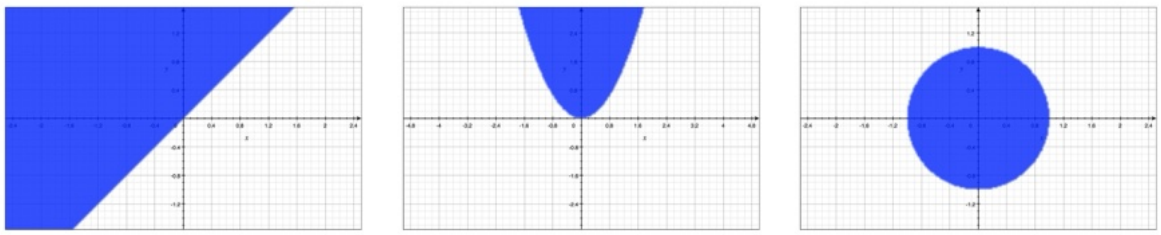

a) $x_2 > x_1$ b) $x_2 > x_1^2$ c) $x_1^2 + x_2^2 < 1$

Figure 2.3: Geometry of LMIs

(which is equivalent to this nonlinear constraint $x_2 - x_1^2 > 0$) represents also a second-order cone and is a convex set (see Fig. 2.3 b).

Finally, the following LMI [1]:

$$F(x) = \begin{bmatrix} 1 & x_1 & x_2 \\ x_1 & 1 & 0 \\ x_2 & 0 & 1 \end{bmatrix} \succ 0 \tag{2.2}$$

represents a disk ($x_1^2 + x_2^2 < 1$) and is a convex set shown in Fig. 2.3 c.

Remarks:

1. Any matrix inequality as $F(x) \succ 0$ can be represented as an LMI if its elements are affine with respect to x. For example the inequality in (2.2) can be written in the standard form of an LMI as:

$$F(x) = \underbrace{\begin{bmatrix} 1 & 0 & 0 \\ 0 & 1 & 0 \\ 0 & 0 & 1 \end{bmatrix}}_{F_0} + x_1 \underbrace{\begin{bmatrix} 0 & 1 & 0 \\ 1 & 0 & 0 \\ 0 & 0 & 0 \end{bmatrix}}_{F_1} + x_2 \underbrace{\begin{bmatrix} 0 & 0 & 1 \\ 0 & 0 & 0 \\ 1 & 0 & 0 \end{bmatrix}}_{F_2}$$

2. Any matrix inequality which is affine w.r.t $F(x)$ and symmetric, e.g. $A^T F(x) + F(x)A \succ 0$, is also an LMI.
3. An LMI can be seen as the intersection of some sets related to the nonlinear constraints associated to the positivity of its leading principal minors. Each nonlinear constraint is a polynomial function of x.

Example 2.3. Consider the following LMI: [1]

$$F(x) = \begin{bmatrix} 1 - x_1 & x_1 + x_2 & x_1 \\ x_1 + x_2 & 2 - x_1 & 0 \\ x_1 & 0 & 1 + x_2 \end{bmatrix} \succ 0$$

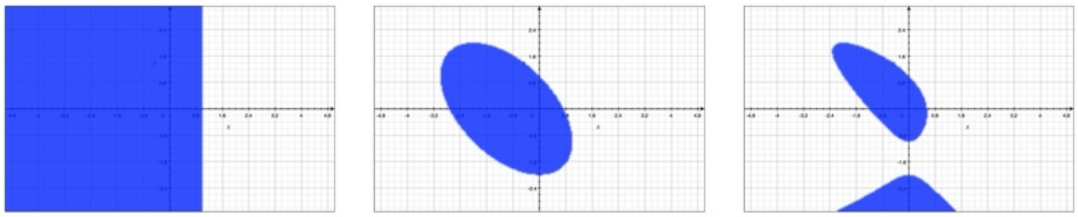

$m_1 > 0$ $m_2 > 0$ $m_3 > 0$

Figure 2.4: LMI as the intersection of nonlinear polynomial constraints related to the positiveness of the determinants of principal minors.

If we write the conditions on the positivity of its leading principal minors, we obtain:

$$\begin{aligned} m_1 > 0: &\quad 1 - x_1 > 0 \\ m_2 > 0: &\quad (1 - x_1)(2 - x_1) - (x_1 + x_2)^2 > 0 \\ m_3 > 0: &\quad x_1^2(x_2 - 2) + (1 + x_2)[(1 - x_1)(2 - x_2) - (x_1 + x_2)^2 > 0 \end{aligned}$$

The sets related to these inequalities are depicted in Fig. 2.4. The intersection of the three sets is the convex set around the origin in the third plot ($m_3 > 0$), which corresponds to the LMI $F(x) \succ 0$.

Schur Lemma

Some nonlinear matrix inequalities can be converted to an LMI using the so called Schur Lemma.

Lemma 2.1. *Let $F(x) \succ 0$ be an LMI and $F(x)$ can be partitioned as:*

$$F(x) = \begin{bmatrix} A & B \\ B^T & C \end{bmatrix}$$

where $A = A^T$, $C = C^T$ and B are affine with respect to x and have appropriate dimensions. Then $F(x) \succ 0$ if and only if

$$A \succ 0 \quad \textit{and} \quad C - B^T A^{-1} B \succ 0$$

Proof. Let a nonsingular full rank matrix M be defined as:

$$M = \begin{bmatrix} I & -A^{-1}B \\ 0 & I \end{bmatrix}$$

We know from property (7) that $M^T F M \succ 0$. Then it can be verified easily that:

$$M^T F M = \begin{bmatrix} A & 0 \\ 0 & C - B^T A^{-1} B \end{bmatrix} \succ 0$$

that leads to $A \succ 0$ and $C - B^T A^{-1} B \succ 0$. □

There are some other variants of the Schur lemma that can be proved in the same way. More specifically, it can be shown that:

$$\begin{aligned} F(x) \succ 0 &\iff C \succ 0, \text{ and } A - BC^{-1}B^T \succ 0 \\ F(x) \prec 0 &\iff A \prec 0, \text{ and } C - B^T A^{-1} B \prec 0 \\ F(x) \prec 0 &\iff C \prec 0, \text{ and } A - BC^{-1}B^T \prec 0 \end{aligned}$$

It should be mentioned that $A - BC^{-1}B^T$ and $C - B^T A^{-1} B$ are called Schur complements.

LMIs in Control

Many control problems can be formulated using linear matrix inequalities. Two simple examples are given here to show the importance of LMIs in control.

Stability analysis: Consider the asymptotic stability analysis of a continuous-time autonomous linear system $\dot{x}(t) = Ax(t)$, where $A \in \mathbb{R}^{n \times n}$. The asymptotic stability means that $\lim_{t \to \infty} x(t) = 0$ for all $x(0) \neq 0$. It is well known that the system is asymptotically stable if and only if the real parts of all eigenvalues of A are negative. An alternative is the Lyapunov stability theorem. It states that the system is stable if and only if there exists a function $V(x) \geq 0$ and $\dot{V}(x) < 0$ for all $t > 0$. If we take $V(x) = x^T(t) P x(t)$ with $P \succ 0$, then

$$\dot{V}(x) = \dot{x}^T(t) P x(t) + x^T(t) P \dot{x}(t) = x^T(t)[A^T P + PA] x(t)$$

The necessary and sufficient condition for $\dot{V}(x) < 0$ is $A^T P + PA \prec 0$. This condition together with $P \succ 0$ can be put to one LMI as:

$$\begin{bmatrix} P & 0 \\ 0 & -(A^T P + PA) \end{bmatrix} \succ 0$$

Therefore, the system is asymptotically stable if and only if there exists a symmetric matrix P that satisfies the above LMI.

Stabilization with state feedback: Consider the following linear time-invariant system:

$$\dot{x}(t) = Ax(t) + Bu(t)$$

The objective is to find a stabilizing state feedback law $u(t) = -Kx(t)$. Replacing $u(t)$ in the above equation, we find an autonomous system $\dot{x}(t) = (A - BK)x(t)$. This system is stable if and only if there exists a symmetric matrix $P \succ 0$ such that:

$$(A - BK)^T P + P(A - BK) \prec 0$$

Since both P and K are unknown, the above inequality is not an LMI on P and K. However, if we introduce new variables we may obtain an LMI on new variables. Let's

multiply the above inequality from left and right by $L = P^{-1}$ (we use the properties 4 and 7 of the positive matrices):

$$L(A - BK)^T + (A - BK)L \prec 0$$

Then we define a new variable $Y = KL$ that makes the above matrix inequality an LMI as:

$$LA^T - Y^T B^T + AL - BY \prec 0$$

Therefore, if the intersection of $L \succ 0$ and $LA^T - Y^T B^T + AL - BY \prec 0$ is not empty, the system can be stabilized by the state feedback controller $K = YL^{-1}$.

2.2.3 Convex Optimization

One of the main problems in numerical optimization is the existence of local minima and local maxima. The main interest of convex functions is related to the absence of local minima.

Local and global minima: A function $f(x)$ has a local minimum at $x_0 \in \mathbb{S}$ if there exists a neighbourhood $\mathbb{N} \subset \mathbb{S}$ of x_0 such that $f(x_0) \leq f(x)$ for all points $x \in \mathbb{N}$. It is a global minimum if $f(x_0) \leq f(x)$ for all $x \in \mathbb{S}$. According to this definition every global minimum is a local minimum as well.

Lemma 2.2. *Suppose that $f(x) : \mathbb{S} \to \mathbb{R}$ is convex. If $f(x)$ has a local minimum at $x_0 \in \mathbb{S}$, then $f(x_0)$ is also a global minimum of $f(x)$. If $f(x)$ is strictly convex, then x_0 is moreover unique.*

Proof. Let $f(x)$ has a local minimum at $x_0 \in \mathbb{S}$. Then for all $x \in \mathbb{S}$ and some sufficiently small $\lambda \in [0\,,\,1]$, we have:

$$f(x_0) \leq f(x_0 + \lambda(x - x_0)) = f(\lambda x + (1 - \lambda)x_0) \tag{2.3}$$

Since $f(x)$ is convex

$$f(\lambda x + (1 - \lambda)x_0) \leq \lambda f(x) + (1 - \lambda)f(x_0) = f(x_0) + \lambda(f(x) - f(x_0)) \tag{2.4}$$

Using (2.3) and (2.4), we obtain:

$$f(x_0) \leq f(x_0) + \lambda(f(x) - f(x_0)) \quad \Rightarrow \quad 0 \leq \lambda(f(x) - f(x_0))$$

This implies that $f(x_0) \leq f(x)$ for all $x \in \mathbb{S}$. So $f(x_0)$ is a global minimum. If $f(x)$ is strictly convex, then the inequalities in (2.4) becomes strict for all $x \in \mathcal{S}$. Hence, x_0 is unique. □

It should be emphasised that this lemma does not make any statement about existence of point $x_0 \in \mathbb{S}$. It only says that all local minima of $f(x)$ are also global minima. As a result, it suffices to compute a local minimum of a convex function to actually determine its global minimum.

Convex problems: In all optimization problems, an objective function should be minimized (or maximized) over a decision space represented by some constraints. If no objective function is defined the problem is called a feasibility problem. The aim of a feasibility problem is to see if the decision space is empty (problem infeasible) or not (problem feasible). In general, we can write an optimization problem as:

$$\begin{aligned} &\min_x f_0(x) \\ &\text{subject to:} \\ &f_i(x) \leq 0 \qquad i = 1, \ldots, n \\ &g_j(x) = 0 \qquad j = 1, \ldots, m \end{aligned}$$

If $f_i(x)$ for $i = 0, \ldots, n$ are convex functions and $g_j(x)$ for $j = 1, \ldots, m$ are affine, the problem is commonly referred to as a convex program. This is probably the only tractable optimization problem in the area of nonlinear optimization theory. The numerical algorithms to solve this problem is not the subject of this course and will not be studied here. We just mention some particular convex problems and the way that they can be solved using the available softwares.

LP: If $f_i(x)$ for $i = 0, \ldots, n$ are affine, the problem is called Linear Programming (LP). This is the simplest constrained optimization problem and can be solved very efficiently even for more than hundred thousands of constraints and variables.

QP: If $f_0(x)$ is a quadratic function and $f_i(x)$ for $i = 1, \ldots, n$ are affine, the problem is called Quadratic Programming (QP). This problem also can be solved very efficiently and is in the second place after LP in terms of reliability and numerical efficiency. The least squares (LS) problem is the simplest optimization problem in this category where there is no constraint ($n = m = 0$).

SDP: If $f_0(x)$ is affine and the constraints are replaced with LMIs $F_i(x) \preceq 0$ or $F_i(x) \succeq 0$ for $i = 1, \ldots, n$ then the problem is called Semi-Definite Programming (SDP). Since many control problems can be reformulated by a system of linear matrix inequalities, SDP has many interests in control theory. The SDP problems can be solved efficiently using the ellipsoid algorithm and interior point methods. There is a Toolbox for Matlab and a few open source softwares for solving the SDP problems.

SIP: If in an SDP problem the constraints are defined for a parameter θ and should be satisfied for all $\theta \in \Theta$ (the number of constraints is infinity but the number of decision variable is finite), the problem is called Semi-Infinite Programming (SIP). This problem is referred to robust optimization as well and is the most complicated convex problem. A practical solution to this problem is to choose a finite set $\Theta_N \subset \Theta$ and convert the problem to SDP. In the randomized approaches the set Θ_N is chosen randomly and the probability of the violation of the constraints by any $\theta \in \Theta \backslash \Theta_N$ is computed.

SDP in Control

Here we introduce two simple examples for the use of SDP in control problems.

Computing $\mathcal{H}_\infty$ norm: In Section 1.3.1 we studied different methods for computing the infinity norm of an LTI system. One of the methods is based on the bounded real lemma and the bisection optimization algorithm. Here, we present the bounded real lemma in which the condition on the Hamiltonian matrix is changed with an equivalent condition on the existence of a solution to a matrix inequality. Then, we reformulate it as an SDP problem and show how it can be solved.

Lemma 2.3. *Let $\gamma > 0$ and*

$$G(s) = \left[\begin{array}{c|c} A & B \\ \hline C & D \end{array}\right]$$

then $\|G\|_\infty < \gamma$ if and only if

$$\begin{bmatrix} A^TP + PA + C^TC & PB + C^TD \\ B^TP + D^TC & D^TD - \gamma^2 I \end{bmatrix} \prec 0 \tag{2.5}$$

Proof. We prove only the sufficient condition. If $u(t)$ is the input and $y(t)$ the output of G then the infinity norm can be defined as the supremum of the system's two-norm gain:

$$\|G\|_\infty = \sup_u \frac{\|y\|_2}{\|u\|_2}$$

The state space representation of G is given by:

$$\begin{aligned} \dot{x}(t) &= Ax(t) + Bu(t) \\ y(t) &= Cx(t) + Du(t) \qquad x(0) = 0 \end{aligned}$$

The LMI in (2.5) can be rewritten as:

$$\begin{bmatrix} A^TP + PA & PB \\ B^TP & -\gamma^2 I \end{bmatrix} + \begin{bmatrix} C^T \\ D^T \end{bmatrix} \begin{bmatrix} C & D \end{bmatrix} \prec 0$$

This implies:

$$\begin{bmatrix} x(t) \\ u(t) \end{bmatrix}^T \left\{ \begin{bmatrix} A^TP + PA & PB \\ B^TP & -\gamma^2 I \end{bmatrix} + \begin{bmatrix} C^T \\ D^T \end{bmatrix} \begin{bmatrix} C & D \end{bmatrix} \right\} \begin{bmatrix} x(t) \\ u(t) \end{bmatrix} < 0$$

$$\begin{bmatrix} x(t) \\ u(t) \end{bmatrix}^T \begin{bmatrix} A^TP + PA & PB \\ B^TP & -\gamma^2 I \end{bmatrix} \begin{bmatrix} x(t) \\ u(t) \end{bmatrix} + [\underbrace{Cx(t) + Du(t)}_{y(t)}]^T [Cx(t) + Du(t)] < 0$$

$$x^T(t)(A^TP+PA)x(t)+x^T(t)PBu+u^T(t)B^TPx(t)-\gamma^2u^T(t)u(t)+y^T(t)y(t)<0$$
$$[\underbrace{Ax(t)+Bu(t)}_{\dot{x}(t)}]^TPx(t)+x^T(t)P[Ax(t)+Bu(t)]-\gamma^2u^T(t)u(t)+y^T(t)y(t)<0$$

Taking a Lyapunov function $V(x)=x^T(t)Px(t)$, we have

$$\dot{V}(x)=\dot{x}(t)^TPx(t)+x^T(t)P\dot{x}(t)$$

that leads to:

$$\dot{V}(x)-\gamma^2u^T(t)u(t)+y^T(t)y(t)<0$$

Taking the integral of the above inequality, we obtain:

$$\int_0^\infty \dot{V}(x)dt-\gamma^2\int_0^\infty u^T(t)u(t)dt+\int_0^\infty y^T(t)y(t)dt<0$$

Using the definition of the two norm of the signals, we obtain:

$$V(x(\infty))-V(x(0))-\gamma^2\|u\|_2^2+\|y\|_2^2<0$$

Since $A^TP+PA\prec 0$ from the LMI in (2.5), G is stable and $x(\infty)=0$ that results in $V(x(\infty))=0$. On the other hand, $x(0)=0$ gives $V(x(0))=0$. Therefore:

$$\frac{\|y\|_2^2}{\|u\|_2^2}<\gamma^2 \quad\Rightarrow\quad \sup_u\frac{\|y\|_2}{\|u\|_2}<\gamma \quad\Rightarrow\quad \|G\|_\infty<\gamma$$

□

As a result, computing the infinity norm of G can be reformulated as an optimization problem:

$$\min_{P,\gamma}\ \gamma^2$$
subject to:
$$\begin{bmatrix} A^TP+PA+C^TC & PB+C^TD \\ B^TP+D^TC & D^TD-\gamma^2I \end{bmatrix}\prec 0$$
$$P\succ 0$$

This SDP problem can be solved using the following Yalmip[1] code:

[1]Free code developed by J. Löfberg accessible at `http://control.ee.ethz.ch/$\sim$joloef/yalmip.php`. Yalmip is an interface that translates an optimization problem to the language of a solver.

```
gamma2=sdpvar(1,1);
P=sdpvar(n,n,'symmetric');
lmi=[A'*P+P*A+C'*C P*B+C'*D; B'*P+D'*C D'*D-gamma2]<0;
lmi=[lmi, P>0];
options=sdpsettings('solver','lmilab');
optimize(lmi,gamma2,options);
gamma2=value(gamma2);
HinfNorm=sqrt(gamma2)
```

Note that γ^2 is replaced with a new variable `gamma2` to make the objective function and the elements of the LMI constraint linear in variable. This, of course, will not change the outcome of the optimization; we should only take the square root of `gamma2` to find the infinity norm at the end. In this code, `sdpvar` is used to define the decision variables. In this problem we have a scalar γ, which is an upper bound on the square of the infinity norm, and a symmetric matrix P whose dimension is equal to the order (number of states) of G. Then, the LMIs are defined straightforwardly using Matlab notation. Using `sdpsettings` the optimization options are defined. Among the options, we can choose an SDP solver. In this example, we use `lmilab` from LMI Toolbox of Matlab. Next, the command `optimize`, take the lmi constraints (`lmi`) and the objective function (`gamma`) to be minimized. Finally the optimal solution is converted from an SDP variable to a double variable of Matlab.

Computing $\mathcal{H}_2$ norm: In Section 1.3.1, we saw that the $\mathcal{H}_2$ norm of a system is equal to the square root of the trace of CLC^T, where $L \succ 0$ is a solution to the following equation:

$$AL + LA^T + BB^T = 0 \tag{2.6}$$

This problem is reformulated as an SDP problem in the following lemma.

Lemma 2.4. *Let $G(s)$ be a strictly proper stable transfer function given by:*

$$G(s) = \left[\begin{array}{c|c} A & B \\ \hline C & 0 \end{array}\right]$$

then $\|G\|_2^2 = trace[CL^\circ C^T]$ where L° is the optimal solution to the following SDP problem:

$$\min_{L} \; trace[CLC^T]$$

$$AL + LA^T + BB^T \preceq 0 \qquad ; \qquad L \succ 0 \tag{2.7}$$

Proof. Let $L^* \succ 0$ be the unique solution to the Riccati equation (2.6). Since L^* satisfies the equality, it also satisfies the inequality in (2.7). Therefore, trace$(CL^\circ C^T) \leq$ trace$(CL^* C^T)$, which implies trace$(C(L^\circ - L^*)C^T) \leq 0$ and hence $L^\circ - L^* \preceq 0$. On the other hand, subtracting (2.6) from (2.7) yeilds $A(L^\circ - L^*) + (L^\circ - L^*)A^T \preceq 0$. By stability of A, this implies $L^\circ - L^* \succeq 0$. Combining both inequalities, we conclude $L^\circ - L^* = 0$, i.e. $L^\circ = L^*$, which complete the proof. □

This can be coded using Yalmip as follows:

```
L=sdpvar(n,n,'symmetric');
lmi=A*L+L*A'+B*B' ≤ 0;
lmi=[lmi, L>0];
options=sdpsettings('solver','lmilab');
optimize(lmi,trace(C*L*C'),options);
L=value(L);
H2Norm=sqrt(trace(C*L*C'))
```

2.3 Model-Based $\mathcal{H}_2$ and $\mathcal{H}_\infty$ Design

When the parametric model of a system is available, there are several methods to design a controller for the system with performance specifications in terms of the minimization of the 2- or infinity-norm of some transfer functions. The optimization problems are different for continuous-time models and discrete-time models, although the approaches are similar. In this section, we present everything for continuous-time models. The control methods can be divided into two categories depending on the controller structure or the desired performance.

Controller structure: Before starting to optimize the controller parameters, we should choose the controller structure among the following choices:

State Feedback: The control law is a linear combination of the states, i.e. $u(t) = -Kx(t)$, where $K \in \mathbb{R}^{m\times p}$ (m is the number of inputs and p is the number of states). The controller is very simple and can be computed using convex optimization programs. However, it can be applied to systems where all states are measurable. Otherwise, it can be combined with a state estimator. In this case, the overall performance may be deteriorated depending on the quality of the estimator.

Output Feedback: When all states are not measured, a simple solution is a static output feedback controller where $u(t) = -Ky(t)$ with $K \in \mathbb{R}^{m\times n}$ (n is the number of outputs). A more general solution is to design a dynamic output feedback controller, where the controller has its dynamic and is represented by a state-space model. This problem has a solution with a convex program when the number of states of the controller is equal to that of the model (called full order controller). It should be mentioned that the decision variables are not the controller parameters but some intermediate variables. The final controller parameters are functions of the intermediate variables.

Fixed Structure: In many applications, a low order controller with a fixed structure is desired. For example the well-known PID controller has a fixed structure (a second order controller with one integrator). The closed-loop performance are optimized

usually by a non-convex optimization algorithm in which the controller parameters are the decision variables. The fixed structure controller is more interesting in multivariable large scale systems when we seek decentralized or distributed controllers.

Performance specification: After choosing the controller structure, we should choose which type of performance and robustness we want to consider for the closed-loop system among the following choices:

Loop shaping: The closed-loop performance can be specified by a desired open-loop transfer function L_d. The objective is to compute a stabilizing controller such that $\|W_L(GK - L_d)\|$ (in 2 or infinity norm) is minimized, where W_L is a frequency weighing function.

$\mathcal{H}_\infty$ performance: The objective is to design a stabilizing controller that minimizes a performance criterion in terms of the infinity-norm of a weighted closed-loop transfer function subject to constraints on the infinity-norm of some other weighted closed-loop transfer functions.

$\mathcal{H}_2$ performance: The objective is to design a stabilizing controller that minimizes a performance criterion in terms of the 2-norm of a weighted closed-loop transfer function subject to constraints on the 2-norm of some other weighted closed-loop transfer functions.

Mixed $\mathcal{H}_2/\mathcal{H}_\infty$: The performance may be represented as a mix of constraints on the 2- and infinity-norm of some weighted closed-loop transfer function while the objective is minimizing the 2- or infinity-norm of a weighted closed-loop transfer function. It is clear that the controller should be stabilizing. In this approach some constraints on the places of the closed-loop poles can be considered as well (regional pole placement).

There are a few Matlab commands in the robust control toolbox that can be used to design such controllers. Namely, `hinfstruc` can be used to compute fixed structure controllers with $\mathcal{H}_\infty$ performance using non-smooth optimization techniques. The commands `h2syn` and `hinfsyn` are used to design $\mathcal{H}_2$ and $\mathcal{H}_\infty$ optimal output feedback controllers, respectively. They use convex optimization methods to compute full-order controllers. Loop shaping performance in the infinity-norm sense can be achieved using `loopsyn` command by convex optimization. The sum of two $\mathcal{H}_2$ and $\mathcal{H}_\infty$ performance criteria is minimized under some constraints on the place of closed-loop poles using `hinfmix` command.

It is clear that we cannot study all of these methods in this section. We will give just an overview of some of the methods without entering into the details in the following subsections. The main principles of controller design using SDP is illustrated by state feedback controller design for $\mathcal{H}_\infty$ and $\mathcal{H}_2$ performance. The linear fractional transformation (LFT) is introduced that presents a general framework for $\mathcal{H}_\infty$ and $\mathcal{H}_2$ optimal output feedback controller design.

2.3.1 State Feedback Control

$\mathcal{H}_\infty$ State Feedback

The objective is to design a stabilizing state feedback controller $u(t) = -Kx(t)$ such that the infinity-norm of a closed-loop transfer function is minimized. To design such a controller, follow these steps:

1. First, write the state-space equations of the plant model.
2. Augment the equations by adding external inputs to the closed-loop system (such as reference signals, disturbance inputs, or measurement noise) that are relevant to the control objectives.
3. Substitute $u(t) = -Kx(t)$ into the system and derive the state-space representation of the resulting closed-loop system.
4. Apply the bounded-real lemma for the closed-loop system to formulate an optimization problem involving matrix inequalities.
5. Transform the optimization problem to a convex problem by changing the variables.

Input disturbance rejection: Consider a controllable state-space representation of a strictly proper LTI system as:

$$\begin{aligned} \dot{x}(t) &= Ax(t) + Bu(t) \\ y(t) &= Cx(t) \end{aligned} \tag{2.8}$$

Suppose that the objective is to design a stabilizing state-feedback controller K such that the infinity-norm of the transfer function between the input disturbance $v(t)$ and the output is minimized.

The control law plus the input disturbance is given by $u(t) = -Kx(t)+v(t)$. Replacing $u(t)$ in (2.8), leads to the following closed-loop state space model:

$$\begin{aligned} \dot{x}(t) &= (A - BK)x(t) + Bv(t) \\ y(t) &= Cx(t) \end{aligned} \tag{2.9}$$

Now, we should apply Lemma 2.3 (bounded-real lemma) to the above system and minimize the infinity norm:

$$\min_{P,\gamma} \gamma^2$$

subject to:

$$(A - BK)^T P + P(A - BK) + C^T C + PB(\gamma^{-2})B^T P \prec 0$$

$$P \succ 0$$

It is clear that the first inequality is not an LMI. However, we can convert it to an LMI using a change of variable. Let's multiply the inequality from left and right by $X = \gamma^2 P^{-1}$ to obtain:

$$X(A - BK)^T\gamma^2 + \gamma^2(A - BK)X + XC^TCX + B\gamma^2B^T \prec 0$$

Then, we define a new variable $KX = Y$ and replace it in the above inequality and divide the inequality by γ^2:

$$XA^T - Y^TB^T + AX - BY + XC^T\gamma^{-2}CX + BB^T \prec 0$$

Now, using the Schur Lemma (2.1), we obtain the following LMIs:

$$\begin{bmatrix} XA^T + AX - Y^TB^T - BY + BB^T & XC^T \\ CX & -\gamma^2 I \end{bmatrix} \prec 0 \quad , \quad X \succ 0$$

The obtained convex problem can be solved to find the optimal values for X and Y. The state feedback controller is given by $K = YX^{-1}$.

Remark: It should be noted that since there is no constraint in other sensitivity function, minimizing one of them will lead to very large norm for the other sensitivity functions. In a good controller design we should always consider some limits for the norm of the control signal to avoid very large values.

State disturbance rejection: Consider again a controllable state-space model of a system with an additional disturbance on the state equation as:

$$\begin{aligned} \dot{x}(t) &= Ax(t) + B_1u(t) + B_2w(t) \\ y(t) &= Cx(t) \end{aligned}$$

The objective is to design a stabilizing state feedback controller that minimizes the infinity-norm of the transfer function between $w(t)$ and $y(t)$ as well as between $w(t)$ and $u(t)$.

We replace $u(t) = -Kx(t)$ in the above equation to find the closed-loop state-space model as:

$$\begin{aligned} \dot{x}(t) &= (A - B_1K)x(t) + B_2w(t) \\ y(t) &= Cx(t) \\ u(t) &= -Kx(t) \end{aligned}$$

Now we define a new output variable $z(t) = [y(t)\,;\, u(t)]$ that regroups the plant output $y(t)$ and the control signal $u(t)$ in one performance output variable. So the objective will be minimizing the infinity-norm of the transfer function between $w(t)$ and $z(t)$. The state space model of the closed-loop system will be:

$$\begin{aligned} \dot{x}(t) &= (A - B_1K)x(t) + B_2w(t) \\ z(t) &= \begin{bmatrix} C \\ -K \end{bmatrix} x(t) \end{aligned}$$

If we apply bounded real lemma to this state-space model we obtain:

$$\min_{P,\gamma} \gamma^2$$

subject to:

$$(A - B_1K)^TP + P(A - B_1K) + C^TC + K^TK + PB_2(\gamma^{-2})B_2^TP \prec 0$$
$$P \succ 0$$

Since the first inequality is not an LMI, we multiply the inequality from left and right by $X = \gamma^2 P^{-1}$, we define a new variable $Y = KX$ and we divide the whole inequality by γ^2 to obtain:

$$XA^T - Y^TB_1^T + AX - B_1Y + XC^T\gamma^{-2}CX + Y^T\gamma^{-2}Y + B_2B_2^T \prec 0$$

which can be rewritten as:

$$XA^T + AX - Y^TB_1^T - B_1Y + B_2B_2^T$$
$$- \begin{bmatrix} XC^T & Y^T \end{bmatrix} \begin{bmatrix} -\gamma^2 I & 0 \\ 0 & -\gamma^2 I \end{bmatrix}^{-1} \begin{bmatrix} XC^T & Y^T \end{bmatrix}^T \prec 0$$

Then applying Schur Lemma the following LMIs are obtained:

$$\begin{bmatrix} XA^T + AX - Y^TB_1^T - B_1Y + B_2B_2^T & XC^T & Y^T \\ CX & -\gamma^2 I & 0 \\ Y & 0 & -\gamma^2 I \end{bmatrix} \prec 0 \quad , \quad X \succ 0$$

The final state feedback controller that achieve this performance is $K = YX^{-1}$.

$\mathcal{H}_2$ State Feedback

The objective is to design a stabilizing state feedback controller that minimizes the 2-norm of a closed-loop transfer function. The method to design such a controller is very similar to that of $\mathcal{H}_\infty$ state feedback controller design. The only difference is that instead of bounded real lemma (Lemma 2.3) the 2-norm lemma (Lemma 2.4) is used.

Input disturbance rejection: Consider the state-space model in (2.8). Design a stabilizing state feedback controller that minimizes the 2 norm of the transfer function between a disturbance added to the control signal and the output of the system.

Similar to the $\mathcal{H}_\infty$ case, we replace $u(t) = -Kx(t) + v(t)$ in (2.8) to obtain (2.9). Then we use the 2-norm lemma and derive the following optimization problem:

$$\min tr(CLC^T)$$
$$(A - BK)L + L(A - BK)^T + BB^T \preceq 0$$
$$L \succ 0$$

It is clear that the first inequality is not an LMI but can be transformed to an LMI with a change of variable as $KL = Y$. This leads to the following LMI:

$$AL + LA^T - BY - Y^T B + BB^T \preceq 0$$

The final controller is $K = YL^{-1}$. This controller, however is not implementable on a real system because when minimizing the norm of one transfer function the norms of other closed-loop transfer functions become too large. A good controller can be designed if, in addition, the two-norm of the control signal is also minimized.

2.3.2 Linear Fractional Transformation

We saw in the previous subsections that we can design state feedback controllers in $\mathcal{H}_2$ and $\mathcal{H}_\infty$ sense by convex optimization programs. However, the norm of only one transfer function from an external signal to a performance output is minimized. We saw that if we have more than one performance output, we can regroup them in a new variable and reformulate the problem. This technique can be generalized to define a new framework for representation of control problems named linear fractional transformation (LFT).

Definition 2.1. *[9] Let M be a complex matrix partitioned as:*

$$\begin{bmatrix} M_{11} & M_{12} \\ M_{21} & M_{22} \end{bmatrix}$$

and let Δ be another complex matrix. Then we can define an LFT with respect to Δ denoted $F_l(M, \Delta)$ as:

$$F_l(M, \Delta) := M_{11} + M_{12}\Delta(I - M_{22}\Delta)^{-1}M_{21}$$

provided that the inverse $(I - M_{22}\Delta)^{-1}$ exists.

The motivation for this definition can be seen from the block diagram in Fig. 2.5. This diagram represents the following set of equations:

$$\begin{bmatrix} z \\ y \end{bmatrix} = \begin{bmatrix} P_{11} & P_{12} \\ P_{21} & P_{22} \end{bmatrix} \begin{bmatrix} w \\ u \end{bmatrix} \qquad ; \qquad u = Ky$$

It is easy to verify that the LFT is in fact the transfer matrix from w to z. Let replace $u = Ky$ in the equations:

$$z = P_{11}w + P_{12}Ky$$
$$y = P_{21}w + P_{22}Ky$$

From the second equation we can find $y = (I - P_{22}K)^{-1}P_{21}w$ and replace it into the first equation:

$$z = [P_{11} + P_{12}K(I - P_{22}K)^{-1}P_{21}]w = F_l(P, K)w$$

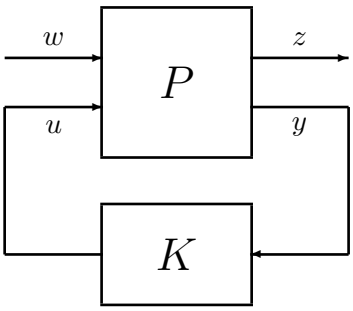

Figure 2.5: The block diagram of an LFT

In a control problem we can define w as a vector containing all external inputs of interest to the closed-loop system. So this vector may include the reference signal, the input disturbance, the output disturbance and the measurement noise. The signal u is the control signal, which is an internal signal in a closed-loop system and connected directly to the actuators. The control signal u is generated by the controller and is its output. The signal z is the collection of all performance indicating signals, that usually we want to minimize, like the tracking error, some of the states, the outputs or the control signal. Note that z may contain the other signals like u and y. Finally, the signal y is the input of the controller (that comes generally from the sensors). Note that the notation is different from a classical closed-loop scheme with unity feedback in which y is the output of the plant and the input of the controller is the tracking error.

For a given P, the objective of a control problem is to design a controller K that minimizes a norm of the transfer function between w and z denoted by T_{zw} or $F_l(P, K)$. It can be shown that many interesting control problems can be reformulated as an LFT. For this purpose, P which is called the augmented plant model should be defined. The augmented plant has two inputs u and w and two outputs z and w (note that all signals are vectors) and includes the plant model and the performance and robustness filters.

Nominal performance: In order to make it clear, let's consider the minimization of $\|W_1\mathcal{S}\|$ as the control performance and try to find the associated augmented plant to this control objective. Figure 2.6 shows a classical closed-loop block diagram in which a filter W_1 is added such that the transfer function between w and z becomes $W_1\mathcal{S}$. Note that all signals in the closed-loop system are denoted such that they are compatible with the notation of a standard LFT. Especially, note that in this scheme y is the input of the controller and not the output of the plant.

In the first step, we should write the equation of the system that relates u and w to z and y. Note that all signals and transfer functions have the argument s for Laplace transform or z for z-transform, which has been dropped out in the following equations.

$$z = W_1(w - Gu) \qquad , \qquad y = w - Gu$$

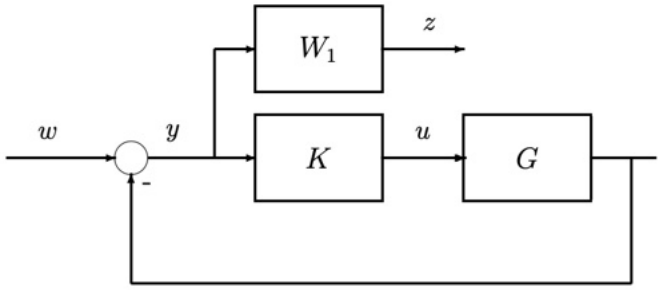

Figure 2.6: Closed-loop block diagram for nominal performance

Therefore we obtain the augmented plant as:

$$\begin{bmatrix} z \\ y \end{bmatrix} = \overbrace{\begin{bmatrix} W_1 & -W_1G \\ 1 & -G \end{bmatrix}}^{P} \begin{bmatrix} w \\ u \end{bmatrix}$$

It is easy to verify that the LFT $F_l(P,K) = W_1\mathcal{S}$:

$$\begin{aligned} F_l(P,K) &= P_{11} + P_{12}K(I - P_{22}K)^{-1}P_{21} \\ &= W_1 + (-W_1G)K(1+GK)^{-1}1 \\ &= W_1\left(1 - \frac{GK}{1+GK}\right) = \frac{W_1}{1+GK} = W_1\mathcal{S} \end{aligned}$$

Robust performance: Consider the robust performance problem for multiplicative uncertainty. It was shown that $\||W_1\mathcal{S}| + |W_2\mathcal{T}|\|_\infty < 1$ should be satisfied. Let's build the block diagram of Fig. 2.7 with one external input w and two performance output z_1 and z_2. We want to investigate which criterion is minimized if we minimize $\|T_{zw}\|_\infty$ in an LFT framework. In the first step we write the equations for the outputs, i.e. z_1, z_2, y of the LFT representation:

$$z_1 = W_1(w - Gu) \qquad , \qquad z_2 = W_2Gu \qquad , \qquad y = w - Gu$$

In the next step we find the augmented plant as:

$$\begin{bmatrix} z_1 \\ z_2 \\ y \end{bmatrix} = \overbrace{\begin{bmatrix} W_1 & -W_1G \\ 0 & W_2G \\ 1 & -G \end{bmatrix}}^{P} \begin{bmatrix} w \\ u \end{bmatrix}$$

In the last step we compute $T_{zw} = F_l(P,K)$ as:

$$\begin{aligned} F_l(P,K) &= P_{11} + P_{12}K(I - P_{22}K)^{-1}P_{21} \\ &= \begin{bmatrix} W_1 \\ 0 \end{bmatrix} + \begin{bmatrix} -W_1G \\ W_2G \end{bmatrix} (K(1+GK)^{-1}1 = \begin{bmatrix} W_1\mathcal{S} \\ W_2\mathcal{T} \end{bmatrix} \end{aligned}$$

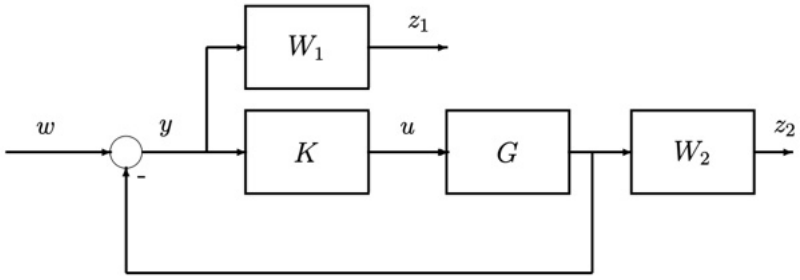

Figure 2.7: Closed-loop block diagram for robust performance

If we minimize $\|T_{zw}\|_\infty$ the following frequency domain function is minimized:

$$\begin{aligned}\|T_{zw}\|_\infty &= \left\| \begin{bmatrix} W_1\mathcal{S} \\ W_2\mathcal{T} \end{bmatrix} \right\|_\infty = \sup_\omega \bar{\sigma} \begin{bmatrix} W_1(j\omega)\mathcal{S}(j\omega) \\ W_2(j\omega)\mathcal{T}(j\omega) \end{bmatrix} \\ &= \sup_\omega \sqrt{|W_1(j\omega)\mathcal{S}(j\omega)|^2 + |W_2(j\omega)\mathcal{T}(j\omega)|^2}\end{aligned}$$

Note that the optimal infinity-norm should be less than $1/\sqrt{2}$ in order to guarantee that the robust performance criterion $\sup_\omega |W_1(j\omega)\mathcal{S}(j\omega)| + |W_2(j\omega)\mathcal{T}(j\omega)| < 1$ is satisfied.

Mixed sensitivity problem: Suppose that in addition to the robust performance problem we are interested to have some constraint on the magnitude of the input sensitivity function $\mathcal{U}$. In other words, we are interested in minimizing $W_3\mathcal{U}$ as well. This can be done by adding a third filter W_3 to Fig. 2.7 such that its input is u and its output is z_3. If we follow the same procedure we will find $F_l(P,K) = [W_1\mathcal{S}\ W_2\mathcal{T}\ W_3\mathcal{U}]^T$. Since usually we are interested in the mixed sensitivity problem, there exists a Matlab command to construct the augmented plant for this problem as `P=augw(G,W1,W3,W2)`. Note that the first filter concerns $\mathcal{S}$, the second one $\mathcal{U}$ and the third one $\mathcal{T}$. The same command can be used for nominal performance problem with `P=augw(G,W1)` and for robust performance problem with `P=augw(G,W1,[],W2)`.

2.3.3 $\mathcal{H}_\infty$ Optimal Control

Given an LFT representation for a system, the optimal $\mathcal{H}_\infty$ control problem is to find all admissible controllers K such that $\|T_{zw}\|_\infty$ is minimized. It should be noted that the optimal $\mathcal{H}_\infty$ controllers are generally not unique for MIMO systems. Furthermore, computing an optimal $\mathcal{H}_\infty$ controller is often theoretically and numerically complicated. Moreover, in practice we are not really interested in designing an optimal $\mathcal{H}_\infty$ controller while we can easily obtain a suboptimal controller which is very close to the optimal one. In a suboptimal $\mathcal{H}_\infty$ control, the objective is to find all admissible controllers, if there are any, such that $\|T_{zw}\|_\infty < \gamma$, where $\gamma > 0$ is given.

Note that in the previous subsection we show that how $P(s)$, which is a matrix of transfer functions, can be computed from the desired performance and robustness requirements. The design of suboptimal $\mathcal{H}_\infty$ controller in an LFT framework needs the augmented plant in state-space form. Assume that a realization of $P(s)$ is given by [9]:

$$\begin{aligned} \dot{x}(t) &= Ax(t) + B_1 w(t) + B_2 u(t) \\ z(t) &= C_1 x(t) + D_{12} u(t) \\ y(t) &= C_2 x(t) + D_{21} w(t) \end{aligned} \tag{2.10}$$

The following assumptions are made:

(A1) (A, B_1, C_1) is controllable and observable. (A, B_2, C_2) is stabilizable and detectable.

(A2) D_{12} has full column rank and D_{21} has full row rank.

(A3) $\begin{bmatrix} A - j\omega I & B_2 \\ C_1 & D_{12} \end{bmatrix}$ has full column rank $\forall\omega$.

(A4) $\begin{bmatrix} A - j\omega I & B_1 \\ C_2 & D_{21} \end{bmatrix}$ has full row rank $\forall\omega$.

Assumption A1 is a standard assumption for controller design in LFT framework. The system with (A, B_1, C_1) which relates the external input w to the performance output z should be controllable and observable. However, for the system (A, B_2, C_2) that relates the control signal to the measured output should only be stabilizable and detectable. Note that stabilizable and detectable are weaker conditions than controllable and observable. In fact, if the uncontrollable states are stable the system is stabilizable and if the unobservable states are stable the system is detectable.

Assumption A2 is related to the rank of D_{12} and D_{21}. If D_{12} has not full column rank, it means that some control inputs have no effect on the performance outputs because $z(t) = C_1 x(t) + D_{12} u(t)$. This will lead to some singularity in solution and can be avoided by adding some weighting filters on these control inputs (even a very small gain to avoid the singularity in the computations). On the other hand, if D_{21} has not full row rank, it means that one of the measured outputs $y(t) = C_2 x(t) + D_{21} w(t)$ is not affected by any of external inputs (the feedback from this output says nothing about the variation in input variables). This makes the problem singular and cannot be solved. The solution is to add some external inputs (noise or disturbance) on all measured output (with a very small gain).

Assumptions A3 and A4 are related to the non existence of poles of the plant model and the weighting filters on the imaginary axis. If there are such poles in the system, they can be perturbed to make these assumptions satisfied. The small perturbation can be done by replacing the term s in the denominator of the model or filters with $(s + \epsilon)$, where $\epsilon > 0$ is a very small value.

Two additional assumptions that are implicit in the assumed realization for $P(s)$ are that $D_{11} = 0$ and $D_{22} = 0$. In fact, D_{22} is usually equal to zero because the plant model is strictly proper. However, it may be non zero when we transform a discrete-time system to a continuous-time system. In this case, we can remove D_{22} from the plant model and re-inject it into the controller afterward. It means that we can solve the problem for $D_{22} = 0$ and compute the controller K_0 and then the final controller is: $K = K_0(I + D_{22}K_0)^{-1}$. The assumption on $D_{11} = 0$ is just for simplicity of the solution formulas and can be relaxed.

A suboptimal $\mathcal{H}_\infty$ can be computed for the augmented plant in (2.10) under the following extra assumption just for simplifying the solution:

(A5) $D_{12}^T \begin{bmatrix} C_1 & D_{12} \end{bmatrix} = \begin{bmatrix} 0 & I \end{bmatrix}$ and $\begin{bmatrix} B_1 \\ D_{21} \end{bmatrix} D_{21}^T = \begin{bmatrix} 0 \\ I \end{bmatrix}$

Theorem 2.1. *[9] Under Assumptions A1 to A5 for the augmented plant in (2.10), there exists a suboptimal controller such that $\|T_{zw}\|_\infty < \gamma$ if and only if there exist $Y \succ 0$ and $X \succ 0$ such that:*

$$XA + A^TX + X(\gamma^{-2}B_1B_1^T - B_2B_2^T)X + C_1^TC_1 \prec 0$$
$$AY + YA^T + Y(\gamma^{-2}C_1^TC_1 - C_2^TC_2)Y + B_1B_1^T \prec 0$$
$$\rho(XY) < \gamma^2$$

where $\rho(\cdot) = |\lambda_{\max}(\cdot)|$ is the spectral radius of a matrix. Moreover, when these conditions hold, the parameters of the state space representation of such controller are:

$$A_K = A + \gamma^{-2}B_1B_1^TX - B_2B_2^TX - (I - \gamma^{-2}YX)^{-1}YC_2^TC_2$$
$$B_K = (I - \gamma^{-2}YX)^{-1}YC_2^T$$
$$C_K = -B_2^TX$$
$$D_K = 0$$

The proof of this theorem can be found in [9]. This problem can be solved using the Matlab command `K=hinfsyn(P)`. In the sequel, it is illustrated how a robust controller can be designed for a system with multimodel uncertainty using the $\mathcal{H}_\infty$ control theory.

Example 2.4. Consider an unstable system $G_n(s) = \frac{2}{s-2}$ as the nominal model with the following multimodel uncertainty:

Extra lag:	$G_1(s) = \frac{2}{(0.06s+1)(s-2)}$
Time delay:	$G_2(s) = \frac{2e^{-0.02s}}{(s-2)}$
High frequency resonance:	$G_3(s) = \frac{2}{s-2}\frac{2500}{(s^2+10s+2500)}$
High frequency resonance:	$G_4(s) = \frac{2}{s-2}\frac{4900}{(s^2+28s+4900)}$
Pole/gain migration:	$G_5(s) = \frac{2.4}{(s-2.2)}$
Pole/gain migration:	$G_6(s) = \frac{1.6}{(s-1.8)}$

A stabilizing controller should be designed to achieve a closed-loop bandwidth of ω_b =10 rad/s and a modulus margin of at least 0.5 for all plant models.

Solution: We start with designing the performance filter to achieve a bandwidth of 10 rad/s and a modulus margin of at least $m = 0.5$. Note that the closed-loop bandwidth is usually higher than the attenuation band ω_a, that is the maximum frequency at which the magnitude of $|\mathcal{S}(j\omega)|$ <-3dB for all $0 < \omega < \omega_a$. For a modulus margin of at least m, we should guarantee that $\max_\omega |\mathcal{S}(j\omega)| < 1/m$. These two conditions are met, if we choose $W^{-1}(s)$ as:

$$W_1^{-1}(s) = \frac{s}{m(s+\omega_b)} = \frac{2s}{s+10}$$

and guarantee that $\|W_1\mathcal{S}\|_\infty < 1$.

In order to satisfy these conditions for all plant model, we should transform the multimodel uncertainty to multiplicative uncertainty and compute the filter $W_2(s)$. Then if $\|W_2\mathcal{T}\|_\infty < 1$ is satisfied we obtain robust stability. For robust performance the mixed sensitivity $\|[W_1\mathcal{S} \quad W_2\mathcal{T}]\|_\infty < 1/\sqrt{2}$ should be satisfied.

In order to compute the uncertainty filter $W_2(s)$, we use the following Matlab code:

```
s=tf('s');
Gn = 2/(s-2);                          % nominal model
G1 = Gn/(0.06*s+1);                    % extra lag
G2 = Gn*(50-s)/(s+50);                 % time delay (Pade approximation)
G3 = Gn*50^2/(s^2+2*.1*50*s+50^2);     % high frequency resonance
G4 = Gn*70^2/(s^2+2*.2*70*s+70^2);     % high frequency resonance
G5 = 2.4/(s-2.2);                      % pole/gain migration
G6 = 1.6/(s-1.8);                      % pole/gain migration

% command to gather the plant models G1 through G6 into one array.

G = stack(1,G1,G2,G3,G4,G5,G6);

% Try a 4th-order filter W2 for Multiplicative uncertainty:

orderW2 = 4;
Gf = frd(G,logspace(-1,3,60));
[Gu,Info] = ucover(Gf,Gn,orderW2,'InputMult');
W2 = Info.W1;
bodemag((Gn-Gf)/Gn,'b--',W2,'r'); grid
```

Note that for $G_2(s)$, the time delay is approximated by a first order Padé function. The Bode plot of the uncertainty filter is given in Fig. 2.8. The following code is used to solve the mixed sensitivity problem:

```
W1=(s+10)/2/(s+0.000001);
K=mixsyn(Gn,W1,[],W2);
```

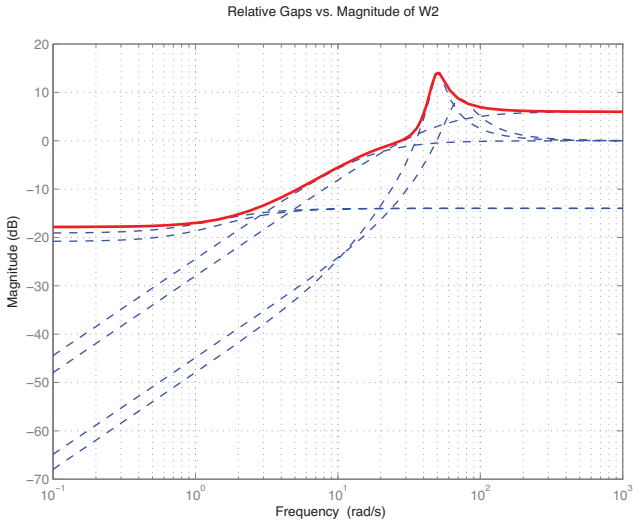

Figure 2.8: The magnitude Bode diagram of the uncertainty filter

Note that since $W_1(s)$ has an integrator, the pole at zero is slightly moved to satisfy Assumptions A3 and A4. The performance of the final controller is illustrated by the step response of the closed-loop system and the control signal in Fig. 2.9. The magnitude Bode plot of the sensitivity function $\mathcal{S}$ is shown in the same figure together with that of the inverse of $W_1(s)$ to show that the robust performance is achieved. It can be seen, however, that the control signal is too large and therefore the controller cannot be implemented in a real experiment. We observe also that, in the same figure, the magnitude of the input sensitivity function $\mathcal{U}$ is too large in high frequency. This will amplify the high frequency measurement noise at the input of the plant. These problems can be fixed by adding $\|W_3\,\mathcal{U}\|_\infty$ to the mixed sensitivity problem. For example, the results can be improved if we choose $W_3(s) = 1/15$ and the following code:

```
W1=(s+10)/2/(s+0.000001);
W3=1/15;
K=mixsyn(Gn,W1,W3,W2);
```

The improved results are shown in Fig. 2.10. It can be seen that the control signal has been significantly reduced and the maximum of the magnitude of $\mathcal{U}$ is much less than that of the initial design.

2.3.4 $\mathcal{H}_2$ Optimal Control

The $\mathcal{H}_2$ control problem and its solution are given in the following theorem [9]:

Theorem 2.2. *Given the augmented plant model in (2.10) together with Assumptions A1 to A4, the controller K stabilizes P internally and minimizes the $\mathcal{H}_2$ norm of the transfer*

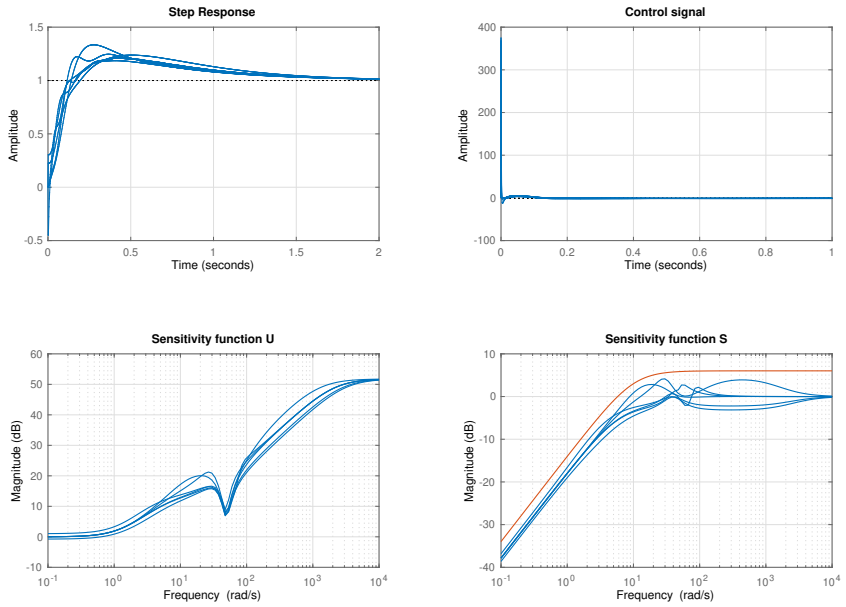

Figure 2.9: Step response, control signal, the sensitivity functions $\mathcal{U}$ and $\mathcal{S}$ for the initial design

matrix T_{zw} from w to z, if and only if there exist $X \succ 0$ and $Y \succ 0$ such that

$$XA_1 + A_1^T X - XB_2 R_1^{-1} B_2^T X + C_1^T (I - D_{12} R_1^{-1} D_{12}^T) C_1 \prec 0$$

$$YA_2^T + A_2 Y - YC_2^T R_2^{-1} C_2 Y + B_1 (I - D_{21}^T R_2^{-1} D_{21}) B_1^T \prec 0$$

where

$$\begin{aligned} A_1 &= A - B_2 R_1^{-1} D_{12}^T C_1 \\ A_2 &= A - B_1 D_{21}^T R_2^{-1} C_2 \\ R_1 &= D_{12}^T D_{12} \quad , \quad R_2 = D_{21} D_{21}^T \end{aligned}$$

Moreover, the parameters of the state space model of such controller are:

$$\begin{aligned} A_K &= A - B_2 R_1^{-1} (B_2^T X + D_{12}^T C_1) - (YC_2^T + B_1 D_{21}^T) R_2^{-1} C_2 \\ B_K &= (YC_2^T + B_1 D_{21}^T) R_2^{-1} \\ C_K &= -R_1^{-1} (B_2^T X + D_{12}^T C_1) \quad , \quad D_K = 0 \end{aligned}$$

The proof of this theorem can be found in [9].

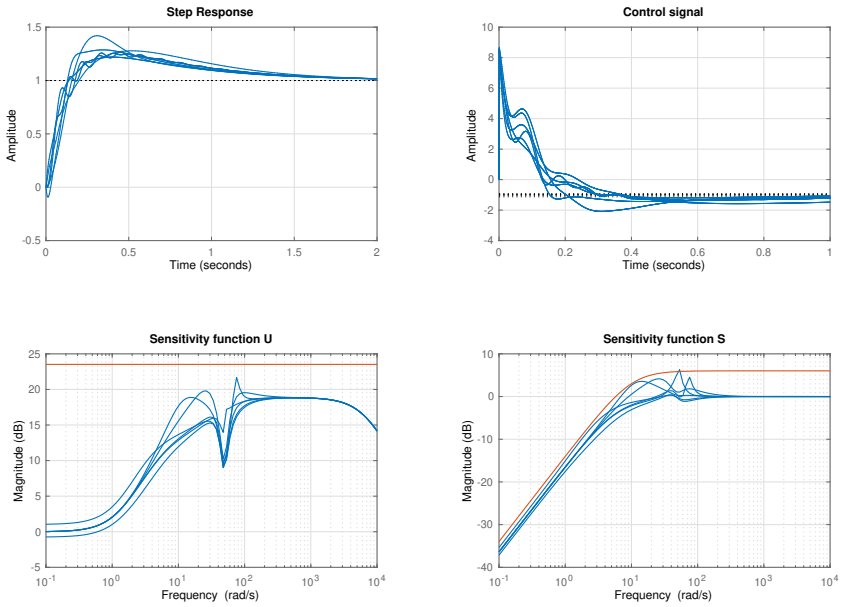

Figure 2.10: Step response, control signal, the sensitivity functions $\mathcal{U}$ and $\mathcal{S}$ for the improved design

2.4 Data-Driven Control

Most controller design methods are based on plant parametric models. A parametric model can be obtained either by first principles modelling or by parameter estimation techniques using measured data. However, it is usually too difficult or time consuming to obtain a parametric model based on physical laws. On the other hand, identification of parametric models is based on several a priori information and user choices like sampling period, time-delay, number of parameters in numerator and denominator of plant and noise model, optimal excitation etc. For these reasons, some data-based methods (in time-domain or in frequency-domain) for controller design have been developed.

Frequency-domain data or spectral models can be easily obtained from input/output data using Fourier or spectral analysis. In this type of models the information is not condensed into a small set of parameters thus avoiding errors of unmodelled dynamics that appear in parametric models. Moreover, an estimate of the uncertainty due to noise can be readily computed.

Although spectral models are largely used in practice, controller design methods based on this type of models are rather limited. These approaches are very intuitive and work well for simple systems that can be approximated by a low-order model with relatively small delay. For unstable and nonminimum-phase systems and systems with parametric and frequency-domain uncertainty, more advanced methods should be used.

Recent developments in the fields of numerical optimization, computer technology, and sensor technology have significantly reduced the computational time of optimization algorithms and increased the availability of large amounts of measured data during a system's operation. These advances make computationally demanding data-driven control design approaches a viable alternative to classical model-based control problems.

This section presents a new approach for designing robust fixed-order controllers. The approach demonstrates that convex optimization can compute robust fixed-order controllers for Linear Time Invariant (LTI) systems represented by nonparametric spectral models. The method is versatile and can be used for designing Proportional-Integral-Derivative (PID) controllers as well as higher order controllers in discrete or continuous time. An important feature of the proposed approach is its ability to treat multimodel uncertainty and systems with time-delay in a straightforward manner.

2.4.1 Frequency Response Data

The system to be controlled is a Linear Time-Invariant Multi-Input Multi-Output (LTI-MIMO) system, and is represented very generally by a multivariable frequency response model $G(j\omega) \in \mathbb{C}^{n\times m}$, where n is the number of outputs and m the number of inputs. The frequency response $G(j\omega)$ is assumed to be bounded in all frequencies. This condition can be relaxed if G has some poles on the stability boundary (the imaginary axis for continuous-time, or the unit circle for discrete-time systems).

The frequency response can be obtained from a parametric model by evaluating:

$$G(j\omega) = G(s = j\omega), \quad \omega \in \Omega = \{\omega \,|-\infty < \omega < \infty\}$$
$$G(e^{j\omega T_s}) = G(z = e^{j\omega T_s}), \quad \omega \in \Omega = \left\{\omega \,\middle|-\frac{\pi}{T_s} \leq \omega \leq \frac{\pi}{T_s}\right\}$$

for continuous-time and discrete-time models respectively, where T_s is the sampling time. A notable advantage of frequency response models as compared to state-space models is that time-delays can be considered exactly, and no approximation is required.

Following a data-driven approach, the frequency response model can also be identified directly from time-domain measurement data using the Fourier analysis method from m sets of input/output sampled data as:

$$G(e^{j\omega T_s}) = \left[\sum_{k=0}^{N-1} \mathbb{Y}(k) e^{-j\omega T_s k}\right] \left[\sum_{k=0}^{N-1} \mathbb{U}(k) e^{-j\omega T_s k}\right]^{-1} \qquad \omega \in \Omega_g$$

where N is the number of data points for each experiment, $\mathbb{U}(k) \in \mathbb{R}^{n_u \times n_u}$ includes the inputs at instant k, $\mathbb{Y}(k) \in \mathbb{R}^{n_y \times n_u}$ the outputs at instant k and T_s is the sampling period. Note that at least n_u different experiments are needed to extract G from the data (each column of $\mathbb{U}(k)$ and $\mathbb{Y}(k)$ represents respectively the input and the output data from one experiment). In order to obtain an accurate model, the input data should have a rich

frequency spectrum such as e.g. a PRBS signal, a sum of sinusoids or a frequency sweep. The main advantage of directly using frequency-domain data is that a parametric model of the plant is not required, and there are no unmodeled dynamics. The only source of uncertainty for an LTI system is the measurement noise, whose influence can be reduced significantly if the amount of measurement data is large.

2.4.2 Controller Structure

In this section, δ will be used to denote both the Laplace variable in the continuous-time case and the z-transform variable in the discrete-time case. The controller structure is chosen as $K = X(\delta)Y^{-1}(\delta)$ where $X(\delta)$ and $Y(\delta)$ are transfer function matrices with bounded infinity norm that are affine with respect to the controller parameters (optimization variables). They can be defined as

$$X(\delta) = \sum_{k=0}^{n} X_k \cdot \frac{\delta^k}{p(\delta)} \tag{2.11}$$

$$Y(\delta) = \sum_{k=0}^{n} Y_k \cdot \frac{\delta^k}{p(\delta)} \tag{2.12}$$

where $p(\delta)$ is a stable polynomial. A possible choice is $p(\delta) = (\delta - \alpha)^n$, $\alpha < 0$ for continuous-time, or $|\alpha| < 1$ for discrete-time systems. Moreover, Y is restricted to be diagonal to avoid increasing the degree of Y when inverted. The final controller is not sensitive to the choice of α as it will be cancelled when forming XY^{-1}. However, its main role is to normalize the constraints and improve the numerical accuracy of the optimization solvers.

This controller structure is very general and covers centralized, decentralized and distributed control structures, as will be shown in the following examples.

Example 2.5. PID controller: In continuous-time, a multivariable PID controller

$$K = XY^{-1} = K_p + \frac{K_i}{s} + K_d\, s\,(T_f s + I)^{-1}$$

corresponds to a fixed-degree controller with $n = 2$, $Y_0 = \mathbf{0}$ and Y_1 and Y_2 diagonal. Show that the PID coefficients can be obtained from X_k, Y_k as follows: $T_f = Y_2 Y_1^{-1}$, $K_i = X_0 Y_1^{-1}$, $K_p = X_1 Y_1^{-1} - K_i T_f$ and $K_d = X_2 Y_1^{-1} - K_p T_f$.

Example 2.6. Distributed controller: Different actuators may be located physically far apart, and the various control inputs can only be computed using a subset of all measurements. Controllers for a distributed control system with ℓ nodes can be designed by choosing Y_k as block diagonal matrices with $\ell \times \ell$ partitions which leads to a block diagonal Y. X is chosen such that the off-diagonal block X_k^{ij} is $\mathbf{0}$ if there is no communication of information from node j to node i. For decentralised controls, all off-diagonal blocks

would be zero. For example, consider a distributed control system with 3 nodes and a communication infrastructure providing bidirectional communication between nodes 1 and 2, and between nodes 2 and 3. Then the partitioned X_k and Y_k for $k \in \{0, 1, \ldots, n\}$ are given by

$$X_k = \begin{bmatrix} X_k^{11} & X_k^{12} & \mathbf{0} \\ X_k^{21} & X_k^{22} & X_k^{23} \\ \mathbf{0} & X_k^{32} & X_k^{33} \end{bmatrix} \tag{2.13}$$

$$Y_k = \begin{bmatrix} Y_k^{11} & \mathbf{0} & \mathbf{0} \\ \mathbf{0} & Y_k^{22} & \mathbf{0} \\ \mathbf{0} & \mathbf{0} & Y_k^{33} \end{bmatrix} \tag{2.14}$$

where red boxes indicate the controllers that use local measurements while blue boxes indicate the controllers that use information from other nodes.

Example 2.7. State-space controller: For designing a state-space controller of order n we can choose :

$$X(\delta) = C_1(\delta I - A)^{-1}B + D_1 \tag{2.15}$$
$$Y(\delta) = C_2(\delta I - A)^{-1}B + D_2 \tag{2.16}$$

where $A \in \mathbb{R}^{n\times n}$ and $B \in \mathbb{R}^{n\times n_y}$ are fixed and can be freely chosen, with only the requirement that A is stable, the pair (A, B) is controllable, and B full column rank. The optimization variables are C_1, C_2, D_1 and D_2 which leads to an affine parametrization of X and Y. A minimal realization of $K = XY^{-1}$ is given by

$$K = \left[\begin{array}{c|c} A - BD_2^{-1}C_2 & BD_2^{-1} \\ \hline C_1 - D_1D_2^{-1}C_2 & D_1D_2^{-1} \end{array}\right] \tag{2.17}$$

2.4.3 Control Performance

This section demonstrates how classical loop-shaping, $\mathcal{H}_2$, and $\mathcal{H}_\infty$ control performance constraints can be converted into constraints on the spectral norm of systems. To proceed, let's consider the following Quadratic Matrix Inequality (QMI):

$$\begin{bmatrix} A & B \\ B^* & \Phi^*\Phi \end{bmatrix} \succ 0 \tag{2.18}$$

where A is a positive definite matrix belonging to $\mathbb{R}^{n\times n}$ and $B, \Phi \in \mathbb{C}^{n\times n}$ are linear in the optimization variables. The Schur complements of this QMI are:

$$\Phi^*\Phi - B^*A^{-1}B \succ 0 \tag{2.19}$$
$$A - B(\Phi^*\Phi)^{-1}B^* \succ 0 \tag{2.20}$$

This type of constraints is called a convex-concave constraint and can be convexified using the following lemma:

Lemma 2.5. *The QMI in (2.18) or its Schur complements in (2.19) and (2.20) have at least a feasible solution if the following LMI is satisfied:*

$$\begin{bmatrix} A & B \\ B^* & \Phi^*\Phi_c + \Phi_c^*\Phi - \Phi_c^*\Phi_c \end{bmatrix} \succ 0 \tag{2.21}$$

where $\Phi_c \in \mathbb{C}^{n\times n}$ is any known matrix.

Proof. The proof uses the following inequality:

$$\Phi^*\Phi \succeq \Phi^*\Phi_c + \Phi_c^*\Phi - \Phi_c^*\Phi_c \tag{2.22}$$

which comes directly from the expansion of

$$(\Phi - \Phi_c)^*(\Phi - \Phi_c) \succeq 0$$

It is clear that in $\Phi^*\Phi - B^*A^{-1}B \succ 0$ we can replace $\Phi^*\Phi$ with a smaller or equal value (i.e. the right side of 2.22), which leads to (2.21) using Schur Lemma. □

The upcoming sections will present the convex formulation of various performance specifications that are commonly used in robust control. However, it is important to note that the method is not limited only to the presented specifications. Essentially, any $\mathcal{H}_\infty$ or $\mathcal{H}_2$ objective or constraint on any weighted transfer function can be formulated within the presented framework. This results in a highly flexible and powerful tool that is suitable for a wide range of applications.

Furthermore, the performance objectives are generally specified through weighting filters $W(j\omega)$. These weighting filters can be defined e.g. as transfer functions, scalar values, or even arbitrary non-smooth functions such as piece-wise continuous functions, which greatly simplifies the problem formulation.

$\mathcal{H}_\infty$ Performance

Constraints on the infinity-norm of any weighted sensitivity function can be considered. For example, consider the following design objective:

$$\min_K \|W_1\mathcal{S}\|_\infty$$

where $\mathcal{S} = (I + GK)^{-1}$ is the sensitivity function and W_1 is a performance weight. The infinity norm of a stable system is equal to:

$$\|H\|_\infty = \max_{\omega\in\Omega} \sigma_{\max}(H(j\omega))$$

where $\sigma_{\max}$ is the maximum singular value of a matrix. Therefore, this problem can be converted to an optimization problem on the spectral norm as:

$$\begin{aligned} &\min_{K} \gamma \\ &\text{subject to:} \\ &(W_1\mathcal{S})(W_1\mathcal{S})^* \prec \gamma I, \qquad \forall \omega \in \Omega \end{aligned} \tag{2.23}$$

where $\gamma \in \mathbb{R}$ is an auxiliary scalar variable and * stands for complex conjugate transpose. Note that the argument $j\omega$ has been omitted for $W_1(j\omega)$, $\mathcal{S}(j\omega)$ and $K(j\omega)$ in order to simplify the notation. The above constraint can be rewritten as:

$$[W_1(I+GK)^{-1}][W_1(I+GK)^{-1}]^* \prec \gamma I$$

Replacing $K = XY^{-1}$, we obtain:

$$W_1Y(Y+GX)^{-1}[(Y+GX)^{-1}]^*(W_1Y)^* \prec \gamma I$$

Then, taking $\Phi = Y + GX$, we can rewrite the above inequality as:

$$\gamma I - W_1Y(\Phi^*\Phi)^{-1}(W_1Y)^* \succ 0$$

which has exactly the same form as (2.20). Therefore, Lemma 2.5, can be used to find the following convex optimization problem:

$$\begin{aligned} &\min_{X,Y} \gamma \\ &\text{subject to:} \\ &\begin{bmatrix} \gamma I & W_1Y \\ (W_1Y)^* & \Phi^*\Phi_c + \Phi_c^*\Phi - \Phi_c^*\Phi_c \end{bmatrix} \succ 0 \ , \ \forall \omega \in \Omega \end{aligned} \tag{2.24}$$

where $\Phi_c = Y_c + GX_c$ is chosen based on an initial controller $K_c = X_cY_c^{-1}$. This convex constraint is a sufficient condition for the spectral constraint in (2.23) for any choice of initial controller $K_c = X_cY_c^{-1}$.

Analogously, the following $\mathcal{H}_\infty$ constraints on the weighted stable closed-loop sensitivity functions:

$$\|W_2\mathcal{T}\|_\infty < 1 \ , \quad \|W_3\mathcal{U}\|_\infty < 1$$

where $\mathcal{T} = GK(I+GK)^{-1}$, $\mathcal{U} = K(I+GK)^{-1}$ can be expressed as:

$$\begin{bmatrix} I & W_2GX \\ (W_2GX)^* & \Phi^*\Phi_c + \Phi_c^*\Phi - \Phi_c^*\Phi_c \end{bmatrix} \succ 0 \ , \ \forall \omega \in \Omega$$

$$\begin{bmatrix} I & W_3X \\ (W_3X)^* & \Phi^*\Phi_c + \Phi_c^*\Phi - \Phi_c^*\Phi_c \end{bmatrix} \succ 0 \ , \ \forall \omega \in \Omega$$

The derivation is straightforward and will be left as an exercise for the students.

Mixed sensitivity problem: Another classical example is the mixed sensitivity problem:

$$\min_K \left\| \begin{array}{c} W_1\mathcal{S} \\ W_3\mathcal{U} \end{array} \right\|_\infty \tag{2.25}$$

which can be written for stable closed-loop systems as minimizing γ subject to:

$$[W_1(I+GK)^{-1}]^*[W_1(I+GK)^{-1}] + [W_3K(I+GK)^{-1}]^*[W_3K(I+GK)^{-1}] \prec \gamma I$$

for all $\omega \in \Omega$. Replacing again $K = XY^{-1}$ and $\Phi = Y + GX$ we obtain:

$$Y^*W_1^*\gamma^{-1}W_1Y + X^*W_3^*\gamma^{-1}W_3X - \Phi^*\Phi \prec 0$$

This inequality can be rewritten as:

$$\Phi^*\Phi - \left[\begin{array}{c} W_1Y \\ W_3X \end{array} \right]^* \left[\begin{array}{cc} \gamma I & 0 \\ 0 & \gamma I \end{array} \right]^{-1} \left[\begin{array}{c} W_1Y \\ W_3X \end{array} \right] \succ 0$$

which has exactly the form of (2.19). Then using Lemma 2.5, it can be converted to the following optimization problem:

$$\begin{array}{c} \min\limits_{X,Y} \gamma \\ \left[\begin{array}{ccc} \Phi^*\Phi_c + \Phi_c^*\Phi - \Phi_c^*\Phi_c & (W_1Y)^* & (W_3X)^* \\ W_1Y & \gamma I & 0 \\ W_3X & 0 & \gamma I \end{array} \right] \succ 0 \qquad \forall \omega \in \Omega \end{array} \tag{2.26}$$

$\mathcal{H}_2$ Performance

The method can also accommodate $\mathcal{H}_2$ control performance objectives. As an example, consider the following $\mathcal{H}_2$ control performance for a stable, discrete-time system:

$$\min_K \|W_1\mathcal{S}\|_2^2 = \min_K \int_{-\frac{\pi}{T_s}}^{\frac{\pi}{T_s}} \text{trace}[(W_1(I+GK)^{-1})^*W_1(I+GK)^{-1}]d\omega$$

This is equivalent to:

$$\min_K \int_{-\frac{\pi}{T_s}}^{\frac{\pi}{T_s}} \text{trace}[\Gamma(\omega)]d\omega$$

subject to:

$$\left[W_1(I+GK)^{-1}\right)^* \left(W_1(I+GK)^{-1}\right] \prec \Gamma(\omega) \ , \ \forall \omega \in \Omega$$

where $\Gamma(\omega) \succ 0$ is an unknown matrix function $\in \mathbb{C}^{n\times n}$. Replacing K with XY^{-1} and $\Phi = Y + GX$ in the above inequality, we obtain:

$$W_1Y(\Phi^*\Phi)^{-1}(W_1Y)^* \prec \Gamma(\omega)$$

which, using Lemma 2.5, leads to the following convex problem:

$$\min_{X,Y,\Gamma(\omega)} \int_{-\frac{\pi}{T_s}}^{\frac{\pi}{T_s}} \text{trace}[\Gamma(\omega)] d\omega$$

$$\begin{bmatrix} \Gamma(\omega) & W_1 Y \\ (W_1 Y)^* & \Phi^*\Phi_c + \Phi_c^*\Phi - \Phi_c^*\Phi_c \end{bmatrix} \succ 0, \quad \forall \omega \in \Omega$$

Remark: The unknown function $\Gamma(\omega)$ can be approximated by a polynomial function of finite order as:

$$\Gamma(\omega) = \Gamma_0 + \Gamma_1 \omega + \cdots + \Gamma_h \omega^h$$

In case the constraints are evaluated for a finite set of frequencies

$$\Omega_g = \{\omega_1, \ldots, \omega_g\}$$

$\Gamma(\omega)$ can also be replaced with a matrix variable Γ_k at each frequency ω_k.

Loop Shaping

Assume that a desired loop transfer function L_d is available and that the objective is to design a controller K such that the loop transfer function $L = GK$ is close to L_d in the 2- or ∞-norm sense.

∞-Norm: The objective function for the ∞-norm case is to minimize:

$$\min_K \|L - L_d\|_\infty$$

and can be expressed as follows:

$$\min_K \gamma$$
$$(GK - L_d)(GK - L_d)^* \prec \gamma I \ , \ \forall \omega \in \Omega$$

Replacing K with XY^{-1} in the constraint, we obtain:

$$\gamma I - (GX - L_d Y)(Y^*Y)^{-1}(GX - L_d Y)^* \succ 0 \qquad \forall \omega \in \Omega$$

Again using Lemma 2.5 the following convex formulation is obtained:

$$\min_{X,Y} \gamma$$

$$\begin{bmatrix} \gamma I & GX - L_d Y \\ (GX - L_d Y)^* & Y^*Y_c + Y_c^*Y - Y_c^*Y_c \end{bmatrix} \succ 0 \qquad \forall \omega \in \Omega$$

2-Norm: In a similar way, minimizing $\|L - L_d\|_2^2$ can be written as:

$$\min_{X,Y} \int_{-\frac{\pi}{T_s}}^{\frac{\pi}{T_s}} \text{trace}[\Gamma(\omega)] d\omega$$

$$(GK - L_d)(GK - L_d)^* \prec \Gamma(\omega) \ , \ \forall \omega \in \Omega$$

Then, the constraint can be reformulated as:

$$(GX - L_dY)(Y^*Y)^{-1}(GX - L_dY)^* \prec \Gamma(\omega)$$

and using Lemma 2.5, the following convex optimization problem can be solved:

$$\min_{X,Y} \int_{-\frac{\pi}{T_s}}^{\frac{\pi}{T_s}} \text{trace}[\Gamma(\omega)] d\omega$$

$$\begin{bmatrix} \Gamma(\omega) & GX - L_dY \\ (GX - L_dY)^* & Y^*Y_c + Y_c^*Y - Y_c^*Y_c \end{bmatrix} \succ 0 \qquad \forall \omega \in \Omega \tag{2.27}$$

Multimodel Uncertainty

The case of robust control design with multimodel uncertainty is very easy to incorporate in the given framework. Systems that have different frequency responses in q different operating points can be represented by a multimodel uncertainty set:

$$\mathbb{G}(e^{j\omega}) = \{G_1(e^{j\omega}), G_2(e^{j\omega}), \ldots, G_q(e^{j\omega})\}$$

Note that the models may have different orders and may contain pure input/output time delays. This can be implemented by formulating a different set of constraints for each of the models. Let $P_i = Y + G_iX$ and $P_{c_i} = X_{c,i} + G_iY_{c,i}$, where $K_{c,i}$ is a stabilizing controller for model G_i. Again taking the mixed sensitivity problem from (2.26) as an example, the formulation of this problem would be:

$$\min_{X,Y} \gamma$$

subject to:

$$\begin{bmatrix} \Phi_i^*\Phi_{c_i} + \Phi_{c_i}^*\Phi_i - \Phi_{c_i}^*\Phi_{c_i} & (W_1Y)^* & (W_2X)^* \\ W_1Y & \gamma I & 0 \\ W_2X & 0 & \gamma I \end{bmatrix} \succ 0$$

for $i = 1, \ldots, q \quad ; \quad \forall \omega \in \Omega$

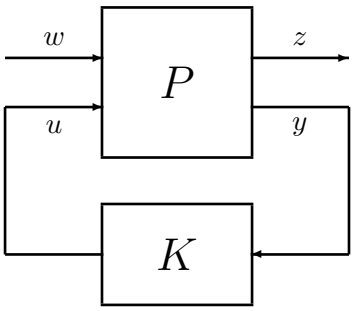

Figure 2.11: Linear fractional transform interconnection of system and controller

2.4.4 LFT Framework

A generalized Linear Time-Invariant (LTI) system, mapping exogenous disturbances $w \in \mathbb{R}^{n_w}$ and control inputs $u \in \mathbb{R}^{n_u}$ to performance channels $z \in \mathbb{R}^{n_z}$ and measurements $y \in \mathbb{R}^{n_y}$ is given as follows:

$$\begin{aligned} z &= P_{11}w + P_{12}u \\ y &= P_{21}w + P_{22}u \end{aligned} \tag{2.28}$$

We assume that only the FRF of the generalized system

$$P(j\omega) = \begin{bmatrix} P_{11}(j\omega) & P_{12}(j\omega) \\ P_{21}(j\omega) & P_{22}(j\omega) \end{bmatrix} \tag{2.29}$$

is available, where $P_{ij}(j\omega)$ are FRFs of appropriate size. The frequency response of the (discrete-time) plant $P_{22} = -G$ can be estimated using the Fourier analysis method from n_u sets of finite input/output sampled data.

The synthesis objective is to design a fixed-structure feedback controller K that regulates the effect of the exogenous disturbances w onto the performance channels z. The corresponding block-diagram, shown in 2.11, is commonly referred to as a lower linear fractional transformation (LFT) and is given by

$$T_{zw} = P_{11} + P_{12}K(I - P_{22}K)^{-1}P_{21}. \tag{2.30}$$

Under the assumption that the closed-loop system is stable, the norm of T_{zw} can be expressed using only its FRF:

$$\|T_{zw}\|_2^2 = \frac{1}{2\pi}\int_{\Omega} \operatorname{trace}\left(T_{zw}(j\omega)T_{zw}^*(j\omega)\right) d\omega \tag{2.31}$$

$$\|T_{zw}\|_\infty^2 = \sup_{\omega\in\Omega} \overline{\sigma}\left(T_{zw}(j\omega)T_{zw}^*(j\omega)\right) \tag{2.32}$$

The controller design problem can be formulated as the minimization of an upper bound

on the system norms

$$\begin{array}{rl} & \min\limits_{K,\,\Gamma}\ \gamma \\ \text{subject to :} & K \text{ stabilizes the closed-loop} \\ & T_{zw}(j\omega)T_{zw}^{*}(j\omega) \preceq \Gamma(j\omega), \quad \forall\omega \in \Omega \end{array} \tag{2.33}$$

For the $\mathcal{H}_\infty$ norm, $\Gamma(j\omega) = \gamma I$, where $\gamma \in \mathbb{R}$ and for the $\mathcal{H}_2$ norm, we have:

$$\gamma = \frac{1}{2\pi}\int_{\Omega} \text{trace}\left(\Gamma(j\omega)\right) d\omega \tag{2.34}$$

The following assumptions will be made for the generalized plant model:

A1 One of the following is true

- **(a)** $P_{21}(j\omega)$ has full row rank $\forall\omega \in \Omega$.
- **(b)** $P_{12}(j\omega)$ has full column rank $\forall\omega \in \Omega$.

A2 $P(j\omega)$ is bounded for all $\omega \in \Omega$.

Remark: A1 is related to the control performance specifications, and similar equivalent assumptions exist on the rank of some matrices in the state-space model-based approaches. A1(a) is made to ensure that any possible disturbances have an effect on the measurements. Such a situation, from a control design perspective, indicates that either more sensors or better placement is required for the desired objective. Similarly, A1(b) ensures that any possible control input has an effect on the performance channels, and its relaxation indicates the need for a better selection of performance channels.

Assume that G_{21} has full row rank and the controller is factorized as $K = XY^{-1}$. However, if G_{21} is not full row rank but $P_{12}(j\omega)$ has full column rank a controller factorization as $K = Y^{-1}X$ can be used for the problem.

Then, the transfer function T_{zw} can be rewritten as

$$T_{zw} = P_{11} + P_{12}X\left(Y - P_{22}X\right)^{-1}P_{21} \tag{2.35}$$

Since P_{21} has full row rank, its right inverse $P_{21}^{\mathsf{R}} = P_{21}^{*}(P_{21}P_{21}^{*})^{-1}$ exists, and we can define

$$\Phi = P_{21}^{\mathsf{R}}\left(Y - P_{22}X\right) \tag{2.36}$$

which is linear in controller parameters. If Φ has full column rank, i.e., the feedback interconnection is well-posed, its left inverse $\Phi^{\mathsf{L}} = (\Phi^{*}\Phi)^{-1}\Phi^{*}$ is given by $\left(Y - P_{22}X\right)^{-1}P_{21}$. Denoting $\Psi = I - \Phi\Phi^{\mathsf{L}} = I - P_{21}^{\mathsf{R}}P_{21}$, then the closed-loop transfer function can be written as

$$\begin{aligned} T_{zw} &= P_{11} + P_{12}X\Phi^{\mathsf{L}} = P_{11}(\Phi\Phi^{\mathsf{L}} + \Psi) + P_{12}X\Phi^{\mathsf{L}} \\ &= \left(P_{11}\Phi + P_{12}X\right)\Phi^{\mathsf{L}} + P_{11}\Psi \end{aligned} \tag{2.37}$$

The inequality in (2.33) can then be reformulated as

$$T_{zw}T_{zw}^{*} = (P_{11}\Phi + P_{12}X)\,(\Phi^{*}\Phi)^{\mathsf{L}}\,(P_{11}\Phi + P_{12}X)^{*} + (P_{11}\Psi)\,(P_{11}\Psi)^{*} \preceq \Gamma \tag{2.38}$$

using the fact that $\Phi^{\mathsf{L}}\Psi^{*} = \Phi^{\mathsf{L}}\Psi = \Phi^{\mathsf{L}} - \Phi^{\mathsf{L}}\Phi\Phi^{\mathsf{L}} = \mathbf{0}$. Since P_{21} was assumed to have full row rank, $\Phi^{*}\Phi$ is a full rank square matrix and $(\Phi^{*}\Phi)^{\mathsf{L}} = (\Phi^{*}\Phi)^{-1}$. Using the Schur complement lemma on (2.38) results in

$$\begin{bmatrix} \Gamma - \Lambda & (P_{11}\Phi + P_{12}X) \\ \star & \Phi^{*}\Phi \end{bmatrix} \succeq \mathbf{0} \tag{2.39}$$

where $\Lambda = (P_{11}\Psi)\,(P_{11}\Psi)^{*}$. Using Lemma 2.5, and subject to closed-loop stability, the synthesis problem can be written as the following convex optimization problem:

$$\begin{aligned} &\min_{X,Y,\Gamma}\ \gamma \\ &\text{subject to} \\ &\begin{bmatrix} \Gamma - \Lambda & (P_{11}\Phi + P_{12}X) \\ \star & \Phi^{*}\Phi_c + \Phi_c^{*}\Phi - \Phi_c^{*}\Phi_c \end{bmatrix}(j\omega) \succeq \mathbf{0}, \forall\omega \in \Omega \end{aligned} \tag{2.40}$$

where the choice of Φ_c is an important factor in guaranteeing closed-loop stability.

2.4.5 Stability Analysis

The stability of the closed-loop system is not necessarily guaranteed even if the spectral norm of a weighted sensitivity function is bounded. In fact, an unstable system with no pole on the stability boundary has a bounded spectral norm. In this section, we show that the closed-loop stability can be guaranteed if some conditions in the linearization of the constraints are met. More precisely, the initial controller $K_c = X_cY_c^{-1}$ plays an important role in guaranteeing the stability of the closed-loop system with the resulting controller K.

The stability analysis is based on the Nyquist stability criterion for MIMO systems and winding number of complex functions around origin that are recalled here.

Definition 2.2. *Let $F(s)$ or $F(z)$ be a continuous- or discrete-time transfer function. Let wno$\{F\}$ be the winding number, in the counterclockwise sense, of the image of F around the origin when s or z traverses the Nyquist contour with some small detours around the poles of F on the stability boundary.*

Since the winding number is related to the phase of the complex function, we have the following properties:

$$\begin{aligned} \text{wno}\{F_1F_2\} &= \text{wno}\{F_1\} + \text{wno}\{F_2\} \\ \text{wno}\{F\} &= -\text{wno}\{F^{*}\} \\ \text{wno}\{F\} &= -\text{wno}\{F^{-1}\} \end{aligned}$$

Theorem 2.3. (Nyquist stability theorem) *The closed-loop system with the plant model G and the controller K is stable if and only if GK has no unstable hidden modes*[2]*, and the Nyquist plot of* $\det(I + GK)$

(a) *makes $N_G + N_K$ counterclockwise encirclements of the origin, where N_G and N_K are the number of unstable poles of G and K, and*

(b) *does not pass through the origin.*

Through Cauchy's argument principle, wno$\{f\}$ can be related to the number of poles and zeros of f inside the contour. This is used for the stability analysis of the closed-loop systems using the Nyquist stability criterion by defining an adequate Nyquist contour.

For continuous-time systems, the Nyquist contour is chosen as the union of the imaginary axis and a semicircle with an infinite radius enclosing the right-half plane. Since this contour is chosen clockwise oriented, wno$\{f\}$ will be equal to the number of unstable poles minus the number of unstable zeros. Note that, for a proper transfer function, the image of the semicircle with infinite radius will be constant and therefore the winding number when traversing the Nyquist contour or only the imaginary axis will be the same.

For discrete-time systems, the Nyquist contour is chosen as the counterclockwise-oriented unit circle. Therefore, the winding number is equal to the number of stable zeros minus the number of stable poles. However, if f is bi-proper, the difference in the number of stable zeros and stable poles is equal to the difference in the number of unstable poles and unstable zeros.Although the Nyquist contours are oriented differently in continuous- and discrete time, the wno in both cases is the number of unstable poles minus the number of unstable zeros. As a result, a single theorem can be used for the stability analysis of continuous- and discrete-time systems.

Main Stability Result

Using the Nyquist criterion, a single theorem can be used for the stability analysis of continuous- and discrete-time systems.

Theorem 2.4. *Given the frequency response $P(j\omega)$ of a generalized model satisfying the assumptions A1(a) and A2, the closed loop system with controller $K = XY^{-1}$ is stable if*

(C1): $\det(Y)$ *and* $\det(Y_c)$ *has no zeros on the stability boundary.*

[2]A hidden unstable mode is an unstable pole of GK that does not appear in $\det(GK)$. An example are pole-zero cancellations, or the following transfer function:

$$GK = \begin{bmatrix} \frac{1}{s+1} & \frac{1}{s-1} \\ 0 & \frac{1}{s+2} \end{bmatrix}$$

(C2): $\Phi^*\Phi_c + \Phi_c^*\Phi - \Phi_c^*\Phi_c \succeq 0 \quad \forall \omega \in \Omega$, *where* Φ *is defined in* (2.36) *and*

$$\Phi_c = P_{21}^{\mathsf{R}} \left(Y_c - P_{22} X_c\right) \tag{2.41}$$

with X_c, $Y_c \in \mathcal{RH}_\infty$ *such that* $K_c = X_c Y_c^{-1}$ *is a stabilizing controller.*

Proof. The winding number of the determinant of $\Phi^*\Phi_c$ is given by

$$\operatorname{wno}\{\det(\Phi^*\Phi_c)\} = \operatorname{wno}\left\{\prod_{i=1}^{n} \lambda_i\right\} = \sum_{i=1}^{n} \operatorname{wno}\{\lambda_i\} \tag{2.42}$$

where λ_i are the eigenvalues of $\Phi^*\Phi_c$. If the LMI in C2 holds, and given A1(a), $\Phi^*\Phi_c$ will be a non-Hermitian strictly positive definite matrix and all its eigenvalues have strictly positive real parts. Therefore, λ_i cannot wind around the origin and we must have $\operatorname{wno}\{\lambda_i\} = 0$. As a result $\mathcal{W}\{\Phi^*\Phi_c\} = 0$, where for conciseness $\mathcal{W}\{\cdot\}$ is defined as $\mathcal{W}\{\cdot\} := \operatorname{wno}\{\det(\cdot)\}$.

On the other hand, $\mathcal{W}\{\Phi^*\Phi_c\}$ can be rewritten as:

$$\begin{aligned} \underbrace{\mathcal{W}\{\Phi^*\Phi_c\}}_{=0} &= -\mathcal{W}\{Y - P_{22}X\} + \mathcal{W}\{P_{21}^{\mathsf{R}*}P_{21}^{\mathsf{R}}\} + \mathcal{W}\{Y_c - P_{22}X_c\} \\ &= -\mathcal{W}\{I - P_{22}K\} - \mathcal{W}\{Y\} + \mathcal{W}\{P_{21}^{\mathsf{R}*}P_{21}^{\mathsf{R}}\} + \mathcal{W}\{I - P_{22}K_c\} + \mathcal{W}\{Y_c\} \end{aligned} \tag{2.43}$$

By A1(a),A2 and C1, the Nyquist contour does not cross any zeros or poles, and the winding numbers in (2.43) are well-defined. From A1(a), $P_{21}^{\mathsf{R}*}P_{21}^{\mathsf{R}}$ is a strictly positive definite matrix in all frequencies as P_{21}^{R} has full column rank. Therefore,

$$\mathcal{W}\{P_{21}^{\mathsf{R}*}P_{21}^{\mathsf{R}}\} = 0 \tag{2.44}$$

Since K_c is a stabilizing controller, based on the Nyquist theorem, $\mathcal{W}\{I - P_{22}K_c\} = N_{P_{22}} + N_{K_c}$, where $N_{P_{22}}$ is the number of unstable poles of P_{22}, and N_{K_c} is the number of unstable poles of K_c. Furthermore, since $Y, Y_c \in \mathcal{RH}_\infty$, $\mathcal{W}\{Y\} = -N_K$ and $\mathcal{W}\{Y_c\} = -N_{K_c}$, where N_K is the number of unstable poles of the controller K. Now using (2.43) and (2.44), we obtain

$$\mathcal{W}\{I - P_{22}K\} = \mathcal{W}\{I - P_{22}K_c\} - \mathcal{W}\{Y\} + \mathcal{W}\{Y_c\} = N_{P_{22}} + N_K \tag{2.45}$$

thus K stabilizes the closed-loop system. □

If the LMI (2.40) holds, then C2 must also hold, as the last minor in (2.40) must also be strictly positive. Thus, closed-loop stability is ensured with the choice Φ_c as described in (2.41). The following remarks are in order:

Remark 1: Condition C1 can be removed with some (infinitely small) detours on the Nyquist contour, avoiding all zeros of $\det(Y)$ and $\det(Y_c)$. However, there is no need to evaluate $\text{wno}\{\det(\Phi^*\Phi_c)\}$ on the new contour because its variation around the zeros of $\det(Y)$ and $\det(Y_c)$ is small and can be ignored. Similarly, if P_{22} has some poles on the stability boundary, they can be avoided by some detours on the Nyquist contour. Again, there is no need to evaluate $\text{wno}\{\det(\Phi^*\Phi_c)\}$ on the additional detours because the contribution of $Y - P_{22}X$ and $Y_c - P_{22}X_c$ are equal (dominated by P_{22} around these poles) and therefore cancelled.

Remark 2: Note that any controller leading to unstable pole-zero cancellation in $P_{22}K$ corresponds to a point in the space of the controller parameters, which is not part of the interior of the convex set represented by the LMI in C2. Because of a small variation of the controller parameters, the number of unstable poles of $P_{22}K$ changes, and the closed-loop system becomes unstable. The only possible case is to have pole-zero cancellations on the stability boundary, which are avoided by C2:

- A zero of P_{22} on the stability boundary cannot be canceled as otherwise $Y - P_{22}X$ factors the same zero, Φ becomes rank deficient at the frequency of the canceled zero, and therefore $\Phi^*\Phi_c$ cannot be strictly positive.
- If P_{22} has a pole on the stability boundary, it cannot be canceled, as otherwise there exists a vector e_1 such that $\Phi e_1 = v$ is bounded but $\Phi_c e_1 = w$ is unbounded when ω approaches the frequency of the pole on the stability boundary. This leads to a contradiction with C2 as

$$e_1^* \left(\Phi^*\Phi_c + \Phi_c^*\Phi - \Phi_c^*\Phi_c\right) e_1 = v^*w + vw^* - \|w\|^2 < 0$$

  for ω sufficiently close to the frequency of the canceled pole.

Remark 3: The proof requires an initial stabilizing controller. For stable plants, a sufficiently small gain controller can always be chosen as the initial stabilizing controller. For unstable systems, in a data-driven setting, it is reasonable to assume that a stabilizing controller is known since it is required for data collection.

2.4.6 Implementation Issues

Using the methods described above, we are now able to pose various control design problems as convex optimization problems with linear matrix inequality (LMI) constraints. In this section, various practical aspects concerning the implementation of the algorithm will be discussed.

Frequency Gridding

The optimization problems formulated in this section contain an infinite number of constraints (i.e. $\forall\omega \in \Omega$) and are called semi-infinite problems. A common approach to

handle this type of constraints is to choose a reasonably large set of frequency samples $\Omega_g = \{\omega_1, \ldots, \omega_g\}$ and replace the constraints with a finite set of constraints at each of the given frequencies. For discrete-time plants and/or controllers, the maximum frequency should be chosen as $\omega_g = \pi/T_s$. As the complexity of the problem scales linearly with the number of constraints, g can be chosen relatively large without severely impacting the solver time. The frequency range is usually gridded logarithmically-spaced. Since all constraints are applied to Hermitian matrices, any constraint at a frequency ω_i is automatically imposed at $-\omega_i$ as well, so the grid does not need to cover negative frequencies.

In applications with low-damped resonance frequencies, the density of the frequency points can be increased around the resonant frequencies to prevent constraint violations. An alternative is to use a randomized approach for the choice of the frequencies at which the constraints are evaluated. In this case, the probability of the violation of the constraints can be computed, and decreased by increasing the number of frequency points.

Example 2.8. Loop Shaping Performance: The loop shaping performance objective in 2-norm from (2.27) can be formulated by replacing $\Gamma(\omega)$ with a matrix variable $\Gamma_k \in \{\Gamma_1, \ldots, \Gamma_g\}$ at each frequency $\omega_k \in \Omega_g$. Then, the integral in the objective function can be replaced by the sum of the trace of the matrix variables as follows:

$$\min_{X,Y} \sum_{k=1}^{g} \text{trace}[\Gamma_k]\Delta\omega_k$$

subject to:

$$\begin{bmatrix} \Gamma_k & G_k X_k - L_{d_k} Y_k \\ (G_k X_k - L_{d_k} Y_k)^* & Y_k^* Y_{c_k} + Y_{c_k}^* Y_k - Y_{c_k}^* Y_{c_k} \end{bmatrix} \succ 0$$
$$\Phi_k^* \Phi_{c_k} + \Phi_{c_k}^* \Phi_k - \Phi_{c_k}^* \Phi_{c_k} \succ 0 \qquad \text{for } k = 1, \ldots, g$$

where $\Delta\omega_k = \omega_k - \omega_{k-1}$. It can be ignored if the frequency samples are equally spaced, or if we are interested in more weights in some frequency region by choosing more frequency points at that region. The subscript k for the frequency response functions denotes the frequency response at ω_k, e.g. $G_k = G(e^{j\omega_k})$. Note that the condition C2 is added to the constraints to guarantee the closed-loop stability..

Controller Order

The choice of the order of the controller is sometimes not obvious. Often, a good initial guess of the order can be made from observing the dynamics of the plant (e.g. the number of resonance modes and couplings). Otherwise, a relatively low order of 4 to 6 is a good starting guess for most systems. Once a controller has been designed, its order can be adjusted by evaluating its performance. If the desired specifications have been met, the order can often be reduced while still achieving the desired result. However, if the final controller deviates significantly from the desired specifications, increasing its order can improve its performance. Furthermore, it has been demonstrated that approaching optimal performance can be achieved by increasing the controller's order.

Iterative Algorithm

Once a stabilizing initial controller K_c is available, it is used to formulate the optimization problem. Any Semi Definite Programming (SDP) solver can be utilized to solve the optimization problem and compute a suboptimal controller K around the initial controller K_c. Since we are only solving an inner convex approximation of the original optimization problem, K heavily relies on the initial controller K_c, and the performance criterion can significantly deviate from the optimal value. To address this issue, an iterative approach can be adopted, which solves the optimization problem multiple times, utilizing the final controller K of the previous step as the new initial controller K_c. This approach always guarantees closed-loop stability, assuming the initial choice of K_c is stabilizing. Since the objective function is non-negative and non-increasing, the iteration converges to a locally optimal solution of the original non-convex problem. The iterative process can be terminated once the change in the performance criterion becomes sufficiently small.

Numerical Issues

All LMI constraints formulated so far are strict positive definiteness constraints. This is important especially for the stability constraints, where strict positive definiteness is crucial. However, numerical optimization generally does not support strict inequalities, meaning the stability constraints may be violated due to numerical precision. This issue can be mitigated by defining a non-strict constraint with a sufficient margin:

$$\begin{bmatrix} \Phi^*\Phi_c + \Phi_c^*\Phi - \Phi_c^*\Phi_c & (W_1 Y)^* \\ W_1 Y & I \end{bmatrix} \succeq \epsilon I$$

where $\epsilon \in \mathbb{R}$ is a small number. Practical experience has shown that often values around 10^{-10} can serve to improve numerical robustness without affecting the achieved performance.

To improve the numerical robustness of the optimization it is also crucial that the constraints are scaled properly. Especially for MIMO systems, all inputs and outputs of the plant should be normalized properly in order to obtain good results. If necessary, individual LMI constraints can be scaled to increase the precision. Assume the following QMI:

$$\frac{1}{\eta}(\Phi^*\Phi - B^*A^{-1}B) \succ 0$$

where $\eta \in \mathbb{R}$ is a scaling factor. This can be transformed to either of the following convexified constraints:

$$\begin{bmatrix} \gamma I & \frac{1}{\sqrt{\eta}}B \\ \frac{1}{\sqrt{\eta}}B^* & \frac{1}{\eta}(\Phi^*\Phi_c + \Phi_c^*\Phi - \Phi_c^*\Phi_c) \end{bmatrix} \succ 0$$

$$\begin{bmatrix} \eta\gamma I & B \\ B^* & \frac{1}{\eta}(\Phi^*\Phi_c + \Phi_c^*\Phi - \Phi_c^*\Phi_c) \end{bmatrix} \succ 0$$

2.4.7 Simulation Examples

In this section, several simulation examples demonstrate the applicability of the method to general problems, and the obtained performance is compared with several state-of-the-art methods [3].

Example 2.9. Hard-disk Drive: This example is drawn from Matlab's Robust Control Toolbox and treats the control design for a 9th-order model of a head-disk assembly in a hard-disk drive. In the Matlab example, *hinfstruct* is used to design a robust controller such that a desired open-loop response is achieved while satisfying a certain performance measure. We will show that an equivalent controller of the same order can be designed using the method presented in this section.

The desired open-loop transfer function is given by $L_d(s) = 1000/s$. Additionally, a constraint on the closed-loop transfer function is introduced to increase the robustness and performance: $\|W_2\mathcal{T}\|_\infty \leq 1$ and $W_2 = 1$. To stay in line with the data-driven aspect, we choose to design a discrete-time controller with the same order as the continuous-time controller given in the Matlab example:

$$K(z) = \frac{X_2 z^2 + X_1 z + X_0}{(z-1)(z+Y_0)}$$

Since the plant is stable, an initial controller is easily found by setting X_0, X_2, Y_0 to zero and choosing a small enough value for X_1. This results in the following initial controller:

$$K_c(z) = \frac{10^{-6} z}{z^2 - z}$$

While with *hinfstruct* the loop-shaping can only be formulated in the ∞-norm sense, we choose to formulate the loop-shaping problem in the 2-norm sense by minimizing $\|L - L_d\|_2$, which will lead to a better performance as shown below.

The semi-infinite formulation is sampled using $g = 1000$ logarithmically spaced frequency points in the interval $\Omega_g = [10, 5 \times 10^4 \pi]$ (the upper limit being equal to the Nyquist frequency). The semi-definite problem is as follows:

$$\min \sum_{k=1}^{g} \gamma_k$$

subject to:

$$\begin{bmatrix} \gamma_k & GX - L_d Y \\ (GX - L_d Y)^* & Y^* Y_c + Y_c^* Y - Y_c^* Y_c \end{bmatrix} (j\omega_k) > 0$$

$$\begin{bmatrix} 1 & (W_2 G X)^* \\ W_2 G X & \Phi^* \Phi_c + \Phi_c^* \Phi - \Phi_c^* \Phi_c \end{bmatrix} (j\omega_k) > 0$$

$$k = 1, \ldots, g$$

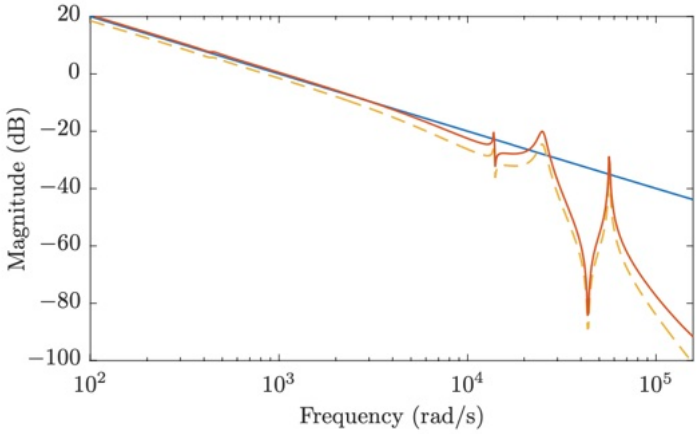

Figure 2.12: Comparison of the open-loop transfer functions. In blue is the desired open-loop function L_d, in red the obtained open-loop function L with the data-driven method, and in dashed yellow the obtained L with the *hinfstruct* controller.

Remark: Note that $\Delta\omega_k = \omega_k - \omega_{k-1}$ has been dropped out in the approximation of the integral by a finite sum in the control objective. For an equally spaced gridding, this will not change anything. However, for a logarithmically spaced gridding, it is equivalent to have more weights in low frequencies and leads to a better fit in those frequencies.

The algorithm converges within 10 iterations to a final, stabilizing controller that satisfies the closed-loop constraint and has the following parameters:

$$K(z) = 10^{-4}\frac{2.287z^2 - 3.15z + 0.8631}{(z-1)(z-0.8598)}$$

Fig. 2.12 shows a comparison of the desired open-loop transfer function and the results produced by the data-driven method as well as the controller calculated in the Matlab example using *hinfstruct*. It can be seen that the result is very similar to the result generated by *hinfstruct*, with the data-driven result being closer to the desired transfer function at lower frequencies. This is especially noticeable when comparing the obtained 2-norm of the objective function, with the data-driven solution achieving a value that is around 30 times smaller. The controller obtained by this method is also already formulated in discrete-time, and no additional controller discretization step is necessary.

Example 2.10. Multivariable Control System: This example demonstrates that the method is able to obtain near-optimal performance for low-order controllers, and shows that the convex approximation of the problem is not restrictive in practice. The mixed sensitivity problem of a 3×3 MIMO continuous-time plant model is considered. The globally optimal solution to this problem with a full-order controller can be obtained via Matlab using *mixsyn*. The plant model is taken from literature and has the following

transfer function:

$$G(s) = \begin{bmatrix} \frac{1}{s+1} & \frac{0.2}{s+3} & \frac{0.3}{s+0.5} \\ \frac{0.1}{s+2} & \frac{1}{s+1} & \frac{1}{s+1} \\ \frac{0.1}{s+0.5} & \frac{0.5}{s+2} & \frac{1}{s+1} \end{bmatrix}$$

The objective is to solve the mixed sensitivity problem:

$$\min_{X,Y} \left\| \begin{array}{c} W_1\mathcal{S} \\ W_2K\mathcal{S} \end{array} \right\|_\infty$$

where the weighting transfer functions are:

$$W_1(s) = \frac{s+3}{3s+0.3}I \quad , \quad W_2(s) = \frac{10s+2}{s+40}I$$

In this example, we design a continuous-time controller to show that the developed frequency-domain LMIs can be used in the same way to design continuous-time controllers. The controller transfer function matrix is defined as $K(s) = X(s)Y^{-1}(s)$:

$$X(s) = [X_p s^p + \ldots + X_1 s + X_0]/(s-a)^p$$
$$Y(s) = [Is^p + \ldots + Y_1 s + Y_0]/(s-a)^p$$

where p is the controller degree, $a = 1$ and $X_i, Y_i \in \mathbb{R}^{3\times 3}$ are full matrices. The optimization problem is sampled using $N = 1000$ logarithmically spaced frequency points in the interval $\Omega_g = [10^{-2}, 10^2]$, resulting in the following optimization problem:

$$\min_{X,Y} \gamma$$
$$\begin{bmatrix} \Phi^*\Phi_c + \Phi_c^*\Phi - \Phi_c^*\Phi_c & (W_1Y)^* & (W_2X)^* \\ W_1Y & \gamma I & 0 \\ W_2X & 0 & \gamma I \end{bmatrix} (j\omega_k) \succ 0$$
$$k = 1, \ldots, g$$

Since the plant is stable, an initial controller can be found by setting the poles of the controller to -1 and choosing a low enough gain: $Y_c = (s+1)^p I$, $X_c = I$.

The problem is formulated for controller degrees p from 1 to 5, implemented in Matlab using Yalmip, and solved with an SDP solver called *Mosek*. The algorithm converges quickly within 3 to 6 iterations. The value of the obtained norm is shown in Fig. 2.13. The number of design parameters is equal to $(2p+1) \times 9$. The figure also shows the globally optimal norm for a full-order state-space controller with 289 design parameters obtained through *mixsyn*. It can be seen that already for $p = 3$ a good value is achieved and for $p = 5$, with only 99 design parameters the global optimum is attained. This example shows that the proposed method is able to reach the global optimum value of the mixed sensitivity norm for a general MIMO transfer function while having a significantly lower number of design parameters than classical state-space methods.

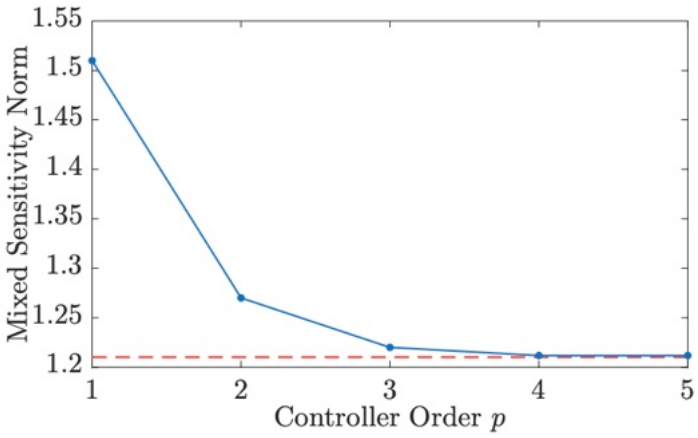

Figure 2.13: Plot of the achieved mixed sensitivity norm for different controller orders p. The dashed red line shows the globally optimal value obtained by *mixsyn*.

2.4.8 Data-Driven Control Design for Atomic-Force Microscopy

An AFM is a mechanical microscope with a resolution on the order of nanometers, and a wide range of applications in various fields such as solid-state physics, semiconductor science, molecular biology and cell biology [5].

The basic functionality of the AFM is shown in Fig. 2.14. The main sensor is a cantilever with a sharp tip that is used to probe the surface of the sample to be studied. The deflection of the cantilever can be measured using a laser that is reflected off its back and collected by a photodetector. From this measurement, the tip-sample interaction force can be extracted, which yields information about various mechanical material properties. Furthermore, the measured deflection is used to control a piezo actuator that moves the vertical position of the sample up and down in order to keep the deflection at a controlled value. Another piezo actuator is used to move the sample in the horizontal plane, and by scanning the sample in a raster an image is acquired point by point. As the deflection of the piezo is proportional to the applied voltage, the image can be reconstructed from the input signal that is extracted from the feedback loop. This also means that the tracking performance of controller used to regulate the piezo actuator plays a crucial role in determining the quality of the image. Ringing in the closed-loop response leads to visible ripples and distortions in the AFM image, and good disturbance rejection is important. Furthermore, the image is acquired line by line as the scanner moves back and forth in the horizontal direction. The relevant metric for the speed is the line rate, which indicates the number of lines per second (L/s) that are recorded. As the scanning motion translates the spatial frequencies of the surface into temporal frequencies, the maximum line rate (and therefore the time required to record an image) directly depends on the closed-loop bandwidth. Simply put, the controller has to be able to track any features of the sample fast enough. A too slow controller leads to distortions in the image, blurs out the features and creates artefacts that obscure the true image.

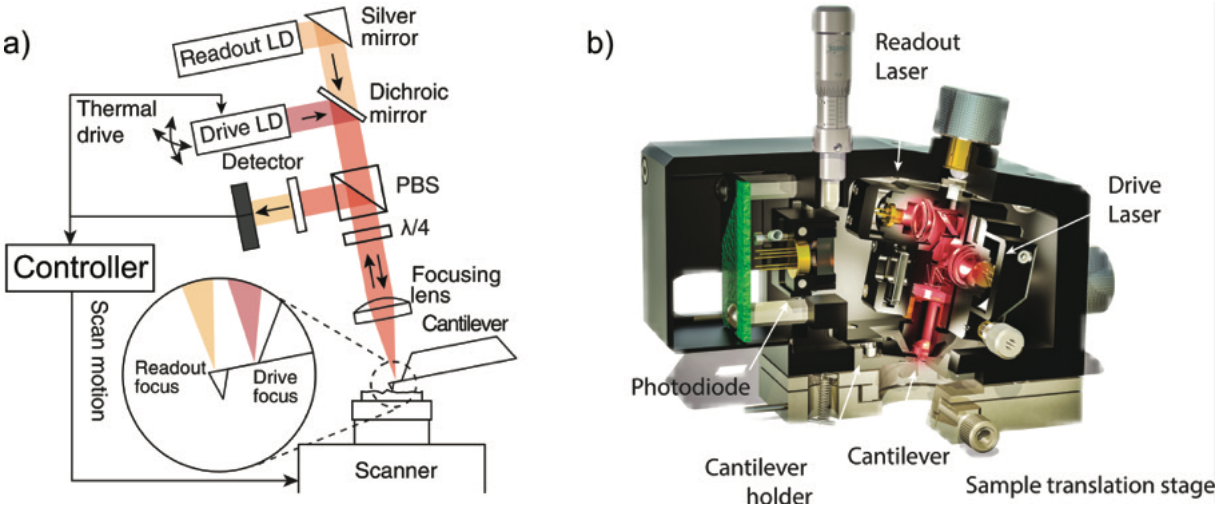

Figure 2.14: a) Block diagram of the functionality of an AFM. b) Exploded view of the head used for the experiments.

Increasing the number of images that can be recorded in a given time enables the observation of processes on the nanoscale in real-time, which is of great interest to many fields. Fast scanning speeds make it possible to record time-lapse image series of processes that could not be observed before. Also, a high controller bandwidth reduces feedback-error-induced force interactions between the tip and the sample, which improves the image quality.

Plant identification: Here, we consider only the control design in the lateral axis. The input of the plant corresponds to the voltage applied to the piezo actuator, and the output corresponds to the deflection of the cantilever (see Fig. 2.14). Both signals are within a range of ±10 V. The system is excited by applying 100 periods of a pseudorandom binary sequence (PRBS) with a length of 8191 samples and a sampling frequency depending on the bandwidth of the system. The frequency response is calculated in Matlab using the `spa` command with a Hann window length of 700. Figure 2.15 shows an example of the evolution of the frequency response over time. The change in the response can be significant, with magnitudes changing by 10 dB or more, and resonance peaks appearing and disappearing over time.

Control performance: The objective is to achieve good tracking performance of the reference input. This is achieved through loop shaping, where a controller is designed such that the loop transfer function $L = GK$ is close to a desired transfer function L_d:

$$\min_K \|L - L_d\|_2 \ , \quad L_d = \frac{\omega_c}{s}$$

where ω_c is the desired bandwidth of the system.

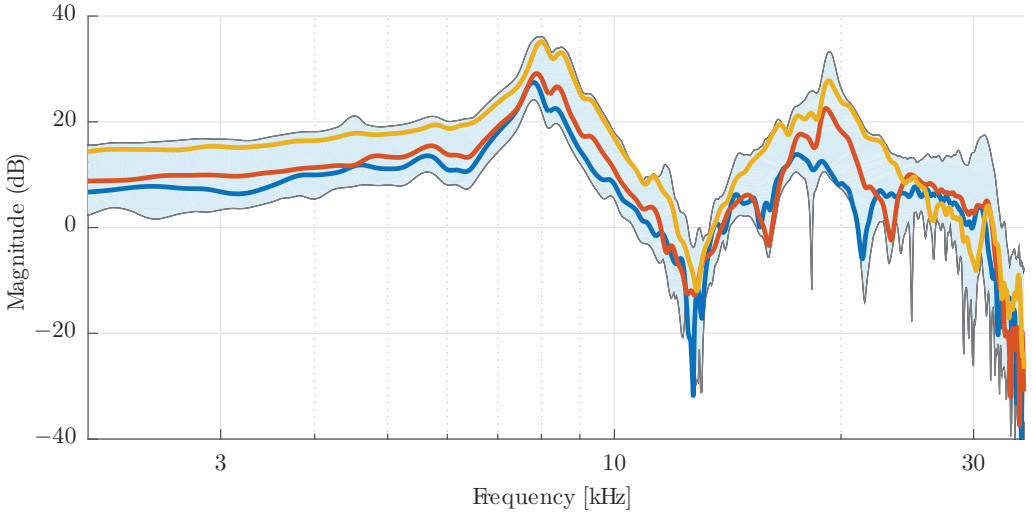

Figure 2.15: Evolution of the frequency response of a J-scanner in liquid over 3 hours. The envelope shows the range of the variations. Three example responses are shown, where blue is at the start, red is after 1 hour and yellow is after 2 hours.

To improve the robustness, $\mathcal{H}_\infty$ constraints on the complementary sensitivity function $\mathcal{T} = GK(I+GK)^{-1}$ and the input sensitivity function $\mathcal{U} = K(I+GK)^{-1}$ are introduced:

$$\|W_2\,\mathcal{T}\|_\infty < 1 \quad ; \quad \|W_3\,\mathcal{U}\|_\infty < 1$$

where W_2, W_3 are chosen as:

$$W_2^{-1} = 1.2B\ , \quad W_3^{-1} = \begin{cases} 10G(0)B & \forall\omega \le \omega_c \\ G(0)B & \forall\omega > \omega_c \end{cases}$$

where B is a second-order discrete-time Butterworth lowpass filter with a cutoff frequency of $1.1\omega_c$. In order to have a generic formulation, the input filter W_3 is scaled by the dc-gain of the plant $G(0)$. This choice of filters enforces a roll-off in the closed-loop and input sensitivities, which improves the robustness of the controller towards plant uncertainties at frequencies above the desired bandwidth.

Controller design: An 11th-order discrete-time transfer function controller K with forced integrator is designed. This choice of order has been found to be sufficient for the systems the method was applied to. To solve the robust design problem, a frequency grid with $g = 500$ logarithmically-spaced frequency points in the interval $\Omega_g = \left\{0.01\frac{\pi}{T_s}, \frac{\pi}{T_s}\right\}$ rad/s is chosen, where the upper limit is the Nyquist frequency of the controller. Since the plants are always stable, an integral controller with low gain is

chosen as initial controller $K_c(z) =: 10^{-3}$, Then, the control design problem is reformulated as a convex optimization problem:

$$\min_{X,Y} \sum_{k=1}^{g} \gamma_k$$

$$\begin{bmatrix} \gamma_k & GX - L_dY \\ (GX - L_dY)^* & Y^*Y_c + Y_c^*Y - Y_c^*Y_c \end{bmatrix} (j\omega_k) \succ 0$$
$$\begin{bmatrix} 1 & W_2GX \\ (W_2GX)^* & \Phi^*\Phi_c + \Phi_c^*\Phi - \Phi_c^*\Phi_c \end{bmatrix} (j\omega_k) \succ 0$$
$$\begin{bmatrix} 1 & W_3X \\ (W_3X)^* & \Phi^*\Phi_c + \Phi_c^*\Phi - \Phi_c^*\Phi_c \end{bmatrix} (j\omega_k) \succ 0$$
$$k = 1, \ldots, N$$

The optimization problem is implemented in Matlab using Yalmip and solved with Mosek. The time to compute a controller is around 1 minute, and since the design is in discrete-time the controller parameters are directly written to the real-time software without requiring any user interaction.

A comparison of the obtained performance of the standard PI controller and the 11th-order controller is shown in Fig. 2.16. It can be seen in subfigure 2.16c) that the bandwidth of the 10th-order controller exceeds the PI by about one order of magnitude. At the same time, the resonance peak in the closed-loop sensitivity function is removed, which also leads to less ringing and better tracking performance.

2.4.9 Data-driven Multivariable Control of a 2-DOF Gyroscope

This experimental example presents the design of a data-driven, robust multivariable controller with multimodel uncertainty to control the gimbal angles of a gyroscope. The controller is then applied on the experimental setup to validate the performance.

System description: The experiment was conducted on a 3-DOF gyroscope setup built by Quanser (see Fig. 2.17). The system consists of a disk mounted inside an inner blue gimbal, which is in turn mounted inside an outer red gimbal. The entire structure is supported by the rectangular silver frame. The disk, both gimbals and the frame can be actuated about their respective axis by electric motors, and their angular positions can be measured using high resolution optical encoders. For this experiment, the position of the silver frame is mechanically fixed in place (to make it 2-DOF). The control objective is to achieve a good tracking performance on the angular positions of the blue and red gimbal and to minimize the coupling between the axes. The dynamics of the system change depending on the angular velocity of the disk, which is included in the control design as a multimodel uncertainty.

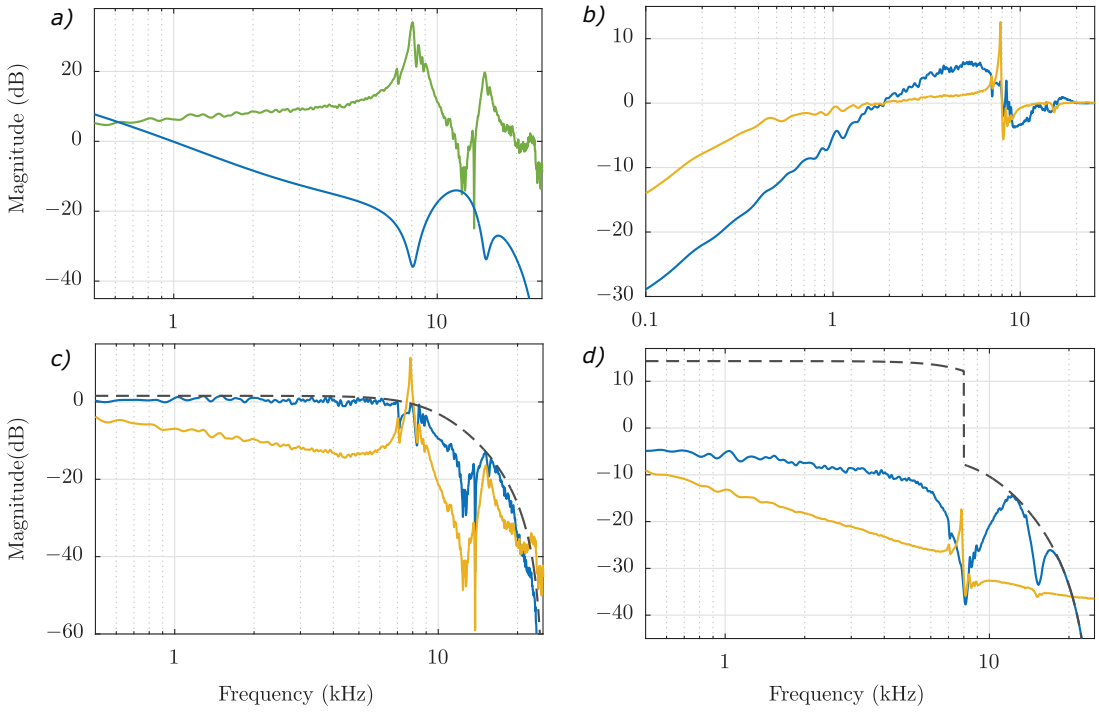

Figure 2.16: Comparison of the nominal closed-loop sensitivities. a) Measured plant frequency response in green, designed 10th-order controller in blue. b)-d) Sensitivity $\mathcal{S}$, closed-loop sensitivity $\mathcal{T}$ and input sensitivity $\mathcal{U}$ for the 10th-order controller in blue and the PI-controller in yellow. Black dashed lines indicate the constraints.

The gyroscope is a strongly nonlinear system, and linear control design methods only achieve good performance in a small range around the operation points. In order to improve this range, a cascaded control architecture was chosen, with a feedback linearization forming the inner loop. The block diagram in Fig. 2.18 shows the structure of the system, where G_m is the real plant and K_f is the feedback linearization controller. The closed-loop response of the inner loop is taken as the new plant G, which is used to design the outer controller K. The variables $\boldsymbol{\theta} = [\theta_b, \theta_r]^T$ and $\boldsymbol{\theta}^* = [\theta_b^*, \theta_r^*]^T$ are vectors containing the measured and desired blue and red gimbal angles, and $\boldsymbol{\theta_u} = [\theta_{ub}, \theta_{ur}]^T$ are the reference gimbal angles given to the feedback linearization.

Frequency response: The black box model G therefore has 2 inputs and 2 outputs, and a single-channel excitation is applied to calculate the frequency response of G. A PRBS signal with an amplitude of $\pm 10°$, a length of $N = 511$ samples and a sampling time of $T_s = 20$ ms was applied for 4 periods to θ_{ub} and θ_{ur} respectively. The non-excited input was set to zero during the process. The frequency response was calculated in Matlab using the `spa` command with a Hann window length of 150. The frequency response was measured for the three different disk velocities $\boldsymbol{v} = [300, 400, 500]$ rpm, resulting in three

Figure 2.17: The gyroscope experimental setup by Quanser.

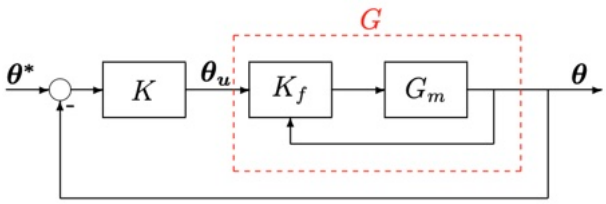

Figure 2.18: Block diagram of the cascaded controller structure of the gyroscope.

models $\mathbb{G} = [G_1, G_2, G_3]$. The frequency responses are shown in Fig. 2.19. It can be seen that the coupling and resonance modes become stronger at higher disk speeds.

Control performance: Based on the three frequency responses, a multivariable controller is designed. The goal is to decouple the system while also achieving good tracking performance of the reference angles θ^*. Therefore, as objective function we choose to minimize the 2-norm $\|L - L_d\|_2$ between the actual open-loop transfer function L and desired open-loop transfer function $L_d = \frac{\omega_c}{s} I$, where a bandwidth of $\omega_c = 4$ rad/s is desired for the decoupled system. To limit the overshoot and guarantee a good roll-off at higher frequencies, an additional $\mathcal{H}_\infty$ constraint is put on the complementary sensitivity function:

$$\|W_2 \mathcal{T}\|_\infty < 1 \ , \ W_2(j\omega) = \frac{j\omega + 6.5}{1.05 \cdot 6.5} I$$

where W_2^{-1} has the form of a low-pass filter to ensure a roll-off at high frequencies. The fact that W_2 is not proper does not create any problem in practice because the constraints are evaluated only for finite values of ω. To prevent input saturation, a constraint on the input sensitivity is included:

$$\|W_3 \mathcal{U}\|_\infty < 1 \ , \ W_3 = 0.05 I$$

where the magnitude of the weighting filter is chosen based on the expected worst-case disturbance.

Controller design: A 5th-order discrete-time controller with a forced integrator is chosen. Note that the desired L_d and the weighting filters can be in continuous-time, while the designed controller is in discrete-time. The optimization problem is sampled using

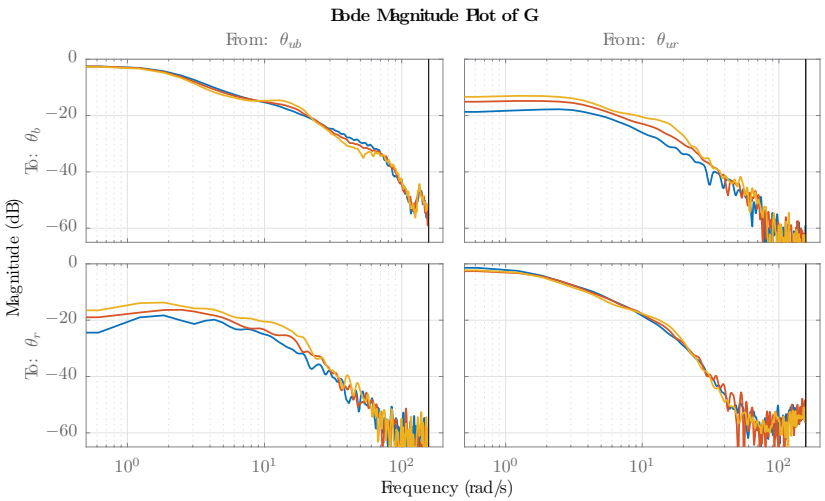

Figure 2.19: The measured frequency response of the blackbox model G at different disk speeds. The blue line is the response at a disk speed of 300 rpm, red at 400 rpm and yellow at 500 rpm.

$g = 500$ logarithmically spaced frequency points in the interval $\Omega_g = [10^{-1}, \pi/T_s]$ (the upper limit being the Nyquist frequency of the controller). The lower limit is chosen greater than zero in order to guarantee the boundedness of $L - L_d$. The constraint sets are formulated for each of the three models $[G_1, G_2, G_3]$, resulting in the following optimization problem :

$$\min_{X,Y} \sum_{i=1}^{3} \sum_{k=1}^{g} \text{trace}[\Gamma_{k_i}]$$

subject to:

$$\begin{bmatrix} Y^*Y_c + Y_c^*Y - Y_c^*Y_c & (G_iX - L_dY)^* \\ G_iX - L_dY & \Gamma_{k_i} \end{bmatrix} (j\omega_k) > 0$$

$$\begin{bmatrix} \Phi_i^*\Phi_{c_i} + \Phi_{c_i}^*\Phi_i - \Phi_{c_i}^*\Phi_{c_i} & (W_2G_iX)^* \\ W_2G_iX & I \end{bmatrix} (j\omega_k) > 0$$

$$\begin{bmatrix} \Phi_i^*\Phi_{c_i} + \Phi_{c_i}^*\Phi_i - \Phi_{c_i}^*\Phi_{c_i} & (W_3X)^* \\ W_3X & I \end{bmatrix} (j\omega_k) > 0$$

$$k = 1, \ldots, N \quad ; \quad i = 1, 2, 3$$

In fact a weighted two-norm of $L - L_d$ is minimized because more frequency points in low frequencies are considered in the objective function (the term $\Delta\omega_k$ has been dropped out in the approximation of the integral).

As the gyroscope is a stable system, the initial controller was chosen as an integral controller with low gain. The optimization problem is implemented in Matlab using Yalmip, and solved with Mosek. The iteration converges to a final controller in 10 steps.

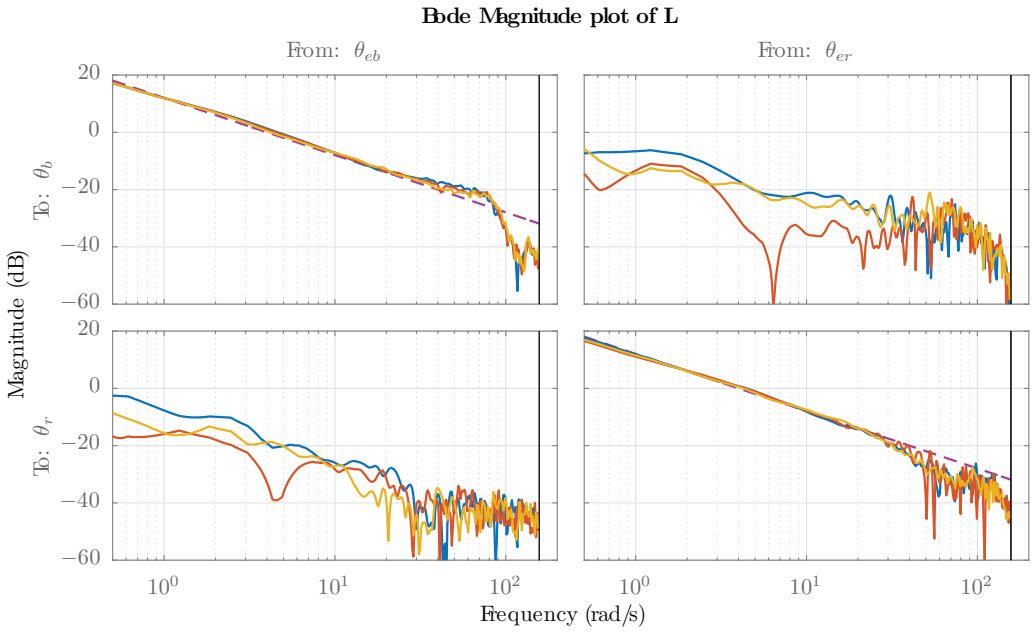

Figure 2.20: Bode magnitude plots of the desired open-loop transfer function L_d and the achieved $L_{1,2,3}$ for the three different plant models. The blue line is the achieved response at a disk speed of 300 rpm, red at 400 rpm and yellow at 500 rpm. The desired L_d is shown in dashed purple.

The Bode magnitude plots of L_d and the obtained $L_{1,2,3}$ for the three different plant models are shown in Fig. 2.20. It can be seen that the designed controller approximates the desired loop shape well at low frequencies, and that the system is well decoupled. The singular value plots of the obtained closed-loop and input sensitivity are displayed in Fig. 2.21. It can be seen that the constraints are satisfied for all three plant models.

Experimental results: To validate the results, the controller was implemented in Labview and applied on the experimental setup. The step responses of the blue and red gimbal angle were measured for varying disk speeds, and the results are shown in Fig. 2.22. It can be seen that the decoupling is good, and that the multimodel uncertainty introduced by the varying disk speed is handled well. The rise time is 0.625 s for the blue and 0.486 s for the red gimbal angle, which matches well the desired bandwidth specified for L_d. Furthermore, the overshoot is limited to less than 10 %.

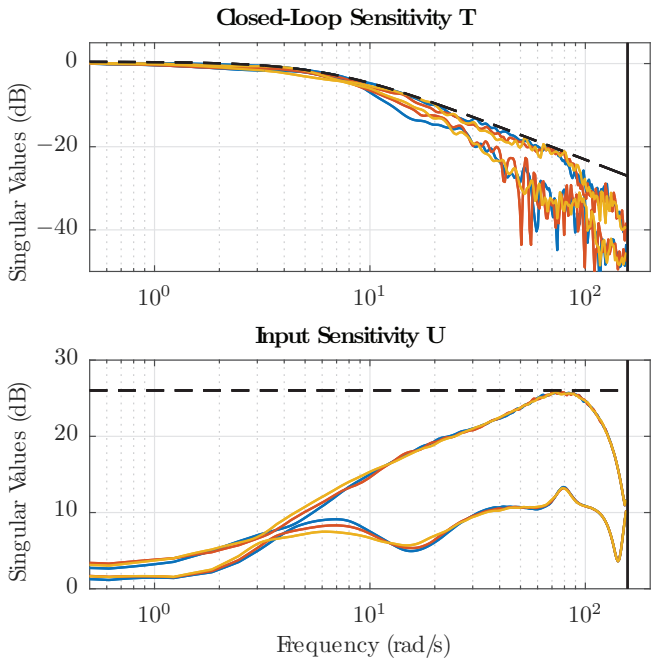

Figure 2.21: Singular value plots of the nominal closed-loop and input sensitivity for the three different plants. The dashed lines indicate the constraints.

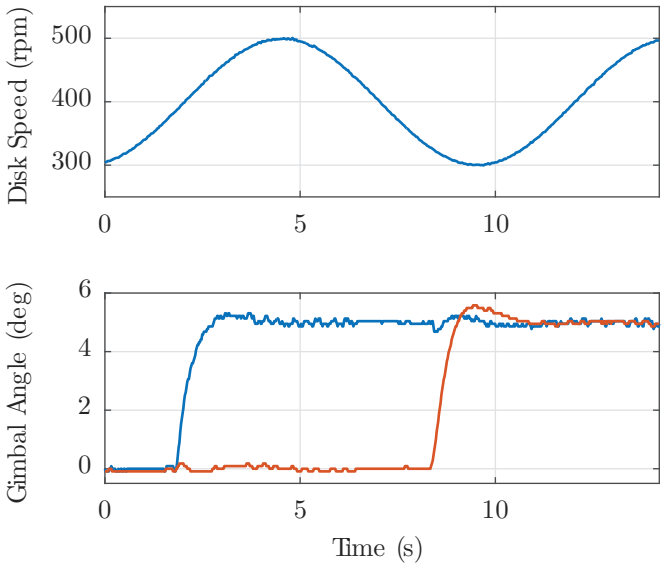

Figure 2.22: Step response of the blue and red gimbal angles during a varying disk velocity.

Chapter 3

ROBUST ADAPTIVE CONTROL

3.1 Introduction

In the presence of model parameter variations or more generally in the presence of variations of the dynamic characteristics of a plant to be controlled, *robust control design* is a powerful tool for achieving a satisfactory level of performance for a family of plant models. This family is often defined by means of a *nominal model* and a size of the uncertainty specified in the parameter domain or in the frequency domain.

The range of uncertainty domain for which satisfactory performance can be achieved depends upon the problem. Sometimes, a large domain of uncertainty can be tolerated, while in other cases, the uncertainty tolerance range may be very small. If the desired performance cannot be achieved for the full range of possible parameter variations, adaptive control has to be considered in addition to a robust control design.

Adaptive Control covers a set of techniques which provide a systematic approach for automatic adjustment of controllers in *real time*, in order to achieve or to maintain a desired level of control system performance when the parameters of the plant dynamic model are unknown and/or change in time.

Furthermore, the tuning of a robust design for the true nominal model using an adaptive control technique will improve the achieved performance of the robust controller design. Therefore, robust control design will benefit from the use of adaptive control in terms of performance improvement and extension of the range of operation. On the other hand, using an underlying robust controller design for building an adaptive control system may drastically improve the performance of the adaptive controller.

Since the adaptive controllers are implemented in computers, the associated controllers are usually digital. Therefore, this chapter starts with a recall on the principles of digital control systems, especially using RST controllers. The pole placement technique is recalled and model reference control problem for an RST structure is studied. The use of Q-parameterisation for improving the robustness of pole placement technique is also investigated. Then, some adaptive control schemes are presented in details. In particu-

lar the parametric adaptation algorithms (PAAs) are introduced and their properties are studied. An overview of the most common adaptive controllers, like direct, indirect and switching adaptive control is given.

3.2 Digital Controller Design

The use of a digital computer or microprocessor in control loops offers several advantages. These include: considerable choice of strategies for controller design; possibility of using complex and more efficient structures than the PID controllers; suited for high order dynamic linear models (including systems with multiple low damped vibration modes) and systems with time delay.

We consider the design of digital controllers for single-input/single-output systems described by discrete-time models in input-output form. The control strategies and the corresponding design assume that the discrete-time plant model is known. In general, one has to solve a joint tracking and regulation problem. The design will also incorporate the *a priori* knowledge upon the disturbances. It is important to note that in many cases the tracking and regulation performances have to be decoupled (as much as possible). This leads us to consider a *two-degree of freedom digital controller*.

Since the plant model is given in the input/output form, it is also reasonable to search for a controller structure which will be fed by the measurements of the output and the desired tracking trajectory (or reference signal) and will generate the control $u(k)$. This controller will also have an input/output form and will consist of three polynomials in the delay operator q^{-1} related to the control $u(k)$, the output $y(k)$ and the desired tracking trajectory $y^\star(k)$.

In many cases the design can be done using a polynomial approach, which in fact corresponds to a design in the frequency domain. This will allow the introduction of specifications in various frequency ranges both for assuring the nominal performances as well as robustness with respect to plant parameter variations, noise etc. The *pole placement* strategy is the basic method that we discuss in this section.

3.2.1 Input-Output Difference Operator Models

We will consider single-input single-output time invariant systems described by input-output discrete-time models of the form:

$$y(k) = -\sum_{i=1}^{n_A} a_i y(k-i) + \sum_{i=0}^{n_B} b_i u(k-i) \tag{3.1}$$

where k denotes the normalized sampling time, $u(k)$ is the input, $y(k)$ is the output, a_i and b_i are the parameters (coefficients) of the models. As such the output of the system at instant k is a weighted average of the past output over an horizon of n_A samples

plus a weighted average of present and past inputs over an horizon of n_B samples. This input-output model (3.1) can be more conveniently represented using a coding in terms of backward shift operators defined as:

$$q^{-1}: \quad q^{-1}y(k) = y(k-1) \tag{3.2}$$

Using the notation:

$$\begin{aligned} A(q^{-1}) &= 1 + a_1 q^{-1} + \cdots + a_{n_A} q^{-n_A} && (3.3)\\ B(q^{-1}) &= b_0 + b_1 q^{-1} + b_2 q^{-2} + \cdots + b_{n_B} q^{-n_B} && (3.4) \end{aligned}$$

Eq. (3.1) can be rewritten as:

$$A(q^{-1})y(k) = B(q^{-1})u(k). \tag{3.5}$$

Note that in the discrete-time systems, there is always some delay between the inputs and outputs such that the first leading coefficients of $B(q^{-1})$ becomes equal to zero. The number of these coefficients is called delay and denoted by d. Because of sampling time delay the output $y(k)$ will not depend on $u(k)$ (b_0 is always zero and so the delay d is always greater than or equal to 1). Using this fact Eq. (3.1) can be rewritten forward in time as:

$$\begin{aligned} y(k+1) &= -\sum_{i=1}^{n_A} a_i y(k-i+1) + \sum_{i=d}^{n_B} b_i u(k-i+1) && (3.6)\\ &= -A^\star(q^{-1})y(k) + B^\star(q^{-1})u(k-d+1) && (3.7) \end{aligned}$$

where

$$\begin{aligned} A^\star(q^{-1}) &= a_1 + a_2 q^{-1} + \cdots + a_{n_A} q^{-n_A+1} && (3.8)\\ B^\star(q^{-1}) &= b_d + b_{d+1} q^{-1} + \cdots + b_{n_B} q^{-n_B+d} && (3.9) \end{aligned}$$

Observe that Eq. (3.6) can also be expressed as (the *regressor form*):

$$y(k+1) = \theta^T \varphi(k) \tag{3.10}$$

where θ defines the vector of parameters

$$\theta^T = [a_1, \cdots a_{n_A}, b_d, \cdots b_{n_B}] \tag{3.11}$$

and $\varphi(k)$ defines the vector of measurements (or the regressor)

$$\varphi^T(k) = [-y(k) \cdots - y(k-n_A+1), u(k-d+1) \cdots u(k-n_B+1)] \tag{3.12}$$

The form of Eq. (3.10) will be used in order to estimate the parameters of a system model from input-output data. Consider Eq. (3.5). Passing the quantities in the left and in the right through a filter $\frac{1}{A(q^{-1})}$ one gets:

$$y(k) = G(q^{-1})u(k) \tag{3.13}$$

where:

$$G(q^{-1}) = \frac{B(q^{-1})}{A(q^{-1})} = \frac{q^{-d}B^{\star}(q^{-1})}{A(q^{-1})} \tag{3.14}$$

is termed the *transfer operator*.[1]

Computing the z-transform of Eq. (3.1), one gets the pulse transfer function characterizing the input-output model of Eq. (3.1)[2]:

$$G(z^{-1}) = \frac{z^{-d}B^{\star}(z^{-1})}{A(z^{-1})} \tag{3.15}$$

Observe that the transfer function of the input-output model of Eq. (3.1) can be formally obtained from the *transfer operator* by replacing the time operator q by the complex variable z. However, one should be careful since the domains of these variables are different. Nevertheless in the linear case with constant parameters one can use either one and their appropriate signification will result from the context.

Note also that the transfer operator $G(q^{-1})$ can be defined even if the parameters of the model (3.1) are time varying, while the concept of pulse transfer function does simply not exist in this case.

Theorem 3.1. *The order r of the system model (3.1), is the dimension of the minimal state space representation associated to the input-output model (3.1) and in the case of irreducible transfer function it is equal to:*

$$r = \max(n_A, n_B) \tag{3.16}$$

which corresponds also to the number of the poles of the irreducible transfer function of the system.

The order of the system is immediately obtained by expressing the transfer operator (3.14) or the transfer function (3.15) in the forward operator q and respectively the complex variable z. The passage from $H(z^{-1})$ to $H(z)$ is obtained multiplying by z^r:

$$G(z) = \frac{\bar{B}(z)}{\bar{A}(z)} = \frac{z^{r-d}B(z^{-1})}{z^r A(z^{-1})} \tag{3.17}$$

Example 3.1.

$$G(z^{-1}) = \frac{z^{-3}(b_1 z^{-1} + b_2 z^{-2})}{1 + a_1 z^{-1}} \quad \Rightarrow \quad r = \max(1,5) = 5 \quad , \quad G(z) = \frac{b_1 z + b_2}{z^5 + a_1 z^4}$$

[1]Note that (3.14) is not mathematically well defined because the devision by a polynomial in shift operator q^{-1}. However, it is understood that this notation has the same meaning as (3.5).

[2]A number of authors prefer to use the notation $G(z)$ for this quantity, instead of $G(z^{-1})$, in order to be coherent with the definition of the z-transform.

Note that if $n_B > n_A$, the system will have $n_B - n_A$ poles at the origin ($z = 0$). In general we will assume that the model of Eq. (3.1) and the corresponding transfer function (3.15) is irreducible. However, situations may occur where this is indeed not the case (an estimated model may feature an almost pole zeros cancellation). The properties of the system model in such cases are summarized below:

- The presence of pole zeros cancellations correspond to the existence of unobservable or uncontrollable modes.
- If the common poles and zeros are stable (they are inside the unit circle) the system is termed *stabilizable*, i.e., there is a feedback law stabilizing the system.
- If the common poles and zeros are unstable, the system is *not stabilizable* (a feedback law stabilizing the system does not exist).

The co-primeness of $A(z^{-1})$ and $B(z^{-1})$ is an important property of the model. A characterization of the co-primeness of $A(z^{-1})$ and $B(z^{-1})$ without searching the roots of $A(z^{-1})$ and $B(z^{-1})$ is given by the Sylvester Theorem.

Theorem 3.2. *: The polynomials $A(q^{-1})$, $B(q^{-1})$ are relatively prime if and only if their eliminant matrix M (known also as the Sylvester Matrix) is nonsingular, where M is a square matrix with $n_A + n_B$ columns given by:*

$$M = \overbrace{\begin{bmatrix} 1 & 0 & \cdots & 0 \\ a_1 & 1 & \ddots & \vdots \\ \vdots & a_1 & \ddots & 0 \\ \vdots & \vdots & \ddots & 1 \\ \vdots & & & a_1 \\ a_{n_A} & & & \vdots \\ 0 & a_{n_A} & & \vdots \\ \vdots & \ddots & \ddots & \vdots \\ 0 & \cdots & 0 & a_{n_A} \end{bmatrix}}^{n_B} \overbrace{\begin{bmatrix} b_0 & 0 & \cdots & 0 \\ b_1 & b_0 & \ddots & \vdots \\ \vdots & b_1 & \ddots & \vdots \\ \vdots & \vdots & \ddots & b_0 \\ \vdots & & & b_1 \\ b_{n_B} & & & \vdots \\ 0 & b_{n_B} & & \vdots \\ \vdots & \ddots & \ddots & \vdots \\ 0 & \cdots & 0 & b_{n_B} \end{bmatrix}}^{n_A} \Bigg\} n_A + n_B \tag{3.18}$$

Remarks:

- The non-singularity of the matrix M implies the controllability and the observability of the associated state space representation.
- The condition number of M allows to evaluate the ill conditioning of the matrix M, i.e., the closeness of some poles and zeros.

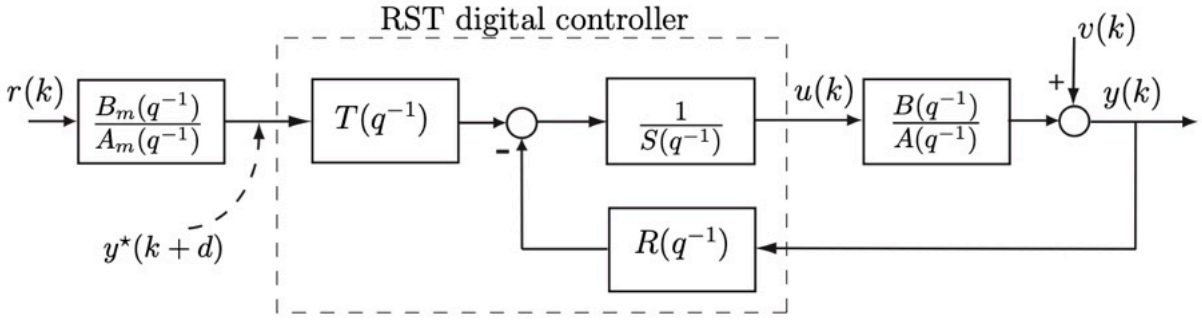

Figure 3.1: Control loop with RST digital controller

3.2.2 RST Controller Structure

A general (canonical) form of a two-degree of freedom digital controller is given by the equation:

$$R(q^{-1})y(k) + S(q^{-1})u(k) = T(q^{-1})y^\star(k+d) \tag{3.19}$$

where $y^\star(k+d)$ represents the *desired tracking trajectory* given with d steps in advance which is either stored in the computer or generated from the reference signal $r(k)$ via a *tracking reference model*

$$y^\star(k+d) = \frac{B_m(q^{-1})}{A_m(q^{-1})}r(k) \tag{3.20}$$

(with $B_m(q^{-1}) = b_{m0} + b_{m1}q^{-1} + \cdots$). The corresponding block diagram is shown in Fig. 3.1.

The controller of equation (3.19) is termed "RST controller" and its *two-degree of freedom* capabilities come from the fact that the *regulation* objectives are assured by the R-S part of the controller and the *tracking* objectives are assured by an appropriate design of the T polynomial.

RST controllers are very appealing because their implementation is very easy by the use of Eq. (3.19). Moreover, all types of two-degree of freedom controllers can be converted to an RST controller. Figure 3.2 shows a very general output feedback control system where $K_1(q^{-1}), K_2(q^{-1})$ and $K_3(q^{-1})$ are rational transfer operators:

$$K_1(q^{-1}) = \frac{N_1(q^{-1})}{D_1(q^{-1})} \quad , \quad K_2(q^{-1}) = \frac{N_2(q^{-1})}{D_2(q^{-1})} \quad , \quad K_3(q^{-1}) = \frac{N_3(q^{-1})}{D_3(q^{-1})}$$

Therefore, we have:

$$u(k) = K_1(q^{-1})\left[K_2(q^{-1})r(k) - K_3(q^{-1})y(k)\right]$$

or

$$N_1(q^{-1})N_3(q^{-1})D_2(q^{-1})y(k) + D_1(q^{-1})D_2(q^{-1})D_3(q^{-1})u(k) = N_1(q^{-1})N_2(q^{-1})D_3(q^{-1})r(k)$$

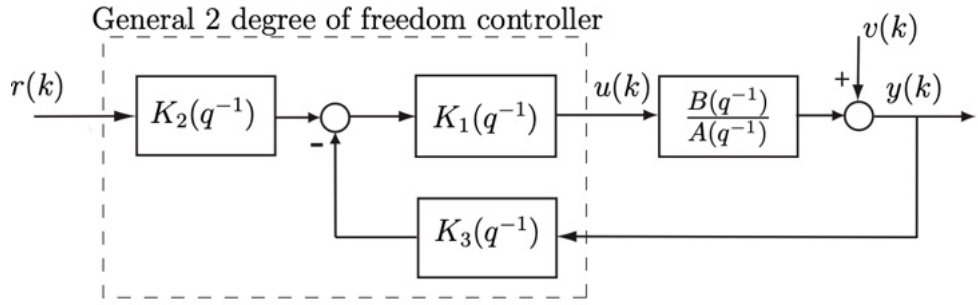

Figure 3.2: General two degree of freedom control system

If we compare this equation with that of an RST controller in (3.19) we get:

$$R(q^{-1}) = N_1(q^{-1})N_3(q^{-1})D_2(q^{-1}) \tag{3.21}$$
$$S(q^{-1}) = D_1(q^{-1})D_2(q^{-1})D_3(q^{-1}) \tag{3.22}$$
$$T(q^{-1}) = N_1(q^{-1})N_2(q^{-1})D_3(q^{-1}) \tag{3.23}$$

The classical one degree of freedom controller in the forward path is a particular case with $K_2(q^{-1}) = K_3(q^{-1}) = 1$ for which we have $R(q^{-1}) = N_1(q^{-1}), S(q^{-1}) = D_1(q^{-1})$ and $T(q^{-1}) = N_1(q^{-1})$. For the controller in the feedback path with $K_1(q^{-1}) = K_2(q^{-1}) = 1$, we obtain $R(q^{-1}) = N_3(q^{-1}), S(q^{-1}) = D_3(q^{-1})$ and $T(q^{-1}) = D_3(q^{-1})$.

3.2.3 Pole Placement Technique

The pole placement strategy allows the design of an RST digital controller both for stable and unstable systems:

- Without restriction on the degrees of the polynomials $A(q^{-1})$ and $B(q^{-1})$ of the discrete-time plant model (provided that they do not have common factors)
- Without restriction on the time delay
- Without restriction on the plant zeros (stable or unstable)

The only restriction concerns the possible common factors of $A(q^{-1})$ and $B(q^{-1})$, which must be simplified before the computations are carried out.

The structure of the closed-loop system is given in Figure 3.1. The plant to be controlled is characterized by the transfer operator (irreducible):

$$G(q^{-1}) = \frac{B(q^{-1})}{A(q^{-1})} \tag{3.24}$$

The closed-loop transfer function is given by

$$H_{cl}(q^{-1}) = \frac{T(q^{-1})B(q^{-1})}{P(q^{-1})} \tag{3.25}$$

where

$$P(q^{-1}) = A(q^{-1})S(q^{-1}) + q^{-d}B(q^{-1})R(q^{-1}) = 1 + p_1 q^{-1} + p_2 q^{-2} + \cdots \tag{3.26}$$

is the closed-loop characteristic polynomial that plays an essential role for the regulation behavior. The behavior with respect to an output disturbance is given by the sensitivity function:

$$\mathcal{S}(q^{-1}) = \frac{A(q^{-1})S(q^{-1})}{P(q^{-1})} \tag{3.27}$$

Desired Closed-Loop Poles

The desired performance is related to the polynomial $P(q^{-1})$. Consider the following example.

Example 3.2. Let $P(q^{-1}) = 1 + p_1 q^{-1}$ with $p_1 = -0.5$. When there is no reference, i.e. $r(k) \equiv 0$, the free output response is defined by

$$y(k+1) = -p_1 y(k) = 0.5y(k)$$

One thus obtains a relative decrease of 50% for the output amplitude at each sampling instant. It is clear that the disturbance rejection speed can be tuned by choosing p_1 between -0.2 and -0.8.

Nevertheless, generally speaking, $P(q^{-1})$ is chosen in the form of a second-order polynomial by discretization of a second-order continuous-time system. In what follows, we recall how time-domain performance is related to the place of the poles of a second-order system.

Consider a second-order continuous-time system given by:

$$H(s) = \frac{\omega_n^2}{s^2 + 2\zeta\omega_n s + \omega_n^2} \tag{3.28}$$

where ω_n is the natural frequency in rad/s ($\omega_n = 2\pi f_n$) and ζ is the damping factor. The poles of $H(s)$ are

$$s_{1,2} = -\zeta\omega_n \pm j\omega_n\sqrt{1-\zeta^2} \tag{3.29}$$

for $|\zeta| < 1$, we have two complex poles (oscillatory response) and for $|\zeta| \geq 1$, two real poles (aperiodic response). It is clear that for $\zeta > 0$ the system is asymptotically stable and for $\zeta < 0$ the system is unstable.

The step response of the second-order model $H(s)$ is given by (for $0 < \zeta < 1$):

$$y(t) = 1 - \frac{1}{\sqrt{1-\zeta^2}} e^{-\zeta\omega_n t}\left[\sin\left(\sqrt{1-\zeta^2}\, t + \psi\right)\right] \qquad t > 0 \tag{3.30}$$

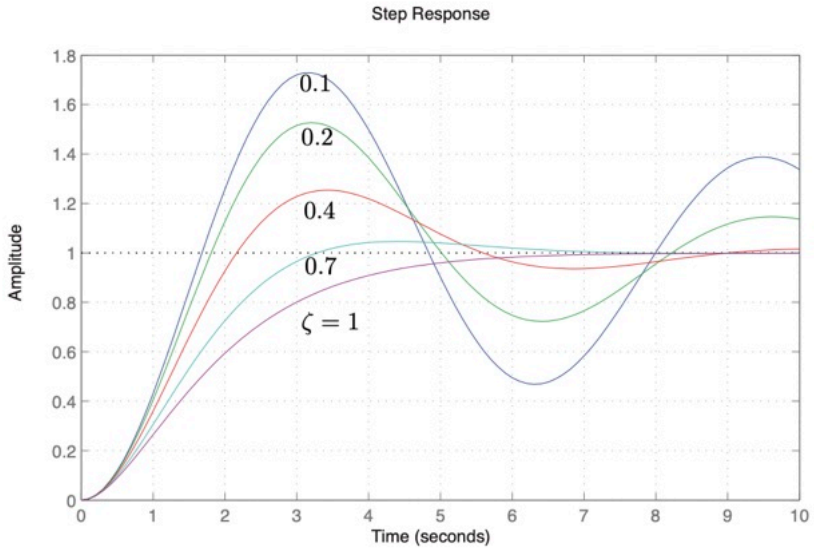

Figure 3.3: Step response of a second-order system for various damping factor ζ.

where $\psi = \cos^{-1}\zeta$. The step response is shown in Fig. 3.3 for a fixed $\omega_n = 1$ and various values of the damping factor ζ. As ζ decreases, the roots approach the imaginary axis, and the response becomes oscillatory. The peak value M_p is a function of the damping factor and is computed by:

$$M_p = 1 + e^{-\zeta\pi/\sqrt{1-\zeta^2}} \tag{3.31}$$

The settling time, T_{set} is defined as the time required for the step response to settle within a certain percentage of the final value. The settling time of a second-order system for which the response remains within 2% of the final value, occurs approximately when

$$e^{-\zeta\omega_n T_{set}} < 0.02 \qquad \text{or} \qquad \zeta\omega_n T_{set} \approx 4 \tag{3.32}$$

The swiftness of step response can be measured as the time it takes to rise from 10% to 90% of the final value. This is the definition of the rise time T_r. Although it is difficult to obtain exact analytic expression for T_r, the following approximations can be used:

$$T_r \approx \frac{2.16\zeta + 0.6}{\omega_n} \qquad \text{or} \qquad T_r \approx \frac{1.8}{\omega_n} \tag{3.33}$$

which is accurate enough for $0.3 \leq \zeta \leq 0.8$.

Example 3.3. Consider the problem of finding ω_n and ζ to obtain a rise time of 1s with an overshoot of 5%. From Eq. (3.31) we have:

$$e^{-\zeta\pi/\sqrt{1-\zeta^2}} = 0.05 \quad \Rightarrow \quad \zeta \approx 0.7$$

Then, from the first relation in Eq. (3.33), $\omega_n = 2.11$ is computed. This corresponds to the following poles $s_{1,2} = -1.4784 \pm j1.507$ for the continuous-time model.

In the next step, using the transformation $z_{1,2} = e^{s_{1,2}h}$, where h is the sampling period, the equivalent discretized poles can be computed. The following formula can be used for a general transformation :

$$(z - e^{s_1 h})(z - e^{s_2 h}) = z^2 + p_1 z + p_2 \tag{3.34}$$

with

$$p_1 = -2e^{-\zeta\omega_n h}\cos\left(\omega_n h\sqrt{1-\zeta^2}\right) \tag{3.35}$$

$$p_2 = e^{-2\zeta\omega_n h} \tag{3.36}$$

Example 3.4. Compute the desired discrete-time closed-loop polynomial to have an overshoot of 10% and a settling time of 1.2 s. Suppose that the sampling period $h = 0.1s$. From Eq. (3.31) for 10% overshoot we have:

$$e^{-\zeta\pi/\sqrt{1-\zeta^2}} = 0.1 \quad \Rightarrow \quad \zeta \approx 0.6$$

The natural frequency is computed from Eq. (3.32) as $\omega_n \approx 5.55$. Then from Eqs (3.35) and (3.36) we obtain:

$$P(q^{-1}) = 1 + p_1 q^{-1} + p_2 q^{-2} \qquad \text{with} \quad p_1 = -1.294 \quad , \quad p_2 = 0.513$$

that corresponds to the following desired poles:

$$z_{1,2} = 0.647 \pm j0.308$$

The loci of the roots of $P(q^{-1})$ can also be found for fixed values of ζ and ω_n. Fig. 3.4 shows the loci for $\zeta = 0.1$ to 0.9 and ω_n for $0.1\pi/h$ to π/h (the Nyquist frequency). Using this figure, which can be plotted in Matlab, the desired closed-loop poles can be chosen very easily. For example if $\zeta = 0.7$ (5% overshoot) and $\omega_n h = 0.628$, the roots of $P(q^{-1})$ will be at the intersections of the loci of the poles with $\zeta = 0.7$ and $\omega_n = 0.2\pi/h$. This leads to $z_{1,2} = 0.5806 \pm j0.2794$ which is illustrated in Fig. 3.4.

The typical values for ζ and ω_n are:

$$\frac{0.25}{h} \leq \omega_n \leq \frac{1.5}{h} \quad ; \quad 0.7 \leq \zeta \leq 1$$

Auxiliary poles: If it is desired to introduce a filtering action in certain frequency regions (or to reduce the effect of the noise on the measurements, or to smooth the variations of the control signal, or to improve the robustness), the poles of the corresponding filter, defined by a polynomial $P_f(q^{-1})$, should also be the poles of the closed loop. As a consequence, the polynomial $P(q^{-1})$ defining the desired closed-loop poles will be the product of the polynomials $P_d(q^{-1})$ and $P_f(q^{-1})$ specifying dominant and auxiliary closed-loop poles, respectively.

$$P(q^{-1}) = P_d(q^{-1})\, P_f(q^{-1}) \tag{3.37}$$

As a general rule, the poles named "auxiliary poles" are faster than the "dominant poles". That is expressed, for the case of discrete-time models, by the property that the roots of $P_f(q^{-1})$ should have a real part smaller than the real part of the roots of $P_d(q^{-1})$.

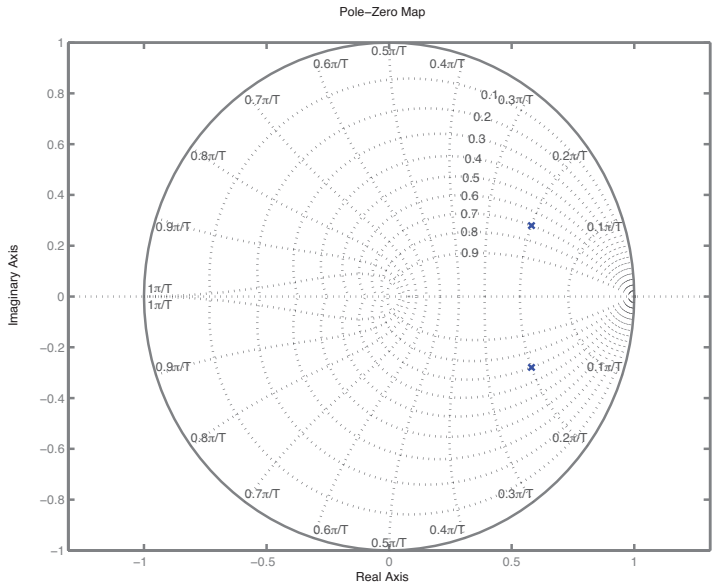

Figure 3.4: Desired closed-loop poles with the loci for constant ζ and ω_n

Regulation: Computation of $R(q^{-1})$ and $S(q^{-1})$

Once $P(q^{-1})$ is specified, in order to compute $R(q^{-1})$ and $S(q^{-1})$, the following equation, known as "Bezout identity" (or Diophantine equation), must be solved:

$$A(q^{-1})S(q^{-1}) + B(q^{-1})R(q^{-1}) = P(q^{-1}) \tag{3.38}$$

Defining

$$n_A = \deg\, A(q^{-1}) \quad ; \quad n_B = \deg\, B(q^{-1}) \tag{3.39}$$

this polynomial equation has a unique solution with minimal degree (when $A(q^{-1})$ and $B(q^{-1})$ do not have common factors) for

$$\begin{aligned} n_R &= \deg\, R(q^{-1}) = n_A - 1 \\ n_S &= \deg\, S(q^{-1}) = n_B - 1 \\ n_P &= \deg\, P(q^{-1}) \leq n_A + n_B - 1 \end{aligned}$$

in which

$$R(q^{-1}) = r_0 + r_1 q^{-1} + \cdots + r_{n_R} q^{-n_R} \tag{3.40}$$

$$S(q^{-1}) = 1 + s_1 q^{-1} + \cdots + s_{n_S} q^{-n_S} = 1 + q^{-1} S^{\star}(q^{-1}) \tag{3.41}$$

Example 3.5. Consider a discrete-time plant model given by:

$$G(q^{-1}) = \frac{b_1 q^{-1} + b_2 q^{-2}}{1 + a_1 q^{-1} + a_2 q^{-2}}$$

The objective is to find the polynomials $R(q^{-1})$ and $S(q^{-1})$ to place the closed-loop poles in the desired places. For this system we have: $n_A = 2, n_B = 2$. Therefore, the controller with the minimal degree has $n_S = 1$ and $n_R = 1$. So three unknown parameters r_0, r_1 and s_1 in $R(q^{-1}) = r_0 + r_1 q^{-1}$ and $S(q^{-1}) = 1 + s_1 q^{-1}$ should be computed. On the other hand, since $n_P \leq 3$ we can place 3 poles in the desired places. Suppose that we choose two complex conjugate poles to meet some conditions on the damping factor and natural frequency, i.e. $n_P = 2$. Therefore, the following Bezout identity should be solved:

$$(1 + a_1 q^{-1} + a_2 q^{-2})(1 + s_1 q^{-1}) + (b_1 q^{-1} + b_2 q^{-2})(r_0 + r_1 q^{-1}) = 1 + p_1 q^{-1} + p_2 q^{-2}$$

By making equal the coefficients of the same powers of q in both sides of the above equation, three linear equations are obtained:

$$\begin{aligned} a_1 + s_1 + b_1 r_0 &= p_1 \\ a_2 + a_1 s_1 + b_2 r_0 + b_1 r_1 &= p_2 \\ a_2 s_1 + b_2 r_1 &= 0 \end{aligned}$$

These equations can be written in the matrix form:

$$\begin{bmatrix} 1 & 0 & 0 & 0 \\ a_1 & 1 & b_1 & 0 \\ a_2 & a_1 & b_2 & b_1 \\ 0 & a_2 & 0 & b_2 \end{bmatrix} \begin{bmatrix} 1 \\ s_1 \\ r_0 \\ r_1 \end{bmatrix} = \begin{bmatrix} 1 \\ p_1 \\ p_2 \\ 0 \end{bmatrix} \tag{3.42}$$

A solution to these equation can be found if the matrix of the coefficients is non singular. We know from Theorem 3.2 that this condition is met if and only if $A(q^{-1})$ and $B(q^{-1})$ do not have common factors.

A general solution to Eq. (3.38) can be written in the matrix form

$$Mx = p \tag{3.43}$$

where

$$x^T = \begin{bmatrix} 1 & s_1 & \dots & s_{n_S} & r_0 & \dots & r_{n_R} \end{bmatrix} \tag{3.44}$$

$$p^T = \begin{bmatrix} 1 & p_1 & \dots & p_{n_P} & 0 & \dots & 0 \end{bmatrix} \tag{3.45}$$

and the matrix M (known as Sylvester matrix or controllability matrix) has the form:

$$M = \overbrace{\left[\begin{array}{cccc} 1 & 0 & \cdots & 0 \\ a_1 & 1 & \ddots & \vdots \\ \vdots & a_1 & \ddots & 0 \\ \vdots & \vdots & \ddots & 1 \\ \vdots & & & a_1 \\ a_{n_A} & & & \vdots \\ 0 & a_{n_A} & & \vdots \\ \vdots & \ddots & \ddots & \vdots \\ 0 & \cdots & 0 & a_{n_A} \end{array}\right.}^{n_B} \overbrace{\left.\begin{array}{cccc} b_0 & 0 & \cdots & 0 \\ b_1 & b_0 & \ddots & \vdots \\ \vdots & b_1 & \ddots & \vdots \\ \vdots & \vdots & \ddots & b_0 \\ \vdots & & & b_1 \\ b_{n_B} & & & \vdots \\ 0 & b_{n_B} & & \vdots \\ \vdots & \ddots & \ddots & \vdots \\ 0 & \cdots & 0 & b_{n_B} \end{array}\right]}^{n_A} \left.\begin{array}{c} \\ \\ \\ \\ \\ \\ \\ \\ \\ \end{array}\right\} n_A + n_B \tag{3.46}$$

The vector x, which contains the coefficients of the polynomials $R(q^{-1})$ and $S(q^{-1})$, is obtained, after the inversion of the matrix M, by the formula

$$x = M^{-1}p \tag{3.47}$$

Note that the inverse of M exists if the determinant of the matrix M is different from zero, i.e. if and only if $A(q^{-1})$ and $B(q^{-1})$ are coprime polynomials (no simplifications between zeros and poles).

For different reasons the polynomials $R(q^{-1})$ and $S(q^{-1})$ may contain, in general, fixed parts specified before the resolution of Eq. (3.38) . In order to take into account these pre-specified fixed parts, the polynomials $R(q^{-1})$ and $S(q^{-1})$ are factorized in the form

$$R(q^{-1}) = R'(q^{-1})H_R(q^{-1}) \tag{3.48}$$
$$S(q^{-1}) = S'(q^{-1})H_S(q^{-1}) \tag{3.49}$$

where $H_R(q^{-1})$ and $H_S(q^{-1})$ are pre-specified polynomials and

$$R'(q^{-1}) = r'_0 + r'_1 q^{-1} + \cdots + r'_{n_{R'}} q^{-n_{R'}} \tag{3.50}$$
$$S'(q^{-1}) = 1 + s'_1 q^{-1} + \cdots + s'_{n_{S'}} q^{-n_{S'}} \tag{3.51}$$

$H_R(q^{-1})$ and $H_S(q^{-1})$ are primarily chosen in relation with the desired nominal performances. $H_S(q^{-1})$ should incorporate the internal model of the disturbance to be rejected (for example $H_S(q^{-1}) = 1 - q^{-1}$, in order to have an integrator which will assure zero steady state error for a step disturbance). $H_R(q^{-1})$ will typically incorporate a filter for reducing the actuator stress in a certain frequency range (by reducing the gain of the controller).

For this parameterization of polynomials $R(q^{-1})$ and $S(q^{-1})$, the closed-loop transfer function will be

$$H_{cl}(q^{-1}) = \frac{T(q^{-1})B(q^{-1})}{A(q^{-1})S'(q^{-1})H_S(q^{-1}) + B(q^{-1})R'(q^{-1})H_R(q^{-1})} = \frac{T(q^{-1})B(q^{-1})}{P(q^{-1})}$$

Therefore, we need to solve the following equation :

$$A(q^{-1})S'(q^{-1})H_S(q^{-1}) + B(q^{-1})R'(q^{-1})H_R(q^{-1}) = P(q^{-1}) \tag{3.52}$$

This can be done after replacing: $A(q^{-1})$ by $A'(q^{-1}) = A(q^{-1})H_S(q^{-1})$ and $B(q^{-1})$ by $B'(q^{-1}) = B(q^{-1})H_R(q^{-1})$ with the restriction that polynomials $[A(q^{-1})H_S(q^{-1})]$ and $[B(q^{-1})H_R(q^{-1})]$ are coprime. The conditions on the orders of the polynomials that allow one to get a unique solution of minimal order, become in this case

$$\begin{aligned} n_{R'} &= \deg R'(q^{-1}) = n_A + n_{H_S} - 1 \\ n_{S'} &= \deg S'(q^{-1}) = n_B + n_{H_R} - 1 \\ n_P &= \deg P(q^{-1}) \leq n_A + n_{H_S} + n_B + n_{H_R} - 1 \end{aligned}$$

For the controller implementation, $S(q^{-1})$ will be given by $S'(q^{-1})H_S(q^{-1})$ and $R(q^{-1})$ by $R'(q^{-1})H_R(q^{-1})$.

Choice of H_R and H_S

Zero steady-state error for a step disturbance: From Fig. 3.1 in the absence of the reference signal (i.e. $r(k) \equiv 0$), one has:

$$y(k) = \frac{A(q^{-1})H_S(q^{-1})S'(q^{-1})}{P(q^{-1})}v(k) \tag{3.53}$$

For a step disturbance we have

$$v(k) = \frac{1}{1-q^{-1}}\delta(k) \tag{3.54}$$

where $\delta(k)$ is the Kronecker impulse ($\delta(k) = 0$ for $t \neq 0$ and $\delta(0) = 1$). The problem can be viewed as either imposing the cancellation of the disturbance model (in this case $(1-q^{-1})$) or as choosing $H_S(q^{-1})$ such that the gain of the transfer function between $v(k)$ and $y(k)$ be zero for the zero frequency (i.e., for $q = z = 1$). Both points of view lead to:

$$H_S(q^{-1}) = (1-q^{-1})$$

Perfect rejection of a harmonic disturbance: In this case the disturbance is:

$$v(k) = \frac{1}{1 + \alpha q^{-1} + q^{-2}} \delta(k)$$

with

$$\alpha = -2\cos(\omega h) = -2\cos(2\pi \frac{f}{f_s})$$

and applying the same reasoning one finds:

$$H_S(q^{-1}) = (1 + \alpha q^{-1} + q^{-2})$$

If we would like only a desired attenuation at the frequency f, one can use a pair of damped zeros in H_S with a damping factor in relation with the desired attenuation.

Opening the loop: In a number of applications, the measured signal may contain specific frequencies which should not be attenuated by the regulation (they correspond in general to signals inherent to the technology of the process). In such cases the system should be in open loop at these frequencies. i.e., this disturbance is made unobservable at the input of the plant. In the absence of the reference, the input to the plant is given by:

$$u(k) = -\mathcal{U}(q^{-1})v(k) = -\frac{A(q^{-1})H_R(q^{-1})R'(q^{-1})}{P(q^{-1})} v(k)$$

and therefore in order to make the input sensitivity function zero at a given frequency f one should introduce a pair of undamped zeros in $H_R(q^{-1})$ i.e.,

$$H_R(q^{-1}) = (1 + \beta q^{-1} + q^{-2})$$

where

$$\beta = -2\cos(\omega h) = -2\cos(2\pi \frac{f}{f_s})$$

In many cases it is desired that the controller does not react to signals of frequencies close to $0.5 f_s$ (where the gain of the system is in general very low). In such cases one uses:

$$H_R(q^{-1}) = (1 + \beta q^{-1})$$

where $0 < \beta \leq 1$. Note that $(1 + \beta q^{-1})^2$ corresponds to a second order with a damped resonance frequency equal to $\omega_s/2$:

$$\omega_0 \sqrt{1 - \zeta^2} = \frac{\omega_s}{2}$$

and the corresponding damping is related to β by

$$\beta = e^{-\frac{\zeta}{\sqrt{1-\zeta^2}}\pi}$$

For $\beta = 1$, the system will operate in open loop at $f_s/2$.

Tracking: Computation of $T(q^{-1})$

In the ideal case we would like to perfectly follow a desired trajectory $y^\star(k+d)$, known d steps ahead, which is stored in the computer or generated from the reference signal via a tracking reference model, i.e.,

$$H_m(q^{-1}) = \frac{B_m(q^{-1})}{A_m(q^{-1})} \tag{3.55}$$

Often, this tracking reference model is determined from the desired tracking performances (rise time, settling time, overshoot) by selecting either an appropriate normalized second order system (defined by ω_n, ζ) or sometimes a cascade of two second orders. Once a continuous-time reference model is selected, one gets by discretization the discrete-time tracking reference model.

The remaining design element of the controller is the polynomial $T(q^{-1})$. The transfer function from the desired reference trajectory to the output is:

$$H_{cl}(q^{-1}) = \frac{T(q^{-1})B(q^{-1})}{P_d(q^{-1})P_f(q^{-1})} = \frac{q^{-d}T(q^{-1})B^\star(q^{-1})}{P_d(q^{-1})P_f(q^{-1})} \tag{3.56}$$

where $B(q^{-1}) = q^{-d}B^\star(q^{-1})$ is used to show clearly the existence of a pure time delay in this transfer function. Two situations may occur.

a) Different dynamics for tracking and regulation.

b) Same dynamics for tracking and regulation.

In the case a) $H_{cl}(q^{-1})$ should have a steady-state gain of 1 and $T(q^{-1})$ should compensate the closed-loop poles i.e.,

$$T(q^{-1}) = \beta P(q^{-1}) \tag{3.57}$$

where

$$\beta = \frac{1}{B(1)} \tag{3.58}$$

The resulting transfer function from the reference to the output is:

$$H_{cl}(q^{-1}) = \frac{B_m(q^{-1})B(q^{-1})}{A_m(q^{-1})B(1)} = \frac{q^{-d}B_m(q^{-1})B^\star(q^{-1})}{A_m(q^{-1})B(1)} \tag{3.59}$$

In the case b)

$$H_m(q^{-1}) = 1 \tag{3.60}$$

$$T(q^{-1}) = \beta P(1) \tag{3.61}$$

If S contains an integrator then $P(1) = B(1)R(1)$ and therefore:

$$T(q^{-1}) = R(1) \tag{3.62}$$

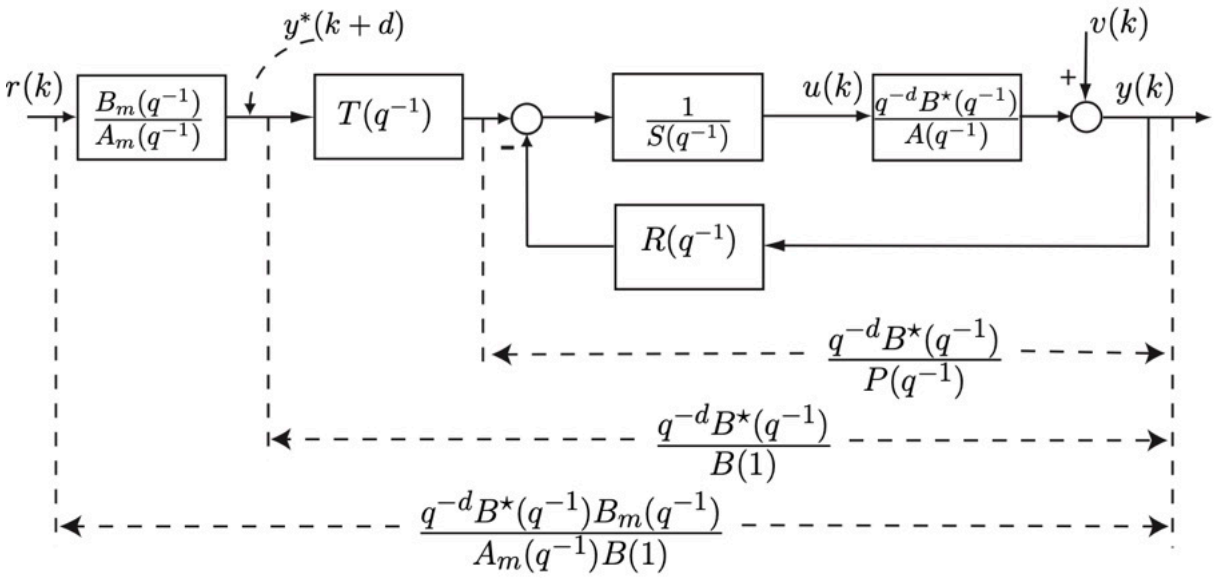

Figure 3.5: Pole placement scheme for tracking and regulation

The resulting transfer function from the reference to the output is in this case:

$$H_{cl}(q^{-1}) = \frac{B(q^{-1})P(1)}{P(q^{-1})B(1)} = \frac{q^{-d}B^\star(q^{-1})P(1)}{P(q^{-1})B(1)} \tag{3.63}$$

Note that better tracking performances can be obtained if the stable zeros of $B(q^{-1})$ are compensated and the unstable ones are partially compensated by using the stable reciprocal inverse. However, this requires a very good knowledge of the coefficient of $B(q^{-1})$.

The complete block diagram of the pole placement for the case a) (different dynamics for tracking and regulation) is shown in Fig. 3.5.

Example 3.6. Consider the following discrete-time second-order plant model:

$$G(q^{-1}) = \frac{0.1q^{-1} + 0.2q^{-2}}{1 - 1.3q^{-1} + 0.42q^{-2}}$$

The sampling period is $h = 1s$. Design an RST controller such that the tracking dynamics is close to the dynamics of a second-order continuous-time model with $\omega_n = 0.5$ rad/s and $\zeta = 0.9$. The regulation dynamics should be close to that of a second-order continuous-time model with $\omega_n = 0.4$ rad/s and $\zeta = 0.9$. The steady state error for an output step disturbance should be zero.

Step 1: From the desired regulation dynamics the dominant closed-loop poles should be computed. Using Eqs (3.35) and (3.36), with $\omega_n = 0.4$ rad/s and $\zeta = 0.9$, we obtain:

$$P(q^{-1}) = 1 - 1.3741q^{-1} + 0.4867q^{-2}$$

Step 2: Zero steady state error is obtained by choosing $H_S(q^{-1}) = 1 - q^{-1}$.

Step 3: The following Bezout equation should be solved:

$$A(q^{-1})H_S(q^{-1})S'(q^{-1}) + B(q^{-1})R(q^{-1}) = P(q^{-1})$$

We have deg $S' = n_B - 1 = 1$ and deg $R = n_A + n_{H_S} - 1 = 2$ and

$$A'(q^{-1}) = A(q^{-1})(1 - q^{-1}) = 1 - 2.3q^{-1} + 1.72q^{-2} - 0.42q^{-3}$$

Therefore the Bezout equation in the matrix form becomes:

$$\begin{bmatrix} 1 & 0 & 0 & 0 & 0 \\ -2.3 & 1 & 0.1 & 0 & 0 \\ 1.72 & -2.3 & 0.2 & 0.1 & 0 \\ -0.42 & 1.72 & 0 & 0.2 & 0.1 \\ 0 & -0.42 & 0 & 0 & 0.2 \end{bmatrix} \begin{bmatrix} 1 \\ s'_0 \\ r_0 \\ r_1 \\ r_2 \end{bmatrix} = \begin{bmatrix} 1 \\ -1.3741 \\ 0.4867 \\ 0 \\ 0 \end{bmatrix}$$

Solving this equation leads to

$$\begin{aligned} R(q^{-1}) &= 3 - 3.94q^{-1} + 1.3141q^{-2} \\ S(q^{-1}) &= (1 + s'_0 q^{-1})(1 - q^{-1}) = 1 - 0.3742q^{-1} - 0.6258q^{-2} \end{aligned}$$

Step 4: The reference model $H_m(q^{-1})$ is computed by discretization of a second-order model with $\omega_n = 0.5$ rad/s and $\zeta = 0.9$:

$$H_m(q^{-1}) = \frac{0.0927q^{-1} + 0.0687q^{-2}}{1 - 1.2451q^{-1} + 0.4066q^{-2}}$$

Finally, the polynomial $T(q^{-1}) = \beta P(q^{-1})$ where $\beta = 1/B(1) = 3.333$:

$$T(q^{-1}) = 3.333 - 4.5806q^{-1} + 1.6225q^{-2}$$

If we wish to have the same dynamics for tracking and regulation, then $H_m(q^{-1}) = 1$ and $T(q^{-1}) = R(1) = 0.3741$.

3.2.4 Model Reference Control

In the conventional pole placement technique we could choose different dynamics for regulation and tracking. However, the transfer function between the reference and the closed-loop output, $H_{cl}(q^{-1})$ in (3.59), contained the zeros of the plant model in addition to the reference model $H_m(q^{-1})$ in (3.55). In Model Reference Control, the zeros of the plant model can also be cancelled that enables the tracking and regulation performance to be achieved without approximation. As a result of the simplification of the zeros, however, this strategy can only be applied to discrete-time models with stable zeros.

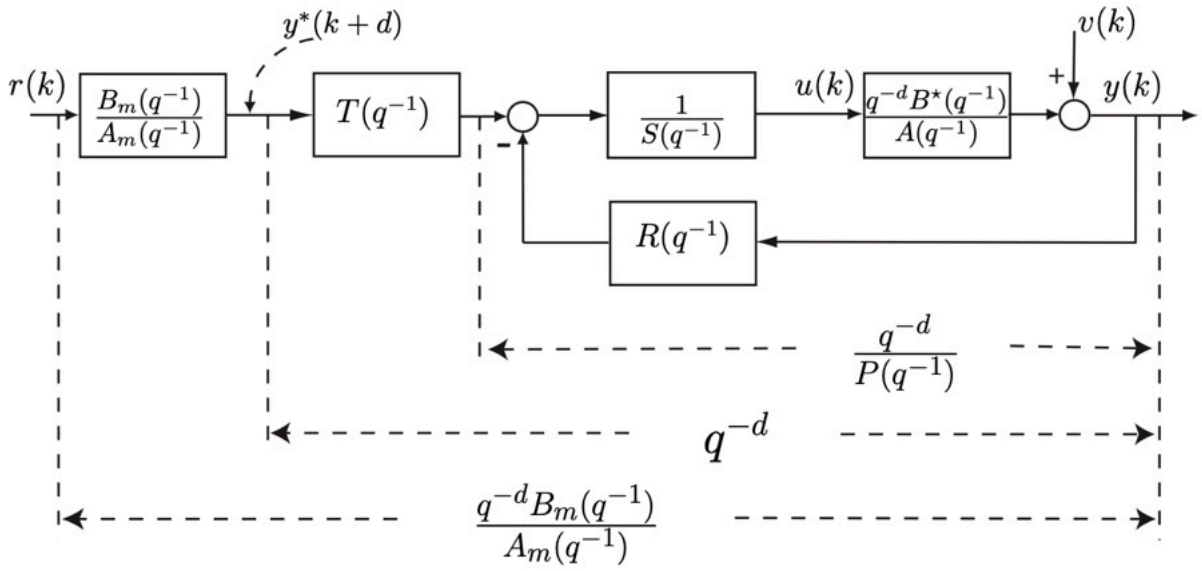

Figure 3.6: Tracking and regulation for Model Reference Control

Note that for continuous-time model, unstable zeros represents non-minimum-phase systems. But for discrete-time models, unstable zeros can be the consequence of too fast sampling (even if the continuous-time zeros are stable). A large fractional delay can also generate unstable zeros which can be avoided by re-identification of a model with augmented delay or resampling. Suppose that the pure time delay of the continuous-time model τ is written as $\tau = dh + L$, where $0 < L < h$ is the fractional delay. It can be shown that if $L > 0.5h$ the identified model will have an unstable zero.

This method can be considered as a particular case of the "pole placement" method. This equivalence can be obtained by imposing that the closed-loop poles contain the zeros of the discrete-time plant model (defined by the polynomial $B^*(q^{-1})$). This is the reason for which the zeros of the plant model must be stable. It is convenient then to verify that, before the application of this method, the zeros of $B^*(q^{-1})$ are stable, and, moreover, that complex zeros have a sufficiently high damping factor ($\zeta > 0.2$). In other words, the zeros should lie inside a region defined by the cardioids related to the constant damping factor $\zeta = 0.2$.

The structure of the closed-loop system is represented in Fig. 3.6. The desired closed-loop poles are defined by a polynomial $P(q^{-1})$ which specifies the desired regulation behavior.

Regulation: Computation of $R(q^{-1})$ and $S(q^{-1})$

The transfer function of the closed loop without precompensator is:

$$H_{cl}(q^{-1}) = \frac{q^{-d}B^\star(q^{-1})}{A(q^{-1})S(q^{-1}) + q^{-d}B^\star(q^{-1})R(q^{-1})} = \frac{q^{-d}B^\star(q^{-1})}{B^\star(q^{-1})P(q^{-1})} \tag{3.64}$$

where $B(q^{-1}) = q^{-d}B^\star(q^{-1})$ and

$$B^\star(q^{-1}) = b_d + b_{d+1}q^{-1} + \cdots + b_{n_B}q^{-n_B+d} \tag{3.65}$$

While $P(q^{-1})$ represents the desired closed-loop poles, the real closed-loop poles will include also $B^\star(q^{-1})$. Standard application of pole placement leads to:

$$A(q^{-1})S(q^{-1}) + q^{-d}B^\star(q^{-1})R(q^{-1}) = B^\star(q^{-1})P(q^{-1}) \tag{3.66}$$

The structure of this equation implies that $S(q^{-1})$ will be of the form:

$$S(q^{-1}) = s_0 + s_1q^{-1} + \ldots + s_{n_S}q^{-n_S} = B^\star(q^{-1})S'(q^{-1}) \tag{3.67}$$

In fact $S(q^{-1})$ will compensate the plant model zeros. Introducing the expression of $S(q^{-1})$ in (3.66) and after simplification by $B^\star(q^{-1})$, one obtains:

$$A(q^{-1})S'(q^{-1}) + q^{-d}R(q^{-1}) = P(q^{-1}) \tag{3.68}$$

Theorem 3.3. *The polynomial equation (3.68) has a unique solution for:*

$$\begin{aligned} n_P &= \deg P \leq n_A + d - 1 && (3.69)\\ n_{S'} &= \deg S' = d - 1 && (3.70)\\ n_R &= \deg R(q^{-1}) = n_A - 1 && (3.71) \end{aligned}$$

and the polynomials R and S' have the form:

$$\begin{aligned} R(q^{-1}) &= r_0 + r_1q^{-1} + \ldots + r_{n_A-1}q^{-n_A+1} && (3.72)\\ S'(q^{-1}) &= 1 + s'_1q^{-1} + \ldots + s'_dq^{-d-1} && (3.73) \end{aligned}$$

Proof. Eq. (3.68) corresponds to the matrix equation

$$Mx = p \tag{3.74}$$

where M is a lower triangular matrix of dimension $(n_A + d) \times (n_A + d)$ of the form:

$$M = \begin{bmatrix} \overbrace{\begin{matrix} 1 & 0 & \cdots & 0 \\ a_1 & 1 & \ddots & \vdots \\ \vdots & a_1 & \ddots & 0 \\ & & & 1 \\ \vdots & & & a_1 \\ a_{n_A} & \vdots & & \\ 0 & a_{n_A} & \ddots & \vdots \\ \vdots & \cdots & 0 & a_{n_A} \end{matrix}}^{d} & \overbrace{\begin{matrix} 0 & \cdots & \cdots & 0 \\ \vdots & & & \vdots \\ \vdots & & & \vdots \\ 0 & \cdots & \cdots & 0 \\ 1 & \ddots & & \vdots \\ 0 & \ddots & \ddots & \vdots \\ \vdots & \ddots & \ddots & 0 \\ 0 & \cdots & 0 & 1 \end{matrix}}^{n_A} \end{bmatrix} \left.\vphantom{\begin{matrix} a \\ a \\ a \\ a \\ a \\ a \\ a \\ a \end{matrix}}\right\} n_A + d \tag{3.75}$$

$$x^T = [1, s'_1, \ldots, s'_d, r_0, \ldots, r_{n_A-1}] \tag{3.76}$$

$$p^T = [1, p_1, \ldots, p_{n_A}, p_{n_A+1}, \ldots, p_{n_A+d-1}] \tag{3.77}$$

Some of the coefficients p_i can be zero. Since M is a lower triangular matrix it is always non-singular which implies that (3.74) (and respectively (3.68)) always has a solution: $x = M^{-1}p$. □

As in the case of the pole placement it is convenient to consider a parameterization of the controller polynomials $S(q^{-1})$ and $R(q^{-1})$ as:

$$S(q^{-1}) = S'(q^{-1})H_S(q^{-1}) \tag{3.78}$$

$$R(q^{-1}) = R'(q^{-1})H_R(q^{-1}) \tag{3.79}$$

where $H_R(q^{-1})$ and $H_S(q^{-1})$ represent the prespecified parts of $R(q^{-1})$ and $S(q^{-1})$. In this case $H_S(q^{-1})$ takes the specific form:

$$H_S(q^{-1}) = B^\star(q^{-1})H'_S(q^{-1}) \tag{3.80}$$

and (3.68) becomes

$$A(q^{-1})H'_S(q^{-1})S'(q^{-1}) + q^{-d}H_R(q^{-1})R'(q^{-1}) = P(q^{-1}) \tag{3.81}$$

All the consideration concerning $H_R(q^{-1})$ and $H'_S(q^{-1})$ discussed in Section 3.2.3 for the pole placement are applicable.

Tracking: Computation of $T(q^{-1})$

The precompensator $T(q^{-1})$ is computed in order to ensure the following transfer function between the reference $r(k)$ and $y(k)$:

$$H_{cl}(q^{-1}) = \frac{q^{-d}B_m(q^{-1})}{A_m(q^{-1})} = \frac{q^{-d}B_m(q^{-1})T(q^{-1})}{A_m(q^{-1})P(q^{-1})} \tag{3.82}$$

From (3.82) one obtains:

$$T(q^{-1}) = P(q^{-1}) \tag{3.83}$$

The input to $T(q^{-1})$ at sampling instant k is the desired trajectory $y^\star$, d steps ahead $(y^\star(k+d))$.

Controller Equation

The controller equation is given by:

$$S(q^{-1})u(k) = -R(q^{-1})y(k) + P(q^{-1})y^\star(k+d) \tag{3.84}$$

Taking into account the form of $S(q^{-1})$

$$S(q^{-1}) = s_0 + s_1 q^{-1} + \ldots + s_{n_S} q^{-n_S} = s_0 + q^{-1} S^\star(q^{-1}) = B^\star(q^{-1}) S'(q^{-1}) \tag{3.85}$$

with

$$s_0 = b_d \tag{3.86}$$

(3.84) takes the form:

$$u(k) = \frac{1}{b_d}\left[P(q^{-1})y^\star(k+d) - S^\star(q^{-1})u(k-1) - R(q^{-1})y(k)\right] \tag{3.87}$$

or in a regressor form:

$$\theta_C^T \phi_C(k) = P(q^{-1})y^\star(k+d) \tag{3.88}$$

where:

$$\phi_C^T(k) = [u(k), \ldots, u(k-n_S), y(k), \ldots, y(k-n_R)] \tag{3.89}$$

$$\theta_C^T = [s_0, \ldots, s_{n_S}, r_0, \ldots, r_{n_R}] \tag{3.90}$$

Observe in (3.87) that low values of $|b_d|$ may lead to very large plant inputs. But this is exactly what happens when one has a significant fractional delay or an unstable zero.

3.2.5 Robust Pole Placement

Using the pole placement technique the closed-loop poles can freely be assigned in the desired places and desired performance in tracking and disturbance rejection can be achieved for the nominal model in simulation. However, the designed controller may not be implemented on the real system for the following reasons:

1. the controller may not be robust with respect to model uncertainty;
2. the control input may be too large and saturated in real experiment.

Therefore, the robustness of the designed controller and the maximum value of the input signal should be verified in simulation before implementation.

Robustness can be verified using the robustness margins like gain, phase and modulus margin. The inverse of the infinity norm of the sensitivity function, the modulus margin M_m, is a good indicator of the robustness margin. A modulus margin $M_m \geq 0.5$ implies a gain margin of greater than 2 and a phase margin of greater than 29°. The robustness can be verified by observing the Bode diagram of the output sensitivity function :

$$\mathcal{S}(z^{-1}) = \frac{A(z^{-1})S(z^{-1})}{A(z^{-1})S(z^{-1}) + B(z^{-1})R(z^{-1})} = \frac{A(z^{-1})S(z^{-1})}{P(z^{-1})}$$

The infinity norm of the sensitivity function $\|\mathcal{S}\|_\infty = \max_\omega |\mathcal{S}(e^{-j\omega})| < 6\text{dB}$ is equivalent to $M_m > 0.5$.

Sensitivity Function Shaping

In general, robustness can be improved and the amplitude of the control input can be reduced by slowing down the swiftness of the closed-loop system. This can be done by reducing the natural frequency ω_n of the dominant desired closed-loop pole and/or by placing the auxiliary poles with greater real part. However, the auxiliary poles should be always faster than the dominant poles. The use of fixed terms in the controller can help improving the robustness and reducing the amplitude of the control input (see Section 3.2.3).

Example 3.7. Consider the following plant model with $h = 1s$:

$$G(q^{-1}) = \frac{q^{-1} + 0.5q^{-2}}{1 - 1.5q^{-1} + 0.7q^{-2}}$$

First we compute a controller to assign the closed-loop poles at $z_{1,2} = 0.3 \pm j0.2$ and to reject a constant disturbance ($H_S(q^{-1}) = 1 - q^{-1}$). Solving the Bezout equation with $P(q^{-1}) = 1 - 0.6q^{-1} + 0.13q^{-2}$, we obtain:

$$R(q^{-1}) = 1.4667 - 1.72q^{-1} + 0.6067q^{-2} \quad ; \quad S(q^{-1}) = 1 - 0.5667q^{-1} - 0.4333q^{-2}$$

The polynomial $T(q^{-1}) = P(q^{-1})/B(1)$ and the reference model $H_m(q^{-1})$ is chosen appropriately to achieve the desired tracking performance. This controller, however, does not have necessarily a good robustness. The modulus margin $M_m = 1/\|\mathcal{S}\|_\infty = 0.39$ is not large enough and the peak-to-peak value of the control input for an impulse disturbance at the output is greater than 5 and its two-norm is 4.05. The maximum of the amplitude of the input sensitivity function is about 17dB which shows poor robustness with respect to additive uncertainty at high frequencies.

There are two approaches to improve the robustness of the closed-loop system. The first one is to slowing down the desired closed-loop poles. A good choice is to choose the

desired poles with the same natural frequency of the open-loop poles but with a larger damping factor. The plant model has two complex poles with $\omega_n = 0.4926$ rad/s and $\zeta = 0.362$. So the desired closed-loop poles with the same natural frequency and $\zeta = 0.9$ are chosen ($z_{1,2} = 0.6272 \pm j0.1368$). This leads to a new controller with:

$$R(q^{-1}) = 0.8721 - 1.29q^{-1} + 0.5231q^{-2} \quad ; \quad S(q^{-1}) = 1 - 0.6264q^{-1} - 0.3736q^{-2}$$

This controller has a modulus margin of $M_m = 0.566$ and a maximum of 10dB for the amplitude of the input sensitivity function. So it is more robust than the original controller. On the other hand, it has better performance in terms of the control input; the peak-to-peak value of the control input is less than 2 and its two norm is $\|\mathcal{U}\|_2 = 1.92$. However, as a result of slower poles, a step disturbance at the output is rejected after 12 seconds while the rejection time for the original controller is 6s. The second solution is to add a fixed term $H_R(q^{-1}) = 1 + q^{-1}$ in the controller to reduce the input sensitivity function at high frequencies. Therefore, the same closed-loop poles as the original controller is chosen ($P(q^{-1}) = 1 - 0.6q^{-1} + 0.13q^{-2}$) and the following controller is computed:

$$\begin{aligned} R(q^{-1}) &= 0.8740 - 0.2382q^{-1} - 0.6973q^{-2} + 0.4149q^{-3} \\ S(q^{-1}) &= 1 + 0.0260q^{-1} - 0.7297q^{-2} - 0.2964q^{-3} \end{aligned}$$

This controller does not improve the modulus margin ($M_m = 0.3913$) but reduces the maximum magnitude of the input sensitivity function to 10dB. It leads to a peak-to-peak value of the control input of about 2 and two-norm of 1.8675. The rejection time of output step disturbance is also fast enough (7s). Figure 3.7 shows the step response for an output disturbance, the control input for an impulse disturbance at the output, the magnitude of the output sensitivity function and the input sensitivity function for the three different controllers designed for this example.

In [7] some iterative methods are proposed to design the fixed terms in the controller that lead to a robust controller. Here, an optimization based approach is proposed to shape the sensitivity function and assign the closed-loop poles. The approach is based on Q-parameterization and uses the convex optimization algorithms.

Q-Parametrization

Suppose that $R_0(q^{-1})$ and $S_0(q^{-1})$ are computed for a nominal model and a given $P(q^{-1})$. Then, the following set of controllers:

$$R(q^{-1}) = R_0(q^{-1}) + A(q^{-1})Q(q^{-1}) \tag{3.91}$$
$$S(q^{-1}) = S_0(q^{-1}) - B(q^{-1})Q(q^{-1}) \tag{3.92}$$

where

$$Q(q^{-1}) = q_0 + q_1q^{-1} + \cdots + q_{n_q}q^{-n_q}$$

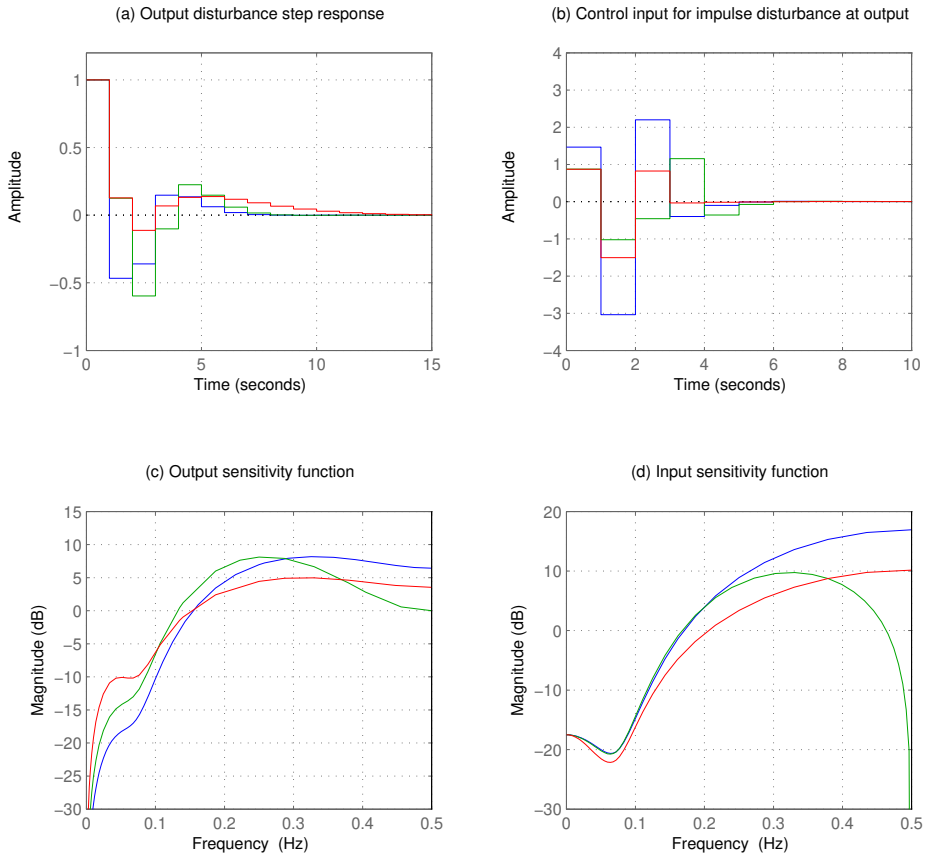

Figure 3.7: Original controller (blue curves), improved controller by slowing down the closed-loop poles (red curves), improved controller by adding a fixed term $H_R(q^{-1}) = 1 + q^{-1}$ (green curves)

are also the solutions of (3.38) which are not necessarily of minimal order. This can be observed by computing the closed-loop poles for the parameterized controller:

$$\begin{aligned} A(q^{-1})S(q^{-1}) + B(q^{-1})R(q^{-1}) &= A(q^{-1})S_0(q^{-1}) - A(q^{-1})B(q^{-1})Q(q^{-1}) \\ &\quad + B(q^{-1})R_0(q^{-1}) + B(q^{-1})A(q^{-1})Q(q^{-1}) \\ &= A(q^{-1})S_0(q^{-1}) + B(q^{-1})R_0(q^{-1}) \end{aligned}$$

Equations (3.91) and (3.92) can be used to tune an initial controller by shaping the sensitivity functions without solving the Bezout equation.

Example 3.8. Suppose that $R_0(q^{-1})$ and $S_0(q^{-1})$ are designed to obtain desired closed-loop poles. Then we decide to add an integrator to the controller and to open the loop at Nyquist frequency which is equivalent to add the fixed terms $H_S(q^{-1}) = 1 - q^{-1}$ and

$H_R(q^{-1}) = 1 + q^{-1}$, respectively. This can be done by Q-parametrization as follows. Let $Q(q^{-1}) = q_0 + q_1 q^{-1}$. An integrator in controller means that $S(1) = 0$ and opening the loop at Nyquist frequency means that $R(-1) = 0$. So q_0 and q_1 can be computed from the following equations:

$$R_0(-1) + A(-1)[q_0 - q_1] = 0 \tag{3.93}$$
$$S_0(1) - B(1)[q_0 + q_1] = 0 \tag{3.94}$$

The main advantage of this parameterization is that while the desired closed-loop poles remain the same, the sensitivity functions will depend linearly on the Q parameters as follows:

$$\begin{aligned} \mathcal{S}(z^{-1}, Q) &= \frac{A(z^{-1})S_0(z^{-1}) - A(z^{-1})B(z^{-1})Q(z^{-1})}{P(z^{-1})} \\ \mathcal{U}(z^{-1}, Q) &= \frac{A(z^{-1})R_0(z^{-1}) + A^2(z^{-1})Q(z^{-1})}{P(z^{-1})} \end{aligned}$$

As a result, any norm of $\mathcal{S}$ or $\mathcal{U}$ is a convex function of the Q parameters. Therefore, after computing a nominal controller that meets the regulation and tracking performance, robustness of the designed controller can be improved by computing the polynomial $Q(q^{-1})$ such that the weighted infinity- or two-norm of the sensitivity functions are minimized. For example the two norm of $\mathcal{U}$ can be minimized under a constraint on the modulus margin and the maximum amplitude of the input sensitivity function. This can be presented as a convex optimization problem:

$$\begin{aligned} &\min_{Q} \|\mathcal{U}(Q)\|_2 \\ &\text{subject to:} \\ &\qquad \|M_m \mathcal{S}(Q)\|_\infty < 1 \\ &\qquad \|\mathcal{U}(Q)\|_\infty < U_{\max} \end{aligned} \tag{3.95}$$

Fixed terms in the controller: If we had some fixed terms in $R_0(q^{-1})$ and $S_0(q^{-1})$, after Q parameterization, they will be lost. It can be seen in (3.91) and (3.92), that a fixed term H_R in R_0 will be preserved in R if it includes in Q as well. In the same way a fixed term H_S in S_0 is preserved in S if it includes in Q. A simple way to include the integrator $H_S(q^{-1}) = 1 - q^{-1}$ in Q, is to add the equality constraint $Q(1) = 0$. In addition to include $H_R(q^{-1}) = 1 + q^{-1}$ in Q, we can add the equality constraint $Q(-1) = 0$. In general, Q can be parameterized as:

$$Q(q^{-1}) = H_R(q^{-1})H_S(q^{-1})Q'(q^{-1})$$

to guarantee that the existing H_R and H_S in R_0 and S_0 will be preserved in R and S, respectively. If R_0 and S_0 do not have the fixed terms but we want to include them in R and S, we can add some equality constraints for R and S to the optimization problem.

For example, to have an integrator in the controller we should have an additional equality constraint $S(1) = 0$, which leads to $Q(1) = S_0(1)/B(1)$, see (3.94).

If we consider again Example 3.7 and we solve the convex optimization problem in (3.95) for a third-order $Q(q^{-1})$ we obtain the following results:

$$\begin{aligned} Q(q^{-1}) &= -0.8952 + 0.3068q^{-1} + 0.3430q^{-2} + 0.2453q^{-3} \\ R(q^{-1}) &= 0.5715 - 0.0704q^{-1} - 0.1372q^{-2} - 0.0544q^{-3} - 0.1279q^{-4} + 0.1717q^{-5} \\ S(q^{-1}) &= 1.0000 + 0.3285q^{-1} - 0.2926q^{-2} - 0.4964q^{-3} - 0.4169q^{-4} - 0.1227q^{-5} \end{aligned}$$

This controller gives a modulus margin $M_m = 0.5$, a maximum amplitude of 3.66 dB and a two-norm of 0.896 for the input sensitivity function. The step response for an output disturbance, the impulse response of the input sensitivity function, the magnitude of the output and input sensitivity functions are given in Fig. 3.8 for the comparison purpose with the results of Example 3.7.

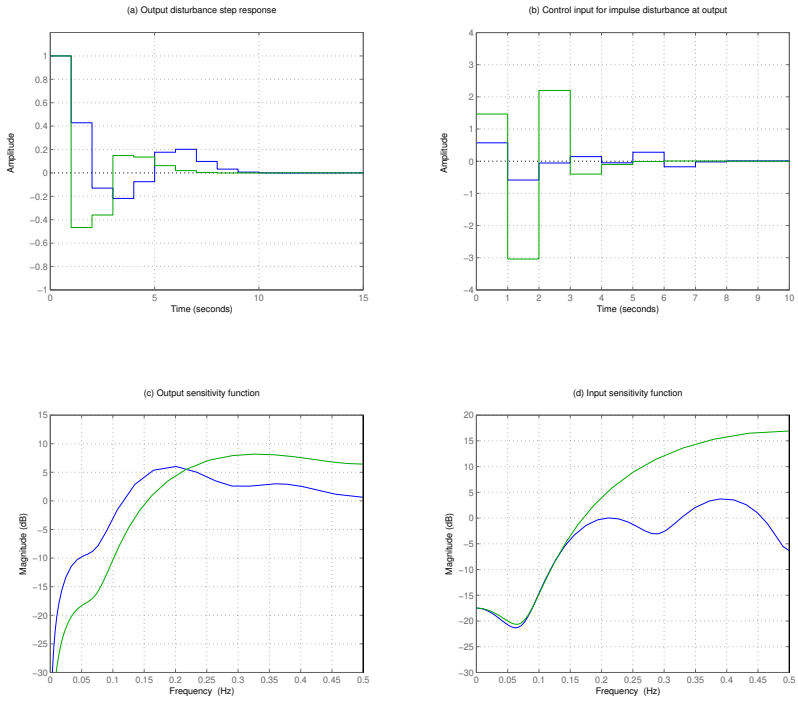

Figure 3.8: Example 3.7 using Q parametrization (blue curves), initial controller (green curves)

3.3 Introduction to Adaptive Control

Adaptive Control covers a set of techniques which provide a systematic approach for automatic adjustment of controllers in *real time*, in order to achieve or to maintain a desired level of control system performance when the parameters of the plant dynamic model are unknown and/or change in time.

Consider first the case when the parameters of the dynamic model of the plant to be controlled are unknown but constant (at least in a certain region of operation). In such cases, although the structure of the controller will not depend in general upon the particular values of the plant model parameters, the correct tuning of the controller parameters cannot be done without knowledge of their values. Adaptive control techniques can provide an automatic tuning procedure in closed loop for the controller parameters. In such cases, the effect of the adaptation vanishes as time increases. Changes in the operation conditions may require a restart of the adaptation procedure.

Consider the second case when the parameters of the dynamic model of the plant change unpredictably in time. These situations occur either because the environmental conditions change (ex: the dynamical characteristics of a robot arm or of a mechanical transmission depend upon the load; in a DC-DC converter the dynamic characteristics depend upon the load) or because we have considered simplified linear models for nonlinear systems (a change in operation condition will lead to a different linearized model). These situations may also occur simply because the parameters of the system are slowly time-varying (in a wiring machine the inertia of the spool is time-varying). In order to achieve and to maintain an acceptable level of control system performance when large and unknown changes in model parameters occur, an *adaptive control* approach has to be considered. In such cases, the adaptation will operate most of the time and the term *non-vanishing adaptation* fully characterizes this type of operation (also called *continuous adaptation*).

Further insight into the operation of an adaptive control system can be gained if one considers the design and tuning procedure of the "good" controller illustrated in Fig. 3.9. In order to design and tune a good controller, one needs to:

1) specify the desired control loop performance;
2) know the dynamic model of the plant to be controlled;
3) possess a suitable controller design method making it possible to achieve the desired performance for the corresponding plant model.

The dynamic model of the plant can be identified from input/output plant measurements obtained under an experimental protocol in open or in closed loop. One can say that the design and tuning of the controller is done from data collected on the system. An adaptive control system can be viewed as an implementation of the above design and tuning procedure in real time. The tuning of the controller will be done in real time from data collected in real time on the system. The corresponding adaptive control scheme is shown in Fig. 3.10.

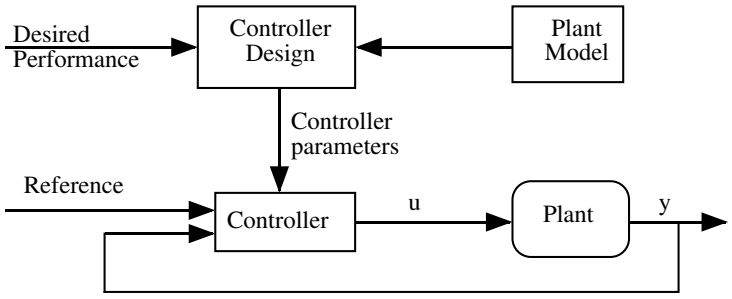

Figure 3.9: Principles of controller design

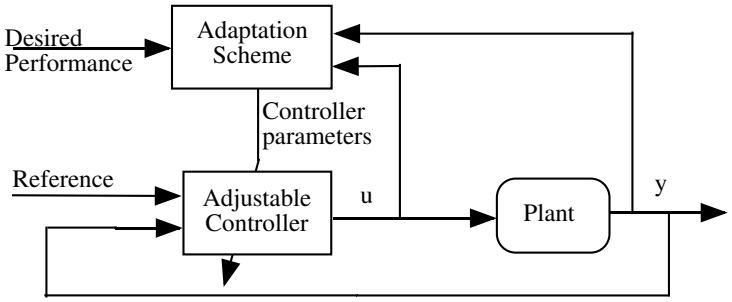

Figure 3.10: An adaptive control system

The way in which information is processed in real time in order to tune the controller for achieving the desired performance will characterize the various adaptation techniques. From Fig. 3.10, one clearly sees that an adaptive control system is nonlinear since the parameters of the controller will depend upon measurements of system variables through the adaptation loop.

Adaptive Control Versus Conventional Feedback Control

The unknown and unmeasurable variations of the process parameters degrade the performance of the control systems. Similarly to the disturbances acting upon the controlled variables, one can consider that the variations of the process parameters are caused by disturbances acting upon the parameters (called parameter disturbances). These parameter disturbances will affect the performance of the control systems. Therefore the disturbances acting upon a control system can be classified as follows:

a) disturbances acting upon the controlled variables;
b) (parameter) disturbances acting upon the performance of the control system.

Feedback is basically used in conventional control systems to reject the effect of disturbances upon the controlled variables and to bring them back to their desired values

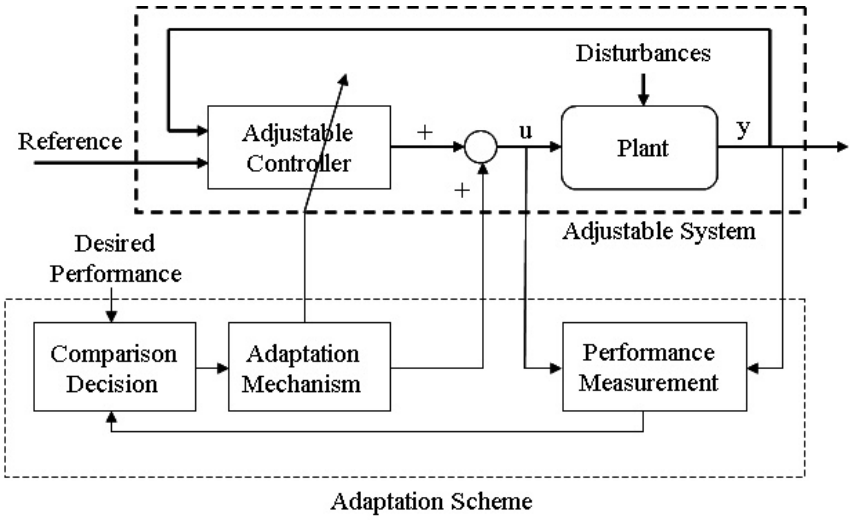

Figure 3.11: Basic configuration for an adaptive control system

according to a certain performance index. To achieve this, one first measures the controlled variables, then the measurements are compared with the desired values and the difference is fed into the controller which will generate the appropriate control.

A similar conceptual approach can be considered for the problem of achieving and maintaining the desired performance of a control system in the presence of parameter disturbances. We will have to define first a *performance index* (PI) for the control system which is a measure of the performance of the system (ex: the damping factor for a closed-loop system characterized by a second-order transfer function is an PI which allows to quantify a desired performance expressed in terms of "damping"). Then we will have to measure this PI. The *measured* PI will be compared to the *desired* PI and their difference (if the measured PI is not acceptable) will be fed into an *adaptation mechanism*. The output of the *adaptation mechanism* will act upon the parameters of the controller and/or upon the control signal in order to modify the system performance accordingly. A block diagram illustrating a basic configuration of an adaptive control system is given in Fig. 3.11.

Associated with Fig. 3.11, one can consider the following definition for an adaptive control system.

Definition 3.1. *An adaptive control system measures a certain performance index (PI) of the control system using the inputs, the states, the outputs and the known disturbances. From the comparison of the measured performance index and a set of given ones, the adaptation mechanism modifies the parameters of the adjustable controller and/or generates an auxiliary control in order to maintain the performance index of the control system close to the set of given ones (i.e., within the set of acceptable ones).*

Note that the control system under consideration is an *adjustable dynamic system*

in the sense that its performance can be adjusted by modifying the parameters of the controller or the control signal. The above definition can be extended straightforwardly for "adaptive systems" in general.

A conventional feedback control system will monitor the controlled variables under the effect of disturbances acting on them, but its performance will vary (it is not monitored) under the effect of parameter disturbances (the design is done assuming known and constant process parameters).

An adaptive control system, which contains in addition to a feedback control with adjustable parameters a supplementary loop acting upon the adjustable parameters of the controller, will monitor the performance of the system in the presence of parameter disturbances.

Consider as an example the case of a conventional feedback control loop designed to have a given damping. When a disturbance acts upon the controlled variable, the return of the controlled variable towards its nominal value will be characterized by the desired damping if the plant parameters have their known nominal values. If the plant parameters change upon the effect of the parameter disturbances, the damping of the system response will vary. When an adaptation loop is added, the damping of the system response will be maintained when changes in parameters occur.

The operation of the adaptation loop and its design relies upon the following fundamental hypothesis: *For any possible values of plant model parameters there is a controller with a fixed structure and complexity such that the specified performance can be achieved with appropriate values of the controller parameters.*

In the context of this chapter, the plant models are assumed to be linear and the controllers which are considered are also linear. Therefore, *the task of the adaptation loop is solely to search for the "good" values of the controller parameters.*

This emphasizes the importance of the control design for the known parameter case (the *underlying control design problem*), as well as the necessity of *a priori* information about the structure of the plant model and its characteristics which can be obtained by *identification* of a model for a given set of operational conditions.

In other words, an adaptive controller is not a "black box" which can solve a control problem in real time without an initial knowledge about the plant to be controlled. This *a priori* knowledge is needed for specifying achievable performance, the structure and complexity of the controller and the choice of an appropriate design method.

3.4 Parameter Adaptation Algorithms

On-line estimation of the parameters of a plant model or of a controller is one of the key steps in building an adaptive control system. Direct estimation of the controller parameters (when possible) can also be interpreted as a plant model estimation in a reparametrized form. Therefore, the problem of on-line estimation of plant model parameters is a generic problem in adaptive control. Such systems will feature a parametric

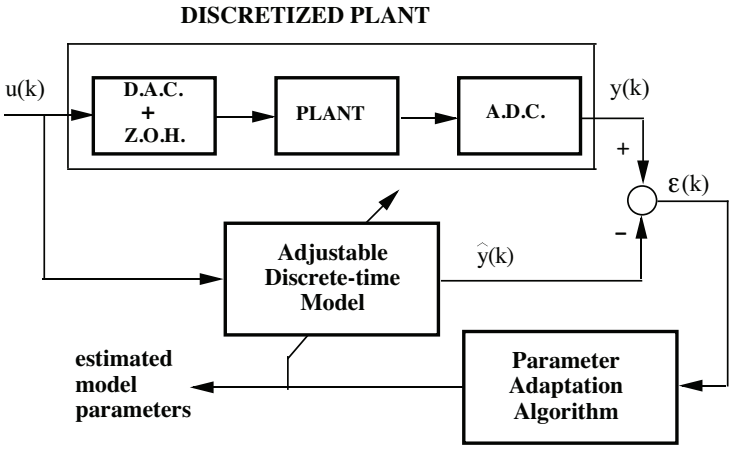

Figure 3.12: Parameter estimation principle

adaptation algorithm which will up-date the estimated parameters at each sampling instant.

On-line plant parameter estimation can also be viewed as a technique for achieving system identification in general by using recursive parametric estimation methods which process a pair of input-output measurements sequentially, as opposed to non recursive (or off-line) identification methods which process an input-output data file acquired over a certain time horizon at once.

The on-line parameter estimation principle for sampled models is illustrated in Fig. 3.12. A discrete-time model with adjustable parameters is implemented on the computer. The error between the system output at instant k, $y(k)$ and the output predicted by the model $\hat{y}(k)$ (called plant-model error or prediction error) is used by the *parameter adaptation algorithm*, which, at each sampling instant, will modify the model parameters in order to minimize this error (in the sense of a certain criterion).

The input to the system is either a low-amplitude frequency-rich signal generated by computer for the case of plant model identification, or the signal generated by the controller in the case of an adaptive control system. It can also be the combination of both (e.g., identification in closed loop).

The key element for implementing the on-line estimation of the plant model parameters is the *parameter adaptation algorithm* (PAA) which drives the parameters of the adjustable prediction model from the data acquired on the system at each sampling instant. This algorithm has a *recursive* structure, i.e., the new value of the estimated parameters is equal to the previous value plus a correcting term which will depend on the most recent measurements.

In general a *parameter vector* is defined. Its components are the different parameters that should be estimated.

Parameter adaptation algorithms generally have the following structure:

$$\begin{bmatrix} New\ estimated \\ parameters \\ (vector) \end{bmatrix} = \begin{bmatrix} Previous\ estimated \\ parameters \\ (vector) \end{bmatrix} + \begin{bmatrix} Adaptation \\ gain \\ (matrix) \end{bmatrix} \times \begin{bmatrix} Measurement \\ function \\ (vector) \end{bmatrix} \times \begin{bmatrix} Prediction\ error \\ function \\ (scalar) \end{bmatrix}$$

This structure corresponds to the so-called *integral type adaptation algorithms* (the algorithm has memory and therefore maintains the estimated value of the parameters when the correcting terms become null). The algorithm can be viewed as a discrete-time integrator fed at each instant by the correcting term. The measurement function vector is generally called the *observation vector*. The prediction error function is generally called the *adaptation error*. The adaptation gain plays an important role in the performance of the parameter adaptation algorithm and it may be constant or time-varying.

The problem addressed in this section is the synthesis and analysis of parameter adaptation algorithms in a deterministic environment. We focus on the least square recursive algorithm, because it is the most used one. Detailed mathematical analysis for the stability and convergence of PAA is given in Appendix A.1 and A.2, respectively.

3.4.1 Recursive Least Squares Algorithm

Consider for example the discrete-time model of a plant described by:

$$y(k+1) = -a_1 y(k) + b_1 u(k) = \theta^T \phi(k) \tag{3.96}$$

where the unknown parameters a_1 and b_1 form the components of the *parameter vector* θ:

$$\theta^T = [a_1, b_1] \tag{3.97}$$

and

$$\phi^T(k) = [-y(k), u(k)] \tag{3.98}$$

is the *measurement vector*. The adjustable prediction model will be described in this case by:

$$\hat{y}^\circ(k+1) = \hat{y}[(k+1)|\hat{\theta}(k)] = -\hat{a_1}(k)y(k) + \hat{b}_1(k)u(k) = \hat{\theta}^T(k)\phi(k) \tag{3.99}$$

where $\hat{y}^\circ(k+1)$ is termed the *a priori* predicted output depending on the values of the estimated parameter vector at instant k:

$$\hat{\theta}^T(k) = [\hat{a_1}(k), \hat{b_1}(k)] \tag{3.100}$$

As it will be shown later, it is very useful to consider also the *a posteriori* predicted output computed on the basis of the new estimated parameter vector at $k+1$, $\hat{\theta}(k+1)$,

which will be available somewhere between $k+1$ and $k+2$. The *a posteriori* predicted output will be given by:

$$\begin{aligned}\hat{y}(k+1) &= \hat{y}[(k+1)|\hat{\theta}(k+1)] \\ &= -\hat{a}_1(k+1)y(k) + \hat{b}_1(k+1)u(k) \\ &= \hat{\theta}^T(k+1)\phi(k) \end{aligned} \tag{3.101}$$

One defines an *a priori* prediction error as:

$$\epsilon^\circ(k+1) = y(k+1) - \hat{y}^\circ(k+1) = y(k+1) - \hat{\theta}^T(k)\phi(k) \tag{3.102}$$

and an *a posteriori* prediction error as:

$$\epsilon(k+1) = y(k+1) - \hat{y}(k+1) = y(k+1) - \hat{\theta}^T(k+1)\phi(k) \tag{3.103}$$

The aim is to find a recursive algorithm, which minimizes the *least squares* criterion:

$$\min_{\hat{\theta}(k)} J(k) = \sum_{i=1}^{k} [y(i) - \hat{\theta}^T(k)\phi(i-1)]^2 \tag{3.104}$$

The term $\hat{\theta}(k)^T\phi(i-1)$ corresponds to:

$$\hat{\theta}^T(k)\phi(i-1) = -\hat{a}_1(k)y(i-1) + \hat{b}_1(k)u(i-1) = \hat{y}[i \mid \hat{\theta}(k)] \tag{3.105}$$

Therefore, this is the prediction of the output at instant $i (i \leq k)$ based on the parameter estimate at instant k obtained using k measurements.

First, a parameter θ must be estimated at instant k so that it minimizes the sum of the squares of the differences between the output of the plant and the output of the prediction model on a horizon of k measurements. The value of $\hat{\theta}(k)$, which minimizes the criterion (3.104), is obtained by seeking the value that cancels $\partial J(k)/\partial\hat{\theta}(k)$:

$$\frac{\partial J(k)}{\partial \hat{\theta}(k)} = -2\sum_{i=1}^{k} [y(i) - \hat{\theta}^T(k)\phi(i-1)]\phi(i-1) = 0 \tag{3.106}$$

From (3.106), taking into account that:

$$[\hat{\theta}^T(k)\phi(i-1)]\phi(i-1) = \phi(i-1)\phi^T(i-1)\hat{\theta}(k)$$

one obtains:

$$\left[\sum_{i=1}^{k} \phi(i-1)]\phi^T(i-1)\right] \hat{\theta}(k) = \sum_{i=1}^{k} y(i)\phi(i-1)$$

and left multiplying by[3]:

$$F(k) = \left[\sum_{i=1}^{k} \phi(i-1)\phi^T(i-1)\right]^{-1} \tag{3.107}$$

one obtains:

$$\hat{\theta}(k) = \left[\sum_{i=1}^{k} \phi(i-1)\phi^T(i-1)\right]^{-1} \sum_{i=1}^{k} y(i)\phi(i-1) = F(k)\sum_{i=1}^{k} y(i)\phi(i-1) \tag{3.108}$$

This estimation algorithm is not recursive. In order to obtain a recursive algorithm, the estimation of $\hat{\theta}(k+1)$ is considered:

$$\hat{\theta}(k+1) = F(k+1)\sum_{i=1}^{k+1} y(i)\phi(i-1) \tag{3.109}$$

$$F^{-1}(k+1) = \sum_{i=1}^{k+1} \phi(i-1)\phi^T(i-1) = F^{-1}(k) + \phi(k)\phi^T(k) \tag{3.110}$$

We can now express $\hat{\theta}(k+1)$ as a function of $\hat{\theta}(k)$:

$$\hat{\theta}(k+1) = \hat{\theta}(k) + \Delta\hat{\theta}(k+1) \tag{3.111}$$

From (3.109) one has:

$$\hat{\theta}(k+1) = F(k+1)\left[\sum_{i=1}^{k} y(i)\phi(i-1) + y(k+1)\phi(k)\right] \tag{3.112}$$

Taking into account (3.108), (3.112) can be rewritten as:

$$\hat{\theta}(k+1) = F(k+1)[F^{-1}(k)\hat{\theta}(k) + y(k+1)\phi(k)] \tag{3.113}$$

From (3.110) after post-multiplying both sides by $\hat{\theta}(k)$ one gets:

$$F^{-1}(k)\hat{\theta}(k) = F^{-1}(k+1)\hat{\theta}(k) - \phi(k)\phi^T(k)\hat{\theta}(k) \tag{3.114}$$

and (3.113), becomes:

$$\hat{\theta}(k+1) = F(k+1)\left\{F^{-1}(k+1)\hat{\theta}(k) + \phi(k)[y(k+1) - \hat{\theta}^T(k)\phi(k)]\right\} \tag{3.115}$$

Taking into account the expression of $\epsilon^\circ(k+1)$ given by (3.102), the result is:

$$\hat{\theta}(k+1) = \hat{\theta}(k) + F(k+1)\phi(k)\epsilon^\circ(k+1) \tag{3.116}$$

[3]It is assumed that the matrix $\sum_{i=1}^{k} \phi(i-1)\phi^T(i-1)$ is invertible. As it will be shown later this corresponds to an *excitation* condition.

The adaptation algorithm of (3.116) has a recursive form but the gain matrix $F(k+1)$ is time-varying since it depends on the measurements. A recursive formula for $F(k+1)$ remains to be given from the recursive formula $F^{-1}(k+1)$ given in (3.110). This is obtained by using the *matrix inversion* lemma.

Lemma 3.1. ***(Matrix Inversion Lemma)****: Let F be a $(n \times n)$ dimensional nonsingular matrix, R a $(m \times m)$ dimensional nonsingular matrix and H a $(n \times m)$ dimensional matrix of maximum rank, then the following identity holds:*

$$(F^{-1} + HR^{-1}H^T)^{-1} = F - FH(R + H^T FH)^{-1}H^T F \tag{3.117}$$

Proof. By direct multiplication one finds that:

$$[F - FH(R + H^T FH)^{-1}H^T F][F^{-1} + HR^{-1}H^T] = I$$

□

For the case of (3.110), one chooses $H = \phi(k)$, $R = 1$ and one obtains from (3.110) and (3.117):

$$F(k+1) = F(k) - \frac{F(k)\phi(k)\phi^T(k)F(k)}{1 + \phi^T(k)F(k)\phi(k)} \tag{3.118}$$

and, putting together the different equations, a first formulation of the recursive least squares (RLS) parameter adaptation algorithm (PAA) is given below:

$$\hat{\theta}(k+1) = \hat{\theta}(k) + F(k+1)\phi(k)\epsilon^\circ(k+1) \tag{3.119}$$

$$F(k+1) = F(k) - \frac{F(k)\phi(k)\phi^T(k)F(k)}{1 + \phi^T(k)F(k)\phi(k)} \tag{3.120}$$

$$\epsilon^\circ(k+1) = y(k+1) - \hat{\theta}^T(k)\phi(k) \tag{3.121}$$

An equivalent form of this algorithm is obtained by introducing the expression of $F(k+1)$ given by (3.120) in (3.119), where:

$$\begin{aligned} [\hat{\theta}(k+1) - \hat{\theta}(k)] &= F(k+1)\phi(k)\epsilon^\circ(k+1) \\ &= F(k)\phi(k)\frac{\epsilon^\circ(k+1)}{1 + \phi^T(k)F(k)\phi(k)} \end{aligned} \tag{3.122}$$

However, from (3.102), (3.103) and (3.122), one obtains:

$$\begin{aligned} \epsilon(k+1) &= y(k+1) - \hat{\theta}^T(k+1)\phi(k) \\ &= y(k+1) - \hat{\theta}(k)\phi(k) - [\hat{\theta}(k+1) - \hat{\theta}(k)]^T\phi(k) \\ &= \epsilon^\circ(k+1) - \phi^T(k)F(k)\phi(k)\frac{\epsilon^\circ(k+1)}{1 + \phi^T(k)F(k)\phi(k)} \\ &= \frac{\epsilon^\circ(k+1)}{1 + \phi^T(k)F(k)\phi(k)} \end{aligned} \tag{3.123}$$

which expresses the relation between the *a posteriori* prediction error and the *a priori* prediction error. Using this relation in Eq. (3.122), an equivalent form of the parameter adaptation algorithm for the recursive least squares is obtained:

$$\hat{\theta}(k+1) = \hat{\theta}(k) + F(k)\phi(k)\epsilon(k+1) \tag{3.124}$$

$$F^{-1}(k+1) = F^{-1}(k) + \phi(k)\phi^T(k) \tag{3.125}$$

$$F(k+1) = F(k) - \frac{F(k)\phi(k)\phi^T(k)F(k)}{1+\phi^T(k)F(k)\phi(k)} \tag{3.126}$$

$$\epsilon(k+1) = \frac{y(k+1) - \hat{\theta}^T(k)\phi(k)}{1+\phi^T(k)F(k)\phi(k)} \tag{3.127}$$

For the recursive least squares algorithm to be exactly equivalent to the non-recursive least squares algorithm, it must be started from a first estimation obtained at instant $k_0 = \dim \phi(k)$, since normally $F^{-1}(k)$ given by (3.107) becomes nonsingular for $k = k_0$. In practice, the algorithm is started up at $k = 0$ by choosing:

$$F(0) = \delta I \qquad \delta \gg 1 \tag{3.128}$$

a typical value being $\delta = 1000$. It can be observed in the expression of $F^{-1}(k+1)$ given by (3.110) that the influence of this initial error decreases with the time. In this case one minimizes the following criterion:

$$\min_{\hat{\theta}(k)} J(k) = \sum_{i=1}^{k} [y(i) - \hat{\theta}^T(k)\phi(i-1)]^2 + [\theta - \hat{\theta}^T(0)]^T F^{-1}(0)[\theta - \hat{\theta}(0)]^T \tag{3.129}$$

A rigorous analysis (based on the stability theory - see Appendix A.1) shows nevertheless that for any positive definite matrix $F(0)[F(0) > 0]$,

$$\lim_{k\to\infty} \epsilon(k+1) = 0$$

The recursive least squares algorithm is an algorithm with a decreasing adaptation gain. This is clearly seen if the estimation of a single parameter is considered. In this case, $F(k)$ and $\phi(k)$ are scalars, and (3.126) becomes:

$$F(k+1) = \frac{F(k)}{1+\phi(k)^2F(k)} \leq F(k); \qquad \phi(k), F(k) \in \mathbb{R}$$

The same conclusion is obtained observing that $F^{-1}(k+1)$ is the output of an integrator which has as input $\phi(k)\phi^T(k)$. Since $\phi(k)\phi^T(k) \geq 0$, one conclude that if $\phi(k)\phi^T(k) > 0$ in the average, then $F^{-1}(k)$ will tends towards infinity, i.e., $F(k)$ will tends towards zero.

The recursive least squares algorithm in fact gives less and less weight to the new prediction errors and thus to the new measurements. Consequently, this type of variation of the adaptation gain is not suitable for the estimation of time-varying parameters, and

other variation profiles for the adaptation gain must therefore be considered. Under certain conditions, the adaptation gain is a measure of the evolution of the covariance of the parameter estimation error.

The least squares algorithm presented up to now for $\hat{\theta}(k)$ and $\phi(k)$ of dimension 2 may be generalized for any dimensions resulting from the description of discrete-time systems of the form:

$$y(k) = \frac{q^{-d}B^{\star}(q^{-1})}{A(q^{-1})}u(k) \tag{3.130}$$

where:

$$A(q^{-1}) = 1 + a_1 q^{-1} + \cdots + a_{n_A} q^{-n_A} \tag{3.131}$$

$$B^{\star}(q^{-1}) = b_d + b_{d+1} q^{-1} \cdots + b_{n_B} q^{-n_B+d} \tag{3.132}$$

Eq. (3.130) can be written in the form:

$$y(k+1) = -\sum_{i=1}^{n_A} a_i y(k+1-i) + \sum_{i=d}^{n_B} b_i u(k-i+1) = \theta^T \phi(k) \tag{3.133}$$

in which:

$$\theta^T = [a_1, \cdots, a_{n_A}, b_d, \cdots, b_{n_B}] \tag{3.134}$$

$$\phi^T(k) = [-y(k) \cdots - y(k-n_A+1), u(k-d+1) \cdots u(k-n_B+1)] \tag{3.135}$$

The *a priori* adjustable predictor is given in the general case by:

$$\begin{aligned} \hat{y}^{\circ}(k+1) &= -\sum_{i=1}^{n_A} \hat{a}_i(k) y(k+1-i) + \sum_{i=d}^{n_B} \hat{b}_i(k) u(k-i+1) \\ &= \hat{\theta}^T(k)\phi(k) \end{aligned} \tag{3.136}$$

in which:

$$\hat{\theta}^T(k) = [\hat{a}_1(k), \cdots, \hat{a}_{n_A}(k), \hat{b}_d(k), \cdots, \hat{b}_{n_B}(k)] \tag{3.137}$$

and for the estimation of $\hat{\theta}(k)$, the algorithm given in equations (3.124) through (3.127) is used, with the appropriate dimension for $\hat{\theta}(k)$, $\phi(k)$ and $F(k)$.

3.4.2 Choice of the Adaptation Gain

The recursive formula for the inverse of the adaptation gain $F^{-1}(k+1)$ given by (3.125) is generalized by introducing two weighting sequences $\lambda_1(k)$ and $\lambda_2(k)$, as indicated below:

$$\begin{aligned} F^{-1}(k+1) &= \lambda_1(k)F^{-1}(k) + \lambda_2(k)\phi(k)\phi^T(k) \\ 0 < \lambda_1(k) \leq 1 \; &; \; 0 \leq \lambda_2(k) < 2 \; ; \; F(0) > 0 \end{aligned} \tag{3.138}$$

Note that $\lambda_1(k)$ and $\lambda_2(k)$ have the opposite effect. $\lambda_1(k) < 1$ tends to increase the adaptation gain (the gain inverse decreases); $\lambda_2(k) > 0$ tends to decrease the adaptation gain (the gain inverse increases). For each choice of sequences, $\lambda_1(k)$ and $\lambda_2(k)$ correspond to a *variation profile* of the adaptation gain and an interpretation in terms of the error criterion, which is minimized by the PAA. Eq. (3.138) allows one to interpret the inverse of the adaptation gain (for constant weighting sequences) as the output of a filter $\lambda_2/(1-\lambda_1 q^{-1})$ having as input $\phi(k)\phi^T(k)$ and as initial condition $F^{-1}(0)$.

Using the *matrix inversion lemma* given by (3.117), one obtains from (3.138):

$$F(k+1) = \frac{1}{\lambda_1(k)}\left[F(k) - \frac{F(k)\phi(k)\phi^T(k)F(k)}{\frac{\lambda_1(k)}{\lambda_2(k)} + \phi^T(k)F(k)\phi(k)}\right] \tag{3.139}$$

Next, a certain number of choices for $\lambda_1(k)$ and $\lambda_2(k)$ and their interpretations will be given.

(A.1) Decreasing gain: In this case $\lambda_1(k) = \lambda_1 = 1$, $\lambda_2(k) = 1$ and $F^{-1}(k+1)$ is given by (3.125), which leads to a decreasing adaptation gain. The minimized criterion is that of (3.104). This type of profile is suited to the estimation of the parameters of stationary systems.

(A.2) Constant forgetting factor: In this case $\lambda_1(k) = \lambda_1$; $0 < \lambda_1 < 1$; $\lambda_2(k) = \lambda_2 = 1$. The typical values for λ_1 are: $\lambda_1 = 0.95$ to 0.99. The criterion to be minimized will be:

$$J(k) = \sum_{i=1}^{k} \lambda_1^{(k-i)}[y(i) - \hat{\theta}^T(k)\phi(i-1)]^2 \tag{3.140}$$

The effect of $\lambda_1(k) < 1$ is to introduce increasingly weaker weighting on the old data ($i < t$). This is why λ_1 is known as the *forgetting factor*. The maximum weight is given to the most recent error. This type of profile is suited to the estimation of the parameters of slowly time-varying systems.

The use of a constant forgetting factor without the monitoring of the maximum value of $F(k)$ causes problems in adaptive regulation if the $\{\phi(k)\phi^T(k)\}$ sequence becomes null in the average (steady state case) because the adaptation gain will tend towards infinity. In this case:

$$F^{-1}(k+i) = (\lambda_1)^i F^{-1}(k)$$

and:

$$F(k+i) = (\lambda_1)^{-i} F(k)$$

For: $\lambda_1 < 1$, $\lim_{i\to\infty}(\lambda_1)^{-i} = \infty$ and $F(k+i)$ will become asymptotically unbounded.

(A.3) Variable forgetting factor: In this case $\lambda_2(k) = \lambda_2 = 1$ and the forgetting factor $\lambda_1(k)$ is given by:

$$\lambda_1(k) = \lambda_0\lambda_1(k-1) + 1 - \lambda_0 \; ; \; 0 < \lambda_0 < 1 \tag{3.141}$$

The typical values being: $\lambda_1(0) = 0.95$ to 0.99 and $\lambda_0 = 0.5$ to 0.99. ($\lambda_1(k)$ can be interpreted as the output of a first order filter $(1-\lambda_0)/(1-\lambda_0 q^{-1})$ with a unitary steady state gain and an initial condition $\lambda_1(0)$).

Relation (3.141) leads to a forgetting factor that asymptotically tends towards 1. The criterion minimized will be:

$$J(k) = \sum_{i=1}^{k} \left[\prod_{j=1}^{k} \lambda_1(j-i) \right] [y(i) - \hat{\theta}^T(k)\phi(i-1)]^2 \tag{3.142}$$

As λ_1 tends towards 1 for large i, only the initial data are forgotten (the adaptation gain tends towards a decreasing gain).

This type of profile is highly recommended for the model identification of stationary systems, since it avoids a too rapid decrease of the adaptation gain, thus generally resulting in an acceleration of the convergence (by maintaining a high gain at the beginning when the estimates are at a great distance from the optimum).

Other types of evolution for $\lambda_1(k)$ can be considered. For example:

$$\lambda_1(k) = 1 - \frac{\phi^T(k)F(k)\phi(k)}{1 + \phi^T(k)F(k)\phi(k)}$$

This forgetting factor depends upon the input/output signals via $\phi(k)$. It automatically takes the value 1 if the norm of $\phi(k)\phi^T(k)$ becomes null. In the cases where the $\phi(k)$ sequence is such that the term $\phi^T(k)F(k)\phi(k)$ is significative with respect to one, the forgetting factor takes a lower value assuring good adaptation capabilities (this is related to the concept of "persistently exciting" signal - see Appendix A.2).

Another possible choice is:

$$\lambda_1(k) = 1 - \alpha\frac{[\epsilon^\circ(k)]^2}{1 + \phi^T(k)F(k)\phi(k)} \; ; \; \alpha > 0$$

The forgetting factor tends towards 1, when the prediction error tends towards zero. Conversely, when a change occurs in the system parameters, the prediction error increases leading to a forgetting factor less than 1 in order to assure a good adaptation capability.

(A.4) Constant trace: In this case, $\lambda_1(k)$ and $\lambda_2(k)$ are automatically chosen at each step in order to ensure a constant trace of the gain matrix (constant sum of the diagonal terms):

$$trF(k+1) = trF(k) = trF(0) = n\delta \tag{3.143}$$

in which n is the number of parameters and δ the initial gain (typical values: $\delta = 0.1$ to 4), the matrix $F(0)$ having the form:

$$F(0) = \begin{bmatrix} \delta & & 0 \\ & \ddots & \\ 0 & & \delta \end{bmatrix} \tag{3.144}$$

The minimized criterion is of the form:

$$J(k) = \sum_{i=1}^{k} \left[\prod_{j=1}^{k} \lambda_1(j-i) \right] \mu(i-1) \left[y(i) - \hat{\theta}^T(k)\phi(i-1) \right]^2 \tag{3.145}$$

with:

$$\mu(k) = \frac{1 + \lambda_2(k)\phi^T(k)F(k)\phi(k)}{1 + \phi^T(k)F(k)\phi(k)} \tag{3.146}$$

Using this technique, at each step there is a movement in the optimal direction of the RLS, but the gain is maintained approximately constant. The value of $\lambda_1(k)$ and $\lambda_2(k)$ are determined from the equation:

$$trF(k+1) = \frac{1}{\lambda_1(k)} tr \left[F(k) - \frac{F(k)\phi(k)\phi^T(k)F(k)}{\alpha(k) + \phi^T(k)F(k)\phi(k)} \right] \tag{3.147}$$

fixing the ratio $\alpha(k) = \lambda_1(k)/\lambda_2(k)$ (Eq. (3.147) is obtained from (3.139)). This type of profile is suited to the model identification of systems with time-varying parameters and for adaptive control with non-vanishing adaptation.

(A.5) Decreasing gain + constant trace: In this case, A.1 is switched to A.4 when:

$$trF(k) \leq n\delta \; ; \; \delta = 0.1 \text{ to } 4 \tag{3.148}$$

in which δ is chosen in advance. This profile is suited to the model identification of time-varying systems and for adaptive control in the absence of initial information on the parameters.

(A.6) Variable forgetting factor + constant trace: In this case A.3 is switched to A.4 when:

$$trF(k) \leq n\delta \tag{3.149}$$

The use is the same as for A.5.

Choice of the Initial Gain $F(0)$

The initial gain $F(0)$ is usually chosen as a diagonal matrix of the form given by (3.128) and, respectively, (3.144). In the absence of initial information upon the parameters to be estimated (typical value of initial estimates $= 0$), a high initial gain (δI) is chosen. A typical value is $\delta = 1000$ (but higher values can be chosen). If an initial parameter estimation is available (resulting for example from a previous identification), a low initial gain is chosen. In general, in this case $\delta \leq 1$.

Since in standard RLS the adaptation gain decreases as the true model parameters are approached (a significant measurement is its trace), the adaptation gain may be interpreted as a measurement of the accuracy of the parameter estimation (or prediction). This explains the choices of $F(0)$ proposed above. Note that under certain hypotheses, $F(k)$ is effectively a measurement of the quality of the estimation.

This property can give indications upon the evolution of a parameter estimation procedure. If the trace of $F(k)$ did not decrease significantly, the parameter estimation is in general poor. This may occur in system identification when the level and type of input used are not appropriate. The importance of the input choice for parameter convergence is discussed in Appendix A.1.

3.4.3 Robust Parameter Estimation

In practice a number of the hypotheses used for the development of parameter adaptation algorithms are violated. Therefore a number of modifications have to be introduced in order to accommodate these situations safely.

The conventional assumptions are:

1. The true plant model and the estimated plant model have the same structure (the true plant model is described by a discrete-time model with known upper bounds for the degrees n_A, n_B).
2. The disturbances are zero mean and of stochastic nature (with various assumptions).
3. For parameter estimation in closed-loop operation, the controller

   a) has constant parameters and stabilizes the closed loop;

   b) contains the internal model of the deterministic disturbance for which perfect state disturbance rejection is assured.

4. The parameters are constant or piece-wise constant.
5. The domain of possible parameter values is in general not constrained.

In this section, we will examine the effects of the violation of these hypotheses and see how they can be overcome. Appropriate modification of the parameter adaptation algorithms in order to obtain a robust parameter estimation will be introduced. This will allow us

to guarantee certain boundedness properties for the parameter estimates and adaptation error, which will be needed for establishing the boundedness of plant input-output signals in adaptive control.

Probably the major difficulty encountered when analyzing adaptive control schemes is caused by the fact that we cannot assume that the plant regressor vector (containing the plant inputs and outputs) is bounded, i.e., that the adaptive controller stabilizes the plant. The boundedness of the regressor vector is a result of the analysis and not an hypothesis (as in the plant model identification in open or closed loop). The robustification of the parameter adaptation algorithms is crucial both for practical and theoretical reasons.

The basic factors in the robustification of the parameter estimation algorithms are explained briefly as follows:

Filtering of input/output data: Filtering of input-output data results naturally if we consider the problem of plant model identification in closed loop using open-loop identification algorithms. Filtering of input-output data also represents a solution for enhancing an input-output spectrum in the "positive real" region of the transfer functions which occurs in convergence conditions of some algorithms. When we would like to estimate a model characterizing the low frequency behaviour of a plant, we have to filter the high-frequency content of input-output, in order to reduce the effect of the unmodelled dynamics.

PAA with dead zone: In a number of applications, it is difficult to assume a stochastic or a deterministic model for the disturbance, but a hard bound for the level of the disturbance can be defined. In such situations, trying to make the (a posteriori) adaptation error smaller than the bound of the disturbance is irrelevant. Therefore, a dead zone is introduced on the adaptation error such that the PAA stops when the adaptation error is smaller or equal to the upper magnitude of the disturbance.

PAA with projection: In many applications, the possible domain of variation of the parameter vector θ (or of some of its components) is known (for example, the model is stable, or the sign of a component of θ is known). Similarly, in a number of parameter estimation schemes, $\hat{\theta}$ or part of the components of $\hat{\theta}$, should be restricted to a stability domain. In such cases, the estimated parameters should be restricted to a given convex domain by projecting the estimates on the admissible domain.

Data normalization: When the estimated model is of lower dimension than the true plant model, the unmodelled response of the plant (if the unmodelled part is stable) can be bounded by a norm or a filtered norm of the reduced order regressor ϕ containing the inputs and outputs over a certain horizon. This unmodelled response can also be considered as a disturbance added to a reduced order model. In the context of adaptive control, since we cannot assume that the regressor ϕ containing plant inputs and outputs does not grow unbounded, we have to assure that the parameter estimates and the adaptation

error remain bounded. This is obtained by defining "normalized" input-output data. This data corresponds to the input-output data divided by a norm of ϕ. This new data cannot become unbounded, and the resulting normalized unmodelled response is also bounded. Therefore, the parameter estimator built from this data, will lead to a bounded adaptation error and using a PAA with dead zone or projection the boundedness of the parameter estimates will be assured.

3.5 Direct Adaptive Control

Direct adaptive control covers those schemes in which the parameters of the controller are directly updated from a signal error (adaptation error) reflecting the difference between attained and desired performance. Direct adaptive control schemes are generally obtained in two ways.

1. Define an equation for a signal error (adaptation error) which is a function of the difference between the tuned controller parameters and the current controller parameters. Use this adaptation error to generate a PAA for the controller parameters.
2. Use an indirect adaptive control approach with an adaptive predictor of the plant output reparameterized in terms of the controller parameters and force the output of the adaptive predictor to follow exactly the desired trajectory.

The second approach allows the direct adaptation of the parameters of the controller without solving an intermediate "design equation". As it will be shown the prediction error used in the PAA is in fact an image of the difference between the nominal and the attained performance because of closed-loop operation. Furthermore, the resulting schemes are governed by the same equations as those obtained by the first approach.

Although direct adaptive control is very appealing, it cannot be used for all types of plant model and control strategies. In fact, the situations where direct adaptive control can be used are limited. The basic hypothesis on the plant model is that, for any possible values of the parameters, the finite zeros of the plant model are inside the unit circle.

It also has to be mentioned that even if the zeros of the plant model are asymptotically stable, it is not possible (or it becomes very complicated) to develop direct adaptive control schemes for pole placement, linear quadratic control or generalized predictive control. The reason is that it is not possible to obtain an adaptation error equation which is linear in the difference between the nominal and estimated controller parameters.

3.5.1 Model Reference Adaptive Control

When the plant parameters are unknown or change in time, in order to achieve and to maintain the desired performance, an adaptive control approach has to be considered and such a scheme known as *Model Reference Adaptive Control (MRAC)* is shown in Fig. 3.13.

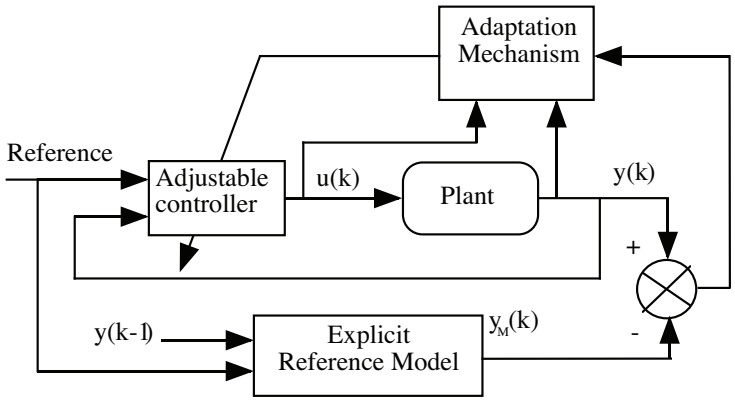

Figure 3.13: Model Reference Adaptive Control scheme

This scheme is based on the observation that the difference between the output of the plant and the output of the reference model (called subsequently plant-model error) is a measure of the difference between the real and the desired performance. This information (together with other information) is used by the *adaptation mechanism* (subsequently called *parameter adaptation algorithm*) to directly adjust the parameters of the controller in real time in order to force asymptotically the plant-model error to zero. Note that in some cases, the reference model may receive measurements from the plant in order to predict future desired values of the plant output.

The model reference control for the case of known plant model parameters has been discussed in detail in Section 3.2.4. For the development of a direct adaptive control scheme, the time-domain interpretation is useful.

The plant model (with unknown parameters) is assumed to be described by:

$$A(q^{-1})y(k) = B(q^{-1})u(k) = q^{-d}B^{\star}(q^{-1})u(k) \tag{3.150}$$

where $u(k)$ and $y(k)$ are the input and the output of the plant respectively.

In the case of known parameters, the objective is to find a control law

$$u(k) = f_u[y(k), y(k-1)\cdots u(k-1), u(k-2)\cdots]$$

such that

$$\epsilon^{\circ}(k+d) = P(q^{-1})[y(k+d) - y^{\star}(k+d)] = 0 \tag{3.151}$$

where $P(q^{-1})$ is an asymptotically stable polynomial defined by the designer. For the case of unknown plant model parameters the objective will be to find a control

$$u(k) = f_u[\hat{\theta}_c(k), y(k), y(k-1)\cdots u(k-1), u(k-2)\cdots]$$

where $\hat{\theta}_c(k)$ denotes the current controller parameters estimates such that with bounded $\{u(k)\}$ and $\{y(k)\}$ we have:

$$\lim_{k\to\infty} \epsilon^{\circ}(k+d) = 0 \tag{3.152}$$

Observe that $\epsilon^\circ(k+d)$ is a measure of the discrepancy between the desired and achieved performance, and as such is a potential candidate to be the adaptation error. This quantity can be generated at each sample ($y^\star(k+d)$ is known d steps ahead).

The next step toward the design of an adaptive control scheme is to replace the fixed controller given in (3.84) or (3.88) by an adjustable controller. Since the performance error for a certain value of plant model parameters will be caused by the misalignment of the controller parameters values, it is natural to consider an adjustable controller which has the same structure as in the linear case with known plant parameters and where the fixed parameters will be replaced by adjustable ones. It will be the task of the adaptation algorithm to drive the controller parameters towards the values assuring the satisfaction of (3.152). Therefore, the control law in the adaptive case will be chosen as:

$$\hat{S}(k,q^{-1})u(k)+\hat{R}(k,q^{-1})y(k)=P(q^{-1})y^\star(k+d) \tag{3.153}$$

where:

$$\hat{S}(k,q^{-1})=\hat{s}_0(k)+\hat{s}_1(k)q^{-1}+\cdots\hat{s}_{n_S}(k)q^{-n_S}=\hat{s}_0(k)+q^{-1}\hat{S}^\star(k,q^{-1}) \tag{3.154}$$

$$\hat{R}(k,q^{-1})=\hat{r}_0(k)+\hat{r}_1(k)q^{-1}+\cdots\hat{r}_{n_R}(k)q^{-n_R} \tag{3.155}$$

which can be written alternatively as (see also Eq. (3.88)):

$$\hat{\theta}_C^T(k)\phi_C(k)=P(q^{-1})y^*(k+d) \tag{3.156}$$

where:

$$\hat{\theta}_C^T(k) = [\hat{s}_0(k)\cdots\hat{s}_{n_S}(k),\hat{r}_0(k)\cdots\hat{r}_{n_R}(k)];\hat{s}_0(k)=\hat{b}_1(k) \tag{3.157}$$

$$\phi_C^T(k) = [u(k)\cdots u(k-n_S),y(k)\cdots y(k-n_R)] \tag{3.158}$$

and the effective control input will be computed as:

$$u(k)=\frac{1}{\hat{s}_0(k)}\left[P(q^{-1})y^*(k+d)-\hat{S}^*(k,q^{-1})u(k-1)-\hat{R}(k,q^{-1})y(k)\right] \tag{3.159}$$

The choice made for the adaptation error in (3.151) and the structure of the adjustable controller leads to the block diagram of the adaptive control system shown in Fig. 3.14. It shows that the adaptation error is defined by the difference between the desired trajectory $y^\star(k)$ generated by the tracking reference model and the plant output $y(k)$ filtered by $P(q^{-1})$. Therefore, $P(q^{-1})$ can be interpreted as a "reference model" for regulation.

Since we have selected a candidate for the adaptation error and a structure for the adjustable controller, the next step will be to give an expression for $\epsilon^\circ(k+d)$ as a function of the controller parameters misalignment. This will allow one to see to what extent $\epsilon^\circ(k+d)$ can be considered as an adaptation error to be used in a PAA of the forms discussed in Section 3.4. We note first that for the case of known parameters where the controller parameters are computed by solving the polynomial equation (3.68), one has

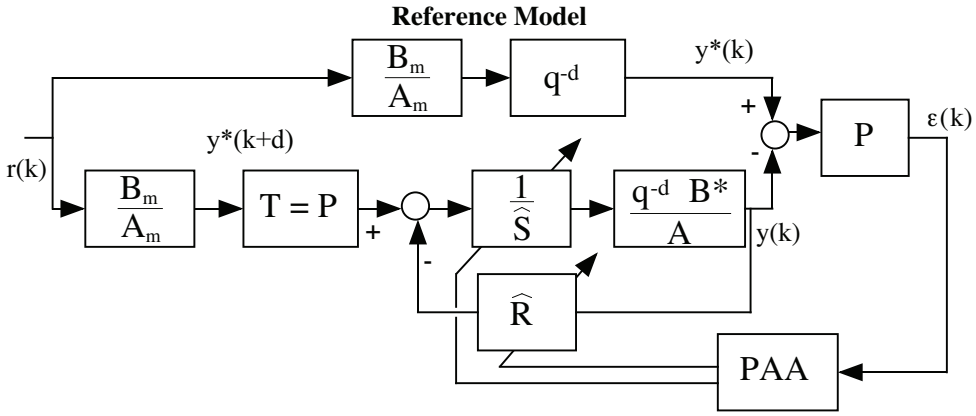

Figure 3.14: The detailed diagram of the model reference adaptive control

$\epsilon^\circ(k+d) \equiv 0$ and using (3.88), one can conclude that the filtered predicted plant output is given by:

$$\theta_C^T \phi_C(k) = P(q^{-1}) y(k+d) \tag{3.160}$$

since in the case of known parameters:

$$P(q^{-1}) y^\star(k+d) = P(q^{-1}) y(k+d) \; ; \; \forall \; k > 0 \tag{3.161}$$

where:

$$\theta_C^T = [s_0 \cdots s_{n_S}, r_0 \cdots r_{n_R}] \tag{3.162}$$

defines the parameter vector of the tuned controller (unknown). Subtracting Eq. (3.154) which contains the parameters of the adjustable controller from Eq. (3.160), one obtains:

$$\begin{aligned} \epsilon^\circ(k+d) &= P(q^{-1}) y(k+d) - P(q^{-1}) y^*(k+d) \\ &= [\theta_C - \hat{\theta}_C(k)]^T \phi_C(k) \end{aligned} \tag{3.163}$$

which has the desired form (linear in the parameter error). Therefore, the PAA to be used for assuring:

$$\lim_{k \to \infty} \epsilon(k+d) = 0 \tag{3.164}$$

is:

$$\hat{\theta}_C(k+d) = \hat{\theta}_C(k+d-1) + F(k) \phi_C(k) \epsilon(k+d) \tag{3.165}$$

$$F^{-1}(k+1) = \lambda_1(k) F^{-1}(k) + \lambda_2(k) \phi_C(k) \phi_C^T(k) \tag{3.166}$$

$$0 < \lambda_1(k) \leq 1; 0 \leq \lambda_2(k) < 2 \; ; \; F(0) > 0$$

To make the above PAA implementable, we have to give an expression of $\epsilon(k+d)$ in terms of the *a priori* adaptation error $\epsilon^\circ(k+d)$ and the parameters $\hat{\theta}(k+i)$ up to and including $i = d-1$. We can associate to (3.161) an a posteriori adaptation error equation

$$\epsilon(k+d) = [\theta_C - \hat{\theta}_C(k+d)]^T \phi_C(k) \tag{3.167}$$

and rewrite it as :

$$\begin{aligned}\epsilon(k+d) &= \epsilon^{\circ}(k+d) + [\hat{\theta}_C(k) - \hat{\theta}_C(k+d)]^T \phi_C(k) \\ &= \epsilon^{\circ}(k+d) - \phi_C^T(k) F(k) \phi_C(k) \epsilon(k+d) \\ &\quad + [\hat{\theta}_C(k) - \hat{\theta}_C(k+d-1)]^T \phi_C(k) \end{aligned} \tag{3.168}$$

from which one obtains:

$$\epsilon(k+d) = \frac{\epsilon^{\circ}(k+d) - [\hat{\theta}_C(k+d-1) - \hat{\theta}_C(k)]^T \phi_C(k)}{1 + \phi_C^T(k) F(k) \phi_C(k)} \tag{3.169}$$

which can also be expressed as:

$$\epsilon(k+d) = \frac{Py(k+d) - \hat{\theta}_C^T(k+d-1) \phi_C(k)}{1 + \phi_C^T(k) F(k) \phi_C(k)} \tag{3.170}$$

The stability of the direct adaptive control is shown in Appendix A.3.

Example 3.9. In this example, we will illustrate the influence of the regulation dynamics (the polynomial $P(q^{-1})$) on the performance of the model reference adaptive control.

Two different plant models are considered. The plant model before a parameter change occurs is characterized by the discrete transfer operator:

$$G_1(q^{-1}) = \frac{q^{-2}(1 + 0.4q^{-1})}{(1 - 0.5q^{-1})[1 - (0.8 + 0.3j)q^{-1}][1 - (0.8 - 0.3j)q^{-1}]}$$

At time $k = 25$, a change of the plant model parameters is made. The new plant model is characterized by the transfer operator:

$$G_2(q^{-1}) = \frac{q^{-2}(0.9 + 0.5q^{-1})}{(1 - 0.5q^{-1})[1 - (0.9 + 0.42j)q^{-1}][1 - (0.9 - 0.42j)q^{-1}]}$$

The simulations have been carried out for two different values of the regulation polynomial:

1. $P_1(q^{-1}) = 1$ (deadbeat control);
2. $P_2(q^{-1}) = 1 - 1.262q^{-1} + 0.4274q^{-2}$.

$P_2(q^{-1})$ corresponds to the discretization ($h = 1$ s) of a continuous-time second-order system with $\omega_0 = 0.5$ rad/s and $\zeta = 0.85$.

The tracking reference model is characterized by:

$$\frac{B_m(q^{-1})}{A_m(q^{-1})} = \frac{(0.28 + 0.22q^{-1})}{(1 - 0.5q^{-1})[1 - (0.7 + 0.2j)q^{-1}][1 - (0.7 - 0.2j)q^{-1}]}$$

In all simulations a PAA with constant trace adaptation gain has been used with $trF(k) = trF(0)$, $F_0 = diag[10]$ and $[\lambda_1(k)/\lambda_2(k)] = 1$.

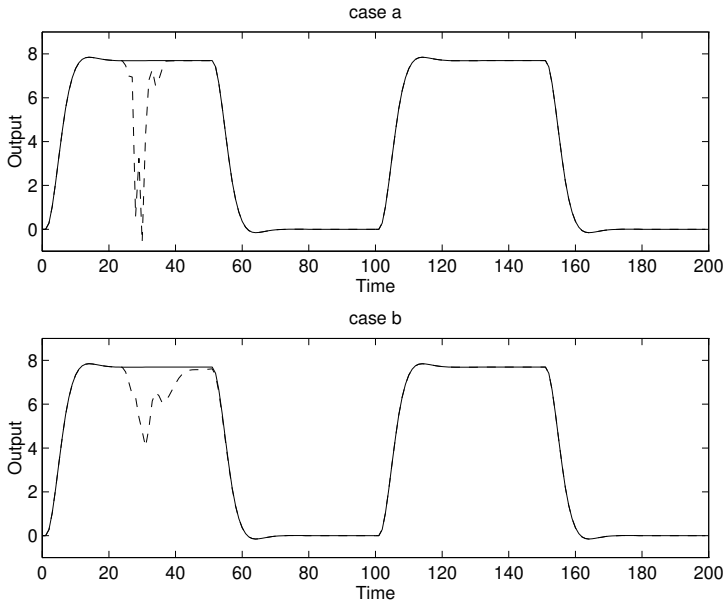

Figure 3.15: Tracking behaviour in the presence of plant model parameters changes at $k = 25$. [–] desired output, [- -] achieved output. a) Regulation dynamics $P(q^{-1}) = 1$, b) Regulation dynamics $P(q^{-1}) = 1 - 1.262q^{-1} + 0.4274q^{-2}$

Fig. 3.15 shows the desired trajectory and the achieved trajectory during a sequence of step changes on the reference and in the presence of the parameter variations occurring at $k = 25$. One can observe that the adaptation transient is much smoother using the $P_2(q^{-1})$ regulation polynomial than in the case $P_1(q^{-1})$.

Fig. 3.16 shows the behaviour in regulation, i.e., the evolution of the output from an initial condition at $k = 0$ in the presence of a change in the parameters at $k = 0$. Same conclusion can be drawn: the poles defined by the regulation polynomial strongly influence the adaptation transient. Too fast dynamics in regulation with respect to the natural response of the system will induce undesirable adaptation transients.

3.6 Indirect Adaptive Control

Fig. 3.17 shows an indirect adaptive control scheme which can be viewed as a real-time extension of the controller design procedure represented in Fig. 3.9. The basic idea is that a suitable controller can be designed on line if a model of the plant is estimated on line from the available input-output measurements. The scheme is termed *indirect* because the adaptation of the controller parameters is done in two stages:

1) on-line estimation of the plant parameters;
2) on-line computation of the controller parameters based on the current estimated

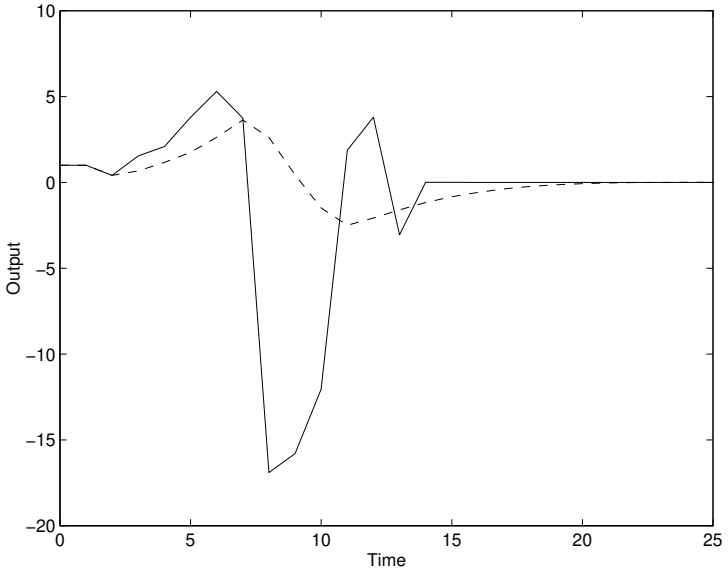

Figure 3.16: Regulation behaviour in the presence of plant model parameters changes at $k = 0$. [–] Regulation dynamics $P(q^{-1}) = 1$, [- -] Regulation dynamics $P(q^{-1}) = 1 - 1.262q^{-1} + 0.4274q^{-2}$

plant model.

This scheme uses current plant model parameter estimates as if they are equal to the true ones in order to compute the controller parameters. This is called the *ad-hoc certainty equivalence* principle.

The indirect adaptive control scheme offers a large variety of combinations of control laws and parameter estimation techniques.

The situation in indirect adaptive control is that in the absence of external rich excitations one cannot guarantee that the excitation will have a sufficiently rich spectrum and one has to analyze when the computation of the controller parameters based on the

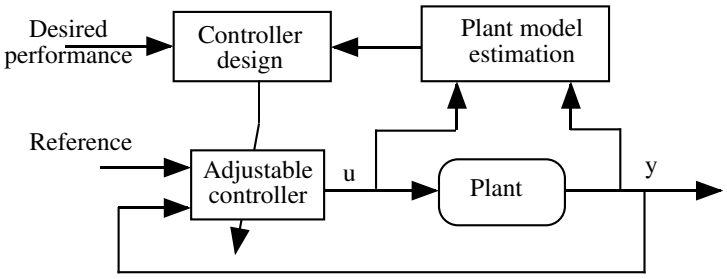

Figure 3.17: Indirect adaptive control (principle)

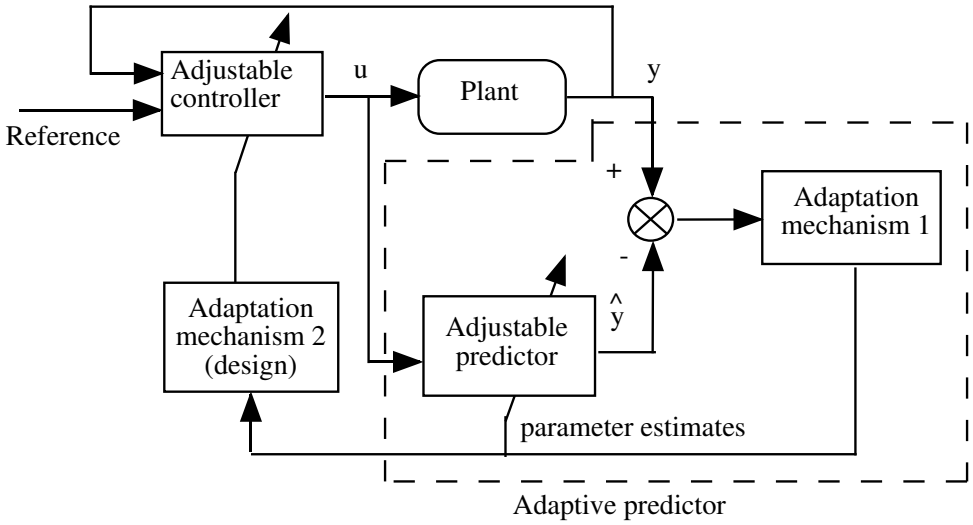

Figure 3.18: Indirect adaptive control (detailed scheme)

parameters of an adaptive predictor will allow acceptable performance to be obtained asymptotically.

Introducing the block diagram for the plant model parameter estimation into the scheme of Fig. 3.17, one obtains the general configuration of an *indirect adaptive control* shown in Fig. 3.18. Using the indirect adaptive control schemes shown in Fig. 3.18, one can further elaborate on the ad-hoc use of the "certainty equivalence" or "separation theorem" which hold for the linear case with known parameters.

In terms of *separation* it is assumed that the adaptive predictor gives a good prediction (or estimation) of the plant output (or states) when the plant parameters are unknown, and that the prediction error is independent of the input to the plant (this is false however during adaptation transients). The adjustable predictor is a system for which full information is available (parameters and states). An appropriate control for the predictor is computed and this control is also applied to the plant. In terms of *certainty equivalence*, one considers the unknown parameters of the plant model as additional states. The control applied to the plant is the same as the one applied when all the "states" (i.e., parameters and states) are known exactly, except that the "states" are replaced by their estimates.

However, as mentioned earlier, the parameters of the controller are calculated using plant parameter estimates and there is no evidence, therefore, that such schemes will work (they are not the exact ones, neither during adaptation, nor in general, even asymptotically). A careful analysis of the behaviour of these schemes should be done. In some cases, external excitation signals may be necessary to ensure the convergence of the scheme toward desired performance. As a counterpart adaptation has to be stopped if the input of the plant whose model has to be estimated is not *rich* enough (meaning a sufficiently

large frequency spectrum).

The resulting control scheme should guarantee that the input and the output of the plant remain bounded and that some indices of performance are achieved asymptotically. This requires a deep analysis of the indirect adaptive control system which is nonlinear and time-varying.

Fortunately, good properties of the indirect adaptive control schemes will be guaranteed if, separately, the parameter estimation algorithm and the control strategy satisfy a number of properties (largely similar to those required for indirect adaptive prediction) which are summarized next:

1. The *a posteriori* adaptation error in the parameter estimation algorithm goes to zero asymptotically.
2. The *a priori* adaptation error does not grow faster than the observation vector (containing the input and output of the plant).
3. The estimated plant model parameters are bounded for all k.
4. The variations of the estimated plant model parameters go to zero asymptotically.
5. The *design equation(s)* provide(s) bounded controller parameters for bounded plant parameter estimates.
6. The estimated plant model is *admissible* with respect to the *design equation* which means that assuming that it corresponds to the exact plant model, the resulting controller has bounded parameters, stabilizes the system and achieves the desired performance.

If these conditions are satisfied, it is then possible to show that the input and the output of the plant remain bounded and that some indices of performance are achieved asymptotically.

Probably, the most difficult problem (at least theoretically) is to guarantee that any estimated model is *admissible* with respect to the control design strategy. For every control strategy, even if the estimated plant parameters are bounded at each time k, the current estimated model may not be admissible in the sense that there is no solution for the controller. For example, if pole placement is used as the control strategy, an estimated model at time k, which features a pole-zero cancellation, will not allow to compute the controller. Furthermore, getting close to non-admissibility situations will lead to numerical problems resulting in very large and undesirable control actions. The consequence of this fact is twofold:

1. One has to be aware of the admissibility conditions and take appropriate ad hoc action in practice, in order to deal with the singularities which may occur during adaptation.
2. One can make a theoretical analysis and develop *modifications* of the parameter estimates (or of the algorithms) in order to avoid the singularities corresponding to the non-admissibility of an estimated plant model.

As indicated earlier (property 6), to remove the singularities one has to assume that the unknown plant model is admissible with respect to the control strategy.

While the various *modifications* of the estimated parameters or of the algorithms resulting from a theoretical analysis are in general complex to implement, they have the merit of showing that there are solutions that avoid the *non-admissibility* of the estimated model and give hints for simple ad hoc modifications to be implemented.

The analysis of the indirect adaptive control schemes is carried out in two steps:

1. One assumes that the estimated models are always in the admissibility set.
2. One modifies the parameter estimation algorithm in order to satisfy the admissibility condition.

The objective of the analysis is to guarantee that a stabilizing controller is obtained without any assumption about the presence or the richness of an external excitation. However, the use of an external or internal excitation signal, even for short periods of time, is useful for speeding up the convergence of the adaptive control scheme since it can be shown that exponential stability is achieved under richness conditions.

3.6.1 Implementation Strategies

To implement an indirect adaptive control strategy effectively, we have two major options. The choice is related to a certain extent to the ratio between the computation time and the sampling period.

Strategy 1

1. Sample the plant output;
2. update the plant model parameters;
3. compute the controller parameters based on the new plant model parameter estimates;
4. compute the control signal;
5. send the control signal;
6. wait for the next sample.

Using this strategy, there is a delay between $u(k)$ and $y(k)$ which will essentially depend upon the time required to achieve (2) and (3). This delay should be small with respect to the sampling period and, of course, smaller than the delay between $u(k)$ and $y(k)$ scheduled in the I/O system. In this strategy, *a posteriori* parameter estimates are used and the *a posteriori* adaptation error will occur in the stability analysis.

Strategy 2

1. Sample the plant output;
2. compute the control signal based on the controller parameters computed during the previous sampling period;
3. send the control signal;
4. update the plant model parameters;
5. compute the controller parameters based on the new plant model parameter estimates;
6. wait for the next sample.

Using this strategy, the delay between $u(k)$ and $y(k)$ is smaller than in the previous case. In fact, this is the strategy used with constant parameters controllers (Steps 4 and 5 are deleted). In this strategy, one uses *a priori* parameter estimates and the *a priori* adaptation error will appear in the stability analysis.

The analysis of the resulting schemes is very similar except that as indicated earlier, in the Strategy 1 the *a posteriori* adaptation error will play an important role, while in the Strategy 2, the properties of the *a priori* adaptation error will be used.

One uses a non-vanishing adaptation gain to get an indirect adaptive control scheme which can react to changes in plant model parameters. One uses a time-decreasing adaptation gain to implement indirect adaptive control schemes for the case of plant models with unknown but constant parameters (over a large time horizon). In the latter case, adaptation can be restarted either on demand or automatically, based on the analysis of an index of performance.

We can also update the estimates of the plant model parameters at each sampling instant, but updating the controller parameters only every N sampling instants. The analysis remains the same as long as N is finite. The use of this approach is related to:

- the possibility of getting better parameter estimates for control design,
- the eventual reinitialization of the plant parameters estimation algorithm after each controller updating,
- the use of more sophisticated control designs requiring complex computations (in particular robust control design),
- the reduction of the risk for getting non-admissible estimated plant models.

3.6.2 Adaptive Pole Placement

We will assume that the system operates in a deterministic environment. The basic algorithm combines a parameter estimation algorithm with the pole placement control strategy presented in Section 3.2.3. The plant model (with unknown parameters) is assumed to be described by:

$$A(q^{-1})y(k) = B(q^{-1})u(k) = q^{-d}B^{\star}(q^{-1})u(k) \tag{3.171}$$

where $u(k)$ and $y(k)$ are the input and the output of the plant and:

$$\begin{aligned} A(q^{-1}) &= 1 + a_1 q^{-1} + \cdots + a_{n_A} q^{-n_A} = 1 + q^{-1} A^\star(q^{-1}) \\ B(q^{-1}) &= b_d q^{-d} + \cdots + b_{n_B} q^{-n_B} = q^{-d} B^\star(q^{-1}) \end{aligned}$$

One assumes that:

- the orders of the polynomials $A(q^{-1}), B(q^{-1})$ and of the delay d are known (n_A, n_B, d - known)[4] ;
- $A(q^{-1})$ and $B(q^{-1})$ do not have common factors (admissibility condition).

Estimation of the plant model parameters: To simplify the analysis, we will assume that a *recursive least squares* type parameter estimation algorithm will be used. The plant output can be expressed as:

$$y(k+1) = \theta^T \phi(k) \tag{3.172}$$

where:

$$\theta^T = [a_1 \cdots a_{n_A}, b_d \cdots b_{n_B}] \tag{3.173}$$

$$\phi^T(k) = [-y(k) \cdots - y(k - n_A + 1), u(k - d + 1) \cdots u(k - n_B + 1)] \tag{3.174}$$

The *a priori* output of the adjustable predictor is given by:

$$\hat{y}^\circ(k+1) = \hat{\theta}^T(k) \phi(k) \tag{3.175}$$

The *a posteriori* output of the adjustable predictor is given by:

$$\hat{y}(k+1) = \hat{\theta}^T(k+1) \phi(k) \tag{3.176}$$

where:

$$\hat{\theta}^T(k) = [\hat{a}_1(k) \cdots \hat{a}_{n_A}(k), \hat{b}_d(k) \cdots \hat{b}_{n_B}(k)] \tag{3.177}$$

Accordingly, the *a priori* and the *a posteriori* prediction (adaptation) errors are given by:

$$\epsilon^\circ(k+1) = y(k+1) - \hat{y}^\circ(k+1) \tag{3.178}$$

$$\epsilon(k+1) = y(k+1) - \hat{y}(k+1) \tag{3.179}$$

The parameter adaptation algorithm is:

$$\hat{\theta}(k+1) = \hat{\theta}(k) + F(k) \phi(k) \epsilon(k+1) \tag{3.180}$$

$$F^{-1}(k+1) = \lambda_1(k) F^{-1}(k) + \lambda_2(k) \phi(k) \phi^T(k);$$

$$0 < \lambda_1(k) \leq 1 \; ; \; 0 \leq \lambda_2(k) < 2 \; ; \; F(0) > 0 \tag{3.181}$$

$$\epsilon(k+1) = \frac{\epsilon^\circ(k+1)}{1 + \phi^T(k) F(k) \phi(k)} \tag{3.182}$$

[4] What is in fact needed is the knowledge of n_B. However, the knowledge of d reduces the number of estimated parameters.

It is also assumed that:

$$F^{-1}(k) \geq \alpha F^{-1}(0) \; ; \; F(0) > 0 \; ; \; \alpha > 0 \; \forall \; t \in [0, \infty] \tag{3.183}$$

Selection of $\lambda_1(k)$ and $\lambda_2(k)$ allows various forgetting profiles to be obtained (see Section 3.4.2) and this leads to:

- a time-decreasing adaptation gain;
- a time-decreasing adaptation gain with reinitialization;
- a non vanishing adaptation gain.

It also allows the introduction of the various modifications in order to have a robust adaptation algorithm. Using this algorithm, one will have the following properties:

- The *a posteriori* adaptation error is bounded and goes to zero asymptotically, i.e.:

$$\lim_{k_1 \to \infty} \sum_{k=1}^{k_1} \epsilon^2(k+1) \leq C < \infty \tag{3.184}$$

$$\lim_{k \to \infty} \epsilon(k+1) = 0 \tag{3.185}$$

- The *a priori* adaptation error satisfies:

$$\lim_{k \to \infty} \frac{[\epsilon^\circ(k+1)]^2}{1 + \phi^T(k) F(k) \phi(k)} = 0 \tag{3.186}$$

- The parameter estimates are bounded for all k

$$\|\hat{\theta}(k)\| \leq C < \infty \; ; \; \forall k \geq 0 \tag{3.187}$$

- The variations of the parameter estimates go to zero asymptotically:

$$\lim_{k \to \infty} \|\hat{\theta}(k+\ell) - \hat{\theta}(k)\| = 0 \; ; \; \forall \ell < \infty \tag{3.188}$$

Computation of the controller parameters and of the control law: We will use Strategy 1 for updating the controller parameters. The controller equation generating $u(k)$ is:

$$\hat{S}(k, q^{-1}) u(k) + \hat{R}(k, q^{-1}) y(k) = \hat{\beta}(k) P(q^{-1}) y^\star(k+d) \tag{3.189}$$

or alternatively:

$$u(k) = -\hat{S}^*(k, q^{-1}) u(k-1) - \hat{R}(k, q^{-1}) y(k) + \hat{\beta}(k) P(q^{-1}) y^\star(k+d) \tag{3.190}$$

where:

$$\hat{\beta}(k) = 1/\hat{B}(k,1) \tag{3.191}$$
$$\hat{S}(k,q^{-1}) = 1 + \hat{s}_1(k)q^{-1} + \cdots \hat{s}_{n_S}(k)q^{-n_S} = 1 + q^{-1}\hat{S}^*(k,q^{-1}) \tag{3.192}$$
$$\hat{R}(k,q^{-1}) = \hat{r}_0(k) + \hat{r}_1(k)q^{-1} + \cdots \hat{r}_{n_R}(k)q^{-n_R} = \hat{r}_0(k) + q^{-1}\hat{R}^*(k,q^{-1}) \tag{3.193}$$

and $\hat{S}(k,q^{-1}), \hat{R}(k,q^{-1})$ are solutions of[5]:

$$\hat{A}(k,q^{-1})\hat{S}(k,q^{-1}) + q^{-d-1}\hat{B}^*(k,q^{-1})\hat{R}(k,q^{-1}) = P(q^{-1}) \tag{3.194}$$

$P(q^{-1})$ in (3.189), (3.190) and (3.194) is the desired closed-loop characteristic polynomial and y^* the desired tracking trajectory. Eq. (3.194) can be reformulated in matrix form:

$$M[\hat{\theta}(k)]\hat{x} = p \tag{3.195}$$

where:

$$\hat{x}^T = [1, \hat{s_1} \cdots \hat{s}_{n_S}, \hat{r}_0, \cdots \hat{r}_{n_R}] \tag{3.196}$$
$$p^T = [1, p_1 \cdots p_{n_P}, 0 \cdots 0] \tag{3.197}$$

and $M[\hat{\theta}(k)]$ is the Sylvester matrix. Therefore, $\hat{S}(k)$ and $\hat{R}(k)$ are given by:

$$\hat{x} = M^{-1}[\hat{\theta}(k)]p \tag{3.198}$$

The admissibility condition for the estimated model is:

$$|\det M[\hat{\theta}(k)]| \geq \delta > 0 \tag{3.199}$$

which can alternatively be evaluated by the condition number:

$$\frac{\lambda_{\min} M[\hat{\theta}(k)]}{\lambda_{\max} M[\hat{\theta}(k)]} > \delta_0 > 0 \tag{3.200}$$

Remark: If Strategy 2 is used, Equations (3.189) through (3.200) remain the same except that the index k becomes $(k-1)$.

Example 3.10. Robust adaptive pole placement
The continuous time plant to be controlled is characterized by the transfer function:

$$G(s) = \frac{2}{s+1} \cdot \frac{229}{(s^2 + 30s + 229)}$$

where the first order part is considered as the dominant dynamics and the second order part as the unmodelled dynamics. The system will be controlled in discrete time with a

[5]In fact $\hat{S}(k,q^{-1}) = \hat{S}'(k,q^{-1})H_S(q^{-1})$, $\hat{R}(k,q^{-1}) = \hat{R}'(k,q^{-1})H_R(q^{-1})$ where $H_S(q^{-1})$ and $H_R(q^{-1})$ are the fixed parts of the controller.

sampling period $h = 0.04$ s. For this sampling period the true discrete time plant model is given by:

$$G(q^{-1}) = \frac{b_1 q^{-1} + b_2 q^{-2} + b_3 q^{-3}}{1 + a_1 q^{-1} + a_2 q^{-2} + a_3 q^{-3}}$$

with:

a_1	a_2	a_3
-1.8912	1.1173	-0.21225
b_1	b_2	b_3
0.0065593	0.018035	0.0030215

Since this model has unstable zeros, it is reasonable to use an indirect adaptive control strategy which can handle unstable zeros. Adaptive pole placement will be used. The plant model will be estimated using a filtered recursive least squares with dynamic data normalization. Adaptation freezing will be enforced in the absence of enough rich information (i.e., the scheduling variable for the dead zone will depend on the signal richness measured by $\bar{\phi}_f^T(k)F(k)\bar{\phi}_f(k)$ - see [7] for details). Estimated models of different orders will be used ($n = 1, 2, 3$).

Figures 3.19, 3.20 and 3.21 summarize the results obtained with various orders for the estimated model. The controller is first initialized using an open-loop recursive identification, then the loop is closed and a series of step reference changes is applied followed by the application of an output disturbance.

For a first order estimated model, while the system is stable and the signals have acceptable form, one can see that the tracking performance is not very good. Second order and third order estimated models give almost the same results and they are very good.

Fig. 3.22 shows the frequency characteristics of the estimated models for $n = 1, 2, 3$. The identified third order model corresponds exactly to the true model. From this figure, one can see that the second and third order models have similar frequency characteristics in the interesting frequency range for control (related to the desired closed-loop poles) while the first order model cannot cope with the frequency characteristics of the third order model in a sufficiently large frequency region. The desired closed-loop poles used are as follows:

$$\begin{aligned} \text{for } n &= 1: \ P(q^{-1}) = (1 - 0.8q^{-1})(1 - 0.9q^{-1}) \\ \text{for } n &= 2, 3: \ P(q^{-1}) = (1 - 0.8q^{-1})(1 - 0.4q^{-1})(1 - 0.2q^{-1})(1 - 0.1q^{-1}) \end{aligned}$$

The controller has an integrator. For the case $n = 2$, a filter $H_R(q^{-1}) = 1 + q^{-1}$ has been introduced in the controller in order to reduce the "activity" of the control action by reducing the magnitude of the input sensitivity function in the high frequencies. Same dynamics has been used in tracking and regulation.

An adaptation gain with variable forgetting factor combined with a constant trace adaptation gain has been used ($F(0) = \delta I$; $\delta = 1000$ desired trace: $tr[F(k)] = 6$). The

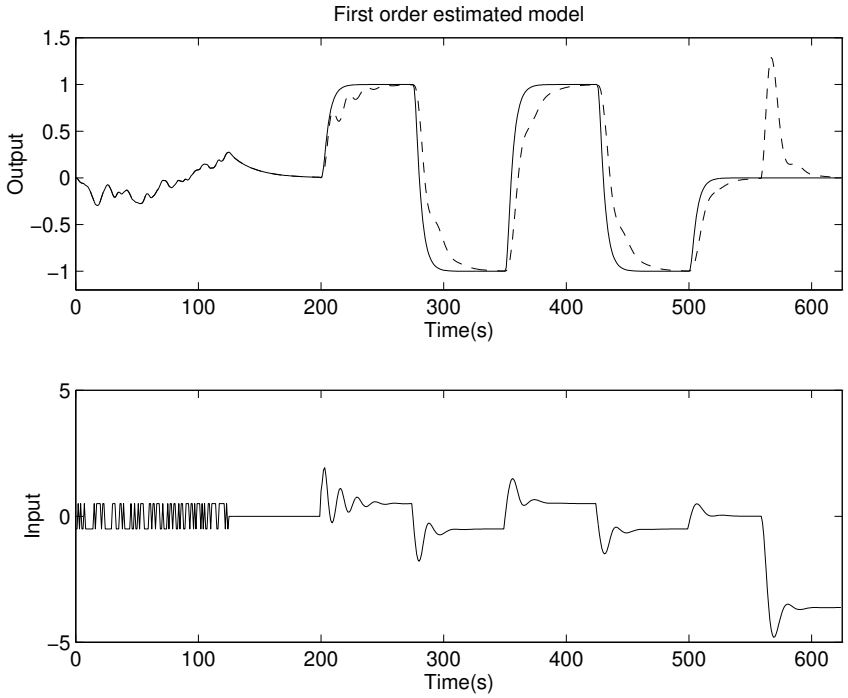

Figure 3.19: First order estimated model

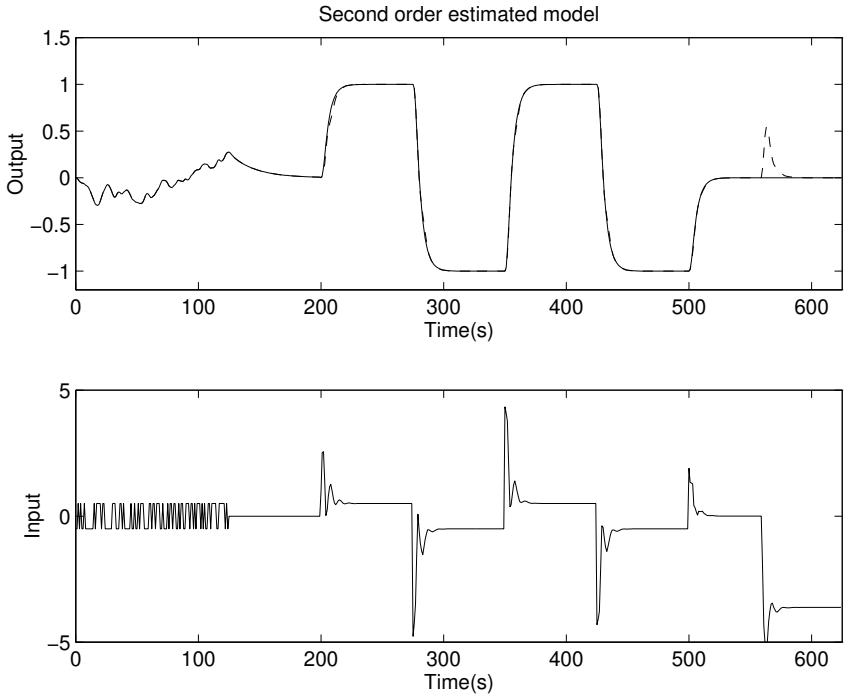

Figure 3.20: Second order Estimated model

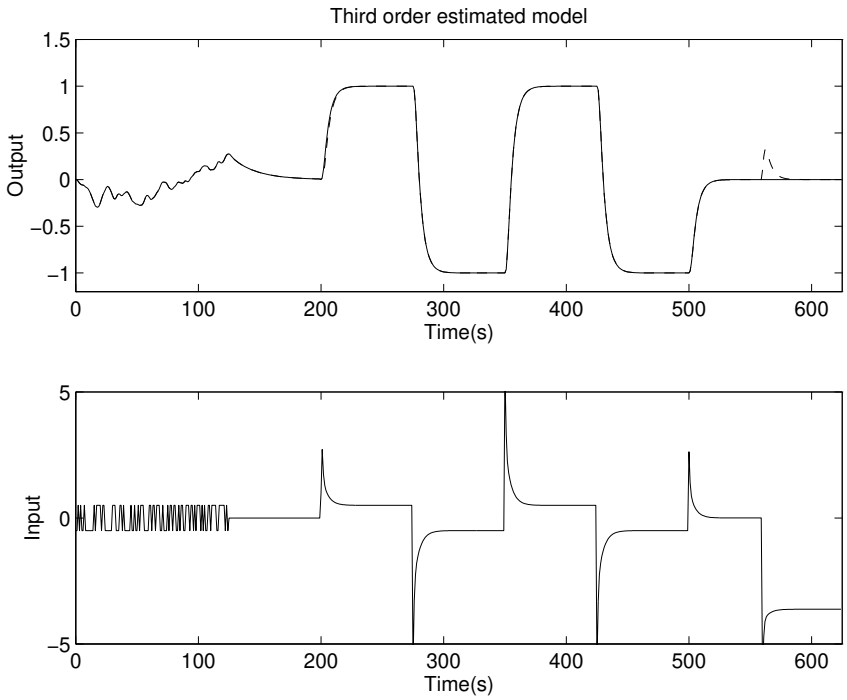

Figure 3.21: Third order estimated model

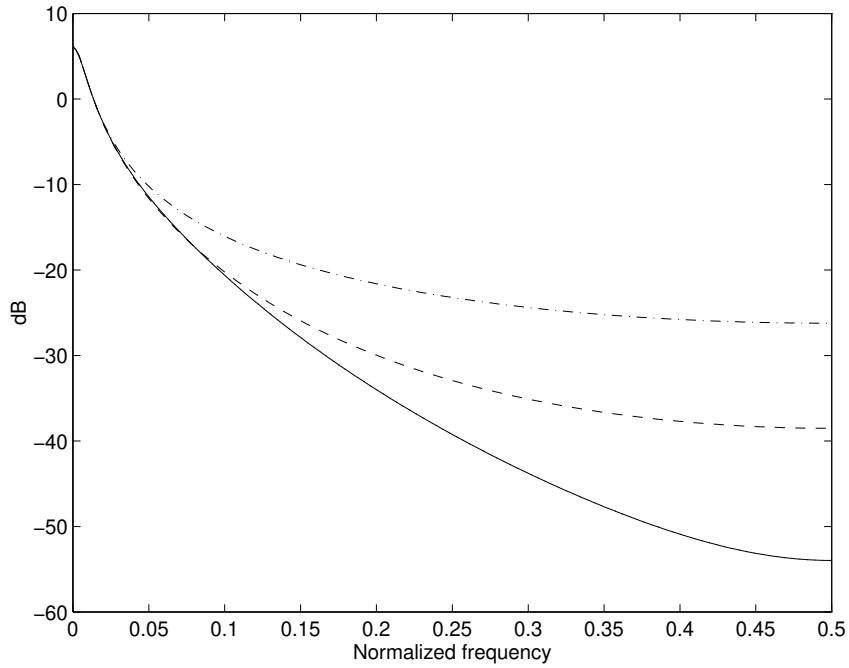

Figure 3.22: Frequency characteristics for $n = 1(-.-), 2(--), 3(-)$

filter used on input/output data is: $L(q^{-1}) = 1/P(q^{-1})$. The normalizing signal $m(k)$ has been generated by $m^2(k) = \mu^2 m^2(k-1) + \max(\|\phi_f(k)\|, 1)$ with $\mu = 0.9$. For $n = 1$, taking into account the unmodelled dynamics, the theoretical value for μ is $0.6 < \mu < 1$ (the results are not very sensitive with respect to the choice of the desired trace and μ).

The conclusion is that for this example, despite the fact that a stable adaptive controller can be obtained with a first order estimated model corresponding to the dominant dynamics of the true plant model, one should use a second order estimated model in order to obtain a good performance.

The rule which can be established is that low-order modelling can be used in adaptive control but good performance requires that this model be able to copy the frequency characteristics of the true plant model in the frequency region relevant for control design.

Concluding Remarks

1. Indirect adaptive control algorithms emerged as a solution for adaptive control of systems featuring discrete time models with unstable zeros.
2. Indirect adaptive control offers the possibility of combining (in principle) any linear control strategy with a parameter estimation scheme.
3. The plant model parameter estimator should allow a good prediction of the behavior of the closed loop.
4. The design of the controller based on the estimated plant models should be done such that some robustness constraints on the sensitivity functions be satisfied (in particular on the output and on the input sensitivity functions). This can be achieved by a suitable choice of the desired performance and introduction of some fixed filters in the controller.
5. For each type of underlying linear control strategy used in indirect adaptive control a specific admissibility test has to be done on the estimated model prior to the computation of the control.
6. Robustification of the parameter adaptation algorithms used for plant model parameter estimation may be necessary in the presence of unmodelled dynamics and bounded disturbances.
7. Adaptive pole placement and adaptive generalized predictive control are the most used indirect adaptive control strategies.

3.7 Switching Adaptive Control

The plants subject to abrupt and large parameter variations are generally very difficult to control. A classical adaptive controller or a fixed robust controller encounter difficulties to solve this problem. An adaptive controller is not fast enough to follow the parameter

variations and unacceptable transients occur. Whereas a fixed robust controller normally leads to poor performance because of large uncertainties.

Multimodel adaptive control can be considered as a solution to this problem. In this approach a set of Kalman filters are used to estimate the states of the plant model. A set of state feedback controllers are also designed such that for each Kalman filter there is a state feedback controller in the set. The final control input is the weighted sum of the control inputs from different controllers. The weightings are computed using the covariance matrix of state estimates such that smaller variances lead to larger weights for the corresponding control inputs. In a robust version of this scheme the state feedback controllers are replaced by robust output feedback controllers designed using the H_∞ control approach. Although this method has been successfully applied in a few simulation examples, the stability of the scheme has not yet been proved.

An alternative solution is to choose one of the control inputs that corresponds to the best output estimator and apply it to the real system. This approach which is based on switching among a set of controllers has the advantage that a stability analysis for the closed-loop system can be carried out. Switching is often based on an error signal measured in real-time that represents the difference between the measured and estimated output. In this approach, it is supposed that a set of models for different operating points is *a priori* known. Then at every instant a controller corresponding to the model yielding the minimum of a performance index is used to compute the control input. The precision of the control can be further improved using an adaptive model (a model whose parameters are updated with a parameter adaptation algorithm) in the set of models.

3.7.1 Basic Scheme

In this section, the main structure of adaptive control with switching is presented. This structure, shown in Fig. 3.23, contains four blocks: plant model, multi-estimator, multi-controller and supervisor.

Plant with uncertainty Plant model is supposed to be a member of a very large set of admissible models given by :

$$\mathcal{G} = \bigcup_{\theta \in \Theta} G(\theta) \tag{3.201}$$

where Θ is a compact set and each $G(\theta)$ is a family of models centered around a nominal model $G_0(\theta)$. For example, if we consider multiplicative uncertainty, the plant model can be represented by

$$G(\theta) = G_0(\theta)[1 + W\Delta]$$

where W is the uncertainty filter and Δ is a stable transfer function with $\|\Delta\|_\infty < 1$. As a result, $\mathcal{G}$ represents the parametric uncertainty (or variation) and for each fixed θ, the subfamily of $G(\theta)$ represents the unmodelled dynamics.

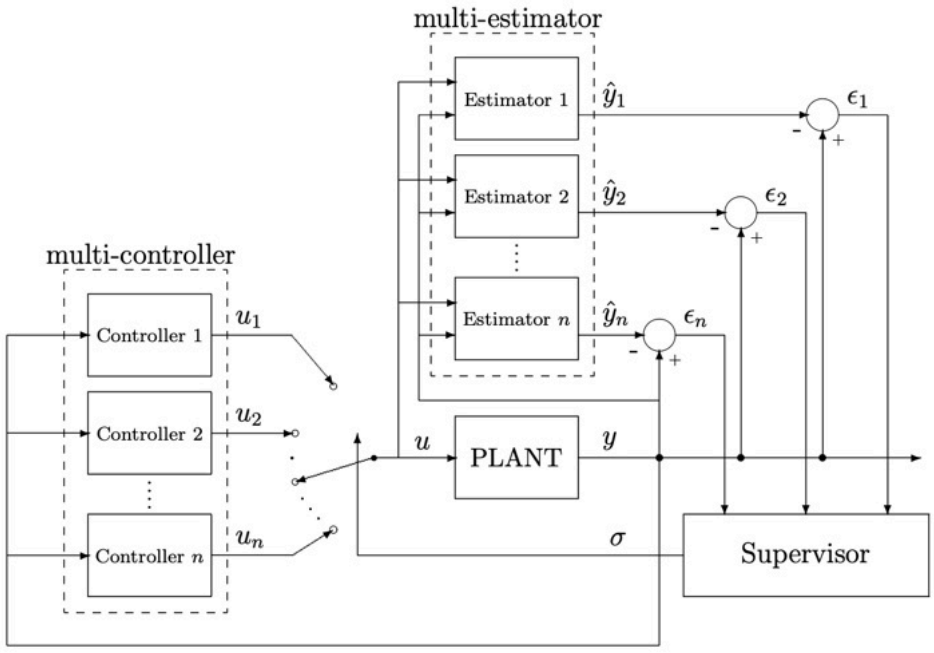

Figure 3.23: Block diagram of adaptive control with switching

Multi-estimator The multi-estimator is a dynamical system whose inputs are the input and output of the plant and whose outputs are the estimates of the plant output. Suppose that Θ is a finite set. In this case, multi-estimator can be chosen as a set of fixed models corresponding to each θ. The fixed models can be considered as output error estimators. However, any other estimators like Kalman filter or ARMAX estimator can be used as well. If Θ is an infinite set, some fixed models and one adaptive model can be considered. Since the number of available models is finite but the number of possible models is generally infinite, the estimation is performed in two steps:

- The model with smallest error with respect to a criterion is rapidly chosen (switching).
- The parameters of the model are adjusted using a parameter adaptation algorithm (tuning).

Multi-controller For each estimator (or fixed model) in the multi-estimator block, a controller should be designed that stabilizes and satisfies the desired performance for the estimator (or fixed model). If Θ is not a finite set but the set of multi-estimators is finite, the controllers should be robust with respect to the parameter uncertainty as well as unmodelled dynamics. If an adaptive model is considered in the multi-estimator set, like the classical adaptive control, the controller should be a function of the model parameters.

Supervisor The supervisor decides the output of which controller should be applied to the real plant at each instant. The decision is based on a monitoring signal and a switching logic. The monitoring signal is a function of the estimation error to indicate the best estimator at each time. It may be defined as follows:

$$J_i(k) = \alpha\epsilon_i^2(k) + \beta\sum_{j=0}^{k} e^{-\lambda(k-j)}\epsilon_i^2(j) \quad \alpha \geq 0 \quad \beta, \lambda > 0 \tag{3.202}$$

where j is the time index and α and β are the weighting factors on the instantaneous measures and the long term accuracy. λ is a forgetting factor which also assures the boundedness of the criterion for bounded $\epsilon_i(k)$. Therefore, the design parameters for the switching part of the control system are α, β and λ. If we choose a large value for α/β and λ, we will obtain a very quick response to the abrupt parameter changing but a bad response with respect to disturbances. It means that, an output disturbance will generate an unwanted switching to another controller which results in a poor control. Contrary, a small value for α/β and λ makes the criterion a good indicator of steady-state identifier accuracy, which reduces the number of unwanted switching but leads to a slow response with respect to the parameter variations.

The switching logic is based on the monitoring signal. A switching signal $\sigma(k)$ indicates which control input should be applied to the plant. In order to avoid chattering, a minimum dwell-time between two consecutive switchings or a hysteresis is usually considered. The switching logic plays an important role on the stability of the switching system which will be discussed in the next section.

A combination of two logics (dwell-time and hysteresis) may also be considered. A small value for T_d, dwell-time, gives too frequent switchings and may lead to instability, while a large T_d leads to a slow response system.

A hysteresis cycle with a design parameter μ is considered between two switchings. It means that a switching to another controller will occur if the performance index concerning a model is improved by μJ_i. With hysteresis, large errors are rapidly detected and a better controller is chosen. However, the algorithm does not switch to a better controller if the performance improvement is not significant.

3.7.2 Stability Issues

The objective of this section is not to give a formal proof for the stability of multimodel adaptive control, but to present the basic idea of the proof and a practical way to compute the dwell-time to ensure the closed-loop stability. It should be mentioned that in this section we suppose that the real plant is fixed but unknown. However, the results can be used for large and abrupt parameter changes but not for frequent parameter variations.

The stability is analyzed in two steps. In the first step we show that under some mild assumptions the stability of the system can be reduced to the stability of a subsystem called the "injected system". This subsystem is a switching system that contains only

stable models. In the second step the stability of this particular switching system is discussed. It is shown that this system can always be stabilized by choosing an appropriate dwell-time.

Stability of adaptive control with switching: Consider a trivial case in which one of the models in the multi-estimator block matches perfectly with the plant model (no unmodelled dynamics). Suppose that there is no measurement noise and that the plant is detectable[6]. In this case, the estimation error for one of the models, say $\varepsilon_k(k)$ goes to zero. Consequently $\varepsilon_\sigma(k)$ goes to zero and the switching signal $\sigma(k)$ goes to k (switching stops after a finite time). It is evident that C_k which stabilizes the k-th model will stabilize the plant based on the certainty equivalence stabilization theorem.

However, in practice, because of unmodelled dynamics and measurement noise, the switching will not necessarily stop after a finite time and the analysis becomes more involved. To proceed, we consider the following assumptions:

A1: In the multi-estimator block there exists at least one "good" estimator. It means that at least for one estimator, say estimator k, the estimation error is "small". The smallness of the estimation error can be defined by an upper bound that depends on the modeling error and noise variance.

A2: $\varepsilon_\sigma(k) = y(k) - y_\sigma(k)$ is small. It means that the monitoring signal, switching criterion $J(k)$, and the switching logic are properly designed (α, β and λ are well tuned and dwell-time or hysteresis are not too large).

It can be shown that under the above assumptions all closed-loop signals and states are bounded if the injected system is stable. The injected system is a dynamical system which has ε_σ as input and u_σ (or u) and y_σ as outputs. Fig. 3.24 is the same as Fig. 3.23 but is drawn differently to make appear the injected system as a separate block from the rest of the system. The supervisor and the switch are replaced by index σ in the output of multi-estimator and multi-controller. It can be observed that if the injected system is stable, the input of the plant u and y_σ are bounded for a bounded ε_σ . It is clear that boundedness of y_σ implies the boundedness of y. So the input and output of the plant are bounded and all internal states of the plant are also bounded if the plant is detectable.

If the switching stops after a finite time, the injected system becomes an LTI system and is naturally stable (each controller stabilizes the corresponding model in the multi-estimator block). However, in presence of noise and unmodelled dynamics, the switching may not stop and the injected system becomes a switching system with arbitrary switching among stable systems. This type of switching systems are not necessarily stable and their stability has been analyzed in the literature. In the next subsection some recent results on the stability of such systems are given.

[6]A system is detectable if and only if all of its unobservable modes are stable.

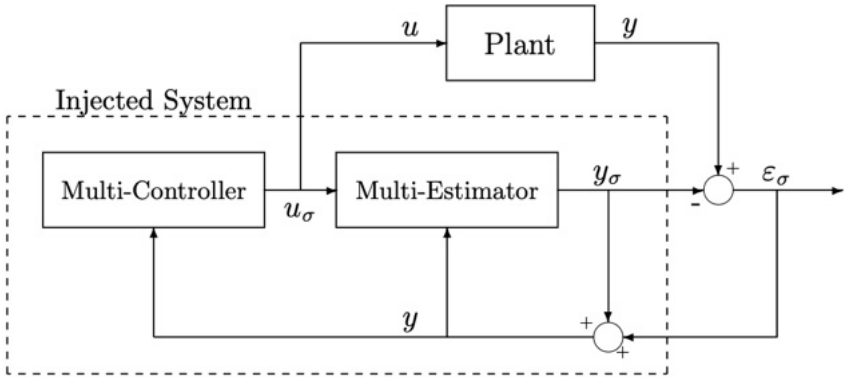

Figure 3.24: Representation of the closed-loop system including the injected system

Stability of the injected system: It is shown that the injected system is a switching system containing only the stable systems constructed by the members of the multi-estimator block and their corresponding controllers in the multi-controller block. In this subsection we study the stability of a switching system containing n stable models in the state space. Consider the following models:

$$x(k+1) = A_1 x(k), \quad x(k+1) = A_2 x(k), \quad \dots \quad x(k+1) = A_n x(k)$$

where $A_1, A_2, \dots, A_n$ are stable matrices. Consider also a switching signal $\sigma(k) \in \{1, 2, \dots, n\}$. Then $x(k+1) = A_\sigma x(k)$ is stable if A_1 to A_n have a common Lyapunov matrix or the minimum time between two switchings is greater than T_d.

Stability with common Lyapunov matrix: The existence of a common Lyapunov matrix P for $A_1, A_2, \dots, A_n$ guarantees the stability of A_σ. It is easy to show that if we take a Lyapunov function $V(k) = x(k)^T P x(k)$ its finite difference

$$\Delta V(k) = V(k+1) - V(k) = x(k)^T (A_\sigma P A_\sigma - P) x(k) < 0$$

if

$$\begin{aligned} A_1^T P A_1 &- P \prec 0 \\ A_1^T P A_1 &- P \prec 0 \\ &\vdots \\ A_n^T P A_n &- P \prec 0 \end{aligned}$$

The above inequalities are linear with respect to P and represent a set of Linear Matrix Inequalities (LMIs). Therefore, the existence of P can be easily verified using Semi Definite Programming (SDP) solvers. The main interest of this stability test is that the stability is guaranteed for arbitrary fast switching. However, it is well known that this stability test is too conservative.

Stability by minimum dwell-time: It can be shown that if $A_1, A_2, \ldots, A_n$ are stable, there exists always some dwell-time $T_d \geq 1$ such that the switching system $x(k+1) = A_\sigma x(k)$ is stable. This result is expressed in the following theorem:

Theorem 3.4. *Assume that for some $T_d \geq 1$, there exists a set of positive definite matrices $\{P_1, \ldots, P_n\}$ such that:*

$$A_i^T P_i A_i - P_i \prec 0, \qquad \text{for } i = 1, \ldots, n \tag{3.203}$$

and

$$[A_i^T]^{T_d} P_j [A_i]^{T_d} - P_i \prec 0 \qquad \forall i \neq j = 1, \ldots, n \tag{3.204}$$

Then the switching signal $\sigma(k) = i \in \{1, \ldots, n\}$ with a dwell-time greater than or equal to T_d makes the equilibrium solution $x = 0$ of the switching system $x(k+1) = A_\sigma x(k)$ globally asymptotically stable.

The inequalities in (3.203) and (3.204) are LMIs with respect to Lyapunov matrices and therefore a feasible value for T_d can be readily computed.

Concluding Remarks

1. Large and fast parameter variations may lead to poor transient performance or even instability in classical adaptive control systems.
2. Adaptive control with switching can significantly improve the transient behavior of adaptive systems.
3. The basic idea is to use a multi-estimator instead of a unique estimator in the adaptive control scheme. During the transients, one of the estimator can provide rapidly a good estimate of the plant output and an appropriate controller can be chosen.
4. The main issue in adaptive control with switching is the stability of the closed-loop system. It has been shown that a dwell-time can be computed that guarantees closed-loop stability.
5. The use of robust pole placement technique in adaptive control with switching guarantees quadratic stability of the injected system and consequently stability of the adaptive system with arbitrary fast switching.

3.7.3 Relation with Gain-Scheduled Controller Design

A large class of nonlinear systems can be represented by a set of linear models that approximate the dynamics of the systems in different operating points. Thus, the dynamic behavior of such systems varies as a function of some scheduling parameters. Many electromechanical systems, such as for example component mounters, H-drives and electromagnetic levitation systems belong to this class of systems. For these examples, the

scheduling parameter is the position, as their dynamics change as a function of the position.

Such time-varying behavior cannot be controlled by classical linear control methods, as these methods require a linear time invariant (LTI) model of the system. One solution to this problem is to design an LTI controller that is robust against these varying dynamics. This kind of approaches assures the global stability of the closed-loop system. The major drawback is that the variation of the dynamics as a function of the scheduling parameters is treated as uncertainty. This often leads to poor closed-loop performance.

The performance of the controlled system can be improved if the knowledge of the scheduling parameters is included in the controller by making it dependent on these parameters. The corresponding synthesis procedure is commonly referred as gain-scheduling.

The classical gain-scheduling methods proceed in two steps. First, a finite grid of operating points is chosen within the whole range of operating points, then a controller is designed for each of these selected operating points based on the local model. Secondly, an interpolation between the controllers is done to get a gain-scheduled controller. The classical gain-scheduling methods give good closed-loop performance and are simple to use: controllers can be designed easily using for example a classical loop-shaping method; the implementation of the controller is straightforward. The major drawback lies in the fact that the global stability of the closed-loop system is not always assured, in particular for fast variations of the scheduling parameters.

The main difference between the gain-scheduling method and the adaptive switching methods are:

1. For the gain-scheduling method the scheduling parameters are measured in real time (usually with some sensors) to detect the operating point, while in the adaptive switching method the variation of the operating point is detected by supervising a performance criterion (no additional sensor).
2. In the gain-scheduling method the parameters of the controllers between two operating points are interpolated to find the intermediate controllers, while there is no interpolation in switching adaptive control.
3. A proof of stability exists for switching adaptive control, while the stability of the gain-scheduled controllers can be proved only for a class of Linear Parameter Varying (LPV) systems and controllers.

Data-Driven Gain-Scheduled Control

The two steps of gain-scheduled controller design can be combined in a data-driven setting and solved with convex optimization. Assume that the frequency response of the system $G(e^{j\omega}, \theta)$ is a function of a scheduling parameter $\theta \in \Theta$. Then we define a gain-scheduled controller structure as:

$$K(\theta) = X(\theta)Y^{-1}(\theta)$$

For example assume that $\theta = [\theta_1\, \theta_2\, \theta_3]$ is a three-dimensional vector and we are seeking a gain-scheduled controller with linear interpolation. In this case, we have:

$$X(\theta) = X_0 + \sum_{i=1}^{3} \theta_i X_i \qquad ; \qquad Y(\theta) = Y_0 + \sum_{i=1}^{3} \theta_i Y_i$$

where X_i and Y_i for $i = 0, \ldots, 3$ are stable transfer function matrices of a chosen order. Consider a second example, where θ is a scalar and we are interested in second order interpolation of the scheduling parameter in the controller. In this case the controller structure becomes:

$$X(\theta) = X_0 + \theta X_1 + \theta^2 X_2$$
$$Y(\theta) = Y_0 + \theta_1 Y_1 + \theta^2 Y_2$$

It is clear that for a given known θ, $X(\theta)$ and $Y(\theta)$ are linear with respect to the controller parameters. Therefore, all performance specifications mentioned in Section 2.4 can be used to design a gain scheduled controller by convex optimization.

For instance, consider minimizing $\|W_1 \mathcal{S}\|_\infty$ as a control objective. The optimization problem in (2.24) is slightly modified to design a gain-scheduled controller:

$$\min_{X,Y} \gamma$$

$$\begin{bmatrix} \gamma I & W_1 Y(\theta) \\ Y(\theta)^* W_1^* & P(\theta)^* P_c(\theta) + P_c(\theta)^* P(\theta) - P_c(\theta)^* P_c(\theta) \end{bmatrix} \succ 0 \qquad \forall \omega \in \Omega \qquad \forall \theta \in \Theta$$

where $P(\theta) = Y(\theta) + G(\theta)X(\theta)$ and $P_c(\theta) = Y_c(\theta) + G(\theta)X_c(\theta)$. The initial controller K_c can be the same for all θ or even be chosen differently for each scheduling parameter $K_c(\theta) = X_c(\theta)Y^{-1}(\theta)$. Note that this problem is convex with respect to the controller parameters and nonlinearity of G, X and Y with respect to θ does not make any problem because θ is the scheduling parameter and not an optimization variable. The problem, however, is to satisfy the constraints for all $\omega \in \Omega$ and for all $\theta \in \Theta$, which is a semi-infinite program (SIP). As it was discussed before, this problem can be solved by gridding in frequency and the scheduling parameters. It should be mentioned that the number of constraints will be multiplied by the number of grid points for the frequency and the scheduling parameters. Therefore, a controller can be designed in a reasonable time if the number of the grid points for the scheduling parameters are small (100 frequency points and 100 scheduling points leads to 10000 LMI constraints).

In the next section we see how the gain-scheduled controller combined with a PAA can be applied to a benchmark problem for active suspension systems.

3.8 Active Suspension Benchmark

The objective of the benchmark is to design a controller for the rejection of unknown/time-varying multiple narrow band disturbances located in a given frequency region. The

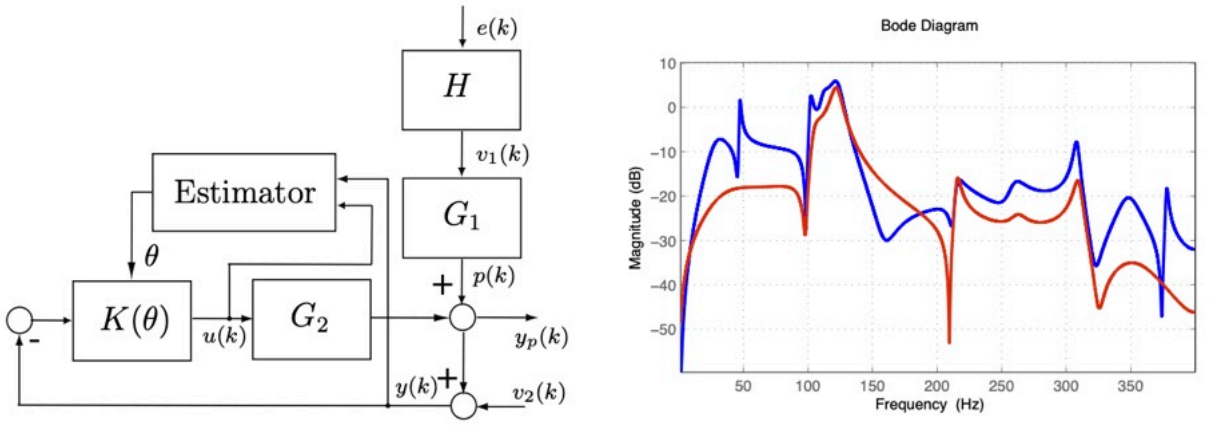

Figure 3.25: Block diagram of the active suspension system and the frequency response of the primary (red) and the secondary path (blue)

proposed controllers will be applied to the active suspension system of the Control Systems Department in Grenoble (GIPSA - lab). The block diagram of the active suspension system together with the proposed gain scheduled controller is shown in Fig. 3.25.

The system is excited by a sinusoidal disturbance $v_1(k)$ generated using a computer-controlled shaker, which can be represented as a white noise signal, $e(k)$, filtered through the disturbance model H. The transfer function G_1 between the disturbance input and the residual force in open-loop, $y_p(k)$, is called the primary path. The signal $y(k)$ is a measured voltage, representing the residual force, affected by the measurement noise. The secondary path is the transfer function G_2 between the output of the controller $u(k)$ and the residual force in open-loop. The control input drives an inertial actuator through a power amplifier. The magnitude Bode diagram of the primary and the secondary path models sampled at 800Hz are shown in Fig. 3.25 that contain several high resonance modes.

The disturbance consists of one sinusoidal signal whose frequency is unknown but lies in an interval from 50 to 95Hz. The controller should reject the disturbance as fast as possible.

Controller Design

An H_∞ gain-scheduled controller $K(\theta) = X(\theta)Y^{-1}(\theta)$, based on the internal model principle to reject the disturbances, is considered as follows:

$$X(z,\theta) = \frac{X_0(z) + \theta X_1(z)}{(z-\alpha)^n}$$

$$Y(z,\theta) = \frac{F_y(z,\theta)}{(z-\alpha)^n}$$

where $0 < \alpha < 1$ can be chosen arbitrarily, $X_0(z)$ and $X_1(z)$ are n-th order polynomials in z and $Y(z, \theta)$ includes only a fixed term and no other parameter for simplicity:

$$F_y(z, \theta) = z^2 + \theta z + 1$$

The fixed-term in Y is in fact the denominator of the disturbance model for a sinusoidal disturbance with frequency $f = \cos^{-1}(-\theta/2)/2\pi$. Based on the internal model principle, this fixed term will asymptotically reject the sinusoidal disturbance. In order to improve the transient response, the infinity-norm of the transfer function between the disturbance and the output, $HG_1\mathcal{S}$, should be minimized. However, since the primary path model G_1 could not be used in the benchmark, it is replaced by a constant gain and F_y^{-1} is considered for the disturbance model.

On the other hand, in order to increase the robustness and prevent the activity of the command input at frequencies where the gain of the secondary path is low, the infinity norm of the input sensitivity function $\|\mathcal{U}\|_\infty$ should be decreased as well. Another constraint on the modulus margin $M_m = 0.5$ is also considered according to the benchmark requirements (not to amplify the noise at other frequencies). As a result the following control problem is defined:

$$\min_{X,Y} \gamma$$

$$\left\| \begin{array}{c} W_1\mathcal{S}(\theta) \\ W_3\mathcal{U}(\theta) \end{array} \right\|_\infty < \gamma \quad ; \quad \|\mathcal{S}(\theta)\|_\infty < 2 \quad ; \quad \forall \theta \in \Theta$$

where $W_1 = F_y^{-1}$ and $W_3 = 1$. The first constraint is for disturbance rejection and reducing the input sensitivity function while the second constraint is to guarantee a modulus margin of 0.5. A gain-scheduled controller is designed using the following choices:

1. Because of many high resonance modes in the secondary path model, a very fine frequency grid with a resolution of 0.5 rad/s (5027 frequency points) is considered.
2. The interval of the disturbance frequencies is divided to 46 points (a resolution of 1Hz), which corresponds to 46 points in the interval $[-1.8478\,,\, -1.4686]$ for the scheduling parameter θ.
3. The controller order is chosen equal to 10 (the controller order is increased gradually to obtain acceptable results). Note that it is much less than the order of the plant model (26).

This gain-scheduled controller gives very good transient performance and satisfies the constraint on the maximum modulus of the sensitivity function for all values of the scheduling parameter. Figure 3.26 shows the magnitude of the output sensitivity functions $\mathcal{S}$ and the input sensitivity functions $\mathcal{U}$, respectively, for 46 gridded values of the disturbance frequencies. One can observe very good attenuation at the disturbance frequencies and the satisfaction of the modulus margin of at least 6dB for all disturbances.

(a) Input sensitivity function $\mathcal{U}$ (b) Output sensitivity function $\mathcal{S}$

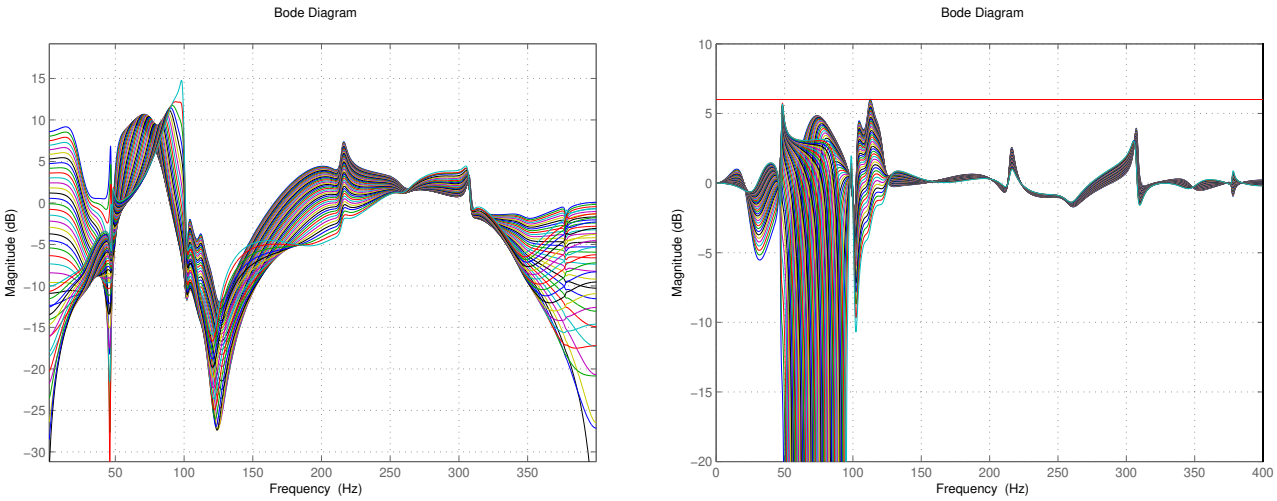

Figure 3.26: Magnitude of $\mathcal{U}$ and $\mathcal{S}$ for disturbance frequencies from 50Hz to 95Hz

Estimator design

The scheduling parameter θ used in the controller is estimated using a parameter adaptation algorithm. To estimate the parameters of the disturbance model, we need to measure the disturbance signal $p(k)$ (see Fig. 3.25). If we model $p(k)$ as the output of an ARMA model with white noise as input, we have:

$$D_p(q^{-1})p(k) = N_p(q^{-1})e(k), \tag{3.205}$$

where $e(k)$ is a zero mean white noise with unknown variance. Estimation of the parameters of N_p and D_p could be performed by the standard *Recursive Extended Least Squares* method [7], if $p(k)$ was measured. Since $p(k)$ is not available, it is estimated using the measured signal $y(k)$ and the known model of the secondary path. From Fig. 3.25, we have:

$$p(k) = y(k) - G_2(q^{-1})u(k) - v_2(k), \tag{3.206}$$

where:

$$G_2(q^{-1}) = \frac{q^{-d}B^\star(q^{-1})}{A(q^{-1})}$$

is the parametric model of the secondary path. Since $v_2(k)$ is a zero mean noise signal, unbiased estimate of $p(k)$ is given as

$$\bar{p}(k) = y(k) + [A(q^{-1}) - 1][y(k) - \bar{p}(k)] - B^\star(q^{-1})u(k-d)$$

For the asymptotical rejection of sinusoidal disturbance, there is no need to identify the whole model of the disturbance path, i.e. HG_1 as shown in Figure 3.25. The information

needed is just the frequency of the disturbance. So, by setting $D_p(q^{-1},\theta) = 1 - \theta q^{-1} + q^{-2}$ and $N_p(q^{-1}) = 1 + c_1 q^{-1} + c_2 q^{-2}$, a simple parameter estimation algorithm can be developed. Let us define :

$$\begin{aligned} z(k+1) &= \bar{p}(k+1) + \bar{p}(k-1) && (3.207)\\ \psi^T(k) &= [-\bar{p}(k), \varepsilon(k), \varepsilon(k-1)]^T && (3.208)\\ \Theta^T(k) &= [\theta, c_1, c_2]^T && (3.209) \end{aligned}$$

where $\varepsilon(k) = z(k) - \hat{z}(k)$ is the *a posteriori* prediction error. Now, the following recursive adaptation algorithm can be used to estimate the scheduling parameter θ:

$$\begin{aligned} \varepsilon^\circ(k+1) &= z(k+1) - \hat{\Theta}(k)\psi(k)\\ \varepsilon(k+1) &= \frac{\varepsilon^\circ(k+1)}{1 + \psi_f^T(k)F(k)\psi_f(k)}\\ \hat{\Theta}(k+1) &= \hat{\Theta}(k) + F(k)\psi_f(k)\varepsilon(k+1) && (3.210)\\ F(k+1) &= \frac{1}{\lambda_1(k)}\left[F(k) - \frac{F(k)\psi_f^T(k)\psi_f(k)F(k)}{\frac{\lambda_1(k)}{\lambda_2(k)} + \psi_f^T(k)F(k)\psi_f(k)}\right] \end{aligned}$$

where $\psi_f(k) = \frac{1}{N_p(q^{-1})}\psi(k)$, $\varepsilon^\circ(k)$ is the *a priori* prediction error and $\lambda_1(k)$ and $\lambda_2(k)$ define the variation profile of the adaptation gain $F(k)$. A constant trace algorithm is used for the adaptation gain.

Simulation and experimental results

Figure 3.27 shows the simulated residual force in closed-loop using the gain-scheduled controller and the scheduling parameter estimator. The transients are greater than that of linear controllers because of the adaptation time of the estimator. The experimental results for the same test are also shown in the same figure. Apart from the disturbance at 50Hz, disturbances at other frequencies are rejected and the transient times and their peak values are slightly smaller than those in simulation. The discrepancy of the simulation and experimental results for the disturbance frequency of 50Hz probably comes from the modeling error of the secondary-path model, around this frequency, used in the simulator of the benchmark. The residual force for a chirp disturbance (from 50 Hz to 95Hz in 4.5 second and then return to 50Hz in 4.5 second) shows that gain scheduled controller can follow the frequency-varying disturbances as well.

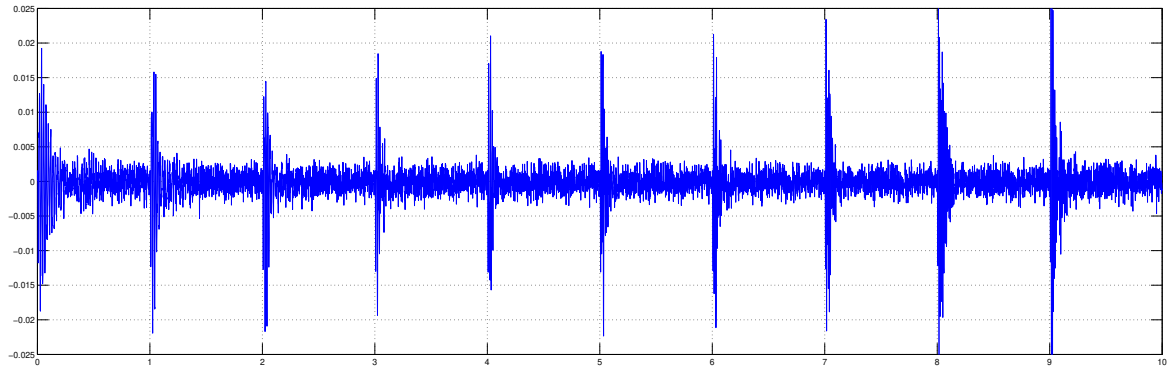

Transient responses in simulation (disturbance frequencies from 50Hz to 95Hz)

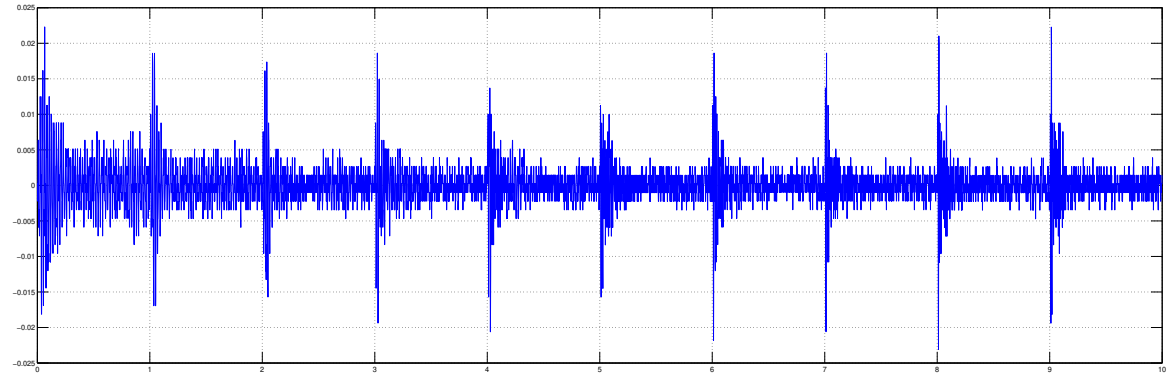

Experimental Transient responses (disturbance frequencies from 50Hz to 95Hz)

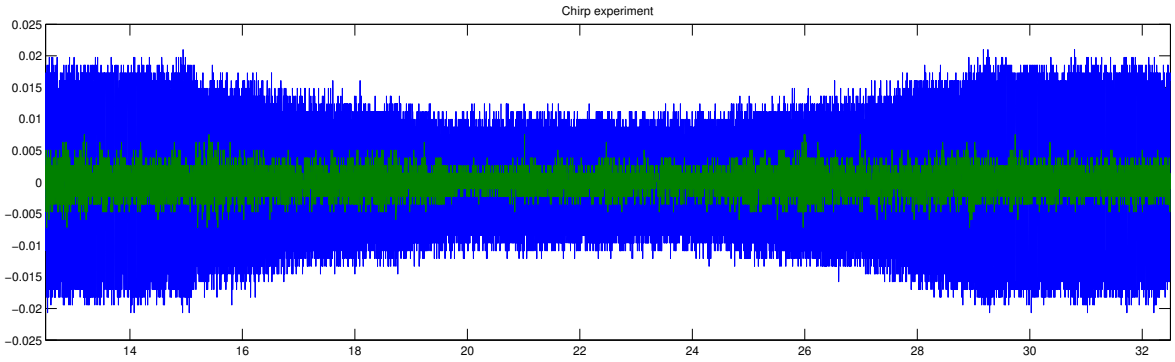

Experimental results for chirp disturbance responses (open-loop: blue; closed-loop: green)

Figure 3.27: Simulation and experimental results for the active suspension system

Appendix A

A.1 Stability of PAA

In the case of recursive least squares the following *a posteriori* predictor has been used:

$$\hat{y}(k+1) = \hat{\theta}^T(k+1)\phi(k) \tag{A.1}$$

where

$$\hat{\theta}^T(k) = [-\hat{a}_1(k), \cdots, -\hat{a}_{n_A}(k), \hat{b}_1(k), \cdots, \hat{b}_{n_B}(k)]$$
$$\phi^T(k) = [-y(k), \cdots, -y(k-n_A+1), u(k-d+1), \cdots, u(k-n_B+1]$$

The PAA has the following form:

$$\hat{\theta}(k+1) = \hat{\theta}(k) + F(k)\phi(k)\epsilon(k+1) \tag{A.2}$$

The parameter error is defined as:

$$\tilde{\theta}(k) = \hat{\theta}(k) - \theta \tag{A.3}$$

Subtracting θ in both sides of (A.2) and, taking into account (A.3), one obtains:

$$\tilde{\theta}(k+1) = \tilde{\theta}(k) + F(k)\phi(k)\epsilon(k+1) \tag{A.4}$$

From the definition of the *a posteriori* prediction error $\epsilon(k+1)$ given by (3.103) and taking into account (3.133) and (A.3), one gets:

$$\epsilon(k+1) = y(k+1) - \hat{y}(k+1) = \phi^T(k)\theta - \phi^T(k)\hat{\theta}(k+1) = -\phi^T(k)\tilde{\theta}(k+1) \tag{A.5}$$

and using (A.4), one can write:

$$\phi(k)\tilde{\theta}(k+1) = \phi^T(k)\tilde{\theta}(k) + \phi^T(k)F(k)\phi(k)\epsilon(k+1) \tag{A.6}$$

Eqs. (A.4) through (A.6) defines an equivalent feedback system represented in Fig. A.1. Eq. (A.5) defines a linear block with constant parameters on the feedforward path, whose

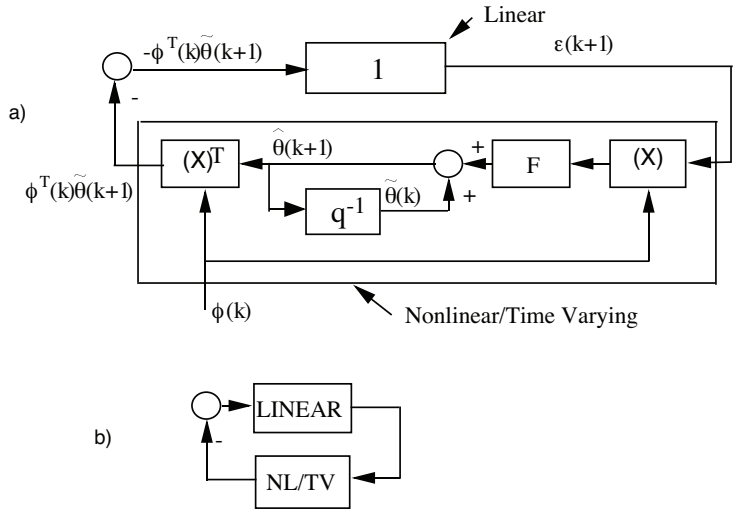

Figure A.1: Equivalent Feedback Representation of PAA, [a] The case of RLS, [b] Generic equivalent representation

input is $-\phi^T(k)\tilde{\theta}(k+1)$. In the case of least squares predictor (known also as equation error predictor or series-parallel predictor) this block is characterized by a unitary gain. Eqs. (A.4) and (A.6) define a nonlinear time-varying block in the feedback path. For the particular case of estimation in open loop operation using recursive least squares this block is only time-varying, since $\phi(k)$ does not depend neither upon ϵ, nor upon $\hat{\theta}$.

The objective of a PAA in a deterministic environment (absence of noise), is to drive the estimated parameter vector $\hat{\theta}$ towards a value such that the *a posteriori* prediction error vanishes asymptotically, i.e., $\lim_{k\to\infty} \epsilon(k+1) = 0$. This objective can be expressed as a condition for the asymptotic stability of the equivalent feedback system associated to the PAA.

It is assumed of course, that the structure chosen for the adjustable model is such that there is a value of the parameter vector which gives a perfect input-output description of the plant (i.e., the plant model and the adjustable predictor have the same structure).

Similar *equivalent feedback representation* (EFR) can be obtained for other PAA and adjustable predictors (like output error predictor or ARMAX predictor). In general, the linear feedforward block will be characterized by a transfer function and the feedback block will be time-varying and nonlinear.

The equivalent feedback representation associated to PAA is always formed by two blocks (see Fig. A.1.b): a linear time-invariant block (LINEAR) and a nonlinear time-varying (NL/TV). It is therefore reasonable to use specific stability analysis tools dedicated to this type of system.

Passivity (hyperstability) properties or Lyapunov functions with two (or several) terms are well suited for the stability analysis of feedback systems. The passivity (hyperstability)

approach is more natural and systematic, but the same results can be obtained by using Lyapunov functions of particular form.

The passivity approach concerns input-output properties of systems and the implications of these properties for the case of feedback interconnection.

We shall next present a pragmatic approach without formal generalized and proven results concerning the use of the passivity approach for the analysis and the synthesis of PAA. Detailed results can be found in [7].

The norm L_2 is defined as:

$$\|x(k)\|_2 = \left(\sum_0^\infty x^2(k) \right)^{1/2}$$

(it is assumed that all signals are 0 for $k < 0$).

To avoid the assumption that all signals go to zero as $k \to \infty$, one uses the so-called extended L_2 space denoted L_{2e} which contains the *truncated* sequences:

$$x_T(k) = \begin{cases} x(k) & 0 \le k \le T \\ 0 & k > T \end{cases}$$

Consider a SISO system G with input u and output y. Let us define the input-output product:

$$\eta(0, k_1) = \sum_{k=0}^{k_1} u(k) y(k)$$

The system G is termed *passive* if:

$$\eta(0, k_1) \ge -\gamma^2 \; ; \; \gamma^2 < \infty \quad \forall \; k_1 \ge 0$$

The system G is termed *(input) strictly passive* if:

$$\eta(0, k_1) \ge -\gamma^2 + \kappa \|u\|_2^2 \; ; \; \gamma^2 < \infty; \; \kappa > 0; \quad \forall \; k_1 \ge 0$$

and *(output) strictly passive* if:

$$\eta(0, k_1) \ge -\gamma^2 + \delta \|y\|_2^2 \; ; \; \gamma^2 < \infty; \; \delta > 0; \quad \forall \; k_1 \ge 0$$

Consider now the feedback interconnection between a block G_1 which is strictly passive (for example strictly input passive) and a block G_2 which is passive as illustrated in Fig. A.2.

One has:

$$\eta_1(0, k_1) = \sum_0^{k_1} u_1(k) y_1(k) \ge -\gamma_1^2 + \kappa \|u\|_2^2 \; ; \; \gamma_1^2 < \infty; \; \kappa > 0; \quad \forall \; k_1 \ge 0$$

$$\eta_2(0, k_1) = \sum_0^{k_1} u_2(k) y_2(k) \ge -\gamma_2^2 \; ; \; \gamma_2^2 < \infty; \quad \forall \; k_1 \ge 0$$

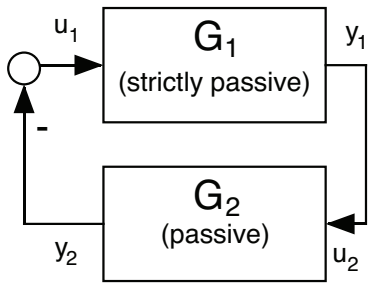

Figure A.2: Feedback interconnection of two passive blocks

The feedback connection corresponds to:

$$u_1 = -y_2;\ u_2 = y_1$$

Taking into account the feedback connection, it results that:

$$\eta_1(0,k_1) = \sum_0^{k_1} u_1(k)y_1(k) = -\sum_0^{k_1} u_2(k)y_2(k) = -\eta_2(0,k_1)$$

and therefore:

$$-\gamma_1^2 + \kappa\|u\|_2^2 \leq \sum_0^{k_1} u_1(k)y_1(k) \leq \gamma_2^2$$

from which one concludes:

$$\kappa\|u\|_2^2 \leq \gamma_1^2 + \gamma_2^2$$

i.e.,

$$\lim_{k_1\to\infty} \sum_{k=0}^{k_1} u_1^2(k) \leq \gamma_1^2 + \gamma_2^2 < \infty$$

which implies that $u(k)$ is bounded and that:

$$\lim_{k\to\infty} u_1(k) = 0$$

If, in addition the block G_1 is a linear asymptotically stable system, then:

$$\lim_{k\to\infty} u_1(k) \Longrightarrow \lim_{k\to\infty} y_1(k) = 0$$

Let us see now how these results can be used for the stability analysis of the *improved gradient algorithm* (which corresponds to recursive least squares using a constant adaptation gain $F(k+1) = F(k) = F > 0$). The equivalent feedback block is characterized by (A.4) and (A.6) with $F(k) = F$:

$$\tilde{\theta}(k+1) = \tilde{\theta}(k) + F\phi(k)\epsilon(k+1) \tag{A.7}$$

$$\begin{aligned} y_2(k) &= \phi^T(k)\tilde{\theta}(k+1) = \phi^T(k)\tilde{\theta}(k) + \phi^T(k)F\phi(k)\epsilon(k+1) \\ &= \phi(k)\tilde{\theta}(k) + \phi^T(k)F\phi(k)u_2(k) \end{aligned} \tag{A.8}$$

The input is the *a posteriori* prediction error $\epsilon(k+1)$ and the output is $\phi^T(k)\tilde{\theta}(k+1)$.

If we want to apply the passivity approach, we should verify first that the feedback path is passive. Taking advantage of (A.7), one gets:

$$\begin{aligned} \sum_{k=0}^{k_1} y_2(k)u_2(k) &= \sum_{k=0}^{k_1} \tilde{\theta}^T(k+1)\phi(k)\epsilon(k+1) \\ &= \sum_{k=0}^{k_1} \tilde{\theta}^T(k+1)F^{-1}\left[\tilde{\theta}(k+1) - \tilde{\theta}(k)\right] \\ &= \sum_{k=0}^{k_1} \left[\tilde{\theta}^T(k+1)F^{-1}\tilde{\theta}(k+1) - \tilde{\theta}^T(k+1)F^{-1}\tilde{\theta}(k)\right] \end{aligned} \tag{A.9}$$

Observe that:

$$\begin{aligned} \left[\tilde{\theta}(k+1) - \tilde{\theta}(k)\right]^T F^{-1}\left[\tilde{\theta}(k+1) - \tilde{\theta}(k)\right] &= \tilde{\theta}^T(k+1)F^{-1}\tilde{\theta}(k+1) \\ &+\tilde{\theta}^T(k)F^{-1}\tilde{\theta}(k) - 2\tilde{\theta}^T(k+1)F^{-1}\tilde{\theta}(k) \geq 0 \end{aligned} \tag{A.10}$$

and therefore:

$$-\tilde{\theta}^T(k+1)F^{-1}\tilde{\theta}(k) \geq -\frac{1}{2}\left[\tilde{\theta}^T(k+1)F^{-1}\tilde{\theta}(k+1) + \tilde{\theta}^T(k)F^{-1}\tilde{\theta}(k)\right] \tag{A.11}$$

Introducing this expression in (A.9), one obtains:

$$\begin{aligned} \sum_{k=0}^{k_1} y_2(k)u_2(k) &\geq \frac{1}{2}\sum_{k=0}^{k_1} \tilde{\theta}^T(k+1)F^{-1}\tilde{\theta}(k+1) - \frac{1}{2}\sum_{k=0}^{k_1} \tilde{\theta}^T(k)F^{-1}\tilde{\theta}(k) \\ &= \frac{1}{2}\tilde{\theta}^T(k+1)F^{-1}\tilde{\theta}(k+1) - \frac{1}{2}\tilde{\theta}^T(0)F^{-1}\tilde{\theta}(0) \\ &\geq -\frac{1}{2}\tilde{\theta}^T(0)F^{-1}\tilde{\theta}(0) = -\gamma_2^2 \;;\; \gamma_2^2 < \infty \end{aligned} \tag{A.12}$$

One concludes therefore that the equivalent feedback path is passive. Taking now into account the feedback connection and the corresponding linear path specified in (A.5), one gets:

$$\begin{aligned} \sum_{k=0}^{k_1} y_1 u_1 &= \sum_{k=0}^{k_1} \epsilon^2(k+1) \\ &= -\sum_{k=0}^{k_1} y_2 u_2 = \sum_{k=0}^{k_1} -\tilde{\theta}^T(k+1)\phi(k)\epsilon(k+1) \\ &\leq \frac{1}{2}\tilde{\theta}^T(0)F^{-1}\tilde{\theta}(0) \end{aligned} \tag{A.13}$$

and, therefore:

$$\lim_{k_1\to\infty}\sum_{k=0}^{k_1}\epsilon^2(k+1)\leq\frac{1}{2}\tilde{\theta}^T(0)F^{-1}\tilde{\theta}(0)=\gamma_2^2 \tag{A.14}$$

from which one concludes that $\epsilon(k+1)$ is bounded and:

$$\lim_{k_1\to\infty}\epsilon(k+1)=0 \tag{A.15}$$

i.e., the global asymptotic convergence to zero of the *a posteriori* prediction (adaptation) error for any finite initial condition on the parameter error and any adaptation gain $F>0$.

Taking into account the relationship between the *a priori* and the *a posteriori* prediction error:

$$\epsilon(k+1)=\frac{\epsilon^\circ(k+1)}{1+\phi^T(k)F\phi(k)} \tag{A.16}$$

one also concludes that $\lim_{k\to\infty}\epsilon(k+1)=0$ implies $\lim_{k\to\infty}\epsilon^\circ(k+1)=0$ when $\phi(k)$ is bounded. In this example, $\phi(k)$ contains the inputs and the outputs of a system assumed to be stable and excited by an input assumed to be bounded and then, it will be bounded. Therefore, the conclusion of this analysis is that the *improved gradient algorithm* is asymptotically stable for any finite value of the adaptation gain F, which is positive definite.

A.2 Parametric Convergence of PAA

As will be shown, the convergence toward zero of the adaptation or prediction error does not imply in every case that the estimated parameters will converge toward the true parameters. The objective will be to determine under what conditions the convergence of the adaptation (prediction) error will imply the convergence toward the true parameters.

We will make the hypothesis that such a value of parameter vector exists, i.e.,

$$\exists\theta\ ;\ \nu(k+1)\mid_{\hat{\theta}=\theta}=0$$

This is based on the assumption that the structure of the adjustable model is identical to that of the system and that the orders n_A, n_B of the adjustable model are equal or higher than those of the system model.

In order to illustrate the influence of the excitation signal for the parametric convergence, let us consider the discrete-time system model described by:

$$y(k+1)=-a_1y(k)+b_1u(k) \tag{A.17}$$

and consider an estimated model described by:

$$\hat{y}(k+1)=-\hat{a}_1y(k)+\hat{b}_1u(k) \tag{A.18}$$

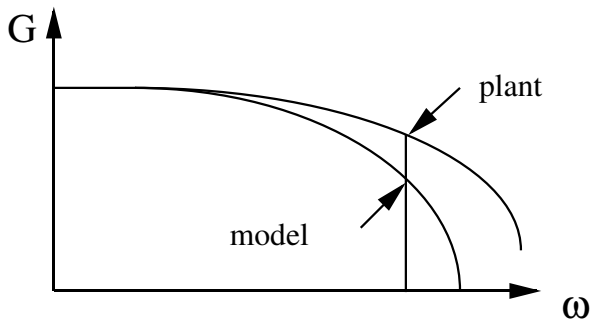

Figure A.3: Gain frequency characteristics of two systems with the same steady state gain

in which $\hat{y}(k+1)$ is the output predicted by the estimation model with the constant parameters $\hat{a}_1, \hat{b}_1$.

Now assume that $u(k) = \textit{constant}$ and that the parameters $a_1, b_1, \hat{a}_1, \hat{b}_1$ verify the following relation:

$$\frac{b_1}{1+a_1} = \frac{\hat{b}_1}{1+\hat{a}_1} \tag{A.19}$$

i.e., the steady state gains of the system and of the estimated model are equal even if $\hat{b}_1 \neq b_1$ and $\hat{a}_1 \neq a_1$. Under the effect of the constant input $u(k) = u$, the plant output will be given by:

$$y(k+1) = y(k) = \frac{b_1}{1+a_1} u \tag{A.20}$$

and the output of the estimated prediction model will be given by:

$$\hat{y}(k+1) = \hat{y}(k) = \frac{\hat{b}_1}{1+\hat{a}_1} u \tag{A.21}$$

However taking into account Eq. (3.4.4), it results that:

$$\begin{aligned} \epsilon(k+1) = y(k+1) - \hat{y}(k+1) = 0 \\ \text{for } u(k) = \textit{constant}\,;\ \hat{a}_1 \neq a_1\ ;\ \hat{b}_1 \neq b_1 \end{aligned} \tag{A.22}$$

It can thus be concluded from this example that the application of a constant input does not allow to distinguish the two models, since they both have the same steady state gain.

If the frequency characteristics of both systems are represented, they will superpose each other at zero frequency and the difference between them will appear for frequencies other than zero since the poles of the two systems are different. Such a situation is shown in Fig. A.3. Figure A.3 indicates that in order to highlight the difference between the two models (i.e., between the parameters) a signal $u(k) = \sin \omega t$ ($\omega \neq 0$) must be applied instead of signal $u(k) = \textit{constant}$.

Let us analyze the phenomenon in more detail. From (A.17) and (A.18), one obtains:

$$\begin{aligned} \epsilon(k+1) &= y(k+1) - \hat{y}(k+1) \\ &= (a_1 - \hat{a}_1)y(k) + (b_1 - \hat{b}_1)u(k) = 0 \end{aligned} \tag{A.23}$$

From (A.17), $y(k)$ can be expressed as a function of $u(k)$ using the system transfer operator:

$$y(k) = \frac{b_1 q^{-1}}{1 + a_1 q^{-1}} u(k) \tag{A.24}$$

Introducing the expression $y(k)$ given by (A.24) in (A.23) and after multiplying by $(1 + a_1 q^{-1})$, one obtains:

$$\begin{aligned} \epsilon(k+1) &= \left[(a_1 - \hat{a}_1)b_1 q^{-1} + (b_1 - \hat{b}_1)(1 + a_1 q^{-1})\right] u(k) \\ &= \left[(b_1 - \hat{b}_1) + q^{-1}(b_1 \hat{a}_1 - a_1 \hat{b}_1)\right] u(k) = 0 \end{aligned} \tag{A.25}$$

We are concerned with finding the characteristics of $u(k)$ so that (A.25) implies zero parametric errors. Denoting:

$$b_1 - \hat{b}_1 = \alpha_0 \; ; \; b_1 \hat{a}_1 - a_1 \hat{b}_1 = \alpha_1 \tag{A.26}$$

Eq. (A.25) is thus written as:

$$(\alpha_0 + \alpha_1 q^{-1}) u(k) = 0 \tag{A.27}$$

which is a difference equation having a solution of the discretized exponential type.

Let us:

$$u(k) = z^k = e^{skh} \tag{A.28}$$

where h is the sampling period. Eq. (A.27) is then written:

$$(\alpha_0 + z^{-1}\alpha_1) z^k = (z\alpha_0 + \alpha_1) z^{k-1} = 0 \tag{A.29}$$

and it will be verified for z, which is the solution of the characteristic equation:

$$z\alpha_0 + \alpha_1 = 0 \tag{A.30}$$

One obtains:

$$\begin{aligned} z &= -\frac{\alpha_1}{\alpha_0} = e^{\sigma h} \\ \sigma &= \text{real} \; ; \; (\frac{\alpha_1}{\alpha_0} < 0) \end{aligned} \tag{A.31}$$

and the nonperiodic solution:

$$u(k) = e^{\sigma k h} \tag{A.32}$$

leads to the verification of (A.27) and (A.25) respectively without $\hat{b}_1 = b_1$ and $\hat{a}_1 = a_1$. Indeed the signal $u(k) = \textit{constant}$ previously considered, corresponds to $\sigma = 0$, i.e., $-\alpha_1 = \alpha_0$. However:

$$\begin{aligned} -\alpha_1 = \alpha_0 \quad &\Longrightarrow \quad b_1 - \hat{b}_1 = a_1\hat{b}_1 - b_1\hat{a}_1 \\ &\Longrightarrow \quad \frac{b_1}{1+a_1} = \frac{\hat{b}_1}{1+\hat{a}_1} \end{aligned} \tag{A.33}$$

In conclusion, if $u(k) = \textit{constant}$, only the steady state gain of the system is correctly estimated. In order to correctly estimate the system model parameters, $u(k)$ must thus be found such that $\epsilon(k) = 0$ implies $\hat{b}_1 = b_1$ and $\hat{a}_1 = a_1$. This will be obtained if $u(k)$ is not a possible solution of (A.27).

Let us:

$$u(k) = e^{j\omega kh} \text{ or } e^{-j\omega kh} \tag{A.34}$$

For $u(k) = e^{j\omega kh}$, (A.27) becomes:

$$\left(e^{j\omega h}\alpha_0 + \alpha_1\right) e^{j\omega h(k-1)} = 0 \tag{A.35}$$

Since α_0 and α_1 are real, $e^{j\omega kh}$ cannot be a root of the characteristic equation (A.35) and therefore $\epsilon(k+1) = 0$ will be obtained only if:

$$\alpha_0 = \alpha_1 = 0 \Longrightarrow \hat{b}_1 = b_1; \hat{a}_1 = a_1 \tag{A.36}$$

A non zero frequency sinusoid is thus required in order to identify two parameters. The signal $u(k)$ which in this case is a sinusoid, is a *persistently exciting signal* of order 2 (allowing to estimate 2 parameters).

We are interested next in the characterization of the *persistently exciting signals*.

A.2.1 Persistently Exciting Signals

In the general case, one considers $u(k)$ signals bounded in average verifying the property:

$$\lim_{k_1\to\infty} \frac{1}{k_1} \sum_{k=1}^{k_1} u^2(k) < \infty \tag{A.37}$$

Defining $\varphi^T(k) = [u(k), u(k-1) \cdots u(k-n+1)]$, the signal $u(k)$ is said to be a *persistently exciting of order n* if:

$$\lim_{k_1\to\infty} \frac{1}{k_1} \sum_{k=1}^{k_1} \varphi(k)\varphi^T(k) > 0$$

One has the following result :

Theorem A.1. *$u(k)$ is a persistently exciting signal of order n if:*

$$\lim_{k_1\to\infty}\frac{1}{k_1}\left[\sum_{k=1}^{k_1}L(q^{-1})u(k)\right]^2>0 \tag{A.38}$$

for all nonzero polynomials $L(q^{-1})$ of order $n-1$.

This theorem is nothing else that a generalization of the previous example. In this example, $L(q^{-1})$ was a polynomial of order 1 (formed by differences between true and estimated parameters) and we have searched a persistently exciting signal $u(k)$ of order 2. The resulting signal was a sinusoid of nonzero frequency. It results that a sum of $n/2$ sinusoids of distinct frequencies is a persistently exciting signal of order n. Effectively, in the case of the estimation of n parameters, $\epsilon(k+1)=0$ leads to an equation $L(q^{-1})u(k)=0$ where $L(q^{-1})$ is a polynomial of order $n-1$ whose coefficients depend upon the difference between the estimated parameters and the true parameters. Depending on whether $(n-1)$ is odd or even, the equation $L(q^{-1})u(k)=0$ admits as solution a sum of p sinusoids of distinct frequencies.

$$u(k)=\sum_{k=1}^{p}\sin\omega_i kh$$

with $p\leq(n-1)/2$. This leads to the conclusion that a sum of p sinusoids of distinct frequencies with $p\geq n/2$ (n =even) or $p\geq(n+1)/2$ (n =odd) cannot be a solution of the equation $L(q^{-1})u(k)=0$, and therefore:

$$\begin{aligned} p &= \frac{n}{2} \quad \forall\, n=\text{even} \\ p &= \frac{n+1}{2} \quad \forall\, n=\text{odd} \end{aligned}$$

leads to a persistent excitation signal of order n, allowing to estimate n parameters.

The persistently exciting signals have a frequency interpretation which is more general than a sum of sinusoids of distinct frequencies. Using the Parseval theorem, Eq. (A.38) becomes:

$$\lim_{k_1\to\infty}\frac{1}{k_1}\sum_{k=1}^{k_1}\left[L(q^{-1})u(k)\right]^2=\frac{1}{2\pi}\int_{-\pi}^{\pi}\mid L(e^{j\omega})\mid^2\phi_u(\omega)d\omega>0$$

where $\phi_u(\omega)$ is the spectral density of the input signal. Since $L(q^{-1})$ is of order $n-1$, $L(e^{j\omega})=0$ at most $n-1$ points between $[-\pi,\pi]$. If $\phi_u(\omega)\neq 0$ for at least n points in the interval $-\pi\leq\omega\leq\pi$, $u(k)$ is a persistently exciting signal of order n.

A signal whose spectrum is different from zero over all the interval $0\leq f\leq 0.5f_s$ is a persistently exciting signal of any order. Such an example is the discrete gaussian white noise which has a constant spectral density between 0 and $0.5f_s$.

In practice, one uses for system identification *pseudo-random binary sequences* (PRBS) which approach the characteristic of a white noise. Their main advantage is that they have

a constant magnitude (the stochastic character coming from the pulse width variation) which permits the precise definition of the level of instantaneous stress on the process (or actuator).

A.2.2 Parametric Convergence Condition

For the parameter estimation of a model of the form ($d = 1$):

$$y(k+1) = -A^{\star}y(k) + B^{\star}u(k) = \theta^T\varphi(k) \tag{A.39}$$

where:

$$\theta^T = [a_1 \cdots a_{n_A}, b_1 \cdots b_{n_B}] \tag{A.40}$$

$$\varphi^T(k) = [-y(k) \cdots y(k-n_A+1), u(k) \cdots u(k-n_B+1)] \tag{A.41}$$

using an *equation error* type adjustable predictor:

$$\hat{y}(k+1) = \hat{\theta}^T(k+1)\phi(k) = \hat{\theta}^T(k+1)\varphi(k) \tag{A.42}$$

one has the following result:

Theorem A.2. *Given the system model described by (A.39) and using an adjustable predictor of the form of (A.42), the parameter convergence, i.e.*

$$\lim_{k\to\infty} \hat{a}_i(k) = a_i \qquad i = 1 \cdots n_A$$

$$\lim_{k\to\infty} \hat{b}_i(k) = b_i \qquad i = 1 \cdots n_B$$

is assured if:

1) One uses a PAA which assures

$$\lim_{k\to\infty} \epsilon(k+1) = \lim_{k\to\infty} [y(k+1) - \hat{y}(k+1)] = 0$$

2) The orders n_A and n_B are known exactly.

3) The plant model to be identified is characterized by an irreducible transfer function in z^{-1} (i.e., $A(q^{-1})$ and $B(q^{-1})$ are relatively prime).

4) The input $u(k)$ is a persistently exciting signal of order $n = n_A + n_B$.

Proof. The proof is a generalization of the example considered in this section combined with the definition and properties of persistently exciting signals.

Under the assumption that $\lim_{k\to\infty} \epsilon(k+1) = 0$, the adjustable predictor becomes asymptotically a fixed predictor described by:

$$y(k+1) = \hat{\theta}^T\varphi(k) \tag{A.43}$$

where:

$$\hat{\theta}^k = [\hat{a}_1 \cdots \hat{a}_{n_A}, \hat{b}_1 \cdots \hat{b}_{n_B}] \tag{A.44}$$

contains the final values of the estimated parameters (i.e. $\hat{a}_i = \lim_{k\to\infty} \hat{a}_i(k)$, $\hat{b}_i = \lim_{k\to\infty} \hat{b}_i(k)$), and one has:

$$\lim_{k\to\infty} \epsilon(k+1) = -\left(\sum_{i=1}^{n_A}(a_i - \hat{a}_i)q^{-i+1}\right) y(k) + \left(\sum_{i=1}^{n_B}(b_i - \hat{b}_i)q^{-i+1}\right) u(k) = 0 \tag{A.45}$$

Taking into account Assumption (3) and replacing $y(k)$ by:

$$y(k) = \frac{B(q^{-1})}{A(q^{-1})}u(k) \tag{A.46}$$

Eq. (A.45) becomes:

$$\left[-\left(\sum_{i=1}^{n_A}(a_i - \hat{a}_i)q^{-i+1}\right) B(q^{-1}) + \left(\sum_{i=1}^{n_B}(b_i - \hat{b}_i)q^{-i+1}\right) A(q^{-1})\right] u(k) = \left(\sum_{i=0}^{n_A+n_B-1} \alpha_i q^{-i}\right) u(k) = 0 \tag{A.47}$$

with:

$$\alpha_0 = \Delta b_1 \tag{A.48}$$

$$\alpha_1 \cdots \alpha_{n_A+n_B-1} = \Delta b_1[a_1 \cdots a_{n_A}, 0 \cdots 0] + [\Delta b_2 \cdots \Delta b_{n_B}, -\Delta a_{n_A} \cdots - \Delta a_1]R(a_i, b_i) \tag{A.49}$$

and condition (4) assures the desired persistence of excitation. □

A.3 Stability of Direct Adaptive Control

The fact that the PAA of (3.165), (3.166) and (3.169) assures that (3.164) holds, does not guarantee that the objective of the adaptive control scheme defined by (3.152) will be achieved (i.e., the a priori adaptation error should goes to zero) and that $\{u(k)\}$ and $\{y(k)\}$ will be bounded. This is related to the boundedness of $\phi_C(k)$. Effectively from (3.169), one can see that $\epsilon(k+d)$ can go to zero without that $\epsilon^\circ(k+d)$ goes to zero if $\phi_C(k)$ becomes unbounded. Since $\phi_C(k)$ contains the input and the output of the plant, it is necessary to show that the PAA achieves the objective of (3.152) while assuring that $\phi_C(k)$ remains bounded for all k.

An important preliminary remark is that the plant model in (3.150) is a difference equation with constant coefficients and therefore $y(k+1)$ cannot become unbounded for

finite k if $u(k)$ is bounded. Therefore if $u(k)$ is bounded, $y(k)$ and respectively $\phi_C(k)$ can become unbounded only asymptotically.

Bearing in mind the form of (3.159), it is also clear that in order to avoid $u(k)$ becoming unbounded the adjustable parameters must be bounded and $\hat{s}_0(k) = \hat{b}_d(k) \neq 0$ for all k. This will assure $\phi_C(k)$ can become eventually unbounded only asymptotically.

In order to assure that $\hat{b}_d(k) \neq 0$ for any k, knowing that b_d cannot be zero and its sign is assumed to be known, one fixes a minimum value $|\hat{b}_d(k)| \geq \delta > 0$. If $|\hat{b}_d(k)| < \delta$ for some k, one either simply uses the value δ (with the appropriate sign), or one takes advantage of the weighting sequences $\lambda_1(k), \lambda_2(k)$ and recomputes $\hat{\theta}_C(k)$ for different values of $\lambda_1(k-d-1), \lambda_2(k-d-1)$ (for example: $\lambda_1' = \lambda_1 + \Delta\lambda_1$, $\lambda_2' = \lambda_2 + \Delta\lambda_2$) such that $|\hat{b}_d(k)| > \delta$.

After these preliminary considerations, the next step is to show that (3.152) is true and $\phi_C(k)$ is bounded. To proceed, we will use the "bounded growth" lemma.

Lemma A.1. *Assume that:*

$$\|\phi(k)\|_{F(k)} = [\phi^T(k)F(k)\phi(k)]^{1/2} \leq C_1 + C_2 \max_{0\leq k\leq t+d+1} |\epsilon^\circ(k)|$$
$$0 < C_1,\ C_2 < \infty,\ F(k) > 0 \tag{A.50}$$

and

$$\lim_{k\to\infty} \frac{[\epsilon^\circ(k+d)]^2}{1 + \|\phi(k)\|^2_{F(k)}} = 0 \tag{A.51}$$

Then: $\|\phi(k)\|$ *is bounded and* $\lim_{k\to\infty} \epsilon^\circ(k+d) = 0$

Proof. The proof is trivial if $\epsilon^\circ(k)$ is bounded for all k. Assume now that $\epsilon^\circ(k+d)$ is asymptotically unbounded. Then there is a particular subsequence such that: $\lim_{k_n\to\infty} \epsilon^\circ(k_n) = \infty$ and $|\epsilon^\circ(k+d)| < |\epsilon^\circ(k_n)|$; $k+d \leq k_n$. For this sequence one has:

$$\frac{|\epsilon^\circ(k+d)|}{(1+\|\phi(k)\|_F^2)^{1/2}} \geq \frac{\epsilon^\circ(k+d)}{1+\|\phi(k)\|_{F(k)}} \geq \frac{|\epsilon^\circ(k+d)|}{1+C_1+C_2|\epsilon^\circ(k+d)|}$$

but:

$$\lim_{k\to\infty} \frac{|\epsilon^\circ(k+d)|}{1+C_1+C_2|\epsilon^\circ(k+d)|} = \frac{1}{C_2} > 0$$

which contradicts (A.51) and proves that neither $\epsilon^\circ(k+d)$ nor $\|\phi(k)\|$ can become unbounded and that $\lim_{k\to\infty} \epsilon^\circ(k+d) = 0$. □

The application of this lemma is straightforward in our case. From Eq. (3.161) one has:

$$P(q^{-1})y(k+d) = P(q^{-1})y^\star(k+d) + \epsilon^\circ(k+d) \tag{A.52}$$

Since $P(q^{-1})$ has bounded coefficients and $y^\star$ is bounded, one gets immediately from Eq. (A.52) that:

$$|y(k)| \leq C_1' + C_2' \max_{0\leq k\leq t+d} |\epsilon^\circ(k)| \tag{A.53}$$

Using the assumption that $B^\star(z^{-1})$ has all its zeros inside the unit circle, the inverse of the system is asymptotically stable and one has:

$$|u(k)| \leq C_1'' + C_2'' \max_{0 \leq k \leq t+d+1} |y(k+d)| \tag{A.54}$$

From Eqs. (A.53) and (A.54), one concludes that:

$$\|\phi_C(k)\|_{F(k)} \leq C_1 + C_2 \max_{0 \leq k \leq t+d+1} |\epsilon^\circ(k)| \tag{A.55}$$

and, on the other hand, one has (A.51). Therefore the assumptions of Lemma A.1 are satisfied allowing to conclude that (3.152) is satisfied and that $\{u(k)\}$ and $\{y(k)\}$ are bounded. The results of the previous analysis can be summarized under the following form:

Theorem A.3. *: Consider a plant model of the form (3.150) controlled by the adjustable controller (3.153) whose parameters are updated by the PAA of Eqs. (3.165), (3.166) and (3.170) where:*

$$\epsilon^\circ(k+d) = Py(k+d) - Py^\star(k+d)$$

Assume that: the integer delay d is known; upper bounds on the degrees of the polynomials A and $B^\star$ are known; for all possible values of the plant parameters, the polynomial $B^\star$ has all its zeros inside the unit circle and the sign of b_d is known. Then:

- $\lim_{k \to \infty} \epsilon^\circ(k+d) = 0$
- *The sequences $\{u(k)\}$ and $\{y(k)\}$ are bounded.*

Remarks:

- Various choices can be made for $\lambda_1(k)$ and $\lambda_2(k)$ as indicated in Section 3.4.2. This will influence the properties and the performance of the scheme. In particular for $\lambda_1(k) \equiv 1$ and $\lambda_2(k) > 0$, one will obtain a PAA with decreasing adaptation gain. The *constant trace algorithm* is probably the most used algorithm for obtaining an adaptive control scheme which is continuously active.
- Monitoring the eigenvalues of $F(k)$ is recommended in order to assure $0 < \delta < \|F(k)\| < \infty$ for all k.
- The choice of $P(q^{-1})$ which influences the robustness of the linear design also influences the adaptation transients. Taking $P(q^{-1}) = 1$, one gets oscillatory adaptation transients (and the linear design will be very sensitive to parameters change) while $P(q^{-1})$ in the range of the band pass of the plant will both improve the robustness of the linear design and the smoothness of the adaptation transient.

Bibliography

[1] D. Arzelier and D. Henrion. *Optimisation LMI et Application*. `http://homepages.laas.fr/henrion/courses/edsys04/`, Slides of a course given in LAAS-CNRS, Toulouse, May 2004.

[2] C. J. Doyle, B. A. Francis, and A. R. Tannenbaum. *Feedback Control Theory*. Mc Millan, New York, 1992.

[3] C. Kammer. *Frequency-Domain Control Design in Power Systems*. PhD thesis, Ecole Polytechnique Fédérale de Lausanne, Laboratoire d'Automatique, 1015 Lausanne, Switzerland, 2018.

[4] C. Kammer and A. Karimi. A data-driven fixed-structure control design method with application to a 2-dof gyroscope. In *2018 IEEE Conference on Control Technology and Applications (CCTA)*, pages 915–920. IEEE, 2018.

[5] C. Kammer, A. P. Nievergelt, G. E. Fantner, and A. Karimi. Data-driven controller design for atomic-force microscopy. *IFAC-PapersOnLine*, 50(1):10437–10442, 2017.

[6] A. Karimi and C. Kammer. A data-driven approach to robust control of multivariable systems by convex optimization. *Automatica*, 85:227–233, 2017.

[7] I. D. Landau, R. Lozano, M. M'Saad, and A. Karimi. *Adaptive Control: Algorithms, Analysis and Applications*. Springer-Verlag, London, 2011.

[8] C. Scherer and S. Weiland. *Linear Matrix Inequalities in Control*. `http://www.cs.ele.tue.nl/sweiland/lmi.htm`, Version 3, October 2000.

[9] K. Zhou. *Essentials of Robust Control*. Prentice Hall, New Jersey, 1998.